

**Characterization of active microbial communities in extreme High Arctic cold saline spring
systems with meta'omics**

Elisse Magnuson

Department of Natural Resource Sciences

Faculty of Agricultural and Environmental Sciences

McGill University

March 2023

A thesis submitted to McGill University in partial fulfillment of the requirements of the degree
of Doctor of Philosophy

© Elisse Magnuson, 2023

Detailed table of contents

Abstract	8
Résumé	10
Acknowledgements	12
Contribution to Original Knowledge	14
Contribution of Authors	15
List of Tables and Figures	17
List of Abbreviations	19
Chapter 1. Introduction and Literature Review	22
1.1 Objectives of this thesis.....	22
1.2 Introduction to the cryosphere and its microbial inhabitants.....	24
1.3 The microbial community in cold, hypersaline environments.....	25
1.3.1 Antarctic hypersaline lakes.....	26
1.3.2 Cryopegs.....	28
1.3.3 Sea ice.....	29
1.4 Hypersaline cryoenvironments as astrobiology analogues.....	30
1.4.1 Mars.....	31
1.4.2 Europa and Enceladus.....	32
1.4.3 Analogue environments on Earth.....	33
1.5 Sulfur and methane cycling in the cryoenvironment.....	34
1.5.1 Sulfur cycling.....	34
1.5.2 Methane cycling.....	40
1.6 Utilizing meta'omics in microbial community characterization.....	43

1.6.1	Conventional approaches for characterization of microbial communities	43
1.6.2	Metagenomic sequencing	44
1.6.3	Single-cell genomics	47
1.6.4	Metatranscriptomics	48
1.6.5	Metaproteomics	49
1.7	Cold saline springs on Axel Heiberg Island	50
1.7.1	Gypsum Hill	51
1.7.1.1	Site description	51
1.7.1.2	Previous studies	52
1.7.2	Lost Hammer	54
1.7.2.1	Site description	54
1.7.2.2	Previous studies	55
1.7.3	The springs as analogue environments	56
1.8	Conclusion	57
	Connecting Text	58
	Chapter 2. Active lithoautotrophic and methane-oxidizing microbial community in an anoxic, sub-zero, and hypersaline High Arctic spring	60
2.1	Abstract	61
2.2	Introduction	61
2.3	Materials and Methods	64
2.3.1	Site description and sample collection	64
2.3.2	DNA extraction and metagenome analyses	64
2.3.3	Single cell sorting and SAG analysis	65

2.3.4 mRNA sequencing and analysis	65
2.3.5 Data availability	65
2.4 Results and Discussion	66
2.4.1 MAGs and SAGs capture novel phylogenetic diversity.....	66
2.4.2 Sulfur cycling <i>Gammaproteobacteria</i> and <i>Desulfobacterota</i> are abundant and active	67
2.4.3 Anaerobic methane oxidation by ANME-1 detected at sub-zero temperatures	69
2.4.4 Other C and N cycling metabolisms detected	71
2.4.5 Lithoautotrophic metabolisms relatively predominant in the active microbial community.....	72
2.4.6 Functional potential and adaptations in poorly characterized taxa.....	74
2.4.6.1 ANME-1 genomes reveal potential metabolic flexibility and hypersaline adaptation.....	75
2.4.6.2 Poorly understood DPANN archaea active in LH	77
2.4.6.3 Candidate CG03 phylum is likely fermentative.....	79
2.4.7 LH as an analogue for relevant microbial metabolisms on Mars	80
2.5 Conclusion	82
2.6 Acknowledgements	82
2.7 References.....	89
Connecting Text.....	101
Chapter 3. Sulfur-cycling chemolithoautotrophic microbial community dominates a cold, anoxic, hypersaline Arctic spring.....	102

3.1 Abstract.....	103
3.2 Introduction.....	103
3.3 Materials and Methods	107
3.3.1 Site description and sampling.....	107
3.3.2 DNA extraction, metagenome sequencing, and metagenome analyses	108
3.3.3 mRNA extraction, metatranscriptome sequencing, and analyses.....	111
3.3.4 16S rRNA community profiling and analysis.....	112
3.3.5 Data accession.....	114
3.4 Results and Discussion	114
3.4.1 Metagenomic sequencing and MAGs characterized taxonomic diversity .	115
3.4.2 Sulfur cycling taxa and metabolic genes are abundant in the metatranscriptome.....	116
3.4.3 H ₂ -linked sulfate reduction drives microbial primary production	117
3.4.4 Trace oxygen supports S-oxidizing <i>Gammaproteobacteria</i>	125
3.4.5 Chemolithoautotrophy rather than photoautotrophy likely sustains primary production	129
3.4.6 Gypsum Hill as a Mars analogue	133
3.5 Conclusion	135
3.6 Acknowledgements	136
3.7 References.....	145
Connecting Text.....	159
Chapter 4. <i>Thiomicrothabodus</i> streamers and sulfur cycling in perennial hypersaline cold springs in the Canadian high Arctic	160

4.1 Originality-Significance Statement	161
4.2 Summary	161
4.3 Introduction	162
4.4 Results	165
4.4.1 Phylogenetic classification	165
4.4.2 Metagenome analyses	166
4.4.3 <i>Thiomicrothabodus</i> sp. metagenome-assembled genome	166
4.4.4 Metatranscriptome results	167
4.4.5 Metaproteome results	168
4.4.6 Sulfur metabolism	169
4.4.7 Additional metabolic pathways	170
4.4.8 Stress response	172
4.4.9 Sulfur isotope results	174
4.5 Discussion	174
4.6 Experimental Procedures	181
4.6.1 Study site and sample collection	181
4.6.2 Metagenome library	183
4.6.3 Metatranscriptome library	184
4.6.4 Metaproteomic analyses	186
4.6.5 Sediment mineralogy via XRD	188
4.6.6 S-isotopic analyses	189
4.7 Acknowledgments	191
4.8 References	200

Chapter 5. Discussion	211
5.1 Identifying the microbial community inhabiting the springs	211
5.2 Identifying the active microbial community and metabolisms.....	216
5.3 Identifying microbial stress response capabilities and adaptations.....	219
5.4 Future work.....	221
Final Conclusion and Summary	225
References	227
Appendix 1. Supplementary Materials for Chapter 2	252
Appendix 2. Supplementary Materials for Chapter 3	279
Appendix 3. Supplementary Materials for Chapter 4	293

Abstract

Cryoenvironments, or environments with continuously sub-zero temperatures, present unique challenges to microbial life, including freezing temperatures and high solute concentrations. Study of inhabitant microbes informs our understanding of the cold and saline limits of life on Earth and extraterrestrial bodies. Lost Hammer and Gypsum Hill springs, located on Axel Heiberg Island, Nunavut, in the Canadian High Arctic, are rare examples of perennial cold springs arising in an area of thick permafrost. These springs are perennially sub- or near-zero (-5 to 7°C), hypersaline (7-24%), and anoxic (<1 ppm O₂). Lost Hammer is also the coldest known terrestrial methane seep on Earth. Multi-omics methods were used to characterize the metabolic activities and adaptations sustaining microbial life in situ in these extreme environments. In Lost Hammer, a combination of metagenomics, single-amplified genomics, and metatranscriptomics identified a predominantly lithotrophic active microbial community in the sediment utilizing inorganic compounds (hydrogen sulfide, hydrogen, carbon dioxide) as energy and carbon sources, driven in part by sulfide-oxidizing *Gammaproteobacteria* scavenging trace oxygen. Genomes from active methane-oxidizing archaea (ANME-1), the first identified under ambient sub-zero and hypersaline conditions, showed evidence of putative metabolic flexibility and cold and saline adaptations. Evidence of anaerobic heterotrophic and fermentative lifestyles were identified in candidate phyla DPANN archaea and CG03 bacteria. In Gypsum Hill, metagenomic and metatranscriptomic sequencing and isotopic analysis identified an active microbial community in the spring sediment dominated by sulfur cycling *Desulfobacterota* and *Gammaproteobacteria*. Sulfate reduction was dominated by hydrogen-oxidizing chemolithoautotrophic *Desulfovibrionaceae* sp. and was identified in phyla not typically associated with sulfate reduction in novel lineages of *Spirochaetota* and *Bacteroidota*. Highly

abundant and active sulfur-reducing *Desulfuromusa* sp. expressed non-coding RNAs associated with transcriptional regulation, showing potential evidence of putative metabolic flexibility in response to substrate availability. Despite low oxygen availability, sulfide oxidation was primarily attributed to aerobic chemolithoautotrophic *Halothiobacillaceae*. In the Gypsum Hill spring outflow channels, seasonal microbial streamers were formed by a novel chemolithoautotrophic *Thiomicrothabodus* sp. oxidizing sulfide to elemental sulfur. The *Thiomicrothabodus* sp. genome contained osmotic and cold stress adaptations, including for the production of extracellular polymeric substances suggested to promote streamer formation and provide cold stress protection. This study identified active, predominantly chemolithoautotrophic microbial communities in extreme cold and hypersaline Arctic springs, providing insights into how microbial life is sustained in Earth's cryosphere and what types of microbial life could exist in analogous environments on Mars and other astrobiology targets.

Résumé

Les cryoenvironnements, ou environnements où les températures sont constamment inférieures à zéro, présentent des défis uniques pour la vie microbienne, incluant des températures de congélation et des concentrations élevées de solutés. L'étude des microorganismes vivants nous permet de mieux comprendre les limites froides et salines de la vie sur Terre et dans les corps extraterrestres. Les sources de Lost Hammer et de Gypsum Hill, situées sur l'île Axel Heiberg, au Nunavut, dans le Haut-Arctique canadien, sont des exemples rares de sources froides pérennes apparaissant dans une zone de pergélisol épais. Ces sources sont en permanence à une température inférieure ou égale à zéro (-5 à 7°C), hypersalines (7-24%), et anoxiques (<1 ppm O₂). À Lost Hammer, il s'agit également du suintement de méthane terrestre le plus froid connu sur Terre. Des méthodes multi-omiques ont été utilisées pour caractériser les activités métaboliques et les adaptations permettant de maintenir la vie microbienne in situ dans ces environnements extrêmes. Dans le cas de Lost Hammer, une combinaison de métagénomique, de génomique à amplification unique et de métatranscriptomique a permis d'identifier une communauté microbienne active principalement lithotrophe dans les sédiments, utilisant des composés inorganiques (sulfure d'hydrogène, hydrogène, dioxyde de carbone) comme sources d'énergie et de carbone, mené en partie par des *Gammaproteobacteria* oxydant le sulfure et piégeant les traces d'oxygène. Les génomes des archées oxydant le méthane (ANME-1), dont ces dernières ont été les premières identifiées dans des conditions ambiantes inférieures à zéro et hypersalines, ont montré des preuves de flexibilité métabolique putative et d'adaptation au froid et à la salinité. Des preuves de modes de vie anaérobiques hétérotrophes et fermentaires ont été identifiées dans les phyla candidats d'archées DPANN et de bactéries CG03.

À Gypsum Hill, le séquençage métagénomique et métatranscriptomique ainsi que l'analyse isotopique ont identifié une communauté microbienne active dans les sédiments de la source, dominée par des *Desulfobacterota* et des *Gammaproteobacteria* effectuant les cycles de soufre. La réduction des sulfates était dominée par les *Desulfovibrionaceae* sp. chimiolithoautotrophes oxydant l'hydrogène et a été identifiée dans des phyla non typiquement associés à la réduction des sulfates dans de nouvelles lignées de *Spirochaetota* et *Bacteroidota*. *Desulfuromusa* sp. hautement abondant et actif dans la réduction du soufre, a exprimé des ARN non codants associés à la régulation transcriptionnelle, montrant des preuves potentielles d'une flexibilité métabolique putative en réponse à la disponibilité du substrat. Malgré la faible disponibilité de l'oxygène, l'oxydation des sulfures était principalement attribuée aux *Halothiobacillaceae* chimiolithoautotrophes aérobiques. Dans les canaux d'écoulement de la source de Gypsum Hill, des films ou « streamer » microbiens saisonniers ont été formés par un nouveau *Thiomicrothabodus* sp. chimiolithoautotrophe oxydant le sulfure en soufre élémentaire. Le génome de *Thiomicrothabodus* sp. contient des adaptations au stress osmotique et au froid, y compris pour la production de substances polymères extracellulaires qui suggère de promouvoir la formation de films ou « streamer » et fournir une protection contre le stress au froid. Cette étude a permis d'identifier des communautés microbiennes actives, principalement chimiolithoautotrophes, dans des sources arctiques hypersalines et extrêmement froides, ce qui permet de mieux comprendre comment la vie microbienne se maintient dans la cryosphère terrestre et quels types de vie microbienne pourraient exister dans des environnements analogues sur Mars et d'autres cibles astrobiologiques.

Acknowledgements

Thank you to my supervisor, Dr. Lyle Whyte, for the opportunity to pursue a Ph.D. and for his advice and encouragement. Thank you to my supervisory committee members, Dr. Jennifer Ronholm and Dr. Sébastien Faucher, for their guidance. Thank you to my manuscript co-authors for their invaluable feedback: Dr. Ianina Altshuler, Dr. Miguel Á. Fernández-Martínez, Dr. Ya-Jou Chen, Dr. Catherine Maggiori, Dr. Jacqueline Goordial, Dr. Nadia Mykytczuk, Dr. Andre Pellerin, and Dr. Nastasia J. Freyria. I would especially like to thank Drs. Altshuler and Chen for their advice on sequencing library preparation and Dr. Freyria for help with ordinations.

Thank you to Dr. Catherine Maggiori, Scott Sugden, and Louis-Jacques Bourdages for sample collection in 2017 and 2022. Thank you to Andrew Golsztajn (Department of Chemical Engineering, McGill University) for assistance with TOC, TIC, and TN measurements. Thank you to the Bigelow Single Cell Genomics Center and The Centre for Applied Genomics (SickKids) for sequencing services and advice. Thank you to the Polar Continental Shelf Program and the PCSP staff and pilots for making Arctic field work possible. Thank you to Dr. Brian Driscoll, Dr. Sébastien Faucher, and Simone Clamann for their help with McGill and NRS administrative matters. Thank you to NSERC, FRQNT, the Northern Scientific Training Program, and McGill for funding to allow me to pursue this Ph.D.

Thank you to my fellow Whyte lab members for their invaluable advice and support: Ianina Altshuler, Isabelle Raymond-Bouchard, Miguel Á. Fernández-Martínez, Ya-Jou Chen, Nastasia Freyria, Mira Okshevsky, Madison Ellis, Esteban Góngora Bernoske, Evan Marcolefes, Olivia Blenner-Hassett, David Touchette, Brady O'Connor, Louis-Jacques Bourdages, Scott Sugden,

Antoine Lirette, Avery Albert, Christina Davis, Emma Righi, Melissa Kozey, and Scott Sugden.

I would especially like to thank the Whyte lab post-docs for everything they do. Thank you to Nastasia Freyria for help with French translations.

This thesis is dedicated to Arun, Nova, and Acci, my constant companions.

Contribution to Original Knowledge

This thesis contributes to the current knowledge of microbial life and metabolism in the cryosphere. Specifically:

1. In Chapter 2, I describe the first metatranscriptomic study of a unique sub-zero, hypersaline Arctic terrestrial methane seep. I characterized the functional gene content and expression in 106 bacterial and archaeal genomes, 103 of which were novel genomes. I report the coldest temperature detected for ANME-1 activity and describe the genome content and expression of novel ANME-1 species. I describe the gene content and expression for the first *Iainarchaeota* and QMSZ01 (DPANN archaea) and CG03 spp. detected in sub-zero and hypersaline environments.
2. In Chapter 3, I describe the first metagenomic and metatranscriptomic survey of a cold, hypersaline, sulfate-rich perennial Arctic spring. I characterized the functional gene content and expression in 57 bacterial and archaeal genomes, 55 of which were novel genomes. I describe the functional gene content and expression of novel *Halothiobacillus*, *Desulfurivibrionaceae*, and *Desulfuromusa* spp., and I report the first detection of *Spirochaetota* and *Kapabacteriales* sulfate reduction gene expression under cold and hypersaline conditions.
3. In Chapter 4, I describe and characterize the first metagenome-assembled genome from a novel *Thiomicrothabodus* sp. GH. I describe the first metatranscriptome and metaproteome from unique sulfide-oxidizing microbial streamers and report the first in situ characterization of gene and protein expression in *Thiomicrothabodus* sp. GH.

Contribution of Authors

1. In Chapter 2, I am the first author of the associated published paper. I performed and oversaw the overall experiment. I did the 2019 sample collection; completed the nucleic acid extractions; prepared and sent samples for HiSeq sequencing, SAG generation, and 16S rRNA sequencing; did metatranscriptome and SAG library preparation and MiSeq sequencing; and completed all of the data processing and analysis. I wrote and edited the manuscript. I. Altshuler provided guidance on nucleic acid extraction, library preparation, and sequencing and contributed to Figure 5. M.Á. Fernández-Martínez contributed to the manuscript introduction. C. Maggiori collected samples in 2017. L.G. Whyte conceived and oversaw the study and contributed to the manuscript. All authors provided guidance on the manuscript and data interpretation.
2. In Chapter 3, I am the first author of the associated manuscript. I performed and oversaw the overall experiment. I did the sample collection, nucleic acid extractions and sequencing library preparation; and completed the sequencing data processing and analyses. I wrote and edited the manuscript and prepared the majority of figures. I. Altshuler provided guidance on nucleic acid extraction, library preparation, and sequencing. N.J. Freyria ran the dissimilarity and clustering analyses and prepared Figures 6, S8, and S9. L.G. Whyte conceived and oversaw the study. N.J. Freyria and L.G. Whyte provided guidance on the manuscript and data interpretation.
3. In Chapter 4, I am the first author of the associated published paper. I annotated the metagenome, binned the metagenome, annotated the metagenome-assembled genome, did the comparisons to reference genomes, and did the data interpretation and analysis. I wrote the majority of the manuscript, edited the manuscript, and prepared the majority of the

figures and tables. N.C.S. Mykytczuk did the sample collection; the metagenome library preparation and assembly; the metatranscriptome library preparation and data processing; the metaproteome sample preparation and data processing; and contributed to the manuscript methods, introduction, and Figure 2. A. Pellerin did the S isotopic analysis, wrote the manuscript sections related to S isotopic analysis, and prepared Table 2 and Figure 5. S.M. Twine, S.J. Foote, and K. Fulton did the mass spectrometry. J. Goordial, B. Wing, and L.G. Whyte provided guidance on the manuscript. L.G. Whyte conceived and oversaw the study.

List of Figures and Tables

Table 4.1. Stress response genes in <i>Thiomicrohabdus</i> genomes.....	197
Table 4.2. Characteristics and isotopic compositions of streamers and sediments.	199
Figure 1.1.A. Don Juan Pond, Antarctica.	27
Figure 1.1.B. Lake Vida, Antarctica.....	27
Figure 1.1.C. Blood Falls, Antarctica.....	27
Figure 1.2. Summary of major inorganic sulfur cycling processes.	35
Figure 1.3. Summary of archaeal and bacterial methane cycling.....	42
Figure 1.4.A. An outflow pool and channel at Gypsum Hill Spring.....	52
Figure 1.4.B. The interior of the salt tufa at Lost Hammer Spring.	52
Figure 2.1.A. Comparison of metagenome taxonomic composition to MAG frequency by order.	83
Figure 2.1.B. Phylogenomic tree of high- and medium-quality MAGs and SAGs.....	83
Figure 2.1.C. Level of taxonomic novelty of the MAGs and SAGs by rank.....	83
Figure 2.2. Key metabolic genes expressed in the LH spring sediment.....	84
Figure 2.3. Metabolic potential and gene expression in high-quality MAGs and medium-quality SAGs.....	85
Figure 2.4. Percent relative expression by phylum, including both genes in MAGs and SAGs and unbinned genes classified by JGI.....	86
Figure 2.5. Metabolic reconstruction of ANME-1 SAGs.	87
Figure 2.6. Model for a hypothetical Martian methane cycle.	88
Figure 3.1.A. Relative abundance of orders in 16S rRNA gene amplicon sequencing and shotgun metagenomes and number of MAGs in each order.	137

Figure 3.1.B. Phylogenomic tree of the 57 high- and medium-quality MAGs.....	137
Figure 3.1.C. Level of taxonomic novelty of the MAGs.....	137
Figure 3.2. Metabolic gene relative expression and distribution of gene relative expression by phylum.....	138
Figure 3.3. Total relative expression (tpm) of MAGs and unbinned genes in phyla or classes >1% relative abundance.....	139
Figure 3.4. Pathway and gene presence in MAGs.....	140
Figure 3.5. Genome content of key sulfur cycling MAGs.....	141
Figure 3.6.A. Plot of canonical correspondence analysis (CCA) of 16S rRNA gene sequencing from GH and cold, saline, and sulfur-rich environments.....	142
Figure 3.6.B. Plot of canonical correspondence analysis (CCA) of 16S rRNA gene sequencing from GH and additional comparable environments.....	142
Figure 3.7. Model for a hypothetical sulfur cycling microbial community similar to the GH microbial community in a theoretical Martian environment such as sub-surface sulfate brines.....	144
Figure 4.1. Field photograph of the streamers in the GH springs.....	192
Figure 4.2. Phylogenetic classification of streamers from Gypsum Hill springs.....	193
Figure 4.3. Model of <i>Thiomicrothabodus</i> sp. GH partial genome cellular systems.....	194
Figure 4.4. Model of sulfur compounds in GH spring environment based on isotopic analysis.....	195
Figure 4.5.A. The measurements of multiple sulfur isotope as fractionations relative to the sulfate in the stream.....	196
Figure 4.5.B. The measurements of multiple sulfur isotope and a mixing model.....	196

List of Abbreviations

AAI: Amino Acid Identity

AHI: Axel Heiberg Island

ANI: Average Nucleotide Identity

ANME: Anaerobic methanotrophic archaea

AOM: Anaerobic oxidation of methane

ASV: Amplicon Sequence Variant

Bya: Billion years ago

CARD-FISH: Catalyzed Reporter Deposition – Fluorescence In Situ Hybridization

CBB: Calvin-Benson-Bassham cycle

CCA: Canonical Correspondence Analysis

cDNA: complementary DNA

CDS: Coding sequence

CO: Carbon monoxide

COG: Clusters of orthologous groups

CRS: Chromium Reducible Sulfur

DHAB: Deep Hypersaline Anoxic Basin

DIC: Dissolved Inorganic Carbon

DNA: Deoxyribonucleic acid

DPANN: Diapherotrites, Parvarchaeota, Aenigmarchaeota, Nanoarchaeota, Nanohaloarchaeota

emPAI: Exponentially Modified Protein Abundance Index

EPS: Exopolymeric substances, exopolysaccharides

FACS: Fluorescence-activated cell sorting

GH: Gypsum Hill Spring

GTDB: Genome Taxonomy Database

Gya: Billion years ago

JGI: Joint Genome Institute

LH: Lost Hammer Spring

MAG: Metagenome-assembled genome

MDA: Multiple displacement amplification

MMO: Methane monooxygenase

mRNA: messenger RNA

MS: Mass spectrometry

NMDS: Non-metric Multidimensional Scaling

NSR: NADPH elemental sulfur oxidoreductase

ORP: Oxidation-reduction potential

PCR: Polymerase chain reaction

RNA: Ribonucleic acid

rRNA: ribosomal RNA

RSL: Recurring slope lineae

rTCA: reverse Reductive Tricarboxylic Acid Cycle

SAG: Single-amplified genome

SRB: Sulfate-reducing bacteria

SOB: Sulfur-oxidizing bacteria

SR: Sulfate reduction

TOC: Total organic carbon

tpm: transcripts per million reads

tRNA: transfer RNA

WGA: Whole genome amplification

XRD: X-ray diffraction

Chapter 1. Introduction and Literature Review

1.1 Objectives of this thesis

The objectives of this thesis were to describe and characterize the active microbial community and the metabolisms sustaining microbial life in extreme cold saline springs in the Canadian High Arctic, in order to further our understanding of microbial life in the Earth's cryosphere and potential life on extraterrestrial worlds. The specific questions my research aimed to address were as follows:

1. What microorganisms are active under extreme salt and cold conditions?
2. What metabolisms sustain microbial life under extreme salt and cold conditions?
3. What adaptations and stress response mechanisms allow microbial life to grow under extreme cold and salt conditions?
4. What are the lower temperature limits of microbial life and what are the implications of active cryospheric life for the search for life on other worlds?

I applied these questions to studies of three cold saline spring environments, which are described in the following three chapters, using a combination of meta'omics methods including metagenomics, metatranscriptomics, and single cell genomics. In Chapter 2, I describe the active microbial community inhabiting Lost Hammer Spring, a sub-zero, hypersaline, and anoxic terrestrial methane seep. I assembled over 100 metagenome-assembled genomes and single-amplified genomes and characterized their metabolic pathways, stress response mechanisms, and gene expression through genome-resolved metagenomics and metatranscriptomics. In particular, I closely examined genomes of anaerobic methane-oxidizing archaea from the ANME-1 clade,

and genomes from uncultured candidate phyla including DPANN archaea and CG03 bacteria. I also utilized metatranscriptomics to investigate the nature of primary production in the spring and identify the active microbial community members.

In Chapter 3, I utilized genome-resolved metagenomics and metatranscriptomics to describe active sulfur cycling in sulfate-rich, cold, hypersaline, and anoxic Gypsum Hill Spring. Using this methodology, I identified the most active and abundant microorganisms contributing to sulfur cycling and described their metabolic functions and potential interactions. Additionally, I profiled the microbial community with 16S rRNA gene sequencing and compared the microbial community to those present in other cold, saline, or sulfur-rich environments in order to determine which factors are most important in shaping community structure in these environments.

In Chapter 4, I examine in detail a metagenome-assembled genome representing a novel *Thiomicrothabodus* sp. which seasonally forms microbial streamers in the outflow channels of Gypsum Hill spring. Using a combination of metagenomics, metatranscriptomics, and metaproteomics, I described its metabolic pathways, stress response capability, and potential mechanism of streamer formation. I also compared its stress response genes to those present in related *Thiomicrothabodus* spp. to identify potential unique adaptations to the spring environment.

In these chapters, I additionally discuss the implications of these results for potential habitability and search for life on other worlds such as Mars.

1.2 Introduction to the cryosphere and its microbial inhabitants

The cryosphere comprises the portion of Earth that experiences sub-zero or cold temperatures sufficient for water to freeze (1). It includes diverse environments including glacial and sub-glacial environments, permafrost, and sea ice. It comprises approximately one-fifth of the Earth's surface (1), in addition to the majority of Earth's biosphere which experiences continuously cold (<5°C) temperatures (2).

Microorganisms in these environments typically experience multiple stressors, including cold temperatures. Living microorganisms require liquid water, which in sub-zero cryoenvironments can require freezing point depression through high solute concentrations, e.g. brine veins in permafrost and ice (3, 4), or high pressure as in subglacial lakes (5). Other stressors can include oligotrophy, low water activity, and high UV irradiation (2).

Despite these challenges, the cryosphere contains microbial life which reproduces and is metabolically active, with bacterial respiration detected down to -33°C (6) and bacterial reproduction down to -15°C (7). Microorganisms in these environments are typically psychrophiles (optimal growth <15°C) or psychrotolerant (survival <0°C, optimal growth 20-25°C) (8), and often halophiles (>0.2 M salinity required for growth) or halotolerant (tolerate high salinity but do not require it) (9).

These microorganisms typically contain adaptations to cold and saline conditions. For psychrophilic and psychrotolerant microorganisms, these include adaptations to maintain enzyme

efficiency and cellular flexibility including: increased enzyme catalytic efficiency to overcome low kinetic energy; increased cellular concentrations of enzyme or substrate; increased membrane fluidity through methods such as desaturation of membrane lipid fatty acid chains; and increased protein flexibility to enable activity at low temperatures (10). For halophilic and halotolerant, microorganisms, these include mechanisms to maintain cellular osmotic pressure through increasing salt or solute concentration in the cytoplasm (11). Other effects on inhabitant microorganisms can include slowing of metabolism and reproduction rates due to cold (10) or oligotrophic conditions (12). The range of energetically-favorable metabolisms may also narrow in these environments due to the high energetic costs of osmotic stress response (9, 13).

Cryoenvironments are of particular interest in microbiology as analogues for extraterrestrial habitats, as potential sources for microorganisms and microbial products of use in biotechnology and medical sciences, and as a crucial habitat for study of biogeochemical cycling as the polar regions rapidly warm as a result of climate change (2). This review will focus on the microbial ecology of cold, hypersaline cryoenvironments analogous to extraterrestrial habitats, with a focus on sulfur and methane metabolisms, followed by a review of meta'omics methods for probing the active microbial communities in these environments. Finally, the environments discussed in this thesis will be introduced.

1.3 The microbial community in cold, hypersaline environments

Cold hypersaline brines are found in diverse environments including sea ice, glacial brines, hypersaline Antarctic lakes, and cryopegs. In these environments, cellular abundance can vary significantly from 10^5 cells/mL (sea ice) up to 10^8 cells/mL (cryopegs) (14). Overall, commonly

abundant bacterial phyla include *Bacteroidota* (formerly *Bacteroidetes*) and *Proteobacteria* (commonly *Gammaproteobacteria*), with variable archaeal and eukaryotic abundances (15). Much of the information about inhabitant microbial communities is derived from cultivation of isolates or 16S rRNA gene clone libraries; more recently, culture-independent methods utilizing next-generation sequencing of 16S rRNA gene amplicons and shotgun metagenomes have provided more in-depth pictures of these communities and their metabolic potential.

1.3.1 Antarctic hypersaline lakes

Antarctica hosts a number of hypersaline lake environments, ranging from brine pockets or hypersaline waters sealed under thick surface ice (16, 17) to highly saline lakes that remain perennially unfrozen despite sub-zero water and air temperatures (18). Temperature and salinity in these brines can be highly extreme, reaching to the known limits of metabolic activity, with temperatures down to -20°C and up to 32% salinity (18). More extreme conditions in places such as Don Juan Pond (-30°C, 40% salinity) are evidently prohibitive to even microbial life, with no successful measurements of metabolic activity thus far (19) (Figure 1.1A). In lakes with shallow or no ice coverage, photosynthetic phytoplankton and algae in upper waters act as primary producers, with deeper saline and less oxic waters dominated by bacteria (20, 21). For example, in Organic Lake (-14°C, 23% salinity), dimethylsulfoniopropionate (DMSP) produced by phytoplankton provides an energy and carbon source to dominant bacterial heterotrophs and mixotrophs in the *Bacteroidetes* (*Psychroflexus*) and *Gamma*- and *Alphaproteobacteria* (*Marinobacter*, *Roseovarius*) in the water column (21). Local physical and chemical parameters likely significantly impact inhabitant microbial communities in these lakes; comparison within and between lakes identified increasing abundance of halophilic *Gammaproteobacteria*

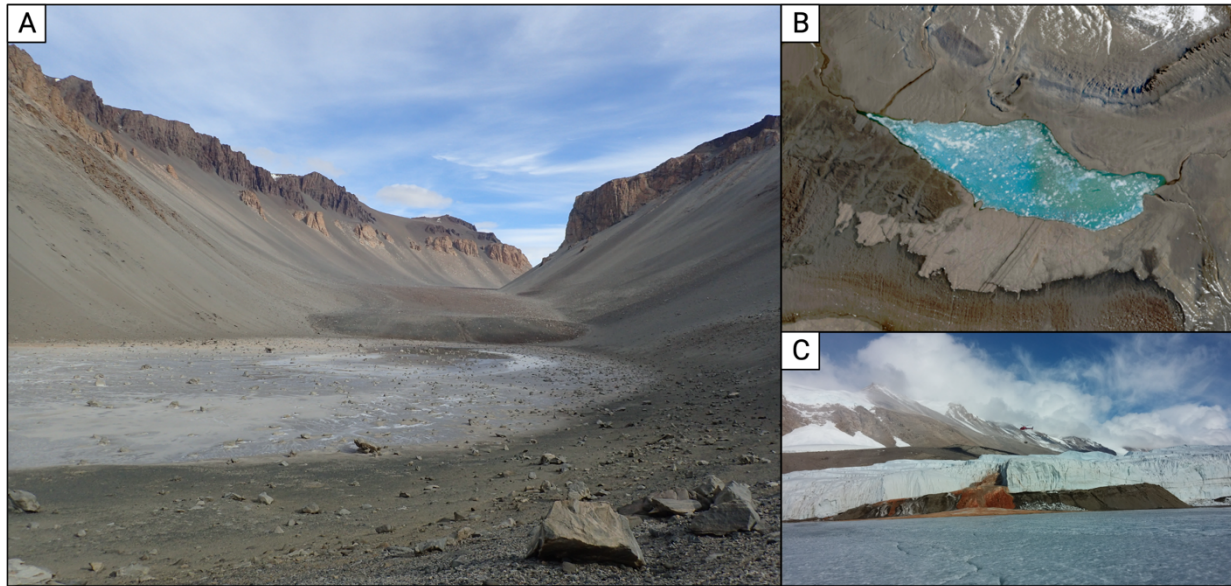


Figure 1.1. A. Don Juan Pond, Antarctica (22). B. Lake Vida, Antarctica (23). C. Blood Falls, Antarctica (24).

(*Marinobacter*, *Halomonas*) with increasing salinity across lake chemoclines (20), and lower bacterial diversity in more saline sediments (18). More divergent communities have also been identified, e.g. in the highly saline Deep Lake (oxic, -20°C , 32% salinity) where primary producing green alga support dominant carbohydrate-degrading haloarchaea rather than bacteria (18, 25).

By contrast, waters and brine pockets in lakes with thick ice coverage are aphotic and putatively chemosynthetic (16, 17, 26), as in Lake Vida (-13°C , 20% salinity), where 16S cDNA sequencing of putatively active microorganisms identified primarily *Gammaproteobacteria* (*Psychrobacter*, *Marinobacter*) and potentially hydrogen-oxidizing *Epsilonproteobacteria* (*Sulfurovum*), as well as fermentative *Firmicutes* and *Sphaerochaeta* (26) (Figure 1.1B). Other aphotic Antarctic environments include sub- and englacial brines (27), the best-studied of which are located at Blood Falls, Antarctica (Figure 1.1C). The brines at Blood Falls (8% salinity) are

sulfate- and iron-rich, and host a predominantly bacterial microbial community containing dominant sulfur and iron cycling *Gammaproteobacteria* (*Thiomicrospira*) and *Deltaproteobacteria* (*Geopsychrobacter*, *Desulfocapsa*) (28, 29). This community is proposed to engage in coupled sulfur-iron cycling, in which organic C is oxidized with Fe(III) as the terminal electron acceptor with intermediary sulfate reduction and subsequent re-oxidation, as a result of low organic C in the absence of photosynthetic production (30).

1.3.2 Cryopegs

Cryopegs are lenses of hypersaline, sub-zero brines within stable permafrost formed from freezing of ancient marine sediments (31). Most studies to date have examined Arctic cryopegs, which range from approximately 3 to 300 meters belowground (32), -11°C – -6°C (15, 31), and 15–20% salinity (31). Cryopegs are highly isolated and undisturbed environments which experience little to no seasonal variation (15, 31) and contain relatively high cellular abundances (10^8 cells/mL) (14, 33) of highly adapted psychrophilic/psychrotolerant and halophilic/halotolerant microorganisms (15, 31, 32). Cryopeg brines contain ample labile organic C, supporting predominantly heterotrophic microbial communities (up to 10^7 cells/mL aerobic heterotrophs) (33), with cellular abundances indicating brines near carrying capacity without nutrient limitation (15). Sequencing of Arctic cryopeg brines identified primarily *Bacteroidetes* and *Gammaproteobacteria*, with dominance of *Marinobacter* sp. (<~70% relative abundance) (14, 15). *Marinobacter* spp. are *Gammaproteobacteria* ubiquitous in cold saline environments; they are highly metabolically flexible, utilizing a range of organic compounds as well as (in some cases) chemolithoautotrophic metabolisms, in addition to being psychro- and halo-tolerant and facultatively aerobic, making them highly successful across many cold and saline

environments (15). Some Arctic cryopegs are also sulfate-rich and can contain low to moderate abundances of sulfate-reducing bacteria (*Deltaproteobacteria*) (10^2 - 10^6 cells/mL), as well as low abundances of methanogenic archaea (10^1 cells/mL) (33).

1.3.3 Sea ice

In contrast to the relatively stable brines in cryopegs, glaciers, and Antarctic lakes, sea ice contains brines that can experience significant seasonal, diurnal, and weather-induced variability (15). These brines form during ice formation through concentration of marine salts and dissolved matter into brine channels and pockets, which form networks along which nutritional, temperature, and salinity gradients can occur, as well as nutrient exchange with seawater (15). Temperature can range from -1°C to -50°C (34) and salinity from 3.8% to 15% (35). Microbial abundances are relatively low (10^5 cells/mL) (14, 15), but high proportions of transcriptionally active cells (<86%) have been detected in sea ice brines down to -20°C (35). Phytoplankton are the dominant primary producers in sea ice, fostering a predominantly heterotrophic bacterial community distinct from marine populations (34) that experiences seasonal succession due to winter darkness. During early winter periods of low productivity, oligotrophic *Alphaproteobacteria* (*Octadecabacter*, *Loktanella*) are dominant; in late winter, cold-adapted *Bacteroidetes* (*Polaribacter*) dominate; and finally, during late spring and summer, light-induced algal productivity fuels copiotrophic *Gammaproteobacteria* (*Paraglaciecola*, *Colwellia*, *Glaciecola*) that utilize algal carbon and EPS derived from *Bacteroidetes* during winter, as well as potentially supplementing with phototrophy (14, 36). Thus, substrate availability is a major driver of microbial community in these brines (36).

In direct comparisons of microbial community composition between cryopegs and sea ice, low temperature and high salinity were sufficient to explain selection at the class level (e.g. similarly high abundances of *Gammaproteobacteria* and *Bacteroidia* in both cryopegs and sea ice brines), with significant differences apparent at the genus level (e.g. highly adapted dominant cryopeg members (*Marinobacter*) vs. greater diversity in sea ice) as a result of local selective pressures such as physical fluctuation and C and N availability (15). Similar patterns can be observed in the cold briny environments reviewed herein, where members of the *Bacteroidota* and *Proteobacteria* phyla are typically abundant (with notable exceptions such as Deep Lake). Cosmopolitan and highly metabolically flexible genera such as *Marinobacter* occupy a diversity of environments. Local physical and chemical parameters including temperature, salinity, nutrient availability, environmental disturbance, and seasonal cycling can significantly impact community abundance at the class level or below, as well as the composition of less-abundant phyla. Modes of primary production in these environments include both photo- and chemosynthesis and also influence community structure, e.g. sea ice dominated by bacterial heterotrophs vs. chemolithoautotrophic iron and sulfur cycling in subglacial brines of Blood Falls.

1.4 Hypersaline cryoenvironments as astrobiology analogues

Astrobiology refers to the study and search for life on extraterrestrial worlds. While no life has yet been discovered on other worlds, conditions that may support life as we know it have been identified in the past and present of extraterrestrial bodies in our solar system and beyond. These conditions for habitability of life as we know it include 1) the presence of water; 2) the presence

of required elements (carbon, hydrogen, nitrogen, oxygen, phosphorus, sulfur, and transition metals); and 3) biologically accessible energy sources (37).

1.4.1 Mars

Mars is considered one of the most promising candidates for extant or past life based on these criteria as well as its accessibility for life detection missions (38). Martian surface features and geological evidence indicate that water features were widespread on Mars during the Noachian and Hesperian periods 3-4 Ga, including springs, crater lakes, and outflow channels (39, 40). As Mars became permanently colder and drier during the late Noachian (~3.7 Ga) (41), its last surface waters would likely have been cold brines. The locations of chloride salt deposits on the Martian surface suggest that small volumes of saline surface waters were present as recently as 2.3 Ga (42). Low atmospheric pressure and freezing temperatures on present-day Mars are prohibitive to standing surface waters, but potential water sources are present in the subsurface. The recurring slope lineae are transient streaks formed on Martian slopes, and are suggested to form from flowing of hydrated salts formed through deliquescence (43) or instability and collapse of surface soils due to gypsum-chloride reactions in thin subsurface brine layers (44). Potential hypersaline lakes were also detected below Mars' southern ice cap (45, 46). Water ice is also present at the polar regions and within high altitude regolith, with conditions overlapping with habitable Earth conditions (47).

A number of potential energy sources are present in the Martian surface and subsurface. Mars is sulfur-rich, with abundant Mg- and Ca-sulfate salts in the surface and subsurface (48). Iron and manganese oxides and perchlorates in the Martian regolith could also act as anaerobic electron

acceptors (38). O₂ is present in nanomolar concentrations in the Martian atmosphere (49), which could support some level of aerobic metabolism as in nanoxic regions on Earth (50). Near-surface brines could also concentrate dissolved O₂, bringing concentrations up to micro-oxic conditions (51).

With abundant CO₂ in the atmosphere (96%) (49), much of Martian habitability has focused on potential chemolithoautotrophic life. However, detection of organic carbon (>50 nM) in lacustrine mudstones in Gale Crater has also raised the possibility of past or present heterotrophy (52). Additionally, trace methane has been detected in the Martian atmosphere (~0.4 ppbv) (53), suggesting the potential for biogeochemical methane cycling on Mars. Serpentinization, which produces H₂ and (under some conditions) methane as a byproduct of water-rock interactions in mafic and ultramafic rocks, may occur in the Martian subsurface (54, 55). The resulting H₂ could be utilized as a potential electron donor for methanogenesis, as well as for chemolithoautotrophic metabolisms such as sulfate reduction, and abiotic or biotic methane could be utilized by methanotrophic microorganisms.

1.4.2 Europa and Enceladus

The icy moons of Europa and Enceladus are two additional primary candidates for life detection in our solar system due to their potential habitability. Jupiter's moon Europa has a liquid ocean covered by an icy crust (56). This liquid ocean is predicted to overlay a rocky ocean floor, as on Earth, with the potential for rock-water interactions such as serpentinization forming energy and carbon sources for chemolithoautotrophic life or for features geochemically favorable for microbial life such as hydrothermal vents (57). Europa's ocean waters are predicted to be cold,

highly saline, and experience high pressure, but within the known limits of life, and elemental sulfur, sulfate, carbon dioxide, and oxygen have been observed on the European surface indicating available energy and carbon for chemolithoautotrophic life (57).

Saturn's moon Enceladus also contains a liquid ocean underneath an icy crust (58). Plumes of ocean water and ice erupting through the crust contain compounds including CO₂, CO or N₂, ammonia, and organic carbon compounds such as methane and propane (59), indicating that Enceladus' ocean contains the potential chemistry to support life. Silica particles identified in the plumes also indicate the presence of high-temperature (>90°C) hydrothermal rock-water reactions, and likely convection or plumes of warm hydrothermal fluids into the ocean (60). The presence of these reactions also constrains ocean salinity (<4%) and pH (8.5-10.5) to well within the known limits of microbial habitability (60), indicating that Enceladus' ocean contains conditions favorable to the presence or development of life.

1.4.3 Analogue environments on Earth

Analogue environments on Earth, or environments that approximate the environmental conditions present in putative habitats on extraterrestrial worlds, are used to study and constrain the known limits and conditions for habitability and biosignature detection on other worlds. Due to the predicted hypersalinity and low temperature of most potential liquid water sources on Mars and in the oceans or ice crusts of Europe and Enceladus, cold briny environments such as cryopegs, hypersaline Antarctic lakes, and ice brine veins are some of the closest terrestrial analogues to putative extraterrestrial habitats (57). The microbial communities inhabiting these environments have been studied in this context to identify putatively habitable environments,

such as ultrathin brine veins in European ice crusts (57), and determine the nutrient sources, energy requirements, and energetic pathways necessary for sustaining microbial life under polyextreme conditions (16, 26, 29). Cultured bacteria from these environments have probed the lower temperature limits of life: microbial respiration in isolates from glacial ice identified metabolism occurring at -33°C (6). Additionally, the absence of life in brines of Don Juan Pond due to extreme temperature and salinity (-36°C , 40% salinity) constrains the boundary conditions for life as we know it (19, 61). Terrestrial cryosphere analogues such as cold saline springs have also been used to interpret geomorphological and geochemical features observed on extraterrestrial bodies, such as identifying potential fluvial features such as springs and lakes on ancient Mars (62) and determining the composition of salts on the European ice crust (63).

1.5 Sulfur and methane cycling in the cryoenvironment

Sulfur and methane cycling are two possible mechanisms by which microorganisms could be supported on extraterrestrial bodies such as Mars. Here I will briefly review these cycles and discuss their relevance to cryoenvironments on Earth.

1.5.1 Sulfur cycling

The range of sulfur oxidation states from sulfate (SO_4^{2-} , +6) to sulfide (H_2S , -2) is utilized by sulfur cycling microorganisms in energy-generating dissimilatory redox reactions (64) (Figure 1.2). Oxidized sulfur (sulfate) is utilized as an electron acceptor in anaerobic respiration, while reduced sulfur (sulfide) can be utilized as an electron donor in aerobic, anaerobic, or phototrophic metabolisms; intermediate sulfur species (i.e. thiosulfate, elemental sulfur, sulfite) can be oxidized, reduced, or disproportionated (64-66). These processes are major drivers of

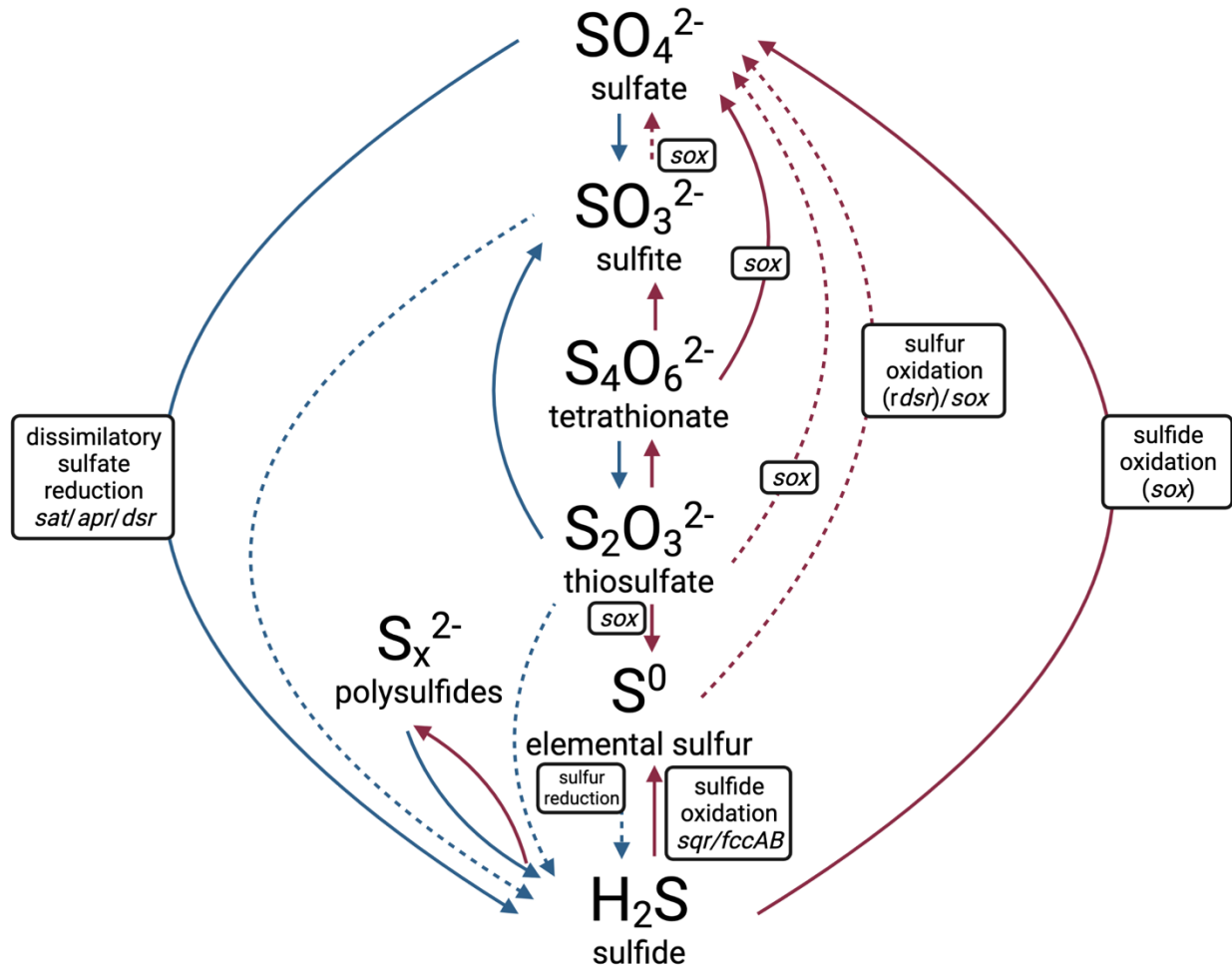


Figure 1.2. Summary of major inorganic sulfur cycling processes discussed in this literature review. Blue lines indicate reductive processes; red lines indicate oxidative processes; dashed lines indicate processes also involved in disproportionation reactions. Genes involved in these processes are indicated in boxes in italics. Adapted from Jorgensen et al. (67). Created with BioRender.com.

bacterial and archaeal metabolism in sulfur-rich ecosystems, including marine waters (68) and sediments (69), hydrothermal vents (70), continental subsurface fluids (71), and sulfidic springs (72).

Sulfate reduction is a major global process, particularly in the sulfate-rich oceans where sulfate-reducing bacteria couple sulfate reduction with up to 30% of global organic carbon

mineralization to the seafloor (73) and up to 50% of anaerobic mineralization in freshwater wetlands (74). The canonical pathway for dissimilatory sulfate reduction to sulfide proceeds via reduction of sulfate to sulfite with sulfate adenylyltransferase (Sat) and adenylyl-sulfate reduction (*aprBA*), followed by sulfite reduction to sulfide (*dsrAB*) (75), typically coupled with oxidation of fermentation products like hydrogen and acetate or carbon compounds including fatty acids, sugars, and amino acids (66). Sulfate-reducing bacteria and archaea (collectively referred to as SRBs) have been cultivated in the *Desulfobacterota* (*Deltaproteobacteria*), *Nitrospirae*, *Firmicutes*, and *Thermodesulfobacteria* bacterial phyla and *Euryarchaeota* and *Crenarchaeota* archaeal phyla (76), and genetic capacity for sulfate reduction has been identified in many additional phyla (75). SRBs may be heterotrophic, autotrophic, or facultatively autotrophic (77), and can commonly also ferment organic carbon to acetate or hydrogen under low sulfate (78). Sulfate reduction is a form of anaerobic respiration, and due to thermodynamic considerations it is limited to environments where oxygen and other more energetically favorable electron acceptors are limited (67); however, many SRBs contain mechanisms to cope with low concentrations or brief exposures to oxygen (79), or may even switch to aerobic respiration (80).

In addition to sulfate, other sulfur intermediates (i.e. elemental sulfur, thiosulfate, tetrathionate) produced by sulfide oxidation reactions or abiotic reactions with sulfide can also be reduced (67). Many of these reactions are more energetically favorable than sulfate reduction and may be preferentially utilized by SRBs, which can typically reduce at minimum thiosulfate and sulfide in addition to sulfate (79), as well as utilized by a diversity of bacteria and archaea that exclusively reduce S intermediates (81, 82). Due to this energetic favorability causing rapid turnover, as well as abiotic reactivity, these intermediates are often detectable only in low concentrations in the

environment (83, 84). Of the intermediates, elemental sulfur is most commonly detected at higher concentrations, due to its relative stability and nonreactivity (67). It is produced from incomplete biotic or abiotic oxidation of sulfide as well as abiotically in volcanic gases (85). Sulfur reducing bacteria and archaea are generally distinct from SRBs (i.e. few SRBs are also able to reduce sulfur), and don't form phylogenetically distinct groups (79): sulfur reducers are found in bacterial phyla including *Desulfobacterota* (*Deltaproteobacteria*), *Campylobacterota* (*Epsilonproteobacteria*), *Aquificiae*, *Firmicutes*, *Thermotogota* (*Thermotogae*), and *Gammaproteobacteria*, and in the archaeal phyla *Euryarchaeota* and *Crenarchaeota* (82). The exact mechanism for sulfur reduction has not been identified in all sulfur reducers, but two distinct mechanisms have been identified to date via a membrane-bound polysulfide reductase PsrABC (studied in the bacterium *Wollinella succinogenes*), and via an NAD(P)H elemental sulfur oxidoreductase (identified in the archaeon *Pyrococcus furiosus*) (85).

Some oxidized sulfur intermediates (elemental sulfur, thiosulfate, sulfite) can also be disproportionated, or utilized as both the electron donor and acceptor with both hydrogen sulfide and sulfate as end products (65). The capacity for thiosulfate and sulfite disproportionation is common among cultivated *Desulfobacterota* SRBs, although not always coupled with growth (65), and has also been identified in *Firmicutes*. Elemental sulfur disproportionators have been identified within *Desulfobacterota*, *Gammaproteobacteria*, and *Firmicutes* (86, 87). Significant proportions of thiosulfate are disproportionated in marine sediments (up to 66% in oxidized sediments) (86), and elemental sulfur disproportionation has also been observed (88). The mechanisms for sulfur intermediate disproportionation have yet to be fully elucidated, but may

utilize the existing sulfate reduction pathway (65); thus, disproportionation capability cannot yet be predicted exclusively from genomic information.

The oxidation of sulfide and intermediate sulfur species provides energy to microbial life in diverse habitats, and chemolithoautotrophic and photoautotrophic sulfur-oxidizing bacteria are major contributors to primary production in environments including marine and lake waters and sediments (69, 89, 90), hydrothermal vents (91), and hot springs (92). S oxidation can be coupled with both anaerobic and aerobic metabolism, and it is present in taxonomically diverse bacteria and archaea including lithoautotrophs, phototrophs, heterotrophs, and mixotrophs (64, 93, 94). There are a diversity of S oxidation enzymes and pathways, with multiple oxidation mechanisms for most S species; species-dependent differences in mechanisms; and concurrence of oxidation mechanisms within microorganisms (64).

One major mechanism by which S oxidation occurs in bacteria is via the Sox multienzyme complex, which can oxidize thiosulfate, sulfite, sulfide, elemental sulfur, and tetrathionate completely to sulfate (95). Sox genes are present in a diversity of bacterial phyla including *Proteobacteria*, *Aquificae*, *Deinococcus-Thermus*, *Chlorobi*, and *Spirochaeta* (95, 96).

Alternatively, in some chemo- and phototrophs missing the SoxCD genes as well as in microorganisms with complete complexes under low pH (97), oxidation with the Sox enzyme proceeds only to elemental sulfur, which can then accumulate intra- or extra-cellularly (95). The elemental sulfur can be oxidized to sulfate when needed by Dsr proteins, typically involved in sulfate reduction, acting in reverse (98). This mechanism is found in the green sulfur bacteria (*Chlorobi*) and purple sulfur bacteria (*Chromatiaceae* and *Ectothiorhodospiraceae* in

Gammaproteobacteria), which utilize sulfur as an electron donor during anaerobic anoxygenic photosynthesis (95). Reverse Dsr proteins have also been identified in *Alphaproteobacteria*, *Betaproteobacteria*, *Deltaproteobacteria*, *Nitrospirae*, *Nitrospinae*, and *Candidatus* *Muproteobacteria* (75), which may utilize the Sox enzyme or other sulfide oxidizing enzymes such as *sqr* or *fccAB* for initial oxidation to sulfur. Additionally, archaeal sulfur oxidizers are found in the *Crenarchaeota* and *Euryarchaeota* and include many thermophiles inhabiting volcanic hot springs and hydrothermal vents (99). Elemental sulfur oxidation is a major process for these archaea, which utilize sulfur oxygenase reductase to aerobically disproportionate elemental sulfur to sulfide, sulfite, and thiosulfate as the first step in oxidation to sulfate (100).

Sulfur cycling contributes to microbial metabolism in many cold, hypersaline, and oxygen-limited environments. As previously noted, sulfate-rich hypersaline subglacial brines in Blood Falls support sulfate-reducing *Deltaproteobacteria* and sulfur-oxidizing *Gammaproteobacteria*, which act as primary producers and ultimately couple organic carbon oxidation to terminal iron (II) reduction (28, 30). Sulfur cycling bacteria are also found in cryopegs (33) and sub-zero Antarctic lake brines (16, 17, 21, 26). Supraglacial and thermal Arctic cold springs in the Canadian High Arctic and Svalbard (0 – 13°C) are supported by chemolithoautotrophic sulfur-oxidizing *Epsilonproteobacteria* (*Sulfurovum*, *Sulfuricurvum*) and *Gammaproteobacteria* (*Thiotrix*) (101-103). As in temperate marine sediments, sulfate-reducing *Deltaproteobacteria* (*Desulfobacteraceae*, *Desulfobulbaceae*) and sulfide-oxidizing *Epsilonproteobacteria* (*Arcobacter*, *Sulfurimonas*, *Sulfurovum*), *Gammaproteobacteria* (*Cocleimonas*), and *Betaproteobacteria* (*Thiobacillus*) contribute to carbon and sulfur cycling in cold Arctic marine sediments (-2°C - 3°C) (104) and exhibit psychrophilic adaptations (105). Halophilic and

halotolerant sulfate-reducing bacteria (*Desulfovibrionales*, *Desulfobacteraceae*) have also been detected in extremely hypersaline soda lakes (<50% salinity) (106) and sulfate-rich lakes (37% salinity) (107). Sulfur cycling also drives energy generation and primary production in marine deep hypersaline anoxic basins (<27% salinity), where sulfate is the most abundant electron acceptor, including by sulfate-reducing *Deltaproteobacteria* (*Desulfobacteraceae*, *Desulfobulbaceae*, *Desulfohalobiaceae*), sulfur-oxidizing *Epsilonproteobacteria* (*Arcobacter*, *Sulfurovum*, *Sulfurimonas*, CT1) and *Gammaproteobacteria* (*Halothiobacillus*), and putatively sulfur cycling *Crenarchaeota* (108, 109). Sulfur cycling is also important in other oxygen-limited marine environments including oxygen-minimum zones and anoxic marine zones, where sulfide-oxidizing *Gammaproteobacteria* (SUP05, EOSA-II) couple S oxidation with N reduction (110, 111).

1.5.2 Methane cycling

Microbial methane metabolism has a major impact on global carbon cycling and occurs commonly in anaerobic environments including in cryospheric permafrost, polar lakes, and cold marine sediments (112, 113). Archaeal methanogens reduce C1 and C2 compounds to methane and are responsible for half of all methane produced per year (114). All known methanogens are archaeal and primarily belong to specialized orders in *Euryarchaeota*; more recently, metagenomic analyses have also identified methanogens in other archaeal phyla including *Ca. Thermoplasmatota* and *Ca. Verstraetearchaeota* (114). Methanogenesis is a strictly anaerobic process and occurs in regions where more energetically favorable electron acceptors (oxygen, nitrate, sulfate, iron) have been depleted. In these locations, methanogens utilize fermentation products including H₂, CO₂, acetate, and methylated compounds for methanogenesis (114)

(Figure 1.3). The key enzyme in methanogenesis is methyl coenzyme-M reductase (Mcr), which catalyzes the terminal step for methane production in all known methanogens and is commonly used as a marker gene for this activity (114). In addition to cryospheric environments such as permafrost (115), methanogens are also found in extreme cold and/or hypersaline anaerobic environments where methanogenesis may be favorable including cryopegs (15, 31), Antarctic lake brine pockets (16, 17), and deep hypersaline anoxic basins (108).

Methane-consuming microorganisms, or methanotrophs, are found in both bacterial and archaeal phyla and attenuate a major fraction of the methane produced by methanogens (up to 90% in marine sediments) (115). Archaeal methanotrophs (referred to as anaerobic methanotrophic archaea, or ANME) belong to clades (ANME-1, ANME-2, and ANME-3) in the *Methanosarcinales* and *Ca. Methanophagales* orders of *Euryarchaeota* and oxidize methane anaerobically through a reversal of the methanogenesis pathway (Anaerobic Oxidation of Methane, or AOM). AOM is most commonly observed in syntrophic consortia of ANME with sulfate-, iron-, or manganese-reducing bacteria, where methane oxidation by ANME is coupled to reduction by the bacterial partner (116). Decoupled AOM has also been observed in nitrate-, iron-, and manganese-reducing ANME in the ANME-2 clade (117-119). AOM and ANME have been identified in a variety of extreme environments, including hypersaline Gulf of Mexico brine pools (120), a Dead Sea aquifer (121), mud volcano cold seeps (122), and near- or sub-zero Arctic environments including marine cold seeps and submarine permafrost down to -2°C (113, 123). These environments are typically occupied by the ANME-1 clade, which evidently possess higher halotolerance than other ANME clades potentially due to adaptations including low membrane permeability and compatible solute production (122).

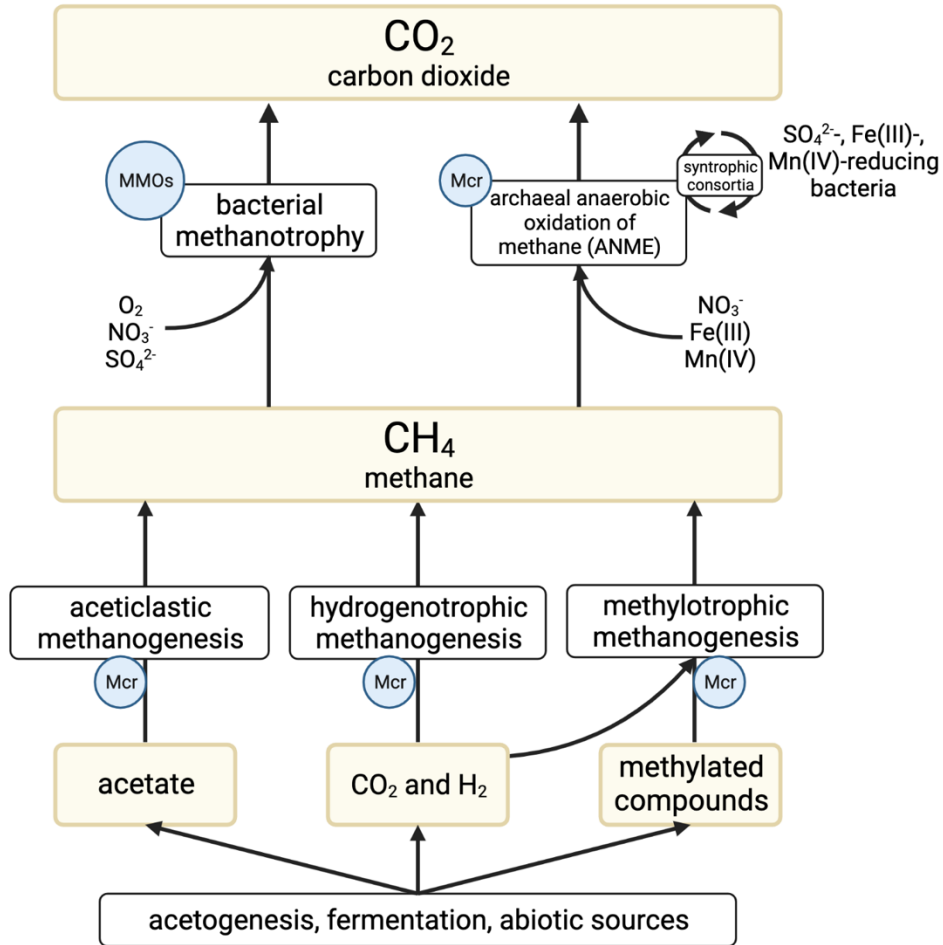


Figure 1.3. Summary of archaeal and bacterial methane cycling processes. Key enzymes are indicated in blue; major processes are indicated in white boxes; major substrates and products are indicated in yellow. Some of the electron acceptors utilized by methanotrophs are additionally indicated with arrows. Adapted from Evans et al. (114). Figure created with BioRender.com.

Methanotrophic bacteria utilize methane diffusing from anaerobic zones in seeps produced by methanogens as well as consume atmospheric methane (124). Bacterial methanotrophs belong to clades in *Gammaproteobacteria* (*Methylococcaceae*), *Alphaproteobacteria* (*Methylocystaceae*), NC10, *Verrucomicrobiota*, and *Chloroflexota* (124-127). They are most commonly aerobic, though some can also couple methane oxidation with nitrate or sulfate reduction (126, 128, 129). The key enzymes in bacterial methanotrophy are methane monooxygenases (MMOs), which catalyze the initial oxidation of methane. Virtually all methanotrophs possess a particulate,

membrane-bound MMO (*pmoABC*), and some additionally possess a soluble MMO encoded by the *mmo* genes (112). Bacterial methanotrophs are widespread in Arctic permafrost and tundra environments, and psychrophilic and halophilic methanotrophs have been isolated from ice-covered and meromictic Antarctic lakes, hypersaline lakes, and permafrost (112, 130).

1.6 Utilizing meta'omics in microbial community characterization

Historically, studies characterizing microbial communities in the environment relied on isolation and cultivation of inhabitant bacteria and archaea in 'culture-dependent' methods. More recently, 'culture-independent' approaches have revolutionized the field of microbial ecology and become standard in community characterization. The principle and utility of these approaches in characterizing environmental microbiomes will be briefly reviewed here, with a particular focus on the meta'omics methods utilized in this study.

1.6.1 Conventional approaches for characterization of microbial communities

Traditional approaches to microbial community characterization rely on culturing-based methods, in which microbial strains are isolated or enriched from the environmental medium and grown in pure or co-cultures in the laboratory. Culturing of microbial isolates enables extensive characterization of their physiological traits and capabilities, and as such it remains a fundamentally important approach (131). Studies utilizing culture-based methods to probe environmental microbiomes may screen isolates for genes or metabolisms of ecological relevance (132, 31), identify adaptations to environmental conditions (133), or examine physiological responses to varying growth conditions (134). However, culture-based methods are limited to ex situ analyses, and may not necessarily reflect the in situ capabilities and activities of

isolated microorganisms. Additionally, only an estimated <1% of microbial diversity is currently culturable through standard methodologies (135) due to factors including inability to mimic physicochemical conditions in the laboratory; inability to identify required substrates and growth conditions; and obligatory symbiosis or syntrophy (133). The majority of microbial abundance in non-human-associated environments belongs to unculturable taxa (136), including in extreme environments like hypersaline lakes, permafrost, and glacial ice (137).

The development of ‘culture-independent’ methods to profile microbial communities, such as through amplification and sequencing of phylogenetic marker genes (primarily the 16S ribosomal RNA gene), enabled the identification of a wide diversity of previously-unknown microorganisms (135). Sequencing of 16S rRNA marker genes remains a standard method in characterizing environmental microbial communities (137). However, 16S rRNA gene profiling is generally limited to describing community taxonomic diversity; inference of the functional potential and ecological role of identified taxa often relies on previous characterizations of related cultivated microorganisms or reference genomes (138). The usefulness of these comparisons can be particularly limited for poorly-studied or extreme environments where many taxa are not closely related to previously cultivated or sequenced microorganisms, e.g. Antarctic environments (138). Other methods used in combination with profiling of 16S rRNA or other marker genes, such as fluorescence in situ hybridization or activity assays such as DNA-stable isotope probing, can help link detected diversity and function (139, 140).

1.6.2 Metagenomic sequencing

‘Meta-omics’ approaches such as metagenomics aim to sequence the entirety of the genetic material present in a sample, allowing both taxonomic and functional profiling of microbial communities. The development of affordable next-generation, high throughput sequencing technologies, which enable rapid and massively parallel sequencing of nucleic acids, made metagenomics approaches feasible for widespread sequencing of complex environmental samples (141). Genome sequencing refers to the DNA sequencing of an individual genome; by contrast, metagenomic sequencing refers to the sequencing of all DNA present in a complex sample, i.e. many genomes. This approach is also referred to as ‘shotgun’ metagenomics, which describes the untargeted sequencing of nucleic acids without prior selection of genomic regions as in methods such as 16S rRNA gene sequencing (142). In a typical environmental metagenomics workflow, total DNA is extracted from an environmental sample, a sequencing library is prepared using the extracted DNA, and the metagenome is sequenced (142). Common next-generation sequencing technologies (e.g. Illumina) produce many short sequencing reads (100-300 base pairs). These short reads may be analyzed as-is, but are most often computationally reconstructed into longer contiguous sequences (‘contigs’) that are collectively referred to as a metagenome assembly (141). The metagenome may then be used for taxonomic profiling through read or marker gene classification. Additionally, gene coding regions (CDS) in the assembly can be identified and taxonomically and functionally annotated by comparison to gene databases (142). Metagenome sequencing therefore allows for both taxonomic and functional characterization of complex microbial communities, without prior selection of genes or microorganisms of interest. The reconstruction of long contigs also enables analysis of gene clusters and linkage of co-occurring genes (141).

Metagenomic analysis has been widely applied in diverse environments: it has been used to characterize pathways of carbon and sulfur cycling along salinity and oxygen gradients in Antarctica's Deep Lake (21) and identify the influence of environmental parameters on microbial community structure, function, and adaptations in Arctic sea ice and cryopegs (14, 143) and Antarctic permafrost (144). However, metagenome sequencing may not capture less abundant taxa or genomic regions due to incomplete assembly or sequencing. Additionally, accurate classification and functional prediction is reliant on incomplete reference databases, which can result in inaccurate annotations and unclassified genes (142).

Metagenome analysis is also limited by the fragmented nature of assemblies, which limits characterization of individual genomes within a complex sample (142). To overcome this limitation, metagenome assemblies can be 'binned' in a process by which contigs are clustered into groups representing a single microorganism or genome. These binned contigs are referred to as 'metagenome-assembled genomes', or MAGs. In *de novo* MAG construction (i.e. binning without reference genomes or databases), contigs are grouped based on shared features including read coverage and nucleotide composition (145). The resulting MAGs can be analyzed as single genomes, allowing characterization of the functional potential, adaptations, and interactions of microorganisms in a complex sample. Extensive taxonomic and genomic diversity has been uncovered through MAG assembly (146, 147), including taxa undetected by 16S rRNA gene surveys due to sequencing primer bias or large gene introns (148). It has been used to characterize microbial adaptations, genomic diversity, and metabolic potential in environments including glacial streams (149), Arctic seawater (150) and lake sediments (151), and hypersaline lakes (152).

Because MAGs are assembled from metagenomes, their quality relies in turn on the quality of sequencing and metagenomic assembly (153). Due to incomplete sequencing, assembly, and binning, MAGs rarely represent complete genomes. They also commonly contain ‘contamination’ from incorrectly binned contigs originating from other microorganisms, which can confound genomic analysis. For these reasons, standards have been established for acceptable completeness and contamination of reported MAGs (154). Additionally, due to the presence of closely-related strains that cannot be distinguished by binning algorithms, MAGs often represent populations of closely-related genomes (‘population genomes’) rather than individual genomes (153), limiting their usage in analysis of strain-level heterogeneity (155). Closely-related strains can also inhibit accurate binning and result in high intraspecies bin contamination; this in combination with incomplete metagenomic assembly and limitations of binning methodologies can result in a lack of MAG recovery for both abundant and rare taxa in an environment (153). This can be especially pronounced for certain groups such as halophiles, which contain high intraspecies diversity and genomic adaptations (high GC content) that reduce unique genomic sequences (156).

1.6.3 Single-cell genomics

While not strictly a meta’omics method, single-cell genomics provides another approach for culture-independent genome sequencing. In this method, individual cells are isolated from a sample, most commonly by fluorescence-activated cell sorting, in which cells stained with a fluorescent dye are separated into individual wells with a cell sorter based on fluorescence and particle size (157). DNA from each cell is then amplified through whole-genome amplification in

order to recover sufficient DNA for sequencing. This is most commonly done with multiple displacement amplification, in which random primers are annealed to DNA followed by strand-displacement synthesis of new DNA copies with the phi29 DNA polymerase (158). The genome from individual cells can then be sequenced, assembled, and annotated, as in whole-genome sequencing of cultured isolates, to produce single-amplified genomes (SAGs) (153).

Because SAGs are derived from individual cells, they are suitable for examination of strain-level heterogeneity (157) and can be used in analysis of intra-population diversity and niche selection (155). Recovery of complete cellular DNA content also enables linkage of host cells with mobile genetic elements (155). Targeted sorting of cells based on phylogeny or function can enable enrichment of cells of particular interest, including rare taxa or those with specialized gene content or function (157). As with MAGs, SAG sequencing has expanded known microbial diversity and enabled examination of the metabolic function and ecological roles of uncultured clades (148, 157, 159). However, due to incomplete and uneven genome amplification, SAGs are typically less complete than MAGs, and amplification techniques can result in formation of chimeric sequences and bias against high GC content genomes (153). Additional bias can occur during cell sorting, where cells attached to particulate matter may not be recovered, and during cell lysis due to lack of universal lysis methods for all taxa (157). In addition, this method is sensitive to contamination during cell sorting and as a result of low DNA concentrations, and ultraclean facilities and reagents as well as sequence decontamination are required (157).

1.6.4 Metatranscriptomics

While microbial genomics can be used to identify the functional potential of a microbial community, it is unable to distinguish active taxa or metabolic activity occurring in situ. Cold, saline, or anoxic environments with low microbial turnover may favor preservation of organic molecules including nucleic acids from dead microorganisms (160, 161), and there may be populations of quiescent or dormant microorganisms under extreme physicochemical or oligotrophic conditions (162). Meta'omics approaches can also be utilized for studies of microbial activity in situ in cold and saline environments.

In metatranscriptomics, the total transcriptome (RNA) in a microbial community is sequenced to identify actively transcribing community members and expressed genes. Following RNA extraction, highly abundant ribosomal RNA reads are depleted in order to preferentially sequence messenger RNA. After mRNA sequencing, reads can be mapped to a reference metagenome or assembled and annotated *de novo* to identify expressed gene coding regions (163). Metatranscriptomics can thus be used to identify active taxa and expressed functional genes to indicate in situ community function, and to compare effects of environmental conditions on gene expression patterns (163, 164). For example, metatranscriptomic sequencing identified differential expression patterns between highly stable cryopegs and seasonally fluctuating sea ice brines (14); key metabolic pathways and taxa contributing to nutrient cycling in oligotrophic hypersaline microbial mats (165); and the effects of oxygen concentration on sulfur cycling gene expression in a sulfidic spring (166).

1.6.5 Metaproteomics

Metatranscriptomic sequencing indicates taxon and gene-specific transcription levels; however, due to post-transcriptional regulation, gene expression does not necessarily correlate to protein expression (167) and thus may not directly reflect microbial community function in situ.

Metaproteomics approaches therefore aim to characterize all proteins present in a microbial community to identify post-translational microbial activity and expression. In a typical liquid chromatography-based metaproteomics workflow, proteins are extracted from a sample and enzymatically digested into shorter peptides, which are then separated by liquid chromatography prior to peptide analysis by mass spectrometry (168). Proteins can then be identified by comparison to protein databases or through de novo peptide sequencing (168). Metaproteomics can be utilized similarly to metatranscriptomics in environmental samples in identifying active taxa and protein expression levels within and between environments, and linking metabolic function to active taxa. In combination with other 'omics approaches it can also be used to identify post-translational modifications and adaptation (167). As in other 'omics approaches, it can be limited by incomplete extraction and under- or over-representation of specific taxa or proteins (167). Peptide annotation can also be limited by incomplete databases, which commonly results in less accurate taxonomic classifications compared to functional annotation.

Metaproteomics is therefore generally best utilized in combination with metagenomics or SAG sequencing to improve annotation (168).

1.7 Cold saline springs on Axel Heiberg Island

Perennial springs are rare in areas of continuous permafrost such as the High Arctic due to prevention of fluid exchange by the permafrost layer (169). Where these springs occur, they can be associated with unusual disruptive features such as deep faults (170, 171) or discharge of

fluids through polythermal glacial ice (172). Axel Heiberg Island, Nunavut, in the Canadian High Arctic, hosts six sets of saline springs that flow perennially from subsurface groundwater through 500-600 meters of permafrost in areas of gypsum-anhydrite diapiric uplift (169). These springs discharge year-round despite their location in a polar desert region with average air temperatures of -15°C , reaching down to -40°C in winter (62). Two of these springs, Gypsum Hill Spring and Lost Hammer Spring, are the focus of this study. Their physicochemical characteristics and previous microbiological studies of these sites will be reviewed below.

1.7.1 Gypsum Hill

1.7.1.1 Site description

The Gypsum Hill (GH) spring area consists of approximately 40 springs and seeps over a 300 x 30 m area along the bank of the Expedition Fjord river (62) (Figure 1.4A). The springs are derived from groundwater in a deep subsurface salt layer, which discharges through the gypsum-anhydrite evaporite piercements to the surface and loses heat to the surrounding permafrost (62). The groundwater is theorized to recharge from subglacial melt or a nearby glacially-dammed, ice-covered alpine lake (62).

The springs at Gypsum Hill maintain constant physicochemical conditions year-round. Their waters are characteristically cold ($-1.3 - 7.2^{\circ}\text{C}$), hypersaline (7 - 8% salinity), reducing ($-287 - -324$ mV oxido-reductive potential), and anoxic (<0.6 $\mu\text{M O}_2$) (132, 139, 173). The spring waters are rich in sulfide (<1.5 mM) and sulfate (~ 41 mM) (132, 169). The spring sediment is also rich in sulfate (1.9 g/kg), and contains low levels of organic carbon (3700 mg/kg total organic carbon) (132). Gas exsolving continuously from the spring sediment is comprised primarily of

nitrogen (<99%), with trace He, Ar, CO₂, and CH₄ (132, 174). While there is no visible microbial biomass in the main spring pools, microbial streamers and mats form in and around the shallow outflow channels (139, 175).

1.7.1.2 Previous studies

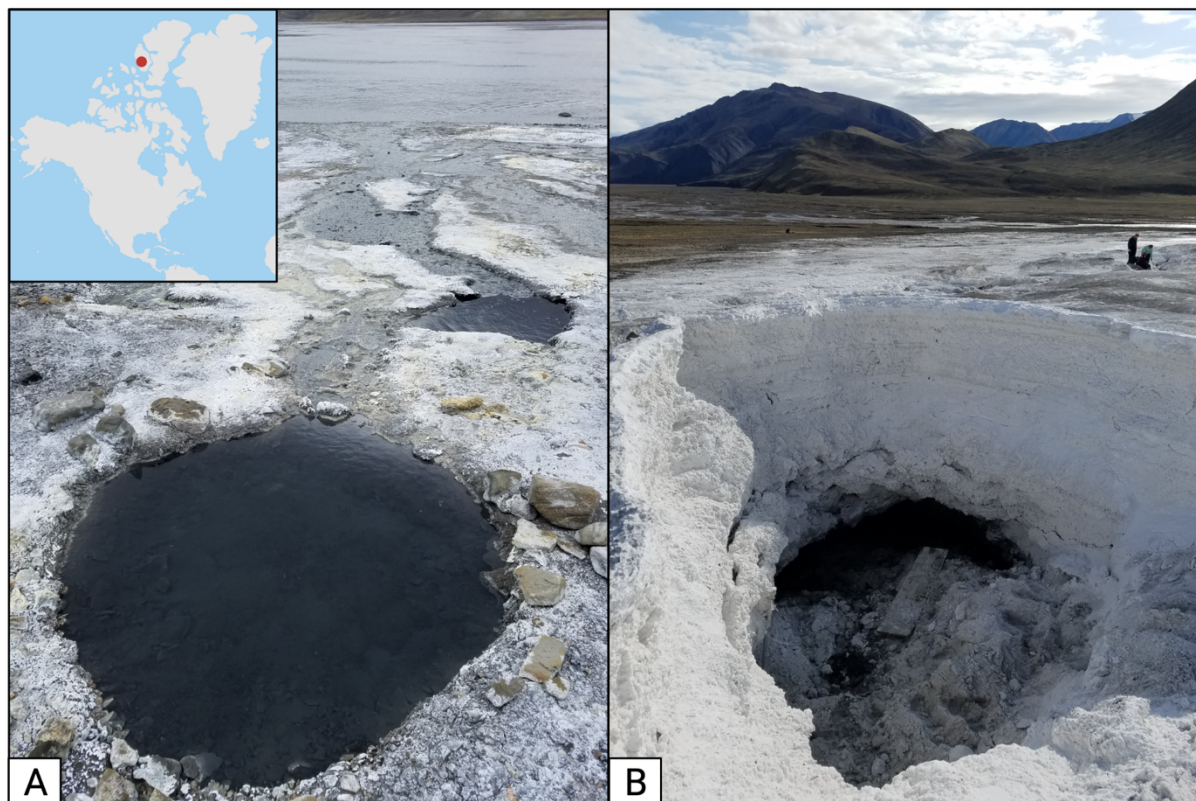


Figure 1.4. **A.** An outflow pool and channel at Gypsum Hill Spring. **B.** The interior of the salt tufa at Lost Hammer Spring. Inset: Approximate location of the Gypsum Hill and Lost Hammer Springs on Axel Heiberg Island, Nunavut. Map generated in QGIS with the Natural Earth dataset. Photos: Elisse Magnuson.

Previous studies of the spring sediments have primarily focused on four of the largest and most stable spring outflow pools (GH-1 to GH-4). Total microbial numbers in these springs are 10^7 cells/g in the spring sediments and 10^3 - 10^4 cells/mL in the spring waters (132). Microbial community composition in the spring sediment has previously been investigated through

cultivation of bacterial isolates as well as 16S rRNA gene clone libraries and high-throughput amplicon sequencing (132, 175-177). Abundant bacterial phyla included *Proteobacteria* (primarily *Gamma*- and *Deltaproteobacteria*), *Bacteroidetes*, *Firmicutes*, *Actinobacteria*, and *Spirochaetes*, and detected archaea were predominantly *Crenarchaeota* and *Euryarchaeota*. Taxa associated with sulfur cycling were abundant, comprising up to 75% of detected phylotypes, including sulfur-oxidizing *Gammaproteobacteria* (*Thiomicrospira*, *Thiobacillus*, *Halothiobacillus*) and sulfur- and sulfate-reducing *Deltaproteobacteria* (*Desulfuromonas*, *Desulfobulbus*, *Desulfobacteraceae*) (175-177), and *soxB* sulfur oxidation marker genes were identified in isolated *Marinobacter*, *Loktanella*, and *Roseobacter* spp. (132). Sulfur oxidation and sulfate reduction were detected in sediment microcosms (132), and sulfur isotopic analysis and radiolabeled sulfate uptake indicated sulfate reduction was occurring in situ in the spring sediments (177). Additionally, isotopic analysis of methane in the spring indicated a biogenic source of methane in the spring through methanogenesis, as well as potential methanotrophy (132). Sequences related to the methanogenic clade *Methanosarcinales* were detected through 16S rRNA gene clone sequencing (176). Uptake of leucine by heterotrophic microorganisms was low in comparison to dark CO₂ uptake. This in combination with little evidence of photoautotrophy (no detected photoautotrophic clades or chlorophyll) suggested a predominantly chemolithoautotrophic microbial community (132). Bacterial isolates were predominantly psychrotolerant, halotolerant, and facultatively anaerobic, indicating the microbial community is adapted to the cold, saline, and sub-oxic spring conditions (132).

Microbial streamers formed in the snow-covered spring outflow channels in winter were found to be dominated by a sulfur-oxidizing *Thiomicrospira* sp. NP51. Microscopy of the streamers

indicated they were comprised of *Thiomicrospira* microbial cells in an exopolymeric organic matrix containing elemental sulfur and other sulfur minerals such as gypsum and halotrichite. Sulfide and thiosulfate consumption and bicarbonate uptake detected in in situ microcosms indicated the *Thiomicrospira* was a chemolithoautotrophic sulfur-oxidizer, and streamer proliferation in the stream channels was suggested to occur due to increased sulfide concentrations under winter snow cover (139).

1.7.2 Lost Hammer

1.7.2.1 Site description

Lost Hammer (LH) Spring (also referred to as Wolf Spring) emerges from the subsurface into a cone-shaped salt tufa approximately two meters in height and three meters in diameter (178) (Figure 1.4B). During summer, the spring brines dissolve through the side of the tufa in a continuous stream, while during winter the outflow is blocked and water fills the interior of the tufa mound and overflows the side (178). The spring arises through a gypsum-anhydrite diapir as in the GH springs, but the source of the spring waters remains unknown as it is not located in close enough proximity to the GH springs to be recharged by the same sources (179).

Despite seasonal emptying and filling of the tufa, conditions in the spring waters and sediments remain highly consistent year-round. The spring waters are sub-zero ($\sim -5^{\circ}\text{C}$), hypersaline (24% salinity), micro-oxic ($<30\ \mu\text{M O}_2$), and highly reducing ($-168\ \text{mV}$ oxidation reduction potential) (179). The sediment and spring water are rich in sulfate (1.04 M and 0.054 M, respectively) and sulfide ($<1.5\ \text{mM}$), and contain low organic carbon ($<0.45\%$ in the sediment) (177, 180). LH continually emits a gas mixture of $\sim 50\%$ methane, 35% N_2 , 10% CO_2 , and trace ($<1\%$) H_2 , He,

and short-chain alkanes (ethane, propane, and butane), making it the coldest known terrestrial methane seep. Isotopic analysis indicated a thermogenic rather than biogenic origin for the methane and hydrocarbons (180).

1.7.2.2 Previous studies

The spring sediment contains 10^5 cells/g. The spring community was predominantly bacterial (80-84%), with >4% archaeal cells (180). Previous sequencing efforts include 16S rRNA gene sequencing and a 454-pyrosequencing metagenome (178, 180, 181). The most abundant taxa in the spring sediment were inconsistent between studies, likely due to the low biomass in the spring. Previously-identified bacterial phyla include *Proteobacteria* (*Alpha*-, *Beta*-, *Delta*- and *Gammaproteobacteria*), *Bacteroidetes*, *Chloroflexi*, *Cyanobacteria*, *Synergistetes*, *Firmicutes*, and *Actinobacteria*, and detected archaeal phyla include *Euryarchaeota*, *Crenarchaeota*, and *Thaumarchaeota*. Initial CARD-FISH and 16S rRNA gene clone library sequencing indicated that anaerobic methanotrophic archaea (ANME) in the ANME-1 clade dominated the sediment archaeal population (180); however, few or no ANME sequences were detected in subsequent studies. Sequencing of 16S rRNA gene cDNA was utilized in two studies to identify the active portion of the microbial community. Significant differences in microbial community relative abundance between cDNA and DNA sequences were observed in both studies, suggesting significant populations of dormant and dead cells. *Chloroflexi*, *Gammaproteobacteria*, *Actinobacteria*, and *Verrucomicrobia* were relatively enriched in the cDNA sequences, while *Cyanobacteria* were suggested to be dormant (178, 181).

Genes for a complete sulfur cycle between sulfate, sulfide, and sulfur intermediates were identified in the metagenome from a diversity of taxa, including *Gammaproteobacteria* (*Thiomicrospira*, *Thiobacillus*) and anoxygenic photosynthetic *Alphaproteobacteria* (*Chlorobium*, *Roseiflexus*, *Chloroflexus*) (181). Hydrogen-dependent reduction of sulfur compounds was detected in microcosms down to -20°C, and was suggested to be sulfate reduction carried out by *Deltaproteobacteria* (*Desulfovibrionales*) (178). No anaerobic methane oxidation could be detected in microcosms, but bacterial clades associated with methanotrophy (*Gamma*- and *Betaproteobacteria*) as well as methanogenic archaeal genera and methanogenesis-related genes were identified, suggesting methane cycling may still occur (178, 181). Additionally, genes involved in nitrogen cycling (nitrogen fixation, denitrification, and ammonia oxidation) and taxa related to hydrocarbon cycling and hydrogen oxidation were detected, indicating additional potential metabolisms in the spring community (178, 181).

1.7.3 The springs as analogue environments

The Axel Heiberg Island cold hypersaline springs, including Gypsum Hill and Lost Hammer, have been characterized extensively as analogues to spring features and cold brines on extraterrestrial bodies (62, 63, 179, 182, 183). Geomorphological structures resembling ancient salt springs have been identified on the Martian surface (40), and recently-formed gully features are suggested to have formed as a result of groundwater seepage or subsurface eutectic brines (184, 185). Salt diapirs may also be present on the Martian surface (186). Thermal and flow modelling of the GH springs applied to present-day Martian conditions indicated that similar cold saline springs could flow through the thick permafrost on Mars, resulting in formation of the observed geomorphological spring or gully features (62, 182). The AHI springs thus provide a

model for microbial communities that could inhabit putative saline springs and other cold brines on past or present Mars, as well as potential biosignatures that could be present in these features (179, 183).

1.8 Conclusion

Cold, hypersaline environments like the Axel Heiberg Island springs are analogous to putative habitats on extraterrestrial bodies such as Mars, Europa, and Enceladus and contain microbial communities despite challenging physicochemical conditions. While previous investigations of these springs and other similar environments have identified microbial community structure and potential metabolisms, relatively few studies have described the active microbial community and functional metabolisms occurring in situ. Previous studies of the Axel Heiberg Island springs have utilized 16S rRNA gene cDNA sequencing and ex situ measurements such as microcosm studies to identify putatively active microorganisms and metabolisms, but have not described in depth the in situ active microbial community or been able to link observed metabolisms to the responsible taxa. This work aimed to characterize the active microbial community inhabiting the springs through combined meta'omics methods in order to improve our understanding of how microbial life is sustained in cryoenvironments on Earth and other worlds.

Connecting Text

Relatively few studies of sub-zero, hypersaline environments have identified active microorganisms and metabolisms in situ. Characterizing these active communities in situ is vital to understanding microbial community structure and function in the cryosphere on Earth and other worlds. Lost Hammer Spring is a highly unique sub-zero, hypersaline terrestrial methane seep and analogue to putative sub-zero briny habitats on extraterrestrial worlds such as Mars. Previous studies identified a low biomass, putatively active microbial community in the spring sediment including sulfate-reducing bacteria and methane-oxidizing archaea. However, no in situ characterization of gene expression had previously been accomplished. In this chapter, I utilized a combination of metagenomics, metatranscriptomics, and single-cell genomics to characterize the active microbial community and metabolisms inhabiting the sub-zero, hypersaline Lost Hammer Spring.

This manuscript appears in:

Magnuson E, Altshuler I, Fernandez-Martinez MA, Chen YJ, Maggiori C, Goordial J, et al. Active lithoautotrophic and methane-oxidizing microbial community in an anoxic, sub-zero, and hypersaline High Arctic spring. *ISME J.* 2022;16(7):1798-808. doi: 10.1038/s41396-022-01233-8.

with

Material from: Magnuson, E., Altshuler, I., Fernández-Martínez, M.Á., Chen, Y.-J., Maggiori, C., Goordial, J., Whyte, L.G., *The ISME Journal*, published 2022, © The Author(s), under exclusive licence to International Society for Microbial Ecology 2022.

Supplementary tables S2.1, S2.4 – S2.9, and S2.11 – S2.18 are available as supplemental material.

Chapter 2. Active lithoautotrophic and methane-oxidizing microbial community in an anoxic, sub-zero, and hypersaline High Arctic spring

Elisse Magnuson¹, Ianina Altshuler², Miguel Á. Fernández-Martínez¹, Ya-Jou Chen¹, Catherine Maggiori¹, Jacqueline Goordial³, Lyle G. Whyte¹

¹Natural Resource Sciences, McGill University, Ste-Anne-de-Bellevue, QC, Canada

²School of Architecture, Civil and Environmental Engineering, Ecole Polytechnique Fédérale de Lausanne, Lausanne, Switzerland

³School of Environmental Sciences, University of Guelph, Guelph, ON, Canada

2.1 Abstract

Lost Hammer Spring, located in the High Arctic of Nunavut, Canada, is one of the coldest and saltiest terrestrial springs discovered to date. It perennially discharges anoxic (<1 ppm dissolved oxygen), sub-zero (~ -5°C), and hypersaline (~24% salinity) brines from the subsurface through up to 600 meters of permafrost. The sediment is sulfate-rich (1 M) and continually emits gases composed primarily of methane (~50%), making Lost Hammer the coldest known terrestrial methane seep and an analogue to extraterrestrial habits on Mars, Europa, and Enceladus. A multi-omics approach utilizing metagenome, metatranscriptome, and single-amplified genome sequencing revealed a rare surface terrestrial habitat supporting a predominantly lithoautotrophic active microbial community driven in part by sulfide-oxidizing *Gammaproteobacteria* scavenging trace oxygen. Genomes from active anaerobic methane-oxidizing archaea (ANME-1) showed evidence of putative metabolic flexibility and hypersaline and cold adaptations. Evidence of anaerobic heterotrophic and fermentative lifestyles were found in candidate phyla DPANN archaea and CG03 bacteria genomes. Our results demonstrate Mars-relevant metabolisms including sulfide oxidation, sulfate reduction, anaerobic oxidation of methane, and oxidation of trace gases (H₂, CO₂) detected under anoxic, hypersaline, and sub-zero ambient conditions, providing evidence that similar extant microbial life could potentially survive in similar habitats on Mars.

2.2 Introduction

Axel Heiberg Island in the High Arctic region of Nunavut, Canada, hosts perennial cold saline springs discharging through up to 600 meters of continuous permafrost (1, 2). Lost Hammer (LH) Spring (79°7'N, 90°21'W) is the most extreme of the springs in terms of temperature and

salinity, with liquid water flowing at -5°C and 24% salinity (3). LH continuously exudes gas comprised primarily of methane (50%), making it the coldest terrestrial methane seep discovered to date (3). It emerges in an area of gypsum-anhydrite diapiric uplift through a two-meter-high salt tufa that experiences seasonal emptying and filling; despite this seasonality, conditions in the outflow sediment remain stable. The sediment is nearly anaerobic with trace amounts of O_2 (0.25 ppm), highly reducing (-165 mV), and sulfate-rich (1 M) (3).

Microbial life in cryoenvironments, or environments with continuous sub-zero temperatures, is dependent on the presence of liquid water, typically enabled by freezing point depression through high concentrations of salts or other solutes (4). Such habitats include permafrost ultrathin brine films surrounding soil particles and cryopegs (5, 6), brine veins in sea ice (7), and highly unique habitats like Lake Vida in the Antarctica dry valleys (8). Microorganisms in these environments contend with multiple stressors, and study of these microorganisms informs our understanding of the cold and saline limits of life on Earth and putative extraterrestrial habitats in the subsurface of Mars and the icy moons Europa and Enceladus (4). For example, recent evidence obtained through orbital radar sounding indicated the presence of subglacial, hypersaline lakes ~800m below Mars' southern ice cap (9, 10). Recurring slope lineae may be another possible episodic source for liquid water closer to the Martian surface; modelling suggests they may form through hydration and deliquescence of near-surface sulfate-chloride salt brines (11). Geomorphological features resembling ancient salt springs have also been proposed (12, 13), and as Mars became much colder and drier ~3.7 bya, the last habitable surface environments would likely have been highly saline cryoenvironments; chloride salt deposit imaging suggests surface brines persisted 2-2.5 bya (14). Indeed, the search for extant and/or

past life on Mars, Europa, and Enceladus is a primary driver for current and future planetary science missions (15, 16). The cold, salty, and anoxic oceans on Europa and Enceladus putatively contain redox components that could support microbial life, including methane in water plumes erupting from Enceladus (17, 18).

Previous studies characterized LH as a low-biomass, microbially dominated ecosystem ($\sim 10^5$ cells/g sediment) with anaerobic methane-oxidizing archaea (ANME-1) and sulfate-reducing bacteria (SRBs) identified via 16S rRNA gene clone libraries and a 454 pyrosequencing metagenome (3, 19, 20). However, due to low biomass and high salinity that make nucleic acid extraction difficult, these surveys likely did not capture the complete microbial diversity of the system, as determined by rarefaction curves and low sequencing depth (19, 20). Sediment incubations identified SRBs capable of metabolism at *in situ* temperatures, and limited studies have identified putatively active microbiota through sequencing of 16S rRNA (cDNA) transcripts (19, 20); however, no transcriptome has previously been successfully sequenced.

In this context, the objectives of the present study were to identify the dominant taxonomic and metabolic diversity through genome-resolved metagenomic sequencing combined with metagenome-assembled genome (MAGs) and single-amplified genome (SAG) analyses. In parallel, we attempted to identify the primary active members and metabolisms of the LH spring sediments through metatranscriptomic analyses and to identify adaptations to the polyextreme LH environment focusing on MAGs and SAGs from poorly characterized phylogenetic groups. Lastly, we interpreted the identified active microbial ecosystem members and metabolisms as

potential life forms that could exist in very cold and saline environments on other planetary bodies such as Mars.

2.3 Materials and Methods

Detailed descriptions of the following are in Supplementary Materials.

2.3.1 Site description and sample collection

Lost Hammer discharges through a precipitated mineral salt tufa as described in previous publications (3, 13, 19, 20) (Figure S2.1). Physical and geochemical parameters (Table S2.1) have remained highly stable since 2005, allowing comparison among samples collected in different years. For this study, sediment samples were collected in July 2017 and July 2019. Sediment from 2017 was used for metagenomic sequencing, and sediment from 2019 was used for RNA and SAG sequencing.

2.3.2 DNA extraction and metagenome analyses

DNA was extracted from two 5 g sediment portions. Resulting DNA from each sample was concentrated and sequenced on a HiSeq2500 (Illumina, San Diego, CA, USA) at The Centre for Applied Genomics (Toronto, ON, Canada). Reads were trimmed with Trimmomatic (21) and classified with Kaiju (22) and phyloFlash (23). The metagenomes were co-assembled with Megahit (24) and contigs were binned with MetaBAT (25). Bin quality was assessed with CheckM (26). The co-assembly was annotated with the Joint Genome Institute's IMG/M server (27, 28). Bins were classified with Genome Taxonomy Database Toolkit (29). Additional

annotation is described in Supplementary Materials. Sequencing and assembly statistics are in Tables S2.2 and S2.3.

2.3.3 Single cell sorting and SAG analysis

Fluorescence-activated cell sorting and genome amplification was done at the Bigelow Laboratory for Ocean Sciences (East Boothbay, ME, USA). Whole genome sequencing libraries were prepared and sequenced on a MiSeq (Illumina). Reads were trimmed with BBDuk and contaminant human reads were removed with DeconSeq (30). Genomes were assembled with SPAdes (31). Genome annotation was as described for the metagenome.

2.3.4 mRNA sequencing and analysis

RNA was extracted in triplicate, treated to remove contaminating DNA, then pooled and concentrated. Ribosomal RNA was depleted and the generated cDNA library was sequenced on a NovaSeq 6000 at The Center for Applied Genomics. Reads were trimmed with Trimmomatic and rRNA reads were removed with SortMeRNA (32). Remaining reads were aligned to metagenome and SAG contigs with bowtie2 (33). Reads aligned to CDS were counted with HTSeq (34) and transcripts per million reads (tpm) was calculated to normalize gene expression values.

2.3.5 Data availability

Sequencing reads, metagenome, MAGs, and SAGs are in NCBI under BioProject PRJNA699472. JGI metagenome and SAG annotations are available under GOLD Study ID Gs0135943 (SAG IDs in Table S2.4).

2.4 Results and Discussion

2.4.1 MAGs and SAGs capture novel phylogenetic diversity

We sequenced the metagenome and constructed MAGs in order to characterize microbial diversity within the LH sediment. The majority of classified metagenomic reads were bacterial (98%) (Figures 2.1A, S2.2). The most abundant phyla were *Bacteroidota* (37%), *Proteobacteria* (23%), *Desulfobacterota* (20%), and *Campylobacterota* (5%). Metagenome binning produced 32 high-quality MAGs (>90% completeness, <5% contamination) and 60 medium-quality MAGs (>50% completeness, <10% contamination) (Table S2.5). All MAGs were classified as bacterial, representing 12 phyla (Figure 2.1B) including the most abundant orders (>1.5%) in the metagenome (Figure 2.1A).

SAGs captured additional diversity. Fourteen medium-quality and 53 low-quality SAGs were obtained, of which 33 were bacterial and 34 were archaeal. We intentionally sought to sequence archaeal genomes as no ANME-1 genomes have been previously recovered from LH. These SAGs represented 31 species following identification of closely related genomes based on 16S rRNA gene similarity (>98.6%) and average nucleotide identity (ANI) (>95%). The majority of these species (28 of 31) were found at low abundance (<1%) in the metagenome; discussion on why this occurred is in Supplementary Materials. Correspondingly, there was little overlap between SAGs and MAGs: ANI analysis classified one low-quality SAG (S38) as the same species as MAGs (M8 and M38). The 14 medium-quality SAGs represented primarily archaeal species, including five ANME-1 SAGs and six SAGs representing QMZS01 (formerly in

Candidatus Aenigmarchaeota) and *Iainarchaeota* (*Candidatus* Diapherotrites) in the DPANN superphylum (Figure 2.1A).

Genome novelty was assessed using assigned rank of taxonomic classification by comparison to the GTDB database, based on placement in a reference tree and whole-genome comparisons to reference genomes (29). The majority (97%) of MAGs and SAGs were unclassified at the species level, with 23% of genomes unclassified at higher taxonomic ranks (genus (29 genomes), family (5 genomes), and order (1 genome)) (Figure 2.1C). Comparatively, a recent compendium of 530 Arctic Ocean MAGs found 83% novelty at the species level (35). The high level of genomic novelty reflects the uniqueness of LH as well as the relative undersampling of genomes from polar and extreme environments.

2.4.2 Sulfur cycling Gammaproteobacteria and Desulfobacterota are abundant and active

We identified the active microbial community and metabolisms present in the spring by mapping the metatranscriptome to the metagenome, MAGs, and SAGs. Due to the challenges of extracting RNA from LH sediment, the metatranscriptome had relatively low sequencing depth (4.2 million reads). Therefore, some transcripts were likely not detected in our study and their absence herein does not preclude their presence in the environment. Additionally, the metatranscriptome and metagenome were sequenced from sediment collected in different years; while spring conditions are stable, we cannot exclude the possibility of variation in the sampled microbial communities contributing to observed differences between the two datasets.

The LH sediment contains abundant sulfate (~100 000 mg/kg), and typical sulfur-cycling taxa were among the most abundant in the metagenome, including *Desulfobulbales* (15%), *Campylobacterales* (5%), and *Halothiobacillales* (3.6%) (Figure 2.1A). Sulfide oxidation genes were among the most highly expressed metabolic genes (5027 tpm) (Figure 2.2; Table S2.6). Multiple mechanisms of sulfide oxidation were evident, including through elemental sulfur (*sqr*, *fccAB*), thiosulfate (*sox*), and tetrathionate (*tsdA*) intermediates; elemental sulfur detected in LH is putative evidence of this activity in situ (3, 13, 36). Relative expression indicated oxidation was largely driven by the versatile Sox multi-enzyme complex (4662 tpm), which can utilize multiple sulfur compounds for complete or partial oxidation (36). The majority (71%) of total oxidation gene relative expression was attributed to *Guyparkeria* MAGs M8 and M38 (Table S2.7) in *Halothiobacillales*. These MAGs contained complete Sox pathways and also expressed sulfide-oxidizing *sqr* and *fccAB* genes, indicating they oxidize sulfide completely to sulfate (Figure 2.3; Table S2.8). Previously cultivated *Guyparkeria* are characteristically halophilic sulfur-oxidizers, identified in marine and hypersaline waters and sediments (37, 38).

Expression of Sox genes was also detected in nine additional *Gammaproteobacteria*, *Alphaproteobacteria*, and *Campylobacterota* MAGs (Figure 2.3; Table S2.8). Variation in partial versus complete Sox pathways and co-expression of other oxidation genes including *sqr* and *rdsrAB* was observed in the eleven MAGs with Sox gene expression, suggesting variation in oxidation pathways and substrate utilization as a potential source of niche differentiation, similar to sulfidic environments (39, 40). Eight MAGs co-expressed cytochrome c oxidases, while one (M37) additionally expressed denitrification genes, suggesting they scavenge for the low amounts of O₂ as well as utilize anaerobic electron acceptors; trace nitrite/nitrate has been

detected in the sediment (2.87 mg/kg). These MAGs all contained high-affinity *cbb3*-type cytochrome c oxidases (*coxABCD*), which enable aerobic respiration in microaerobic environments (41), exclusively or in addition to low-affinity oxidases; five MAGs expressed these high-affinity oxidases.

Expression of reductive sulfur cycling genes (*dsrAB*, *ttrAB*, and *psr/phsA*) was dominated by *Desulfobacterota*, with all expression of these genes mapped to MAGs and unbinned genes in the *Desulfobulbales* order (106 tpm). Complete dissimilatory sulfate reduction (SR) pathways were identified in the three *Desulfobulbales* MAGs, and expression of reductive *dsrAB* was identified in BM506 MAG M19 (Table S8). *Desulfobacterota*, including *Desulfobulbales*, have previously been characterized in hypersaline and subzero ice-covered lakes and sub-glacial brines (8, 42).

Our previous microcosm experiments detected H₂-dependent SR in LH sediments down to -20°C (19), suggesting hydrogen (~0.65%) exsolving from the spring as a likely electron donor for SRB. The two MAGs that expressed SR genes in our study have unexpressed hydrogen-oxidizing NiFe hydrogenase genes; however, expression was identified for hydrogenase subunits in another *Desulfobacterota* MAG (SURF-3 sp. M58) (Table S2.8) and SAG (*Desulfurivibrionaceae* sp. S23) (Table S2.9). Thus, hydrogen oxidation is likely coupled with SR for at least some LH SRB, confirming this observed metabolism in situ.

2.4.3 Anaerobic methane oxidation by ANME-1 detected at sub-zero temperatures

Methane seeps have been studied extensively due to their importance in global carbon cycling, most commonly in marine environments where methanotrophy is dominated by anaerobic oxidation of methane (AOM) by anaerobic methane-oxidizing archaea (ANME) (43). ANME have been detected in hypersaline environments including marine cold seeps and mud volcanoes (44, 45), but are generally absent from sub-zero brines such as cryopegs (46, 47). ANME have previously been reported in one sub-zero environment (thawing Arctic sub-marine permafrost) where isotopic evidence indicated AOM down to -1°C (48). LH continuously exudes methane (11 g/day), with sediment concentrations of ~ 100 nmol/g (49), and ANME-1 have previously been detected in the sediment (3). In our study, expression of genes involved in AOM (*mcrAB*, *mtrC*, *frhB*) (165 tpm) was identified in ANME-1 SAGs (Figure 2.3), indicating that AOM is occurring under *in situ* conditions and providing some of the strongest evidence to date that AOM occurs at sub-zero temperatures as low as -5°C .

AOM is typically coupled with SR in syntrophic consortia with SRB, though associations with iron- and manganese-reducing bacteria also occur (50). In LH, co-occurrence of active SRB suggests SR-coupled AOM as a putative mechanism. The SRB genomes include *Desulfobulbales*, which are known to form consortia with ANME (51). However, our previous CARD-FISH microscopy did not observe close associations of ANME-1 with other cells (3). Similar observations of unattached ANME, usually ANME-1, suggests they can carry out AOM alone, with potential alternate electron acceptors including metal oxides and humic acids (52). Decoupled AOM has been shown in nitrate-, iron-, and manganese-reducing ANME-2 species (53-55). It is unclear what the electron acceptor is for LH ANME-1.

Expression of bacterial methanotrophy marker genes for methane monooxygenase (*pmoABC*; 102 tpm) was identified in *Methylobacter* MAG M5 (Figure 2.3). Transcripts also mapped to formylmethanofuran dehydrogenase (*fmdB*; 18 tpm), involved in downstream oxidation of formaldehyde to formate. *Methylobacter* oxidize methane in environments including seep oxic zones and anoxic lakes (56, 57). The presence of both cytochrome c oxidase and nitrate reduction genes in MAG M5 suggests possible facultative anaerobic methane oxidation by *Methylobacter* could be occurring in the micro-oxic sediment although expression of these genes was not detected.

Despite the availability of methane, both ANME-1 and *Methylobacter* were at low abundance (<1%) in the metagenome. While *Methylobacter* may be restricted by competition for nitrate and/or oxygen, electron acceptor restriction is unlikely for ANME-1 if coupled with SR given the abundance of sulfate and SRBs. Their activity may be inhibited by the low energy yield of SR-coupled AOM, which is predicted to be unfavorable under *in situ* LH conditions (6.1 kJ/mol electron⁻¹; Table S2.10); although ANME-1 have reached abundances of ~50% in hypersaline marine cold seeps (58), they may be less adapted to sub-zero conditions. As ANME are also oxygen-sensitive (59), micro-oxic conditions in LH may be sufficient to restrict their abundance as observed in marine water columns (60) and sediment (61).

2.4.4 Other C and N cycling metabolisms detected

In addition to methane, the gas emitted in LH contains significant amounts of nitrogen (~35%) and carbon dioxide (~10%), as well as trace gases (~<1%) including short-chain alkanes (3). Expression of aerobic short-chain alkane oxidation genes was detected (180 tpm; Figure 2.2),

indicating that these gases provide additional energy and carbon sources. Dissimilatory nitrate reduction (*napA/narG/nirB*; 197 tpm), denitrification (*napA/narG/nirKS/norBC/nosZ*; 505 tpm), and nitrogen fixation (*nifH*; 2 tpm) genes were also expressed (Figure 2.2). Dissimilatory nitrate reduction and denitrification genes with mapped transcripts were classified as *Proteobacteria*, *Actinobacteriota*, and *Desulfobacterota*; *nifH* had mapped transcripts in *Sulfuricurvum* MAG M14 (*Campylobacterota*) (Figures 2.2, 2.3). The lack of detected nitrification gene expression represents a gap in the nitrogen cycle, although a small number of bacterial *amoA* genes in the metagenome suggests nitrification may be carried out by low-abundance taxa. No evidence of anaerobic ammonia oxidation was found.

Photosynthetic gene transcripts were also detected (*psaAB/psbABCDTZ*; 5337 tpm), mapping to unbinned cyanobacterial (74% of tpm) and eukaryotic genes (Figure 2.2). However, months-long winter darkness at LH (~October to February) means this activity is necessarily seasonal. All cyanobacterial 16S rRNA sequences in the metagenome were most similar to chloroplast 16S rRNA, indicating this detected activity may be due to plant or soil matter blown into the spring tufa. Alternatively, *Cyanobacteria* may be dormant during the winter months; previous metagenomic sequencing found cyanobacterial dormancy genes (20). Anoxygenic photosynthesis gene expression was also detected by unbinned alphaproteobacterial and eukaryotic genes (*pufLMC*; 11 tpm), indicating some photosynthetic activity occurs through H₂S oxidation.

2.4.5 Lithoautotrophic metabolisms relatively predominant in the active microbial community

We hypothesized that lithoautotrophic metabolisms primarily sustain the spring microbial community, as the potential for photoautotrophy is limited due to long seasonal darkness and heterotrophic metabolism would be limited by low organic C (0.45% TOC) in the sediment. Approximately 40% of the MAGs and SAGs contained CO₂-fixation genes, and 73% of MAG and SAG relative expression was attributed to those autotrophic genomes (Figure S2.3). However, this did not account for the majority of relative expression (61%) attributed to unbinned genes. In order to estimate the total relative contributions of autotrophs to the active LH community, we multiplied the relative expression in each phylum, including unbinned genes, by its proportion of autotrophic genomes (Figure 2.4). Using this method, we estimated 60% of relative expression originated from autotrophic microorganisms. These results suggest the LH microbial community may potentially primarily use lithoautotrophy, though additional in situ evidence (e.g. a bicarbonate mineralization assay) is required to support this finding. Notably, 23% of relative expression was attributed to sulfide-oxidizing *Gammaproteobacteria* genomes containing Calvin-Benson-Bassham cycle genes, suggesting that they are significant contributors to primary production. Sulfide-oxidizing *Gammaproteobacteria* are major contributors to carbon fixation in light-limited environments including anoxic coastal sediments, hydrothermal vents, and other hypersaline Axel Heiberg springs (39, 62, 63); they also comprise major clades at marine cold seeps where methane oxidation and sulfate reduction produce abundant sulfide and CO₂ (43).

Mixotrophic growth using trace carbon monoxide (CO) as an energy source is a proposed survival mechanism for heterotrophs under organic carbon limitation (64). CO dehydrogenase (*coxL*) genes were present in 11 heterotrophic *Alphaproteobacteria* MAGs; furthermore, *coxL*

gene expression was detected in three of these MAGs, indicating that mixotrophy is a relevant lifestyle in LH. No measurement of CO has previously been attempted in LH; it may be a previously undetected component of the LH gas, or microorganisms could be utilizing trace atmospheric CO.

Relative expression by *Bacteroidota* was low (3.5%) compared to their relative abundance in the metagenome (37%) (Figures 2.4, 2.1B), suggesting their reliance on heterotrophy may limit activity. While these results should not be considered conclusive given low coverage and lack of replicates for the metatranscriptome, this relative decrease was also observed in a previous study involving sequencing of cDNA derived from 16S rRNA (20). *Bacteroidota* comprise significant proportions of the microbial community in subglacial brines, sea ice brines, cryopegs, and cold hypersaline marine basins (46, 47, 65), and the most abundant *Bacteroidota* genera in the metagenome (*Gillisia*, *Salegentibacter*, *Lutibacter*) were found in highly saline soil, subglacial brines, and marine solar salterns (46, 66, 67). Their putative salt tolerance may enable survival even with low transcriptional activity.

2.4.6 Functional potential and adaptations in poorly characterized taxa

This study utilized two approaches to recovering microbial genomes through assembly of MAGs and SAGs. MAGs are assembled through clustering of metagenomic contigs; accordingly, MAGs often represent “population genomes” of related strains, which may have differing microniches or metabolisms, rather than single genotypes (68). SAGs are sequenced from individual cells and represent an individual strain rather than population, enabling precise evaluation of amino acid residue substitutions associated with cold and saline adaptation (69).

Our SAGs include genomes for under-studied or candidate taxa, present in low-abundance in LH but with mapped mRNA transcripts indicating metabolic activity. In order to better understand the niches occupied by these microorganisms, the functional potential and gene expression of several SAGs was more closely examined.

2.4.6.1 ANME-1 genomes reveal potential metabolic flexibility and hypersaline adaptation.

Despite extensive study of ANME, much remains unknown due to their recalcitrance to enrichment and culturing. As the LH ANME-1 genomes are the first from species active under ambient sub-zero and hypersaline conditions, we examined them for features enabling their survival. While ANI and marker gene analyses determined that the 17 SAGs (12.3-84.6% completeness) represented multiple species within the ANME-1 family, the genomes are presented together for simplicity.

Two ANME-1 SAGs contained subunits of a Group 1h NiFe hydrogenase, co-localized with the electron-accepting Hdr2 complex, signifying possible respiratory oxidation of hydrogen. In addition, six SAGs encoded butyryl-CoA dehydrogenase, clustered with *mcr* genes, and a downstream butyryl-CoA oxidation pathway. This pathway is involved in oxidation of butane and other short-chain alkanes in archaea closely related to ANME (*Ca. Syntrophoarchaeum*) utilizing *mcr*-like complexes (70), and has been identified in ANME-1 containing *mcr*-like sequences (71). LH butyryl-CoA dehydrogenases were homologous to those from *Ca. Syntrophoarchaeum butanivorans* and *mcr*-like-encoding ANME-1 (40% and 62% amino acid identity, respectively). LH *mcrA* genes were most similar to canonical ANME-1 *mcrA*; nevertheless, the presence of this pathway suggests potential alkane oxidation. Taken together,

these genes signify potential substrate flexibility in LH ANME-1. As SR-coupled AOM yields little energy (72), alternate electron donors may compensate for energy deficits due to costly hypersaline adaptations. Competition for hydrogen and alkanes (<1% of spring gas) may additionally contribute to low ANME-1 abundance.

The ANME-1 SAGs contained osmotic stress adaptations (Figure 2.5), including for uptake and synthesis of compatible solutes and transporters for K⁺ uptake and Na⁺ extrusion (73).

Transcripts mapped to a small conductance mechanosensitive channel involved in maintenance of solute concentration (73), suggesting this accumulation occurs in situ. Based on these genes, LH ANME-1 could utilize either a “salt-in” or “compatible solute” osmoregulation strategy, though predicted proteins did not show the typical enrichment of acidic amino acids found in salt-in microorganisms (Figure S2.4A). Homologous osmotic stress response genes were identified in related ANME-1 genomes (Table S2.11), indicating widespread adaptive capabilities and corroborating observed preferential habitation of hypersaline environments by ANME-1 over other ANME clades (45, 50). Seven SAGs also encoded gas vesicle proteins, proposed to reduce water loss during salt stress (74). Alternatively, they may enable buoyancy regulation, allowing cells to position themselves more favorably in a spring which experiences seasonal changes in water depth (75). The presence of chemotaxis proteins and a flagellum suggest ANME may navigate the sediment to find optimal niches or, potentially, SRB for syntrophic partnerships.

The ANME-1 SAGs contained genes for several multi-heme cytochromes, which have proposed functions in both syntrophic and decoupled AOM (53, 55, 76) (Figure 2.5). In syntrophic AOM,

direct exchange of electrons is proposed to occur via conductive “nanowires” between ANME and SRB (76). Examination of the sulfate-reducing MAG M19 as a potential syntrophic partner identified genes with mapped transcripts required for nanowire construction (77) including multi-heme cytochromes, type IV pili, and outer membrane porins. The ANME-1 SAGs additionally contained archaeal genes suggested to facilitate nanowire construction (78). Syntrophic electron exchange is therefore putatively possible in these microorganisms.

2.4.6.2 Poorly understood DPANN archaea active in LH.

Archaea from the DPANN superphylum were detected with the recovery of *Iainarchaeota* (*Candidatus* Diapherotrites) (one SAG, completeness 52.9%) and QMZS01 (formerly part of *Aenigmarchaeota*) (five SAGs, completeness 57.7-76.2%) SAGs. Within DPANN, these phyla are typically non-extremophilic and have not previously been identified in hypersaline or sub-zero environments (79, 80). The QMZS01 candidate phylum contains only two other genomes, both MAGs from hydrocarbon- and sulfate-rich Guaymas Basin hot hydrothermal sediments (71).

Due to their resistance to laboratory cultivation, the DPANN superphylum has only recently been defined (81). DPANN are characterized by small cell and genome sizes and minimal metabolic function (82), but are proposed to have important roles in organic carbon and hydrogen cycling (80, 83). Characteristically small genomes (<0.7 Mbp, though incomplete), limited anabolic pathways, and acetogenic and hydrogenic fermentation capabilities were observed in LH DPANN SAGs (Figures S2.5, S2.6), indicating reliance on scavenging for cellular components. All SAGs showed evidence of obligately anaerobic and heterotrophic lifestyles. The

Iainarchaeia SAG contained a large subunit form III RubisCO gene (*rbcL*) (Figure S2.7), also identified in *Candidatus Iainarchaeum andersonii* where it was proposed to take part in the adenosine monophosphate metabolism pathway (79). The rest of this pathway was identified in the LH SAG (Figure S2.5), suggesting adenosine degradation to pyruvate as a possible ATP-generating mechanism. The QMZS01 SAGs contained genes involved in polysaccharide degradation (e.g. alpha amylase and endoglucanase) and transcripts mapped to a TrmB-family sugar-specific transcriptional regulator, supporting putative polysaccharide-degradation activity. The two Guaymas Basin QMZS01 MAGs also contain carbohydrate-active enzymes and fermentation genes, indicating similar metabolisms across this phylum. Additionally, LH QMZS01 uniquely contain subunits of group 3b NiFe hydrogenase (*hydDA*) co-localized with a ferredoxin and an oxidoreductase homologous to *hydG* and *hydB* from *Pyrococcus furiosus* (29 and 40% amino acid identity, respectively), which reversibly couple H₂ oxidation with NADPH formation (84). LH DPANN may thus cycle complex carbon compounds, supplying fermentation products including H₂ or acetate to co-occurring hydrogen oxidizers or putative acetate metabolizers including SRB containing the Wood-Ljungdahl pathway or the numerous microorganisms encoding acetate metabolism genes (Tables S2.12, S2.13). Transcripts mapping to DPANN SAGs (2981 tpm) were primarily to non-coding RNA (Table S2.9). The SAGs also contained stress response genes (Figures S2.3, S2.4). While the majority of these genes were detected in other *Iainarchaeota* and QMZS01 genomes (Table S2.11), LH QMZS01 uniquely contained Na⁺/H⁺ antiporter and compatible solute synthesis genes, indicating adaptations to hypersalinity in this clade. DPANN have been detected in High Arctic lakes on Ellesmere Island, including cold (3.5°C) freshwater Lake Hazen (85) and meromictic ice-covered (0-8°C) Lake A (86). DPANN populations in both lakes were primarily *Woesearchaeota*; however, *Iainarchaeota*

and *Aenigmarchaeota* were detected in the saline (~3%), anoxic, and sulfidic layers of Lake A, where they were similarly theorized to recycle microbial biomass. These results demonstrate that, despite minimal biosynthetic capabilities, DPANN archaea are active in extreme, resource-limited Arctic environments.

2.4.6.3 Candidate CG03 phylum is likely fermentative.

SAG S2 was classified in the phylum CG03, a candidate phylum recently defined by GTDB using their methodology based on phylogenetic tree placement and normalization of taxonomic rank using lineage-specific evolutionary distance (87). This poorly characterized phylum contains 15 MAGs in the GTDB database, previously deposited in NCBI primarily as unclassified *Elusimicrobia* and sourced from groundwater and hypersaline sediments; only one study has previously examined some of these CG03 genomes (88). The LH SAG is the first CG03 genome from a sub-zero environment, although CG03 was recently detected in the anaerobic, methane-rich sulfidic Zodletone spring (22°C, 1.2% NaCl) (89). The LH SAG contains a glycolysis/gluconeogenesis pathway, partial TCA cycle, and partial fatty acid oxidation pathway (Figure S2.8), indicating a likely heterotrophic and anaerobic lifestyle. Interestingly, it encodes partial NADH dehydrogenase and ATP synthase complexes but lacks other electron transport chain proteins, corroborating the previous survey of several CG03 genomes which found near-universal partial ATP synthases. The functionality of these complexes is unclear, but their frequency within the phylum implies an active rather than vestigial role. Regardless, the LH CG03 is likely fermentative, as it contains genes involved in both acetogenic (phosphotransacetylase and acetate kinase) and hydrogenogenic (FeFe Group A hydrogenase) processes. It also encodes homologs to carbon monoxide/xanthine dehydrogenase

family proteins. Structure-based functional annotation by I-TASSER (90) confirmed protein similarity to CO dehydrogenase, suggesting possible mixotrophy. These results suggest that, similar to DPANN, CG03 may provide acetate and hydrogen to the microbial community.

Transcripts mapped to the SAG (6718 tpm total) mapped to tRNA genes and a AAA ATPase-family protein, indicating transcriptional activity but providing little indication of metabolic function (Table S2.9). The genome contained several sodium and potassium transporters, but did not have an enrichment in acidic amino acids in predicted proteins (Figure S2.4B), leaving its osmoregulation strategy unclear. It should be noted that the above results are based on a single genome (62.8% completeness) and so should not be considered conclusive.

2.4.7 LH as an analogue for relevant microbial metabolisms on Mars

Terrestrial analogues like LH can help constrain and inform theorized habitability and biosignatures in ancient and extant Martian environments. This study provides in situ evidence of an active microbial ecosystem in a sub-zero hypersaline spring supporting Mars-relevant chemolithoautotrophic metabolisms (91, 92). We identified active ANME-1 putatively capable of AOM, H₂ oxidation, CO₂ fixation, and N₂ fixation. Trace methane (~0.4 ppbv) has been detected in the Mars atmosphere (93) and, while the source is unknown, methane and hydrogen could be produced abiotically in the deep subsurface through rock-water interactions (serpentization; Fischer-Tropsch synthesis) or through putative methanogenesis (Figure 2.6) (94). Regardless of the origin, subsurface gaseous methane or methane clathrates could potentially sustain microbial life by AOM.

Sulfates and trace H₂ (3) in LH support transcriptionally active H₂-oxidizing, SO₄-reducing bacteria containing CO₂-fixation and N₂-fixation genes. Similar conditions for supporting SRBs may exist in the Martian subsurface where sulfate is abundant and may co-localize with H₂ and CH₄ from serpentinization or methanogenesis (95). Atmospheric CO (0.075%) on Mars may also support CO-oxidizing bacteria (91), as in Antarctic desert soils where trace CO may support primary production through high-affinity CO dehydrogenases (96). In this study, CO dehydrogenase genes and transcripts were detected in mixotrophic *Alphaproteobacteria* MAGs, suggesting Martian CO could support near-surface heterotrophs.

The relatively high abundances of lithoautotrophic sulfide-oxidizing bacteria as well as high expression of S-oxidation genes was somewhat surprising given sulfide-oxidizers are generally aerobic while LH sediment is highly reducing and contains only trace O₂. However, extremely low-oxygen environments can sustain aerobic metabolisms (97), including sulfide oxidation in anoxic lakes (98), due to O₂ favorability as an electron acceptor. Gibbs energy calculations for LH show redox reactions with O₂ are more favorable than those with NO₃⁻ or SO₄²⁻, including H₂S/O₂ (-109 kJ/mol electron⁻¹) compared to H₂S/NO₃⁻ (-93.8 kJ/mol electron⁻¹) (Table S2.10). While the Martian atmosphere contains 0.1% O₂, modelling of perchlorate and sulfate brines under Martian surface conditions demonstrated how O₂ can concentrate in near-surface brines allowing for potential micro-oxic and even aerobic metabolisms (99). While methanogens and SRBs are generally considered the most likely candidate life forms on Mars, this study highlights the capability of lithoautotrophic sulfide-oxidizers to also thrive in a hypersaline, sub-zero, and oxygen-depleted environment.

2.5 Conclusion

Lost Hammer supports an active microbial community including sulfur-cycling *Gammaproteobacteria* and *Desulfobacterota* and methane-oxidizing ANME-1, as well as fermentative and heterotrophic populations. Overall, our study provides robust evidence of chemolithoautotrophic metabolisms active in a sub-zero, hypersaline, and anoxic environment similar to those that may exist on Mars.

2.6 Acknowledgements

We thank the Bigelow Single Cell Genomics Center for cell sorting services and support. E.M. was supported by a Natural Sciences and Engineering Research Council of Canada (NSERC) doctoral award (funding reference number CGSD2-534189-2019), Fonds de recherche du Québec – Nature et technologies (FRQNT) doctoral award (funding reference number 272792), and the Northern Scientific Training Program. This research was also supported by the Canada Research Chair Program, the NSERC Discovery and Northern Research Supplement Programs, and the Polar Continental Shelf Project (Arctic logistical support). Field work was carried out with appropriate licensing obtained from the territory of Nunavut and the Nunavut Research Institute (Nunavut Scientific Research License Nos. 02 043 17R-M and 02 051 19N-M).

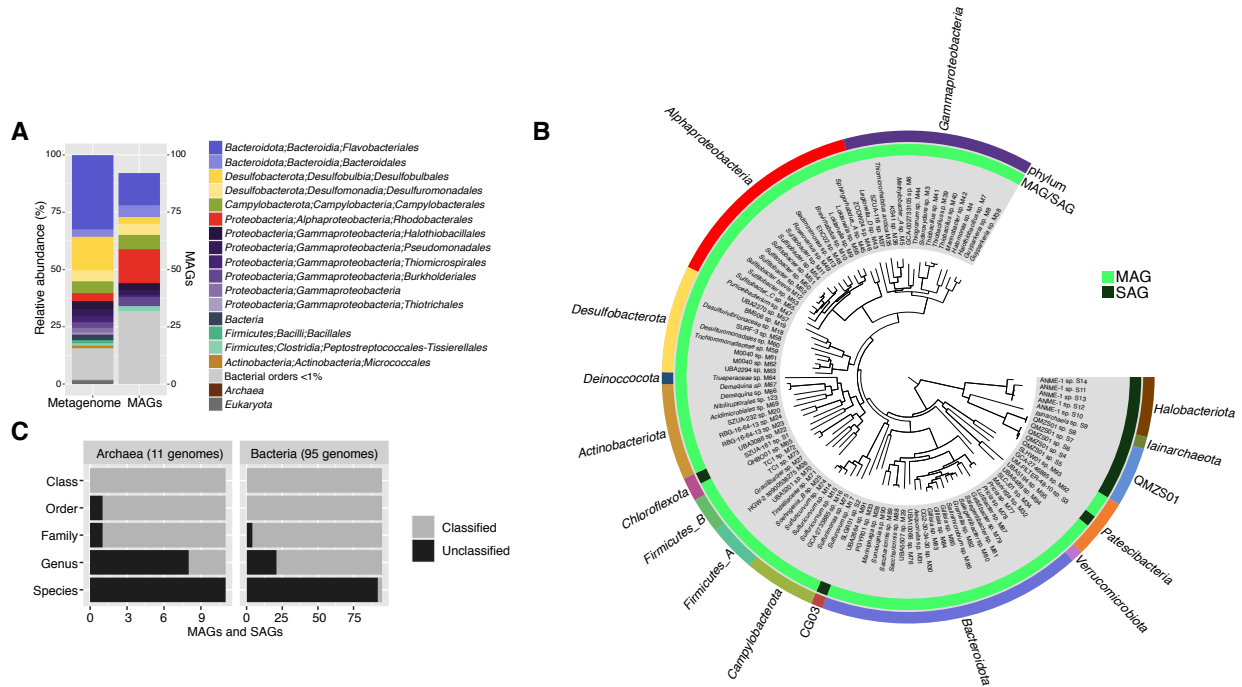


Figure 2.1. **A.** Comparison of metagenome taxonomic composition to MAG frequency by order. Metagenome taxonomic composition was determined with phyloFlash, based on classification of metagenomic reads mapping to the SILVA small subunit ribosomal database. **B.** Phylogenomic tree of high- and medium-quality MAGs and SAGs. The tree was constructed in Anvi'o with FastTree using the Bacteria_71 collection of single-copy genes and midpoint-rooted with FigTree. **C.** Level of taxonomic novelty of the MAGs and SAGs by rank. The number of classified and unclassified genomes at each taxonomic level was determined according to its rank assignment and taxonomic placement by GTDB-tk.

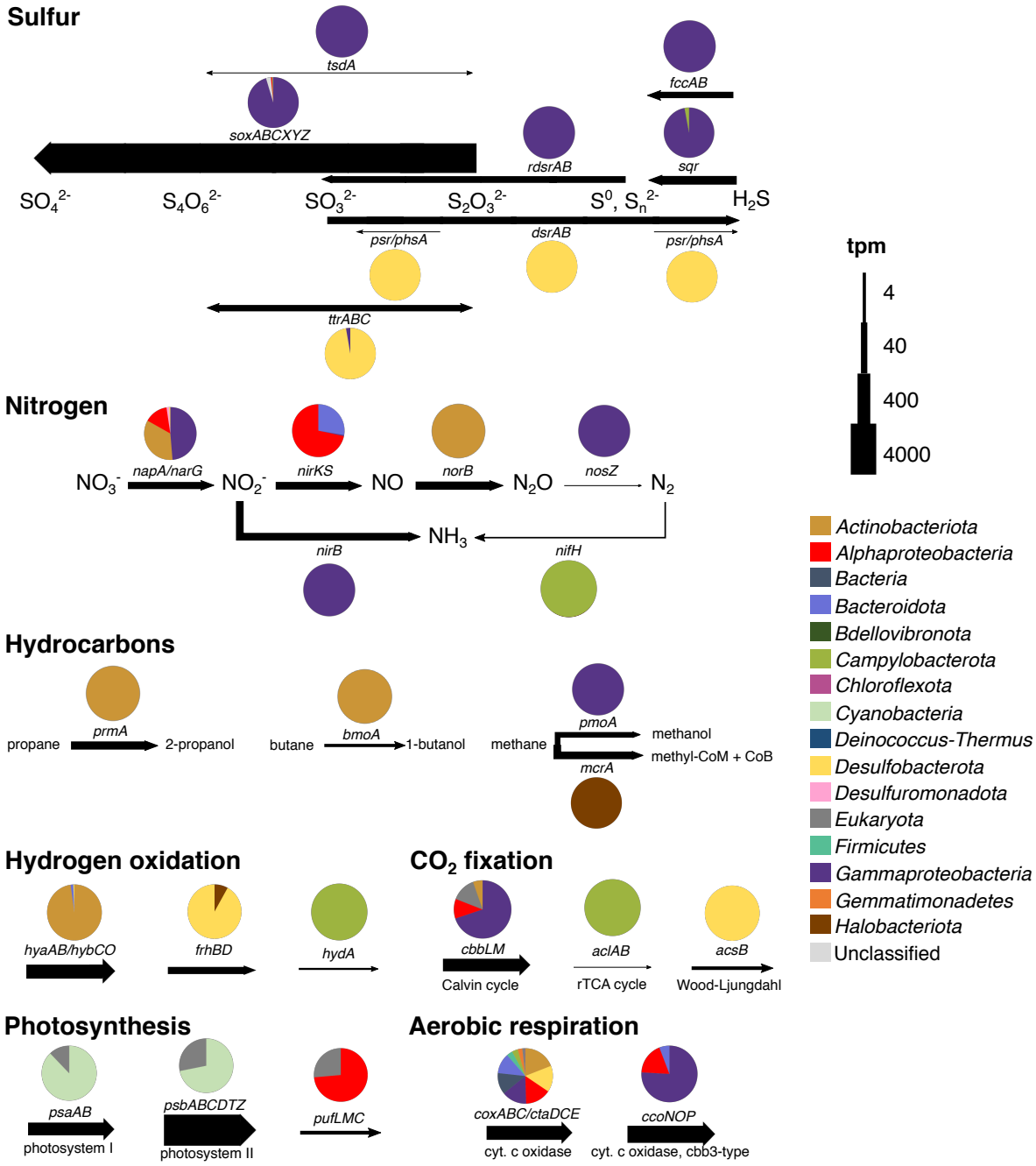


Figure 2.2. Key metabolic genes expressed in the LH spring sediment. Arrow width represents relative expression of genes in transcripts per million reads (tpm). Pie charts represent the phylogenetic classification of relative expression based on presence of the expressed gene in MAGs or SAGs or phylogenetic classification of the gene for unbinned genes. Complete distribution of tpm in MAGs, SAGs, and unbinned genes can be found in Table S2.7.

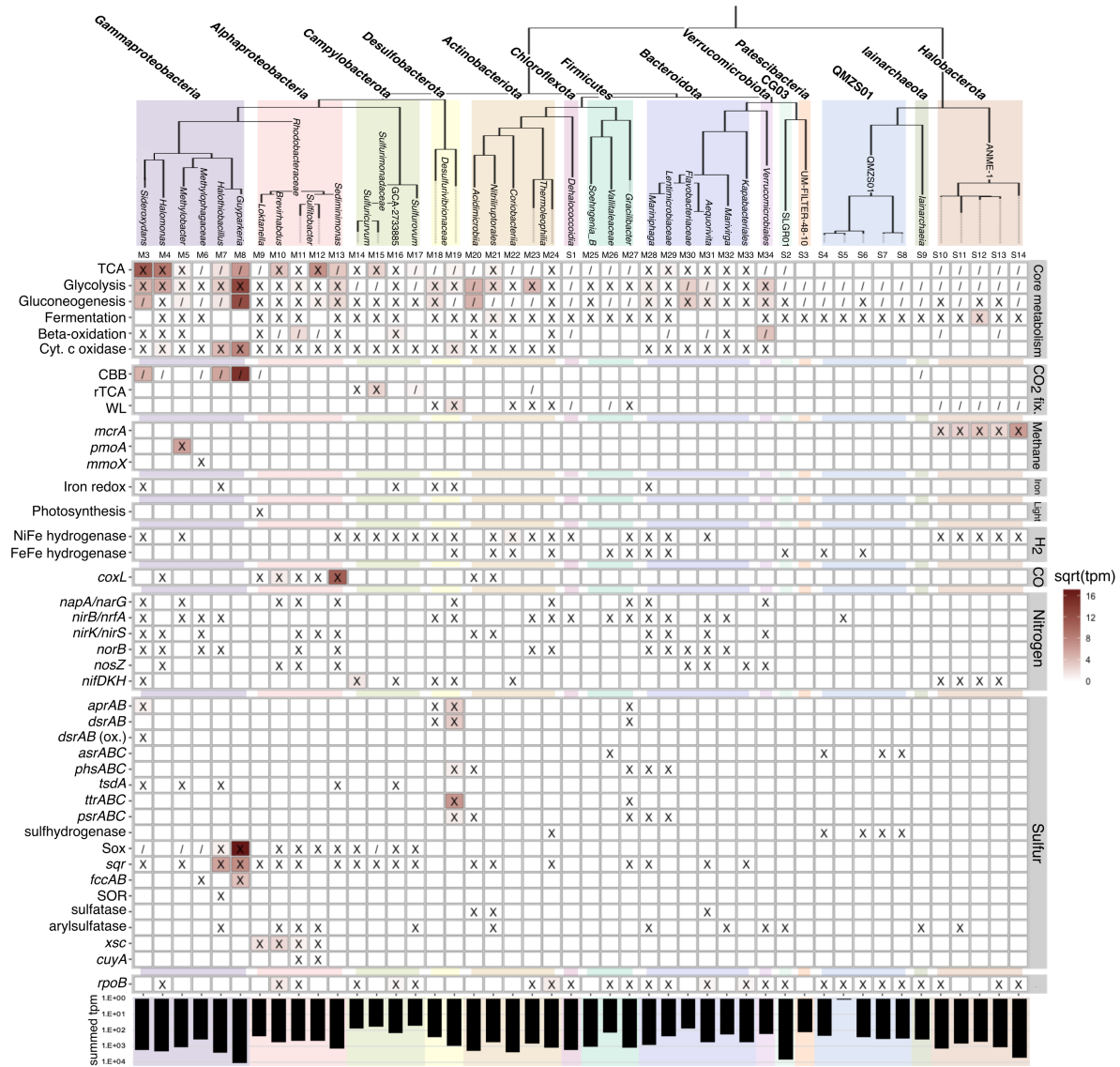


Figure 2.3. Metabolic potential and gene expression in high-quality MAGs and medium-quality SAGs. The identification number for each genome is noted above each column. An ‘X’ indicates the presence of a gene or pathway within the genome; ‘/’ indicates a partial pathway. A complete list of gene IDs and criteria used for denoting the presence of a complete or partial pathway is found in Tables S2.12 and S2.13. The square root of transcripts per million reads (tpm) of metatranscriptome reads mapped to the genome is indicated by a color scale within each square.

The summed tpm indicates the total tpm of reads mapped to the genome on a logarithmic scale.

A corresponding table for medium-quality MAGs is located in Table S2.8.

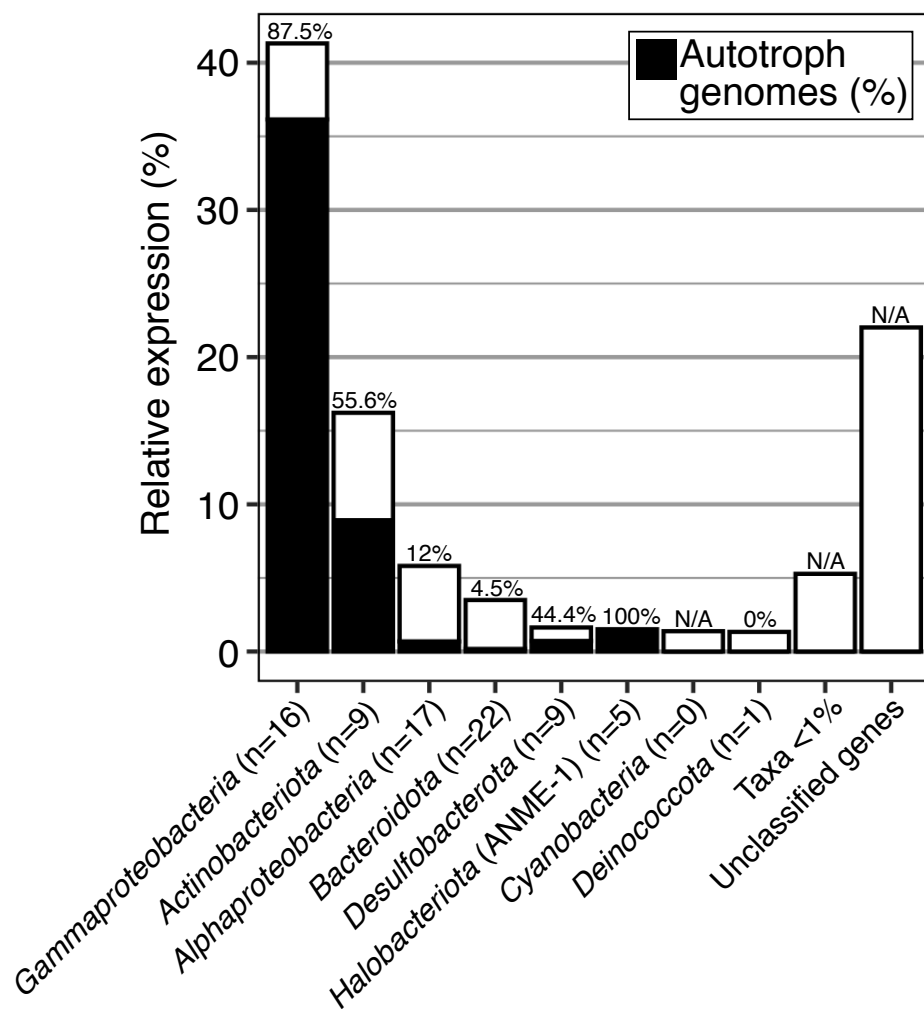


Figure 2.4. Percent relative expression by phylum, including both genes in MAGs and SAGs and unbinned genes classified by JGI. The percentage of autotrophic MAGs and SAGs (containing CO₂ fixation genes) in each phylum is indicated in black and noted above each column. The number of MAGs and SAGs in each phylum is indicated in parentheses in each column label. The percentage of relative expression by autotrophic microorganisms was estimated by multiplying the relative expression by the percentage of autotrophic genomes in each taxon.

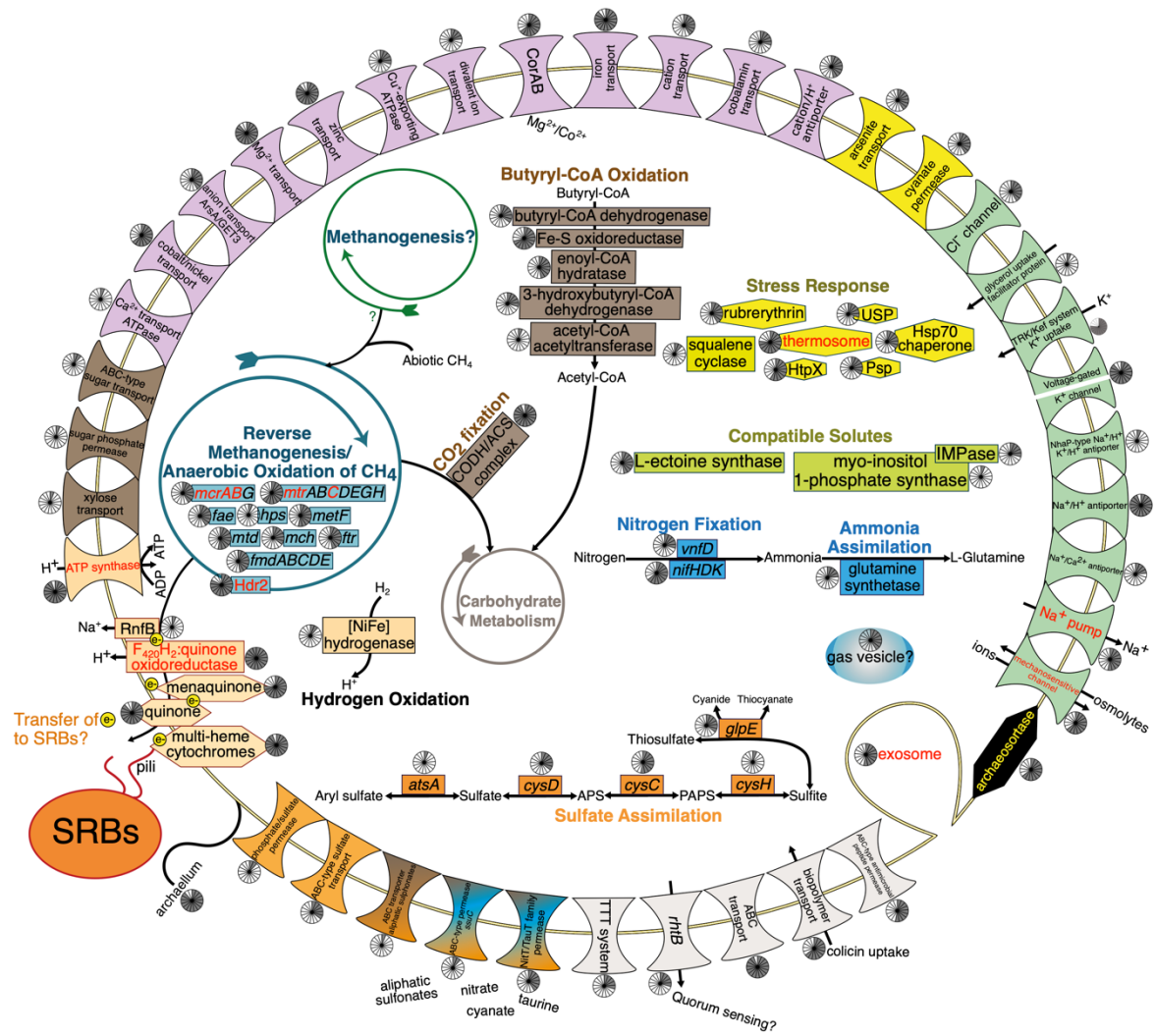


Figure 2.5. Metabolic reconstruction of ANME-1 SAGs. Genome contents were based on a composite of 17 medium- (SAGs S10-S14) and low-quality (SAGs S39-S50) ANME-1 SAGs. Genes with mapped transcripts are denoted by red text. Pie charts indicate the number of SAGs containing each gene (out of 17). A complete list of genes can be found in Table S2.14.

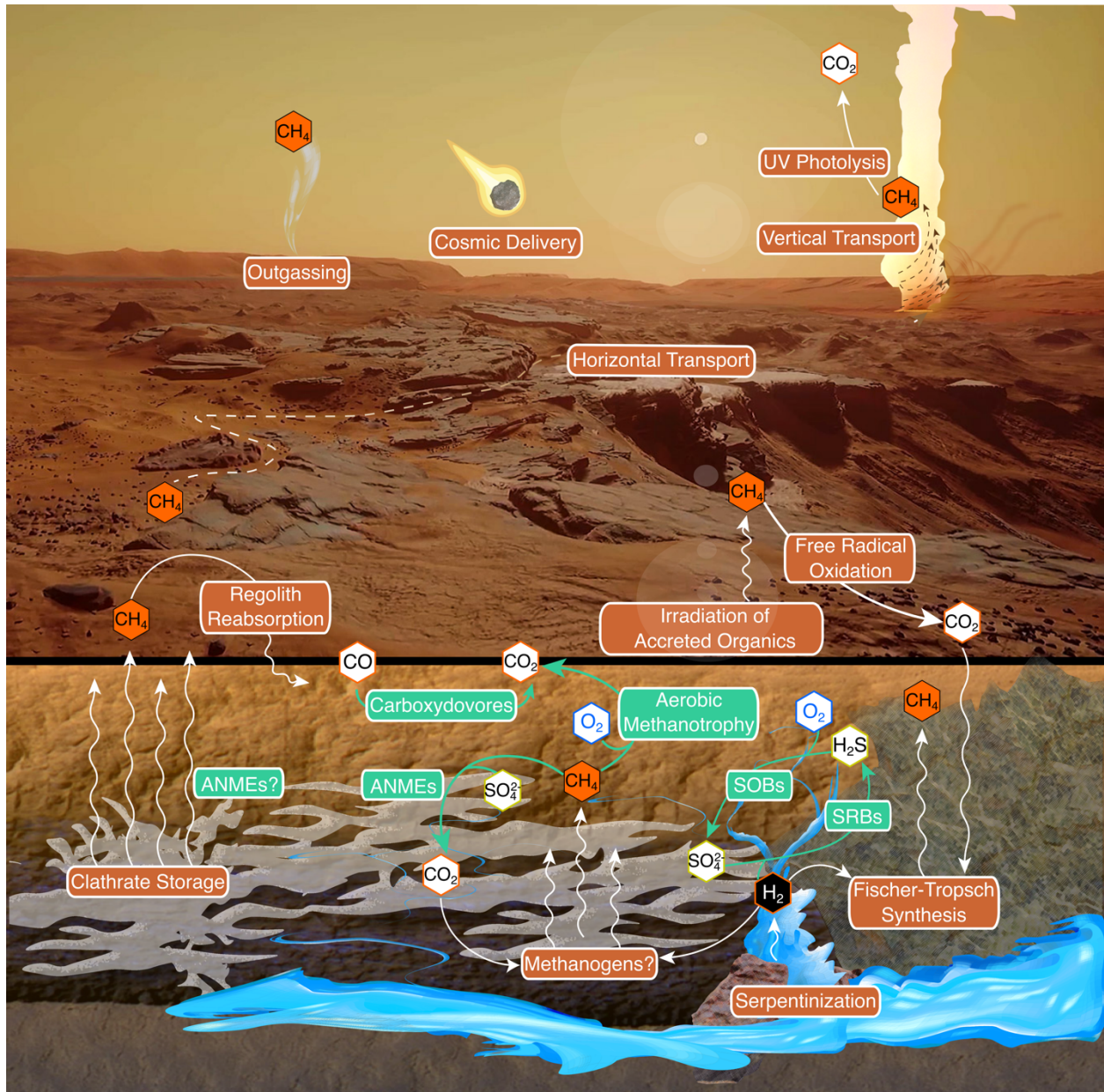


Figure 2.6. Model for a hypothetical Martian methane cycle, adapted and reproduced with permission from Harris et al. (2021) (92). Putative methane sources, sinks, and reservoirs are noted in orange. Mars-relevant metabolisms identified in Lost Hammer are noted in green.

2.7 References

1. Pollard W, Omelon C, Andersen D, McKay C. Perennial spring occurrence in the Expedition Fiord area of western Axel Heiberg Island, Canadian High Arctic. *Can J Earth Sci.* 1999;36:105-20.
2. Andersen DT. Cold springs in permafrost on Earth and Mars. *J Geophys Res.* 2002;107(E3):4-1-4-7.
3. Niederberger TD, Perreault NN, Tille S, Lollar BS, Lacrampe-Couloume G, Andersen D, et al. Microbial characterization of a subzero, hypersaline methane seep in the Canadian High Arctic. *ISME J.* 2010;4(10):1326-39.
4. Goordial J, Lamarche-Gagnon G, Lay CY, Whyte L. Left out in the cold: life in cryoenvironments. In: Seckbach J, Oren A, Stan-Lotter H (eds). *Polyextremophiles.* Springer, New York, 2013. pp. 335-64.
5. Gilichinsky D, Rivkina E, Bakermans C, Shcherbakova V, Petrovskaya L, Ozerskaya S, et al. Biodiversity of cryopegs in permafrost. *FEMS Microbiol Ecol.* 2005;53(1):117-28.
6. Rivkina EM, Friedmann EI, McKay CP, Gilichinsky DA. Metabolic activity of permafrost bacteria below the freezing point. *Appl Environ Microbiol.* 2000;66(8):3230-3.
7. Brown MV, Bowman JP. A molecular phylogenetic survey of sea-ice microbial communities (SIMCO). *FEMS Microbiol Ecol.* 2001;35:267-75.
8. Murray AE, Kenig F, Fritsen CH, McKay CP, Cawley KM, Edwards R, et al. Microbial life at -13 degrees C in the brine of an ice-sealed Antarctic lake. *Proc Natl Acad Sci USA.* 2012;109(50):20626-31.
9. Orosei R, Lauro SE, Pettinelli E, Cicchetti A, Coradini M, Cosciotti B, et al. Radar evidence of subglacial liquid water on Mars. *Science.* 2018;361(6401):490-3.

10. Lauro SE, Pettinelli E, Caprarelli G, Guallini L, Pio Rossi A, Mattei E, et al. Multiple subglacial water bodies below the south pole of Mars unveiled by new MARSIS data. *Nat Astron.* 2021;5:63-70.
11. Bishop JL, Yesilbas M, Hinman NW, Burton ZFM, Englert PAJ, Toner JD, et al. Martian subsurface cryosalt expansion and collapse as trigger for landslides. *Sci Adv.* 2021;7(6):1-13.
12. Allen CC, Oehler, D.Z. A case for ancient springs in Arabia Terra, Mars. *Astrobiology.* 2008;8(6):1093-112.
13. Battler MM, Osinski GR, Banerjee NR. Mineralogy of saline perennial cold springs on Axel Heiberg Island, Nunavut, Canada and implications for spring deposits on Mars. *Icarus.* 2013;224(2):364-81.
14. Leask EK, Ehlmann BL. Evidence for deposition of chloride on Mars from small-volume surface water events into the Late Hesperian-Early Amazonian. *AGU Adv.* 2022;3(1):1-19.
15. Howell SM, Pappalardo RT. NASA's Europa Clipper-a mission to a potentially habitable ocean world. *Nat Commun.* 2020;11(1):1-4.
16. Farley KA, Williford KH, Stack KM, Bhartia R, Chen A, de la Torre M, et al. Mars 2020 mission overview. *Space Sci Rev.* 2020;216(8):1-41.
17. Kargel JS, Kaye JZ, Head JW, Marion GM, Sassen R, Crowley JK, et al. Europa's crust and ocean: origin, composition, and the prospects for life. *Icarus.* 2000;148(1):226-65.
18. Taubner RS, Pappenreiter P, Zwicker J, Smrzka D, Pruckner C, Kolar P, et al. Biological methane production under putative Enceladus-like conditions. *Nat Commun.* 2018;9(1):1-11.
19. Lamarche-Gagnon G, Comery R, Greer CW, Whyte LG. Evidence of *in situ* microbial activity and sulphidogenesis in perennially sub-0 degrees C and hypersaline sediments of a high Arctic permafrost spring. *Extremophiles.* 2015;19(1):1-15.

20. Lay CY, Mykytczuk NC, Yergeau E, Lamarche-Gagnon G, Greer CW, Whyte LG. Defining the functional potential and active community members of a sediment microbial community in a high-arctic hypersaline subzero spring. *Appl Environ Microbiol.* 2013;79(12):3637-48.
21. Bolger AM, Lohse M, Usadel B. Trimmomatic: a flexible trimmer for Illumina sequence data. *Bioinformatics.* 2014;30(15):2114-20.
22. Menzel P, Ng KL, Krogh A. Fast and sensitive taxonomic classification for metagenomics with Kaiju. *Nat Commun.* 2016;7(1):1-9.
23. Gruber-Vodicka HR, Seah BKB, Pruesse E. phyloFlash: rapid small-subunit rRNA profiling and targeted assembly from metagenomes. *mSystems.* 2020;5(5):1-16.
24. Li D, Liu CM, Luo R, Sadakane K, Lam TW. MEGAHIT: an ultra-fast single-node solution for large and complex metagenomics assembly via succinct de Bruijn graph. *Bioinformatics.* 2015;31(10):1674-6.
25. Kang DD, Froula J, Egan R, Wang Z. MetaBAT, an efficient tool for accurately reconstructing single genomes from complex microbial communities. *PeerJ.* 2015;3:1-15.
26. Parks DH, Imelfort M, Skennerton CT, Hugenholtz P, Tyson GW. CheckM: assessing the quality of microbial genomes recovered from isolates, single cells, and metagenomes. *Genome Res.* 2015;25(7):1043-55.
27. Chen IA, Chu K, Palaniappan K, Ratner A, Huang J, Huntemann M, et al. The IMG/M data management and analysis system v.6.0: new tools and advanced capabilities. *Nucleic Acids Res.* 2020;49(D1):D751–D63.
28. Mukherjee S, Stamatis D, Bertsch J, Ovchinnikova G, Sundaramurthi JC, Lee J, et al. Genomes OnLine Database (GOLD) v.8: overview and updates. *Nucleic Acids Res.* 2020;49(D1):D723-D733.

29. Chaumeil PA, Mussig AJ, Hugenholtz P, Parks DH. GTDB-Tk: a toolkit to classify genomes with the Genome Taxonomy Database. *Bioinformatics*. 2019;36(6):1925–7.
30. Schmieder R, Edwards R. Fast identification and removal of sequence contamination from genomic and metagenomic datasets. *PLoS One*. 2011;6(3):1-11.
31. Bankevich A, Nurk S, Antipov D, Gurevich AA, Dvorkin M, Kulikov AS, et al. SPAdes: a new genome assembly algorithm and its applications to single-cell sequencing. *J Comput Biol*. 2012;19(5):455-77.
32. Kopylova E, Noe L, Touzet H. SortMeRNA: fast and accurate filtering of ribosomal RNAs in metatranscriptomic data. *Bioinformatics*. 2012;28(24):3211-7.
33. Langmead B, Salzberg SL. Fast gapped-read alignment with Bowtie 2. *Nat Methods*. 2012;9(4):357-9.
34. Anders S, Pyl PT, Huber W. HTSeq--a Python framework to work with high-throughput sequencing data. *Bioinformatics*. 2015;31(2):166-9.
35. Royo-Llonch M, Sanchez P, Ruiz-Gonzalez C, Salazar G, Pedros-Alio C, Sebastian M, et al. Compendium of 530 metagenome-assembled bacterial and archaeal genomes from the polar Arctic Ocean. *Nat Microbiol*. 2021;6(12):1561-74.
36. Ghosh W, Dam B. Biochemistry and molecular biology of lithotrophic sulfur oxidation by taxonomically and ecologically diverse bacteria and archaea. *FEMS Microbiol Rev*. 2009;33(6):999-1043.
37. Boden R. Reclassification of *Halothiobacillus hydrothermalis* and *Halothiobacillus halophilus* to *Guyparkeria* gen. nov. in the *Thioalkalibacteraceae* fam. nov., with emended descriptions of the genus *Halothiobacillus* and family *Halothiobacillaceae*. *Int J Syst Evol Microbiol*. 2017;67(10):3919-28.

38. Sorokin DY, Abbas B, van Zessen E, Muyzer G. Isolation and characterization of an obligately chemolithoautotrophic *Halothiobacillus* strain capable of growth on thiocyanate as an energy source. *FEMS Microbiol Lett.* 2014;354(1):69-74.
39. Meier DV, Pjevac P, Bach W, Hourdez S, Girguis PR, Vidoudez C, et al. Niche partitioning of diverse sulfur-oxidizing bacteria at hydrothermal vents. *ISME J.* 2017;11(7):1545-58.
40. Headd B, Engel AS. Evidence for niche partitioning revealed by the distribution of sulfur oxidation genes collected from areas of a terrestrial sulfidic spring with differing geochemical conditions. *Appl Environ Microbiol.* 2013;79(4):1171-82.
41. Preisig O, Zufferey R, Thoney-Meyer L, Appleby CA, Hennecke H. A high-affinity cbb3-type cytochrome oxidase terminates the symbiosis-specific respiratory chain of *Bradyrhizobium japonicum*. *J Bacteriol.* 1996;178(6):1532-8.
42. Mikucki JA, Pearson A, Johnston DT, Turchyn AV, Farquhar J, Schrag DP, et al. A contemporary microbially maintained subglacial ferrous “ocean”. *Science.* 2009;324:397-400.
43. Ruff SE, Biddle JF, Teske AP, Knittel K, Boetius A, Ramette A. Global dispersion and local diversification of the methane seep microbiome. *Proc Natl Acad Sci USA.* 2015;112(13):4015-20.
44. Lloyd KG, Lapham L, Teske A. An anaerobic methane-oxidizing community of ANME-1b archaea in hypersaline Gulf of Mexico sediments. *Appl Environ Microbiol.* 2006;72(11):7218-30.
45. Maignien L, Parkes RJ, Cragg B, Niemann H, Knittel K, Coulon S, et al. Anaerobic oxidation of methane in hypersaline cold seep sediments. *FEMS Microbiol Ecol.* 2013;83(1):214-31.

46. Campen R, Kowalski J, Lyons WB, Tulaczyk S, Dachwald B, Pettit E, et al. Microbial diversity of an Antarctic subglacial community and high-resolution replicate sampling inform hydrological connectivity in a polar desert. *Environ Microbiol.* 2019;21(7):2290-306.
47. Cooper ZS, Rapp JZ, Carpenter SD, Iwahana G, Eicken H, Deming JW. Distinctive microbial communities in subzero hypersaline brines from Arctic coastal sea ice and rarely sampled cryopegs. *FEMS Microbiol Ecol.* 2019;95(12):1-15.
48. Winkel M, Mitzscherling J, Overduin PP, Horn F, Winterfeld M, Rijkers R, et al. Anaerobic methanotrophic communities thrive in deep submarine permafrost. *Sci Rep.* 2018;8(1):1-13.
49. Lay CY, Mykytczuk NC, Niederberger TD, Martineau C, Greer CW, Whyte LG. Microbial diversity and activity in hypersaline high Arctic spring channels. *Extremophiles.* 2012;16(2):177-91.
50. Bhattarai S, Cassarini C, Lens PNL. Physiology and distribution of archaeal methanotrophs that couple anaerobic oxidation of methane with sulfate reduction. *Microbiol Mol Biol Rev.* 2019;83(3):1-31.
51. Kleindienst S, Ramette A, Amann R, Knittel K. Distribution and in situ abundance of sulfate-reducing bacteria in diverse marine hydrocarbon seep sediments. *Environ Microbiol.* 2012;14(10):2689-710.
52. Timmers PH, Welte CU, Koehorst JJ, Plugge CM, Jetten MS, Stams AJ. Reverse methanogenesis and respiration in methanotrophic archaea. *Archaea.* 2017;2017:1-22.
53. Leu AO, Cai C, McIlroy SJ, Southam G, Orphan VJ, Yuan Z, et al. Anaerobic methane oxidation coupled to manganese reduction by members of the *Methanoperedenaceae*. *ISME J.* 2020;14(4):1030-41.

54. Haroon MF, Hu S, Shi Y, Imelfort M, Keller J, Hugenholtz P, et al. Anaerobic oxidation of methane coupled to nitrate reduction in a novel archaeal lineage. *Nature*. 2013;500(7464):567-70.
55. Cai C, Leu AO, Xie GJ, Guo J, Feng Y, Zhao JX, et al. A methanotrophic archaeon couples anaerobic oxidation of methane to Fe(III) reduction. *ISME J*. 2018;12(8):1929-39.
56. Oshkin IY, Wegner CE, Luke C, Glagolev MV, Filippov IV, Pimenov NV, et al. Gammaproteobacterial methanotrophs dominate cold methane seeps in floodplains of West Siberian rivers. *Appl Environ Microbiol*. 2014;80(19):5944-54.
57. Cabrol L, Thalasso F, Gandois L, Sepulveda-Jauregui A, Martinez-Cruz K, Teisserenc R, et al. Anaerobic oxidation of methane and associated microbiome in anoxic water of Northwestern Siberian lakes. *Sci Total Environ*. 2020;736:1-16.
58. Orcutt B, Boetius A, Elvert M, Samarkin V, Joye SB. Molecular biogeochemistry of sulfate reduction, methanogenesis and the anaerobic oxidation of methane at Gulf of Mexico cold seeps. *Geochim Cosmochim Acta*. 2005;69(17):4267-81.
59. Knittel K, Losekann T, Boetius A, Kort R, Amann R. Diversity and distribution of methanotrophic archaea at cold seeps. *Appl Environ Microbiol*. 2005;71(1):467-79.
60. Schubert CJ, Coolen MJ, Neretin LN, Schippers A, Abbas B, Durisch-Kaiser E, et al. Aerobic and anaerobic methanotrophs in the Black Sea water column. *Environ Microbiol*. 2006;8(10):1844-56.
61. Wang J, Hua M, Cai C, Hu J, Wang J, Yang H, et al. Spatial-temporal pattern of sulfate-dependent anaerobic methane oxidation in an intertidal zone of the East China Sea. *Appl Environ Microbiol*. 2019;85(7):1-15.

62. Dykstra S, Bischof K, Fuchs BM, Hoffmann K, Meier D, Meyerdierks A, et al. Ubiquitous Gammaproteobacteria dominate dark carbon fixation in coastal sediments. *ISME J*. 2016;10(8):1939-53.
63. Perreault NN, Greer CW, Andersen DT, Tille S, Lacrampe-Couloume G, Lollar BS, et al. Heterotrophic and autotrophic microbial populations in cold perennial springs of the high Arctic. *Appl Environ Microbiol*. 2008;74(22):6898-907.
64. Cordero PRF, Bayly K, Man Leung P, Huang C, Islam ZF, Schittenhelm RB, et al. Atmospheric carbon monoxide oxidation is a widespread mechanism supporting microbial survival. *ISME J*. 2019;13(11):2868-81.
65. Nigro LM, Elling FJ, Hinrichs KU, Joye SB, Teske A. Microbial ecology and biogeochemistry of hypersaline sediments in Orca Basin. *PLoS One*. 2020;15(4):1-25.
66. Rath KM, Fierer N, Murphy DV, Rousk J. Linking bacterial community composition to soil salinity along environmental gradients. *ISME J*. 2019;13(3):836-46.
67. Yoon JH, Lee MH, Kang SJ, Oh TK. *Salegentibacter salinarum* sp. nov., isolated from a marine solar saltern. *Int J Syst Evol Microbiol*. 2008;58(2):365-9.
68. Sangwan N, Xia F, Gilbert JA. Recovering complete and draft population genomes from metagenome datasets. *Microbiome*. 2016;4:1-11.
69. Goordial J, Raymond-Bouchard I, Zolotarov Y, de Bethencourt L, Ronholm J, Shapiro N, et al. Cold adaptive traits revealed by comparative genomic analysis of the eurypsychrophile *Rhodococcus* sp. JG3 isolated from high elevation McMurdo Dry Valley permafrost, Antarctica. *FEMS Microbiol Ecol*. 2016;92(2):1-11.

70. Laso-Perez R, Wegener G, Knittel K, Widdel F, Harding KJ, Krukenberg V, et al. Thermophilic archaea activate butane via alkyl-coenzyme M formation. *Nature*. 2016;539(7629):396-401.
71. Dombrowski N, Teske AP, Baker BJ. Expansive microbial metabolic versatility and biodiversity in dynamic Guaymas Basin hydrothermal sediments. *Nat Commun*. 2018;9(1):1-13.
72. Oren A. Thermodynamic limits to microbial life at high salt concentrations. *Environ Microbiol*. 2011;13(8):1908-23.
73. Gunde-Cimerman N, Plemenitas A, Oren A. Strategies of adaptation of microorganisms of the three domains of life to high salt concentrations. *FEMS Microbiol Rev*. 2018;42(3):353-75.
74. Hechler T, Pfeifer F. Anaerobiosis inhibits gas vesicle formation in halophilic *Archaea*. *Mol Microbiol*. 2009;71(1):132-45.
75. Stokke R, Roalkvam I, Lanzen A, Haflidason H, Steen IH. Integrated metagenomic and metaproteomic analyses of an ANME-1-dominated community in marine cold seep sediments. *Environ Microbiol*. 2012;14(5):1333-46.
76. Wegener G, Krukenberg V, Riedel D, Tegetmeyer HE, Boetius A. Intercellular wiring enables electron transfer between methanotrophic archaea and bacteria. *Nature*. 2015;526(7574):587-90.
77. Skennerton CT, Chourey K, Iyer R, Hettich RL, Tyson GW, Orphan VJ. Methane-fueled syntrophy through extracellular electron transfer: uncovering the genomic traits conserved within diverse bacterial partners of anaerobic methanotrophic archaea. *mBio*. 2017;8(4):1-14.
78. Krukenberg V, Riedel D, Gruber-Vodicka HR, Buttigieg PL, Tegetmeyer HE, Boetius A, et al. Gene expression and ultrastructure of meso- and thermophilic methanotrophic consortia. *Environ Microbiol*. 2018;20(5):1651-66.

79. Youssef NH, Rinke C, Stepanauskas R, Farag I, Woyke T, Elshahed MS. Insights into the metabolism, lifestyle and putative evolutionary history of the novel archaeal phylum '*Diapherotrites*'. ISME J. 2015;9(2):447-60.
80. Castelle CJ, Brown CT, Anantharaman K, Probst AJ, Huang RH, Banfield JF. Biosynthetic capacity, metabolic variety and unusual biology in the CPR and DPANN radiations. Nat Rev Microbiol. 2018;16(10):629-45.
81. Rinke C, Schwientek P, Sczyrba A, Ivanova NN, Anderson IJ, Cheng JF, et al. Insights into the phylogeny and coding potential of microbial dark matter. Nature. 2013;499(7459):431-7.
82. Dombrowski N, Lee JH, Williams TA, Offre P, Spang A. Genomic diversity, lifestyles and evolutionary origins of DPANN archaea. FEMS Microbiol Lett. 2019;366(2):1-12.
83. Wong HL, MacLeod FI, White RA, 3rd, Visscher PT, Burns BP. Microbial dark matter filling the niche in hypersaline microbial mats. Microbiome. 2020;8(1):1-14.
84. Schut GJ, Nixon WJ, Lipscomb GL, Scott RA, Adams MW. Mutational analyses of the enzymes involved in the metabolism of hydrogen by the hyperthermophilic archaeon *Pyrococcus furiosus*. Front Microbiol. 2012;3:1-6.
85. Ruuskanen MO, Colby G, St. Pierre KA, St. Louis VL, Aris-Brosou S, Poulain AJ. Microbial genomes retrieved from High Arctic lake sediments encode for adaptation to cold and oligotrophic environments. Limnol Oceanogr. 2020;65(S1):S233-S247.
86. Vigneron A, Cruaud P, Lovejoy C, Vincent WF. Genomic evidence of functional diversity in DPANN archaea, from oxic species to anoxic vampiristic consortia. ISME Commun. 2022;2(1):1-10.

87. Parks DH, Chuvochina M, Waite DW, Rinke C, Skarshewski A, Chaumeil PA, et al. A standardized bacterial taxonomy based on genome phylogeny substantially revises the tree of life. *Nat Biotechnol.* 2018;36(10):996-1004.
88. Meheust R, Castelle CJ, Matheus Carnevali PB, Farag IF, He C, Chen LX, et al. Groundwater *Elusimicrobia* are metabolically diverse compared to gut microbiome *Elusimicrobia* and some have a novel nitrogenase paralog. *ISME J.* 2020;14(12):2907-22.
89. Hahn CR, Farag IF, Murphy CL, Podar M, Elshahed MS, Youssef NH. Microbial diversity and sulfur cycling in an early earth analogue: from ancient novelty to modern commonality. Preprint at <https://doi.org/10.1101/2021.07.05.451135>. 2021.
90. Yang J, Yan R, Roy A, Xu D, Poisson J, Zhang Y. The I-TASSER Suite: protein structure and function prediction. *Nat Methods.* 2015;12(1):7-8.
91. Rummel JD, Beaty DW, Jones MA, Bakermans C, Barlow NG, Boston PJ, et al. A new analysis of Mars "Special Regions": findings of the second MEPAG Special Regions Science Analysis Group (SR-SAG2). *Astrobiology.* 2014;14(11):887-968.
92. Harris RL, Schuerger AC, Wang W, Tamama Y, Garvin ZK, Onstott TC. Transcriptional response to prolonged perchlorate exposure in the methanogen *Methanosarcina barkeri* and implications for Martian habitability. *Sci Rep.* 2021;11(1):1-16.
93. Webster CR, Mahaffy PR, Atreya SK, Moores JE, Flesch GJ, Malespin C, et al. Background levels of methane in Mars' atmosphere show strong seasonal variations. *Science.* 2018;360:1093-6.
94. Oehler DZ, Etiope G. Methane seepage on Mars: where to look and why. *Astrobiology.* 2017;17(12):1233-64.

95. Marlow JJ, Larowe DE, Ehlmann BL, Amend JP, Orphan VJ. The potential for biologically catalyzed anaerobic methane oxidation on ancient Mars. *Astrobiology*. 2014;14(4):292-307.
96. Ji M, Greening C, Vanwonterghem I, Carere CR, Bay SK, Steen JA, et al. Atmospheric trace gases support primary production in Antarctic desert surface soil. *Nature*. 2017;552(7685):400-3.
97. Berg J, Ahmerkamp S, Pjevac P, Hausmann B, Milucka J, Kuypers MMM. How low can they go? Aerobic respiration by microorganisms under apparent anoxia. *FEMS Microbiol Rev*. 2022:1-37.
98. Berg JS, Pjevac P, Sommer T, Buckner CRT, Philippi M, Hach PF, et al. Dark aerobic sulfide oxidation by anoxygenic phototrophs in anoxic waters. *Environ Microbiol*. 2019;21(5):1611-26.
99. Stamenković V, Ward LM, Mischna M, Fischer WW. O₂ solubility in Martian near-surface environments and implications for aerobic life. *Nat Geosci*. 2018;11(12):905-9.

Connecting Text

Chapter 2 of this study described novel microbial genomes and in situ gene expression in a sub-zero, hypersaline methane seep. This chapter aimed to further examine microbial diversity and activity under cold and hypersaline conditions in the cryosphere. I utilized genome-resolved metagenomics and metatranscriptomics to describe active sulfur cycling in Gypsum Hill Spring and characterize the functional capabilities of highly active microorganisms. I additionally discussed the potential implications for the search for microbial life in extraterrestrial cold brines.

Supplementary tables S3.1 and S3.4 – S3.14 are available as supplemental material.

**Chapter 3. Sulfur-cycling chemolithoautotrophic microbial community dominates a cold,
anoxic, hypersaline Arctic spring**

Elisse Magnuson¹, Ianina Altshuler², Nastasia J. Freyria¹, Lyle G. Whyte¹

¹Natural Resource Sciences, McGill University, Ste-Anne-de-Bellevue, QC, Canada

²School of Architecture, Civil and Environmental Engineering, Ecole Polytechnique Fédérale de
Lausanne, Lausanne, Switzerland

3.1 Abstract

Gypsum Hill Spring, located in Nunavut in the Canadian High Arctic, is a rare example of a cold spring arising through thick permafrost. It perennially discharges cold (~ 7 °C), hypersaline (7-8 % salinity), anoxic (~ 0.04 ppm O_2), and highly reducing (~ -430 mV) brines rich in sulfate (2.2 g.L⁻¹) and sulfide (9.5 ppm), making Gypsum Hill an analogue to putative sulfate-rich briny habitats on extraterrestrial bodies such as Mars. Genome-resolved metagenomics and metatranscriptomics were utilized to describe an active microbial community containing novel metagenome-assembled genomes and dominated by sulfur cycling *Desulfurobacterota* and *Gammaproteobacteria*. Sulfate reduction was dominated by hydrogen-oxidizing chemolithoautotrophic *Desulfovibrionaceae* sp. and was identified in phyla not typically associated with sulfate reduction in novel lineages of *Spirochaetota* and *Bacteroidota*. Highly abundant and active sulfur-reducing *Desulfuromusa* sp. highly expressed non-coding RNAs associated with transcriptional regulation, showing potential evidence of putative metabolic flexibility in response to substrate availability. Despite low oxygen availability, sulfide oxidation was primarily attributed to aerobic chemolithoautotrophic *Halothiobacillaceae*. Low abundance and expression of photoautotrophs indicated sulfur-based chemolithoautotrophy drives primary productivity even during periods of constant illumination. Our results describe an active chemolithoautotrophic sulfur cycling microbial community inhabiting a unique hypersaline spring, providing insights into the microbial life and biosignatures that may be present in similar environments on Mars.

3.2 Introduction

The cold saline springs on Axel Heiberg Island (AHI), located in the High Arctic in Nunavut, Canada, are rare examples of non-volcanic perennial springs discharging in an area of continuous permafrost. The Gypsum Hill (GH) springs (79°24'30''N, 90°43'05''W) are a collection of approximately 40 springs and seeps located on the bank of Expedition River. These springs flow to the surface through 500-600 meters of permafrost in an area of gypsum-anhydrite diapiric uplift, and are suggested to originate in a subsurface salt layer recharged by an ice-covered alpine lake or sub-glacial meltwater (1). They are characteristically cold (~ -1.3 – 7.2 °C) and hypersaline (7-8 % salinity) and maintain stable conditions year-round despite average air temperatures of -15 °C, reaching down to -40 °C in the winter (2). Sediments and waters in the largest spring outlet, referred to as GH-4, are sub-oxic (~0.04 ppm O₂), highly reducing (~ -430 mV oxidation-reduction potential), saturated in dissolved gases (99 % N₂), and rich in sulfate (1.9 g.kg⁻¹ and 2.2 g.L⁻¹ respectively) and sulfide (9.5 ppm) (3, 4).

The AHI saline springs have been described extensively as analogues to sulfurous, cold, saline environments on extraterrestrial bodies such as Mars (1, 5-7). As warm, wet ancient Mars became colder and drier during the Hesperian (~3.7 Gya), the last surface waters were likely cold brines persisting up to 2 Gya (8); sulfate salt enrichments in the former lake basin Gale Crater indicate the presence of widespread sulfate-rich brines during this time (9). The modern Martian surface and subsurface are also rich in Mg- and Ca-sulfates (10). While the atmospheric pressure and temperature on present-day Mars prevents the formation of surficial liquid water, there are potential sources of liquid water in the Martian subsurface. Recent evidence suggests the presence of hypersaline lakes below Mars' southern ice cap (11). Another possible source of liquid water is the recurring slope lineae; recent modelling suggests they may form from near-

surface chloride and sulfate salt brines (12). Geomorphological features resembling gullies formed in the recent geologic past (13) are suggested to have formed from subsurface eutectic brines (14). Thus, the GH springs provide a useful analogue for examining microbial diversity in a sulfate-rich cryoenvironment such as those that may exist or have existed on Mars.

Cycling of inorganic sulfur compounds sustains microbial life in sulfur-rich terrestrial environments including hydrothermal vents (15, 16), marine sediments (17), and sulfidic springs (18, 19), where chemolithoautotrophic sulfur-oxidizing bacteria drive primary production. Sulfur-oxidizing anoxygenic phototrophs inhabit a wide range of anoxic environments, and some can act as primary producers in environments such as hot springs (20) and meromictic lakes (21). Oxidation of sulfide and other reduced sulfur intermediates can be carried out by diverse microorganisms utilizing a multiplicity of oxidation enzymes and biochemical pathways, thus contributing to overall microbial and functional diversity in these environments (17). In the cryosphere, chemolithoautotrophic S-cycling microbes drive primary productivity in a High Arctic sulfur-rich supraglacial spring at Borup Fjord Pass, Ellesmere Island (22), sulfide-rich thermal springs in Svalbard, Norway (22, 23), and sulfate-rich subglacial brines at Blood Falls, Antarctica (24), and have been detected in cold hypersaline environments such as cryopegs (25) and Antarctic lake brines (26). Microbial communities at other hypersaline AHI springs contain abundant sulfur-oxidizing *Gammaproteobacteria* and sulfate-reducing *Desulfobacterota* (formerly *Deltaproteobacteria*) (6, 27). However, microbial community sequencing in many of these cryospheric S-cycling environments, including GH, has been limited to 16S rRNA community profiling or 16S rRNA gene sequencing of isolates. Recent high-throughput shotgun metagenomic and metatranscriptomic sequencing of nearby hypersaline, sub-zero Lost Hammer

Spring revealed previously-undetected bacterial and archaeal species and identified active sulfide-oxidizing *Gammaproteobacteria* driving primary production (27), demonstrating the power of these sequencing approaches in describing sulfur cycling and microbial diversity in these cryospheric Mars analogues. Detection of active microorganisms through approaches such as metatranscriptomic or metaproteomic sequencing are especially crucial in open-system anoxic, cold, hypersaline environments like GH, where dormant or dead populations may be present and organic matter including DNA may be preserved (5). Indeed, detected active microbial communities at AHI springs including Lost Hammer differ from the total microbial biomass (6, 27, 28).

Previous studies of the GH sediment community indicate the presence of a chemolithoautotrophic, primarily sulfur-oxidizing microbial community ($10^6 - 10^7$ cells.g⁻¹ sediment) (3, 4, 29). Sequencing of 16S rRNA genes identified *Gammaproteobacteria* and *Desulfobacterota* phylotypes associated with sulfur cycling (3, 4, 30, 31), and microcosm activity measurements and isotopic analyses indicate sulfur oxidation and sulfate reduction occur in the GH spring sediments (4, 29, 32). However, due to methodological limitations, no studies have yet fully described the taxonomic and metabolic diversity present in the sediment or definitively linked detected metabolic activities to active taxa in situ. As such, this study utilized genome-resolved metagenomics and metatranscriptomics to identify the primary active microbial community in the springs and characterize sulfur cycling metabolisms and taxa in depth in the context of the GH springs as a unique cryospheric analogue to sulfate-rich environments on Mars.

3.3 Materials and Methods

3.3.1 Site description and sampling

As described in previous publications (1-4), the GH springs emerge in approximately 40 outlets across a 300-meter length of the Expedition River bank, 2.5 km downstream from the White and Thompson glaciers. This region experiences seasonal darkness from ~October to February.

Gypsum (CaSO_4), halite (NaCl), and elemental sulfur are the most abundant minerals across the GH site (5). The spring outlet described in this study is referred to here and in previous publications as GH-4. At GH-4, spring water emerges from the subsurface into a primary pool, measuring ~1.7 meters in diameter with a depth of ~45 centimeters, then flows into a shallow outflow channel (Figure S3.1). Dissolved gases bubble continuously through the outflow pool sediment and water and are predominantly comprised of N_2 (~ 99 %) with low levels of CO_2 (0.04 %) and CH_4 (0.5 %) (4, 33). All spring samples and measurements described in this study were taken in the primary outflow pool of GH-4.

Physical and chemical parameters in GH-4 have remained highly stable since 2007 (Table S3.1), allowing for comparison of samples collected in different years. Sediment samples (top ~10 cm) for metagenomic and metatranscriptomic sequencing were collected in July 2019, and sediment samples for 16S rRNA gene community profiling were collected in August 2021. All sediment samples were collected with a sterilized scoop and mixed immediately with Zymo Research DNA/RNA Shield (Irvine, CA, USA) in a sterile Falcon tube filled to maximum to avoid aerobic headspace. Samples were frozen at $-20\text{ }^\circ\text{C}$ after sampling, then kept at $<7\text{ }^\circ\text{C}$ during transport to Montréal where they were again stored at $-20\text{ }^\circ\text{C}$ prior to processing. Thermochron Temperature

Loggers (Baulkham Hills, NSW, Australia) were used to track temperature conditions during transport.

Water temperature, pH, oxidation-reduction potential, salinity, and total dissolved solids were measured in situ with a YSI Professional Plus Multiparameter Instrument (Yellow Springs, OH, USA). Dissolved oxygen was measured in situ with a PyroScience Piccolo2 oxygen meter (Aachen, Germany). Sulfide, sulfate, nitrite, nitrate, phosphate, ammonia, and iron were measured in situ with CHEMetrics Inc. (Midland, VA, USA) test kits. Water for total carbon and total nitrogen measurements was filtered immediately after sampling with a 0.22 μm Whatman Uniflo PES filter (Madstone, UK). Filtered water was stored at $-20\text{ }^{\circ}\text{C}$ and thawed at $4\text{ }^{\circ}\text{C}$ prior to analysis on a Shimadzu TOC-VCPH Total Organic Carbon Analyzer with TNM-L Total Nitrogen Measuring Unit (Kyoto, Japan).

3.3.2 DNA extraction, metagenome sequencing, and metagenome analyses

DNA was extracted from 3 x 10 g portions of sediment with the Qiagen DNeasy PowerMax Soil Kit (Hilden, Germany). Extracted DNA was concentrated with a Thermo Fisher Scientific SpeedVac Vacuum Concentrator (Waltham, MA, USA) and New England Biolabs Monarch PCR & DNA Cleanup Kit (5 μg) (Ipswich, MA, USA). Sequencing libraries were prepared with the Illumina Nextera XT DNA Library Prep Kit and sequenced at The Center for Applied Genomics at the Hospital for Sick Children (Toronto, ON, Canada) on a NovaSeq 6000 (Illumina) with an S Prime 100-cycle flow cell (2 x 100 base pairs).

Metagenome sequencing produced ~109 million reads across the three replicates (sequencing and assembly statistics in Table S3.2). Read quality was checked before and after quality control with FastQC (v.0.11.9). Adapters and reads were trimmed with BBDuk (BBMap v.38.96) with parameters trim=r k=23 mink=11 hdist=1 tpe tbo ftm=5. PhiX contamination was removed with BBDuk using the BBMap PhiX174 reference genome (parameters k=31 hdist=1), and human genome contamination was removed with the BBMap Removehuman.sh script with default parameters using the BBMap GH19 masked human reference genome. After contaminant filtering, all reads <30 bp were removed with BBDuk (minlength=30). Remaining reads were classified with Kaiju (v.1.7.4) (34) with the nr_euk reference database and with phyloFlash (v.3.4) (35).

The three replicate metagenomes were co-assembled with Megahit (v.1.2.9) using three pre-set settings (default, meta-sensitive, and meta-large) (36). The ‘meta-sensitive’ assembly was selected for further analysis based on assembly quality as assessed with MetaQUAST (v.5.0.2) (37). Co-assembly statistics are compiled in Table S3.3. The co-assembly was annotated with the Joint Genome Institute IMG/M Annotation Pipeline (v.5.1.5) using KEGG, COG, and TIGRFAM databases (38, 39). Reads were mapped to the assemblies with Bowtie2 (v.2.4.4) (--very-sensitive) (40) and assemblies were binned with MetaBAT (v.2.14) (41) and MaxBin (v.2.2.7) (42) with minimum contig sizes of 1000, 2000, 2500, and 5000 bp. Bin completeness and contamination were assessed with CheckM (v.1.1.9) (43), and bin taxonomy was assigned with GTDB-Tk (v.2.1.1, reference package R207-v2) (44). A minimum contig size of 2000 bp was selected based on quantity of high-quality bins. Assemblies were additionally binned with CONCOCT (v.1.1.0) (--length_threshold 2000) (45). MetaBAT, MaxBin, and CONCOCT bins

were de-replicated with DAS Tool (46) to create a set of non-redundant bins, and bin contamination was further reduced where possible with RefineM (v.0.0.25) (47).

An additional binning strategy adapted from Chen *et al.* (48) was also used for comparison to ensure the highest bin quality possible. Briefly, the three replicate metagenomes were assembled individually with Megahit and SPAdes (v.3.15.3) (--meta). The SPAdes metagenomes were selected for further analysis based on assembly quality. Read mapping, binning, de-replication, and bin refinement were performed as above to produce a set of non-redundant bins for each metagenome. Following this, the bins from all three metagenomes were pooled and again de-replicated with dRep (v.3.2.2) (49), resulting in a final set of de-replicated bins. After comparison between the two resultant bin sets, the co-assembly bins were selected for all downstream analyses based on prevalence of high-quality bins.

Additional analyses were as follows: Bin abundance in the metagenome was calculated with CoverM (v.0.4.8). A phylogenomic tree of MAGs was created in Anvi'o (v.6.2) (50) with the Bacteria_71 collection of single-copy genes. Amino acid sequences for all genes were concatenated, with a total alignment length of 23,122 bp, and approximately-maximum-likelihood trees were constructed with FastTree (v.2.1) (51) within Anvi'o with midpoint rooting. FeGenie (v.1.2) was used to identify iron-related genes (52). Hydrogenases were classified with hydDB (53). Reductive and oxidative DsrAB were classified as follows: DsrAB amino acid sequences were aligned against reference sequences from Müller *et al.* (54) using MUSCLE (v.3.8.1551) with default settings (55). Maximum likelihood phylogenetic trees were constructed in CLC Genomics Workbench (v.12.0.3; QIAGEN, Aarhus, Denmark) using the

WAG protein substitution model and 1000 bootstraps (Figures S3.2-S3.5). DsrAB were classified as reductive or oxidative based on phylogenetic clustering and the presence of accessory proteins as in Anantharaman *et al.* (56).

3.3.3 mRNA extraction, metatranscriptome sequencing, and analyses

RNA was extracted from 3 x ~6 g sediment samples with the Zymo Research ZymoBIOMICS DNA/RNA Miniprep kit. Each replicate was split into six sub-samples for the extraction.

Extracted RNA was treated with the Invitrogen Turbo DNA-free kit (Carlsbad, CA, USA) to remove contaminating DNA. The six sub-samples in each replicate were then pooled together and concentrated with the New England Biolabs Monarch RNA Cleanup Kit. Extractions were checked for DNA contamination with a Thermo Fisher Scientific Qubit dsDNA HS Assay Kit and by PCR amplification of 16S rRNA genes using DNA primers 27F/1492R (57, 58); only samples with no amplified product (as detected by agarose gel electrophoresis) were used.

Ribosomal RNA was depleted with the New England BioLabs NEBNext rRNA Depletion Kit (Bacteria) and a cDNA sequencing library was prepared with the New England BioLabs Ultra II RNA Library Prep Kit. For one extraction replicate (GH3), two sequencing libraries were prepared from the extraction, with one library undergoing fragmentation (R9) and one not fragmented (R6), in order to optimize library quality based on its RNA Integrity Number. The generated libraries were sequenced at The Center for Applied Genomics at the Hospital for Sick Children on a NovaSeq 6000 (Illumina) with an S Prime 100-cycle flow cell (2 x 100 base reads).

Metatranscriptome library statistics are compiled in Table S3.2. Adapter trimming and PhiX and human contamination removal was done with BBDuk as for the metagenomic reads. Additional quality trimming was done with BBDuk (qtrim=r trimq=15 maq=15 minlen=50). Remaining rRNA reads were removed with SortMeRNA (v.4.3.4) (59). The trimmed reads were classified with Kaiju and mapped to the co-assembly contigs with bowtie2 (--very-sensitive). Reads aligned to metagenome features were counted with htseq-count (-s no-i ID --nonunique=all -r pos -a 0) and transcripts per million reads (tpm) was calculated to normalize expression values for each gene. Counts from the two technical replicates (R6 and R9) were merged prior to tpm calculation. Normalized expressed values represent averages of the three biological replicates unless otherwise noted.

3.3.4 16S rRNA community profiling and analysis

DNA was extracted from 3 x 1 g sediment samples with the Zymo Research ZymoBIOMICS DNA/RNA Miniprep kit. Two negative controls (nuclease-free water) and two replicates of the ZymoBIOMICS Microbial Community Standard were also extracted. All extractions were concentrated with the New England Biolabs Monarch PCR & DNA Cleanup kit. Concentrated DNA was amplified by PCR with 16S rRNA V4 primers 515F-Y and 926R (60) with Illumina overhang adapters (61). Each 25 μL reaction contained 10 μL Qiagen HotStarTaq Plus Master Mix, 0.5 μL each of 10 μM forward and reverse primers, 1 μL 10 $\mu\text{g}\cdot\mu\text{L}^{-1}$ bovine serum albumin, 5 μL extracted DNA, and 3 μL nuclease-free water. PCR cycling proceeded as follows: 5 minutes at 95 $^{\circ}\text{C}$; 35 cycles of 45 seconds at 94 $^{\circ}\text{C}$, 45 seconds at 50 $^{\circ}\text{C}$, and 1 minute at 72 $^{\circ}\text{C}$; and ten minutes at 72 $^{\circ}\text{C}$. Amplicon sequencing libraries were prepared according to the Illumina 16S Metagenomic Sequencing Library Preparation protocol (61). Briefly, PCR products were

cleaned using Cytiva Sera-Mag Select (Marlborough, MA, USA) magnetic beads at a ratio of 0.6 x beads:sample volume. Nextera XT Index Kit v2 Set B dual indices were attached by PCR in 50 μ L reactions containing 25 μ L Invitrogen Platinum Hot Start PCR 2x Master Mix (Waltham, MA, USA), 5 μ L PCR product, 5 μ L each index primers 1 and 2, and 10 μ L PCR-grade water. PCR cycling proceeded as follows: 3 minutes at 95 °C; 8 cycles of 30 seconds at 95 °C, 30 seconds at 55 °C, and 30 seconds at 72 °C; and 5 minutes at 72 °C. The libraries were again cleaned with Cytiva Sera-Mag Select beads at a ratio of 0.8 x beads:sample volume, then pooled at equimolar concentrations and sequenced on an Illumina MiSeq with MiSeq Reagent Kit v3 (600-cycle) (2 x 300 base reads).

The 16S rRNA gene amplicon sequencing statistics are compiled in Table S3.2. An amplicon sequence variant (ASV) count table was generated with the DADA2 pipeline (v.1.24.0) (62). Taxonomy was assigned with the SILVA database (v.138.1) (63). The decontam R package (v. 1.16.0) was used to identify and remove contaminant ASVs (threshold=0.5) in addition to manual removal of ASVs present only in the negative controls and the ZymoBIOMICS Microbial Community Standard. In total, 2885 of 2901 ASVs remained after quality control.

The 16S rRNA gene amplicon sequences from GH were compared to 24 additional 16S rRNA gene amplicon sequencing libraries from similar environments (metadata in Table S3.4). ASV count tables were generated for each library in DADA2 using the SILVA database for taxonomy assignment as above. For single-end libraries (Ion Torrent and 454 metagenomes), the DADA2 pipeline was run with only forward read commands and without read merging. Ion Torrent and 454 metagenomes were also processed with additional parameters as recommended by the

DADA2 pipeline (dada(..., HOMOPOLYMER_GAP_PENALTY=-1, BAND_SIZE=32)). Two data sets did not have sufficient reads to learn error rates (JL94DB and JL95B); for these samples, taxonomy was assigned directly to the reads using the DADA2 assignTaxonomy function without ASV inference. To allow comparison between the data sets, ASV/read counts were summed by taxonomic assignment (Table S3.5). Dissimilarity and clustering analyses were calculated using the ‘vegan’ Community Ecology package (v.2.6-4) in R. Environmental metadata was standardized with the decostand() function using the “standardize” method. Frequencies were calculated for each taxon by dividing each count by total count per taxon, following by standardization with decostand() using the “hellinger” method. A non-metric multidimensional scaling (NMDS) ordination was generated using the metaMDS() function with Bray-Curtis dissimilarity matrix (dist=”bray”). A Canonical Correspondance Analysis (CCA) was done using the cca() function with a Bray-Curtis dissimilarity matrix and 999 permutations. CCA was built by automatic forward selection, with adjusted R^2 to select significant variables. Spearman’s rank correlation was performed using the cor(), rcorr() functions and visualized using corplot() function of the stats, Hmisc and corrgram packages respectively.

3.3.5 Data accession

All sequencing data was deposited in NCBI under BioProject PRJNA915120. Metagenome annotation is available under Analysis Project ID Ga0534206 in the Joint Genome Institute IMG/M system. A list of MAG contigs is supplied in Table S3.6 so IMG metagenome annotation can be attributed to MAGs.

3.4 Results and Discussion

3.4.1 Metagenomic sequencing and MAGs characterized taxonomic diversity.

In order to describe the taxonomic diversity present in the GH sediment, we sequenced 16S rRNA gene amplicons and shotgun metagenomes and constructed metagenome-assembled genomes (MAGs) (Figure 3.1). Metagenomic sequencing recovered primarily bacterial reads, with archaeal and eukaryotic reads constituting <1 % (Figure 3.1a, Figure S3.6). The most abundant phyla in the shotgun metagenome and 16S rRNA gene amplicon sequences were *Desulfobacterota* (25 % and 26 %, respectively), *Bacteroidota* (22 % and 46 %), *Proteobacteria* (17 % and 8.5 %) (primarily *Gammaproteobacteria*, 15 % and 6.6 % of total), and *Spirochaetota* (4.7 % and 6.8 %). Of the 2,885 16S rRNA gene amplicon sequence variants (ASVs), 258 were represented in the metagenome at species-level similarity (>98.6 %); those 258 ASVs comprised 62 % of ASV relative abundance, indicating that the majority of ASVs not also present in the shotgun metagenome were likely from low abundance species. Detected taxonomic diversity was similar to previous studies of the GH sediment; of 49 bacterial isolates obtained in 2008 (4), 47 were related at genus-level or above (>95 % sequence identity of 16S rRNA gene) to ASVs from this study. Similarly, 43 of 46 bacterial 16S rRNA gene clone library sequences obtained in 2007 were related at genus level or above, indicating consistency in the spring microbial community from 2007 to 2019-2021 (this study).

MAG assembly produced 26 high-quality (>90 % complete, <5 % contamination) and 31 medium-quality (>50 % complete, <10 % contamination) bins representing 17 phyla, including bacterial (55 MAGs) and archaeal (2 MAGs) taxa (Figure 3.1b; Table S3.7). Distribution of MAGs across phyla reflected metagenome abundances (Figure 3.1a), with the most highly-represented phyla being *Bacteroidota* (16 MAGs), *Proteobacteria* (8 MAGs), *Spirochaetota* (7

MAGs), and *Desulfobacterota* (6 MAGs). MAGs were recovered for nearly all of the most abundant orders (>1.5 %) in the metagenome. Taxa above 1.5 % relative abundance without representative MAGs were Bacteroidetes VC2.1 Bac22 (ca. Sulfidibacteriales; 1.6 %) and LCP-89 (2.8 %). Both taxa represent uncultured clades found in oxygen-limited, sulfide-rich environments including marine hydrothermal vents and oxygen-minimum zones (VC2.1 Bac22) and Zodletone Spring in Oklahoma, USA (LCP-89) (64, 65).

MAG novelty was estimated using the taxonomic rank of MAGs classified by comparison to the GTDB database with GTDB-tk (44) (Figure 3.1c). The majority of MAGs (97 %) were unclassified at the species level, and 26 % remained unclassified at higher taxonomic ranks (up to order). Similarly, 40 % of ASVs detected by 16S rRNA gene amplicon sequencing were unclassified at genus level or higher (Figure S3.7), indicating a high level of taxonomic novelty in the GH microbial community.

Comparison of the GH MAGs to previously-sequenced MAGs from nearby Lost Hammer (LH) Spring (24 % salinity, -5° C) (27) by amino acid identity (AAI) and average nucleotide identity (ANI) identified 41 GH MAGs (72% of MAGs) related at the family level or above (>45% AAI) to MAGs from LH. Of these, eight GH MAGs belonged to the same genus (>65% ANI) and two to the same species (>95% ANI) as LH MAGs, indicating that while there is considerable similarity between the GH and LH microbial communities (family-level and above), they contain distinct taxa and microorganisms at the genus-level and below.

3.4.2 Sulfur cycling taxa and metabolic genes are abundant in the metatranscriptome.

Metatranscriptomic reads were mapped to the MAGs and metagenomic co-assembly to identify active microorganisms and metabolisms and link detected metabolic activity to microbial taxa. Relative metatranscriptomic expression of MAGs (Figure 3.1b) and metabolic genes of interest (Figure 3.2) indicated that sulfur cycling metabolisms were predominant in this system. Sulfate is abundant in the spring sediment (1.9 g.kg^{-1}) (3) and waters ($\sim 2200 \text{ ppm}$). Previous isotopic analysis indicated that it is derived from the anhydrite (CaSO_4) evaporite diapirs that the GH springs flow through in the subsurface (32). Isotopic analysis also indicated sulfate reduction to sulfide was occurring in the spring sediment; this reducing activity had a quantitatively unimportant impact on fractionation of sulfate flowing into the spring, indicating that sulfate is present in non-limiting quantities for microbial metabolism (32). Sulfide ($\sim 9.5 \text{ ppm}$) and other reduced sulfur compounds are also present in non-limiting quantities (4), suggesting favorable conditions for a diversity of sulfur-based microbial metabolisms. Sulfur cycling taxa were among the most abundant orders in the shotgun metagenome, including *Desulfuromonadales* (11%), *Desulfobacterales* (9%), *Desulfobulbales* (5%), and *Thiomicrospirales* (7%) (Figure 3.1a). The highest proportion of metatranscriptome relative expression was attributed to *Desulfobacterota* MAGs (35%), followed by *Gammaproteobacteria* MAGs (14.5%) (Figure 3.3); all MAGs in these taxa expressed sulfur cycling genes (Figure 3.4). Additionally, sulfate-reducing genes (*dsrAB*, 1240 tpm; *aprBA*, 1044 tpm) were the most highly expressed metabolic genes in the metagenome (Figure 3.2; Table S3.11).

3.4.3 H_2 -linked sulfate reduction drives microbial primary production.

In addition to archetypal sulfate reduction marker genes (*dsrAB*, *aprBA*), genes involved in tetrathionate (*ttrABC*, *otr*), polysulfide and thiosulfate (*psrA/psrA*), and sulfite (*sreB*, *asrBC*;

note that no *asrA* subunits were detected) reduction were also present and expressed. Sulfur species reduction was relatively widespread; 21 MAGs (37 % of total MAGs) had detected expression of sulfur-reduction-related genes, including *Desulfobacterota*, *Bacteroidota*, *Spirochaetota*, CG03, *Campylobacterota*, and *Gammaproteobacteria* (Figure 3.4). This count excludes *hydBGDA* sulfhydrogenase genes, whose direct role in sulfur reduction is considered unlikely but which are highly homologous to a sulfur-reduction-linked membrane-bound oxidoreductase (66, 67).

The majority of S reduction gene expression (86 % of all S reduction gene expression) mapped to the *Desulfurivibrionaceae* sp. GH16 MAG, primarily due to high expression of the sulfate reduction genes *dsrAB* (93 % of total) and *aprBA* (82 %). This MAG was relatively abundant in the metagenome (4 %) and expressed genes for complete sulfate reduction to sulfide (*dsrAB*, *aprBA*, *sat*, *dsrD*; 2238.9 tpm total) (56), as well as tetrathionate (*ttrABC*; 75.5 tpm) and thiosulfate/polysulfide (*phsA/psrA*; 68.3 tpm) reduction. It also expressed genes for dissimilatory nitrate reduction to ammonia (*napA*, 2.3 tpm; *nirB*, 5.6 tpm), indicating flexible use of S and N electron acceptors despite the abundant sulfate in the spring. The MAG also co-expressed a group 1c [NiFe] hydrogenase involved in hydrogenotrophic respiration (221 tpm) (53), indicating that the majority of sulfate reduction in the spring sediment is coupled with H₂ oxidation. Previous measurements of spring gas composition have not identified measurable concentrations of H₂ (4, 33). However, genes involved in fermentative production of hydrogen are present and expressed (e.g., formate hydrogenlyase, Table S3.12), which may represent a putative source of H₂; thus, hydrogen concentrations may be limiting in sulfate reduction activity.

The *Desulfurivibrionaceae* sp. GH16 MAG could only be classified at the family level in comparison to the GTDB database (Table S3.7). A partial 16S rRNA gene (846 bp) present in the MAG aligned at 91% identity to an uncultured *Desulfobacterota* when compared to the SILVA database, suggesting that this GH sulfate-reducing bacterium (SRB) likely represents a novel genus or higher lineage of *Desulfobacterota*. Related MAGs within the *Desulfurivibrionaceae* family in the GTDB database were assembled from hypersaline soda lakes (GCA_003557565.1), as well as marine environments, indicating halotolerance within the family. Hydrogenotrophic sulfate reduction in another AHI spring, Lost Hammer Spring (24 % salinity, -5° C), was attributed to a MAG in the uncultured BM506 genus in *Desulfobacterota*. This BM506 MAG was related at genus level (66 % amino acid identity) to *Desulfurivibrionaceae* sp. GH16, suggesting that closely-related novel taxa of halo- and psychrotolerant SRB are primarily responsible for sulfate reduction in the AHI springs. Hydrogen-dependent sulfate reduction was previously observed in microcosms of Lost Hammer Spring sediment down to -20 °C (28), corroborating the hydrogenotrophic gene expression detected in SRB from both springs and indicating that these SRB are highly adapted to cold down to the known temperature limits of microbial metabolic activity.

While the majority of sulfate reduction activity was attributed to *Desulfurivibrionaceae* sp. GH16, all six *Desulfobacterota* MAGs expressed sulfur species reduction genes (Figure 3.4). Three additional *Desulfobacterota* MAGs expressed sulfate reduction genes, either to sulfide (GH12, GH14) or sulfite (GH13); both GH12 and GH13 co-expressed group 1a or group 1c [NiFe] hydrogenases involved in hydrogenotrophic respiration, supporting hydrogen-coupled

sulfate reduction as a major metabolism in the spring (Figure 3.4). As in GH16, all *Desulfobacterota* MAGs co-expressed N reduction genes and genes for reduction of multiple sulfur species, and all but one contained the Wood-Ljungdahl pathway for CO₂ fixation (Figure 3.4), indicating the GH spring supports a diversity of novel chemolithoautotrophic SRB utilizing S and N compounds as terminal electron acceptors.

Notably, expression of sulfate reduction genes was also identified in MAGs from phyla not typically associated with sulfate reduction activity (56). *Sphaerochaetales* sp. GH28 (*Spirochaetota*) expressed genes for complete sulfate reduction to sulfide, as well as hydrogenotrophic group 1b and 1c [NiFe] hydrogenases and the Wood-Ljungdahl pathway, indicating similar metabolic activity as GH *Desulfobacterota*. *Spirochaetota* (formerly *Spirochaetes*) are typically chemoorganotrophs growing under a wide range of oxygen concentrations (68); the phylum includes halophiles (69), and *Spirochaetota* have been identified in extreme cold hypersaline environments such as brines in ice-covered Lake Vida in Antarctica (-13 °C) (70). Sulfate reduction genes were only recently identified in this phylum, in the anoxic, sulfide-rich Zodletone Spring in Oklahoma, USA (71), and in groundwater in Tennessee, USA (72). *Sphaerochaetales* sp. GH28 was novel at the family level in comparison to the GTDB database, and a 16S rRNA gene in the MAG (1539 bp) had 88 % identity to its closest match in the SILVA database, suggesting this GH MAG represents a highly novel lineage of sulfate-reducing *Spirochaetota*.

Gene expression for complete sulfate reduction to sulfide was also identified in UBA2268 sp. GH34, in the order *Kapabacteriales* and phylum *Bacteroidota*. In the GTDB database, this MAG

was most closely related to a recently-described ca. Kapabacteria from Yellowstone hot spring microbial mats representing the first sulfate-reducing bacterium from the *Bacteroidetes/Chlorobi* superphylum (73). An additional sulfate-reducing ca. Kapabacteria was also recently reported in a deep subsurface aquifer (74). Comparison of genomes by amino acid identity indicated that UBA2268 sp. GH34 was in the same family as both previously-identified ca. Kapabacteria. All three *Kapabacteriales* SRB appear to be heterotrophic and contain genes involved in dissimilatory nitrite reduction (*nrfA*), denitrification (*nosZ* or *norB*), and polysulfide/thiosulfate reduction (*psrA/phaA*), as well as cytochrome c oxidases (*coxBAC* and/or *cydAB*), indicating similar metabolic function despite their presence in the distinct and disparate environments of cold hypersaline GH, 60°C oxygenic phototrophic microbial mats in non-saline hot springs in the USA and Japan, and 20°C anaerobic non-saline subsurface aquifer waters in Western Siberia, Russia. Transcriptional studies of the Yellowstone hot spring ca. Kapabacteria suggested it may be facultatively aerobic and respire both sulfate and oxygen (73); if so, this might give the UBA2268 sp. GH34 a unique niche in the upper portions of the GH sediment where trace oxygen is present compared to strictly anaerobic SRB.

While sulfate reduction genes were the most highly expressed metabolic genes identified in the metatranscriptome, the most abundant *Desulfobacterota* present in the metagenome did not contain any sulfate reduction capabilities. *Desulfuromusa* sp. GH17 was the most abundant MAG in the metagenome (9.4 % relative abundance) and the metatranscriptome, containing 20% of total relative expression (203101.17 tpm) (Figure 3.1b). The *Desulfuromusa* genus also comprised 14.4% of the 16S rRNA gene amplicon sequences, indicating significant abundance and activity of this taxon in the spring sediment (Figure 3.1a). Previous 16S rRNA gene clone

library and amplicon sequencing of the GH sediment also identified *Desulfuromusa* and *Desulfuromonadaceae* comprising up to 60% of detected *Desulfobacterota* (3, 31), demonstrating their abundance in GH over time. Previous comparison of cell-specific sulfur reduction rates with GH sulfur isotopic fractionation indicated that only ~60 % of *Desulfobacterota* in the GH sediment were engaged in active sulfate reduction (31), supporting the presence of significant populations of non-SRB *Desulfobacterota* such as *Desulfuromusa*.

Cultured *Desulfuromusa* are obligate anaerobes that typically oxidize or disproportionate organic C compounds and reduce a variety of electron acceptors including elemental sulfur, iron, manganese, nitrate, and fumarate (75, 76). A psychrophilic *Desulfuromusa* has previously been cultured from cold Arctic marine sediments (-2 °C). *Desulfuromusa* have also been identified by 16S rRNA gene amplicon sequencing and metagenomic sequencing in sulfidic anoxic marine environments such as hydrothermal vent fluids (77) as well as cold (-1.8 – 7.5 °C) and saline (1-5 %) Antarctic lakes (78).

Elemental sulfur (S⁰) has previously been identified in GH sediments, and it is a major component of the precipitate mineral crusts surrounding the springs (5). Elemental sulfur is produced biotically in the spring outflow channels, where microbial streamers formed by *Thiomicrothabodus* sp. oxidize sulfide to elemental sulfur (32, 79). MAGs detected in this study (including *Thiomicrothabodus* sp.) also express sulfide oxidation genes (Figure 3.4) indicating elemental sulfur is also produced biotically in the spring sediment, as discussed below. *Desulfuromusa* 16S rRNA gene clone sequences were identified within the *Thiomicrothabodus* sp. microbial streamers, which contain S⁰ mineral structures (79), and *Desulfuromonadaceae* in

the spring outflow channels increased in abundance with distance from the primary outlet, indicating a potential positive association with *Thiomicrothrix* sp. streamers in the channels (31). While elemental sulfur reduction by *Desulfuromusa* isolates has previously been described, no in-depth description of a *Desulfuromusa* genome has previously been published and the method of elemental sulfur reduction in this genus remains unclear. Two mechanisms of sulfur reduction have previously been characterized, utilizing either an [NiFe] hydrogenase and sulfur or polysulfide reductase (SreABCDE/PsrABC), or via an NADPH elemental sulfur oxidoreductase (NSR) (80, 81). Potential homologs to these proteins were identified in *Desulfuromusa* sp. GH17 by BLAST using query proteins for NSR and NSR-like proteins from S⁰-reducers *Pyrococcus furiosus* and *Thermovibrio ammonificans* as well as Sre/Psr genes from a variety of bacterial taxa (complete output and list of query sequences in Table S3.13). *Desulfuromusa* sp. GH17 contained a homolog to *T. ammonificans* NSR-like protein (31.6 % identity, 152 bitscore) as well as weak homologs to *P. furiosus* NSR (22-24 % identity, 52-56 bitscore). However, these homologs did not contain the conserved cysteine residue required for S⁰ reduction activity in some species (80). A homolog to PsrB (34 % identity, 70 bitscore) and a weak homolog to PsrA (22 % identity, 97 bitscore) were also identified, although they were not located in the same operon as would be expected; additionally, no PsrC homolog was identified. All putative homologs had mapped transcripts. Thus, a mechanism for elemental sulfur reduction is possible in *Desulfuromusa* sp. GH17, potentially utilizing an NSR-like oxidoreductase; detected activity with an isolated strain would be necessary to confirm this activity.

The *Desulfuromusa* sp. GH17 also contains potential pathways for fumarate and malate disproportionation, fumarate reduction, and tetrathionate reduction, indicating possible alternate

electron acceptors to sulfur, as well as acetogenic fermentation (Figure 3.5a). Transporters for acetate, C4-dicarboxylates, and branched-chain amino acids were highly expressed within the MAG (Table S3.14), indicating that it oxidizes or disproportionates organic carbon compounds as found in other *Desulfuromusa* spp.; it also appears to be obligately heterotrophic. However, the majority of relative expression in *Desulfuromusa* sp. GH17 was attributed to a single gene (Ga0534206_017155_28837_29236), accounting for 80.2 % of relative expression in the MAG and 16 % of relative expression in the entire metatranscriptome (162861.6 tpm). This gene was classified as RNase P class A, a ubiquitous ribonuclease responsible for maturation of tRNAs and cleavage of a variety of other RNAs (82). The next two most highly expressed genes in the MAG were also non-coding RNAs classified as 6S/SsrS RNAs (26427.2 and 1196.1 tpm), which act as transcriptional regulators of RNA polymerase. They are associated with switching from exponential to stationary growth phases, but have also been found to regulate large numbers of genes during the exponential phase (83). It is not clear why these non-coding RNAs account for such a large proportion of *Desulfuromusa* sp. GH17 expression. One possibility is that *Desulfuromusa* sp. GH17 modulates its metabolic strategy frequently based on substrate availability, requiring significant regulation of gene expression. This could potentially result from availability of elemental sulfur and organic carbon compounds: while *Desulfuromusa* spp. are typically obligate anaerobes, elemental sulfur-producing microbes such as *Thiomicrothrix* sp. in GH are aerobic. Thus, they likely cannot exist in close proximity on a microscale in the sediment, potentially limiting access of *Desulfuromusa* sp. to biotic elemental sulfur. Organic carbon is also limiting in GH (29), potentially requiring changes in cellular activity, growth, or metabolic strategy based on availability of organic C. If *Desulfuromusa* sp. GH17 are indeed engaged in intensive gene regulation based on substrate availability, this may explain their

significant abundance in the sediment compared to the chemolithoautotrophic

Desulfurobacterota also present in GH, despite their reliance on limited organic C and inability to reduce non-limiting sulfate.

3.4.4 Trace oxygen supports S-oxidizing Gammaproteobacteria.

Oxidation of sulfur species was also widespread, with 15 MAGs (26 %) containing S oxidation-related genes with mapped transcripts in the *Gamma*- and *Alphaproteobacteria*, *Campylobacterota*, *Bacteroidota*, and *Spirochaetota* (Figure 3.4). S oxidation activity was linked with both aerobic and anaerobic metabolism: of the 15 MAGs, 11 co-expressed N-reduction genes and 11 co-expressed terminal oxidases; 8 of these MAGs expressed both N-reduction genes and cytochrome c oxidases, indicating potential facultatively anaerobic microorganisms. Previous isolates from the GH spring sediment, including isolates containing *soxB* genes as markers of sulfur oxidation capability, were found to be predominantly facultative anaerobes, indicating this is likely advantageous in the sub-oxic spring sediment (0.04 ppm O₂). All 11 MAGs expressed high-affinity terminal oxidases (*cydAB* and/or *ccoNOPQ*), exclusively (4 MAGs) or in addition to low-affinity terminal oxidases (7 MAGs), indicating they are able to carry out respiration under low oxygen conditions. The co-expressed low-affinity oxidases may also contribute to respiration even under sub-oxic conditions, and could even be more favorable than high-affinity oxidases at microaerobic O₂ concentrations due to more efficient ATP production, as found in some *Acidobacteria* (84). Six of the 15 MAGs, from the *Gamma*- and *Alphaproteobacteria* and *Campylobacterota*, additionally contained pathways for CO₂ fixation (CBB or rTCA cycles).

The Sox genes were the most highly expressed S oxidation genes (353.9 tpm across 6 genes). The Sox complex oxidizes thiosulfate, sulfite, sulfide, elemental sulfur, and tetrathionate compounds, either completely to sulfate or, in the absence of *soxCD*, to elemental sulfur (85). Sox genes were identified in 8 of the 15 S-oxidizing MAGs, from *Gammaproteobacteria*, *Alphaproteobacteria*, and *Campylobacterota*. Four MAGs contained genes for complete oxidation to sulfate and 3 MAGs contained genes for oxidation to sulfur (the remaining MAG, *Thiomicrothabodus* sp. GH6, contained a partial Sox pathway with unclear functionality) (Figure 4). Other S oxidation genes with high expression were *fccAB* (86.5 tpm) and *sqr* (103.6 tpm), which oxidize sulfide to elemental sulfur and polysulfide, respectively. Nearly all S oxidation gene expression (96%) was attributed to *Gammaproteobacteria* (Figure 3.3). Over half of this expression was attributed to two MAGs, *Halothiobacillus* sp. GH7 (33 % of total S oxidation gene expression) and *Thiomicrothabodus* sp. GH6 (24 %).

Thiomicrothabodus was abundant in the 16S rRNA gene amplicon sequences (4.8 %) (Figure 3.1a), and *Thiomicrothabodus* sp. GH6 was the most abundant S-oxidizing MAG (3.5 % relative abundance; Figure 3.1b) in the shotgun metagenome. *Thiomicrothabodus* spp. are characteristically chemolithoautotrophic S oxidizers and have previously been identified in cold saline environments including Arctic marine sediments (86) and Antarctic sub-glacial brines (87). *Thiomicrothabodus* (previously identified as *Thiomicrospira*) has previously been detected in abundance in the GH sediment (3), and, as noted, it forms microbial streamers in the spring channels where it aerobically and chemolithoautotrophically oxidizes sulfide to elemental sulfur (32). Comparison of *Thiomicrothabodus* sp. GH6 to the *Thiomicrothabodus* sp. MAG recovered from GH streamers by indicated that they were the same species (99.1 % ANI). The genome and

transcriptome of the streamer *Thiomicrothrix* MAG have previously been described in detail (32); as expected, metabolic gene presence and expression in the *Thiomicrothrix* sp. GH6 was largely identical. The most highly expressed S-oxidizing genes in *Thiomicrothrix* sp. GH6 were the *fccAB* genes (85.7 tpm) involved in sulfide reduction to elemental sulfur, comprising nearly all (99%) of *fccAB* expression in the metatranscriptome, corroborating its previously-observed role in biotic elemental sulfur production in the spring. It additionally expresses genes for sulfide oxidation to polysulfide (*sqr*, 26.4 tpm), thiosulfate oxidation (*tsdA*, 0.3 tpm), and sulfur dioxygenase (*sdo*, 1.2 tpm). Expression of Sox genes was also detected (28.1 tpm). As in the streamer *Thiomicrothrix*, only a partial Sox complex (*soxBCD*) was identified in the MAG (Table S9). The *soxBCD* genes were also the only Sox genes identified in the streamer MAG, and while *soxXAY* genes classified as *Thiomicrothrix* were identified in unassembled reads, no *soxZ* was identified in the streamer metagenome. Thus, despite the *soxBCD* comprising a significant proportion of S oxidation gene expression in *Thiomicrothrix* sp. GH6, the functionality of this complex remains unclear.

Halothiobacillus sp. GH7 had the highest expression of S oxidation genes overall (201.2 tpm), and among the highest total expression of the S-oxidizing MAGs (Figure 3.1b). Cultured *Halothiobacillus* spp. are halotolerant, obligately aerobic, and chemolithoautotrophically oxidize S species (88-90), and members of this genus have previously been identified in sulfidic and hypersaline environments (88, 91). The majority of expression of S oxidation genes by *Halothiobacillus* sp. GH7 was attributed to Sox genes (148.3 tpm), comprising 40 % of total Sox gene expression. Homologs to all Sox genes except *soxX* were identified in the MAG (Table S3.9), indicating it likely utilizes the Sox complex for complete oxidation of S species to sulfate.

It also expressed a number of additional S oxidation genes, indicating it can utilize diverse S species including sulfide (*sqr*, 26.2 tpm), persulfides (*sdo*, 19.3 tpm), and thiosulfate (*tsdA*, 7.5 tpm). It is also the only MAG containing sulfur oxygenase/reductase (*sor*, 9.3 tpm), which aerobically disproportionates and oxygenates elemental sulfur to sulfide, sulfite, and thiosulfate in a non-energy-generating reaction as the first step in oxidation of the resulting products (92). Nearly all *sor* expression in the metatranscriptome (97 %) mapped to *Halothiobacillus* sp. GH7, indicating this may be a unique mechanism within the spring microbial community. It also co-expressed all four cytochrome c oxidases and the CBB cycle for CO₂ fixation (Figure 3.4), indicating it is capable of aerobic, chemolithoautotrophic metabolism as in other *Halothiobacillus* spp. Additionally, the *Halothiobacillus* sp. GH7 expressed genes involved in dissimilatory reduction of nitrite (*nirB*) and nitric oxide (*norBC*), as well as nitrogen fixation genes (*nifHDK*), suggesting it is potentially capable of anaerobic respiration. As noted, *Halothiobacillus* spp. are characteristically obligate aerobes, and *Halothiobacillus* found in environments with oxic-anoxic gradients such as marine haloclines have been restricted to oxic or micro-oxic zones (71, 91, 93). However, *Halothiobacillus* in mine tailings containing an oxygen gradient in southern Ontario, Canada, were also found to co-express *nirB*, *norBC*, and Sox genes under micro-oxic conditions, though the majority of Sox gene expression was identified in oxic zones (94). *Halothiobacillus* sp. GH7 N reduction genes were poorly expressed (1.5 tpm) compared to terminal oxidases (54 tpm), indicating these *Halothiobacillus* spp. are primarily aerobic but may be capable of anaerobically respiring nitrogen species when oxygen is scarce. *Halothiobacillus* have been observed to produce nitrite from nitrate but not grow under anaerobic conditions (88), indicating that anaerobic respiration may supplement aerobic respiration but not enable growth.

Sulfur-oxidizing bacteria (SOB) are also major drivers of primary production in other anoxic, cold, hypersaline AHI springs, dominated by *Halothiobacillus* (Colour Peak Spring, 3-6 °C, 15 % salinity) and *Guyparkeria* (Lost Hammer Spring, -5 °C, 24 % salinity). As such, the dominant SOB and major primary producers in all three springs (*Halothiobacillus*, *Guyparkeria*, and *Thiomicrothrix*) are predominantly or obligately aerobic, chemolithoautotrophic genera in the *Halothiobacillaceae* family (*Gammaproteobacteria*). Comparison of GH and Lost Hammer MAGs indicated a high degree of relatedness between *Halothiobacillaceae* in the two sites, with *Halothiobacillus* and *Thiomicrothrix* MAGs in both sites likely belonging to the same species (>95 % ANI) despite the two springs not sharing a common source (1). *Guyparkeria* was also identified in the GH 16S rRNA gene amplicon sequences, albeit in low abundance (0.03 %). The relative dominance of *Guyparkeria* in Lost Hammer may be due to its significantly higher salinity (24 %) compared to GH (8 %), as *Guyparkeria* spp. are typically true halophiles while *Halothiobacillus* spp. are halotolerant (95). Together, the abundance of these aerobic, chemolithoautotrophic SOB across the sub- and micro-oxic AHI springs highlights the importance of trace oxygen scavenging to microbial primary production in these springs.

3.4.5 Chemolithoautotrophy rather than photoautotrophy likely sustains primary production.

Due to the high latitude of the GH spring, it experiences seasonal periods of both constant illumination (~May to July) and complete darkness (~October to February). No evidence of photoautotrophy has previously been identified in the GH spring source, even during summer illumination, and CO₂ uptake in sediments was found to be significantly higher under darkness, indicating that the GH springs are predominantly sustained by chemolithoautotrophy (4).

Seventeen of the GH MAGs contained CO₂ fixation pathways, accounting for 20 % of total relative expression; the majority, accounting for 17 % of total relative expression, were S-cycling microorganisms in the *Desulfobacterota*, *Gamma-* and *Alphaproteobacteria*, *Spirochaetota*, and *Campylobacterota*. No MAGs contained genes indicating photosynthetic capability although expression of photosystem I (*psaAB*; 12.5 tpm) and photosystem II (*psbAB*; 351.6 tpm) marker genes was identified in unbinned genes. Each gene was present in a single copy in the metagenome, and though *psaA/psbA* were initially classified as cyanobacterial, comparison of all four proteins to the NCBI nr database indicated they are most similar to chloroplast in photosynthetic eukaryotes, with *psaAB* most closely related to *Nitzschia anatoliensis* chloroplast genes (~99 % identity) and *psbAB* to *Durinskia baltica* (>99 % identity). *Nitzschia* spp. diatoms include psychrophilic and halotolerant species found in Arctic sea ice (96), while *Durinskia baltica* are dinoflagellates inhabiting freshwater and marine environments (97). Both *Nitzschia* and *Durinskia* rRNA sequences were identified in the metagenome at low abundance (<0.03 %). The low abundance of these eukaryotes, as well as the low abundance of Eukaryota (0.3 % of metagenomic reads, 0.6 % of metatranscriptomic reads) and Cyanobacteria (<0.4 % in both the metagenome and 16S rRNA gene amplicon sequences, 0.1 % of metatranscriptomic reads) indicates that while there is some amount of photoautotrophy occurring in the spring sediment during summer illumination, it is evidently insufficient to sustain large populations of photoautotrophic eukaryotes or bacteria, potentially due to their limitation during the long winter darkness. A small level of expression (0.12 tpm) was detected for *pufM*, involved in anoxygenic photosynthesis. *Alphaproteobacteria* and *Firmicutes* spp. previously isolated from GH contained *pufM* genes, indicating some level of anoxygenic photosynthesis occurs; however, these bacteria are typically photoheterotrophic and would not positively contribute to organic C supply in the

spring sediment (98). Thus, this study indicates that a low level of photosynthesis, including photoautotrophy, occurs in the spring sediment during summer illumination. However, the low abundance and activity of these microbes suggests their contribution to primary production is limited and potentially seasonal, with chemolithoautotrophic sulfur-cycling bacteria likely sustaining the majority of primary production year-round.

Sulfur-based chemolithoautotrophy as a main driver of microbial primary production is common in aphotic and light-limited S-rich environments, such as deep-sea marine environments and cave sulfidic springs (19, 99). It is rare in illuminated surficial environments such as GH where conditions are not prohibitive to photosynthesis, including other Arctic environments that experience seasonal darkness such as sea ice where algae are the primary producers (100). Similar S-based chemolithoautotrophy has also been observed at the Colour Peak and Lost Hammer AHI springs (6, 32), as well as High Arctic glacial sulfidic springs (22), indicating that it occurs where sulfur is present in abundance to power chemosynthetic life.

To contextualize the GH spring community, the 16S rRNA gene amplicon sequences were compared to sequences from 24 hypersaline, cold, and/or S-rich environments. Of the 24 datasets, a subset of 13 with sufficient metadata (including the GH replicates from this study) were selected for canonical correspondence analysis (CCA) to relate microbial community composition to environmental variables, though estimates were still required for some parameters (details in Table S3.4). A large proportion of sample variance was accounted for by the environmental variables (axis 1: 66.43 % and axis 2: 64.82 %, Figure 3.6a), though only pH was a significant factor individually based on ANOVA ($r^2 = 0.589$, p -value = 0.037 *). The GH

data from this study clustered relatively centrally without strong associations with environmental factors compared to very extreme samples from hydrothermal vents (JL95B; 379 °C, 52 mM sulfide, 42 mM sulfate, 3.42 pH) (101) and Deep Hypersaline Anoxic Basins (DHABs) (SRR6942442; 26.7 % salinity) (102). The GH data clustered most closely with saline spring samples representing previous sequencing of the GH spring sediment (SRR8381681) (31) and another AHI spring, Colour Peak (SRR9911876; 5 °C, 16 % salinity) (6). These saline springs were relatively correlated with low oxygen concentration and moderate hypersalinity in comparison with the highly extreme samples as well as with the sulfidic springs, which contain a range of environmental conditions but are characteristically non-saline. Variance in all 27 samples was also analyzed by CCA (Figure 3.6b), though only temperature and salinity could be used as environmental factors due to lack of reported metadata. Despite this, a large proportion of sample variance was again explained by the environmental variables (axis 1: 42.97 % and axis 2: 29.33 %), with the very extreme hydrothermal vents and DHABs once again strongly correlated with temperature and salinity based on ANOVA ($r^2 = 1$, p -value = 0.001 ***). Comparatively, the GH samples and AHI saline springs most closely clustered with cold brines including Arctic cryopegs and Antarctic lake and subglacial brines, and were correlated with low temperature and moderate hypersalinity. A Spearman correlation of the most abundant taxa (top 50) present in the data sets showed the sulfur cycling taxa found in GH (*Thiomicrohabdus*, *Desulfuromusa*, *Desulfobacteraceae*) were positively correlated with salinity and sulfate and negatively correlated with oxygen (Figure S3.8), and both *Thiomicrohabdus* and *Desulfobacteraceae* were also negatively correlated with temperature. An NMDS ordination of a Bray-Curtis dissimilarity matrix for all 27 samples was also plotted to compare the differences between samples based on sample composition (without environmental factors) (Figure S3.9).

Samples broadly clustered by category, reflecting the influence of environmental factors, with the GH and AHI saline springs clustering most closely with some brine samples as well as some sulfidic springs, including those at Borup Fjord in the Canadian Arctic (<5 °C, <0.5 % salinity; SRR654094 and SRR654099) (22) and Zodletone Spring in Oklahoma, USA (22 °C, 1 % salinity; “Youssef”) (65).

3.4.6 Gypsum Hill as a Mars analogue.

Sulfate is abundant on Mars, including in putative cold, briny waters in the present subsurface and past surface of Mars. The sulfate-rich, cold, hypersaline, anoxic GH spring is an excellent analogue site for identifying and constraining the microbial community and metabolisms that might be present in these environments. We identified active and abundant H₂-oxidizing, sulfate-reducing, chemolithoautotrophic *Desulfobacterota* as the likely predominant drivers of microbial primary production in the springs, utilizing abundant sulfate supplied from the subsurface. While hydrogen has not been detected in the near-surface Martian atmosphere, H₂ is postulated to be present in the subsurface as a result of serpentinization reactions (103), where co-localization with sulfate-rich brines could create similar conditions for supporting SRBs to those found in GH.

Sulfide and other sulfur species produced by SRBs in GH also support chemolithoautotrophic S-oxidizing bacteria. The majority of in situ activity was attributed to aerobic *Gammaproteobacteria* despite the highly reducing (-430 mV) and oxygen-limited (~1.25 μM O₂) conditions in the GH sediment, the relative availability of anaerobic electron acceptors such as nitrate (~6.5 μM), and the presence of anaerobic and facultatively anaerobic SOB. However,

even nanomolar concentrations of oxygen can sustain aerobic metabolisms due to the energetic favorability of O₂ as an electron acceptor (104). The relatively high energy yield of aerobic metabolisms is also favorable in hypersaline environments due to the energy expense of osmotic adaptations (105). Oxygen is present in the Martian atmosphere at ~3 nM (103), and thermodynamic modeling of putative Martian near-surface perchlorate and sulfate brines suggested O₂ could concentrate in these brines up to 2 μM, enabling aerobic respiration (106). Our results highlight the potential importance of even trace oxygen concentrations to microbial metabolism in Martian environments. Active aerobic, facultatively aerobic, and anaerobic S cycling bacteria were identified in situ in the GH spring sediments, indicating these oxygen-limited environments on Mars could support diverse S-linked metabolisms and microorganisms.

Genomes and gene expression of SRBs and SOBs in GH indicated redox of multiple S species in addition to sulfate and sulfide, and potential exchange of S intermediates between oxidizers and reducers (Figure 3.5). Measurement of sulfur isotopic fractionation is one proposed method for identification of microbial sulfur metabolism on Mars (7); NASA's Curiosity rover has measured large variations in fractionations of sulfur isotopes in Gale Crater sediments (107). Oxidation and disproportionation redox processes in addition to sulfate reduction increase S isotope fractionations, as can hypersaline stress, low temperatures, and limited available e⁻ donors (organic C, H₂) and acceptors (O₂) as in GH and in putative habitats on Mars (7, 108). Analogue environments like GH can thereby inform interpretation of isotopic measurements on Mars and help distinguish biotic from abiotic signatures (7). Previous sulfur isotope measurements in GH sediment are consistent with sulfate reduction without disproportionation and oxidative processes (32); our results demonstrate that this does not rule out the presence of these metabolisms or

reduction of additional sulfur species like elemental sulfur. This is relevant to the current Mars Science Laboratory mission (Curiosity rover) measuring sulfur isotope fractionations in Gale Crater (107), and for potential future sample return from the Perseverance rover which will allow for a larger suite of isotopic and other analyses. Notably, Perseverance recently cached sedimentary rock samples formed during evaporation of the Jezero lake that are rich in salts and organic carbon, representing an exciting candidate for future biosignature detection and demonstrating the importance of cold hypersaline sediment analogue environments such as GH to current and future biosignature detection efforts.

Our results demonstrate that sulfur-based chemolithoautotrophy in GH supports additional metabolisms including chemoorganotrophs, heterotrophs, and fermenters (Figure 3.4), including highly active and abundant microorganisms such as *Desulfuromusa*. This has implications for putative metabolisms that could exist or have existed in similar environments on Mars and their associated biosignatures (6). For example, the potential for morphological, mineralogical, or isotopic biosignatures in sulfate-rich brines additional to those associated with SRB such as isotope fractionations associated with organoheterotrophy or iron and nitrogen redox; accumulations of trace element cofactors such as copper in cytochrome c oxidases; or deposition of Se and elemental sulfur by sulfide-oxidizers (109).

3.5 Conclusion

Abundant sulfate in Gypsum Hill Spring supports an active microbial community dominated by sulfur cycling metabolisms. A complete sulfur cycle through sulfate and sulfide, including cycling of sulfur intermediate species, supports a diversity of S-reducing and S-oxidizing

microorganisms. The majority of these microorganisms demonstrate putative metabolic flexibility (oxidation and reduction of multiple S species, use of both S and N electron acceptors, facultative anaerobes), potentially in response to low energy availability (e.g. limited organic carbon and oxygen) in the spring. Our results demonstrate the potential for anoxic, cold, sulfate-rich brines to support microbial life on Mars, with implications for biosignature detection in these past/current habitats.

3.6 Acknowledgements

Figures 3.5 and S3.1 were created with BioRender.com. We thank Andrew Golsztajn (Department of Chemical Engineering, McGill University) for total C and N measurements, and we thank Scott Sugden and Louis-Jacques Bourdages for 2022 field measurements. E.M. was supported by a Natural Sciences and Engineering Research Council of Canada (NSERC) doctoral award, Fonds de recherche du Québec doctoral award, and the Northern Scientific Training Program. Arctic field research was supported through the Natural Resources Canada Polar Continental Shelf Project (PCSP). We thank the McGill Space Institute for additional support.

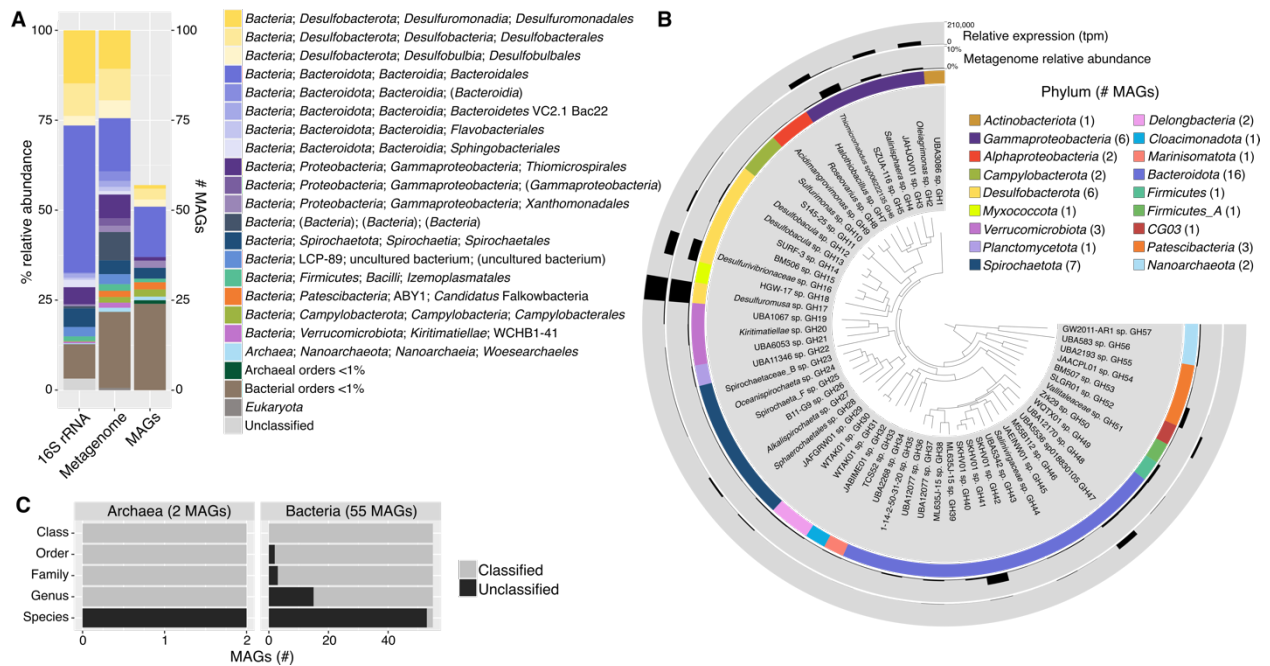


Figure 3.1.A. Relative abundance of orders in 16S rRNA gene amplicon sequencing and shotgun metagenomes and number of MAGs in each order. Shotgun metagenome relative abundance was determined by read mapping to SSU rRNA genes with phyloFlash. **B.** Phylogenomic tree of the 57 high- and medium-quality MAGs with phylum, relative abundance in the metagenome (percentage of mapped metagenome reads), and relative expression (transcripts per million reads of genes in each MAG) indicated. The tree was constructed with the anvi'o Bacteria_71 set of single-copy genes and midpoint-rooted. **C.** Level of taxonomic novelty of the MAGs. The number of classified and unclassified genomes at each taxonomic level was determined according to its rank assignment and taxonomic placement by GTDB-tk.

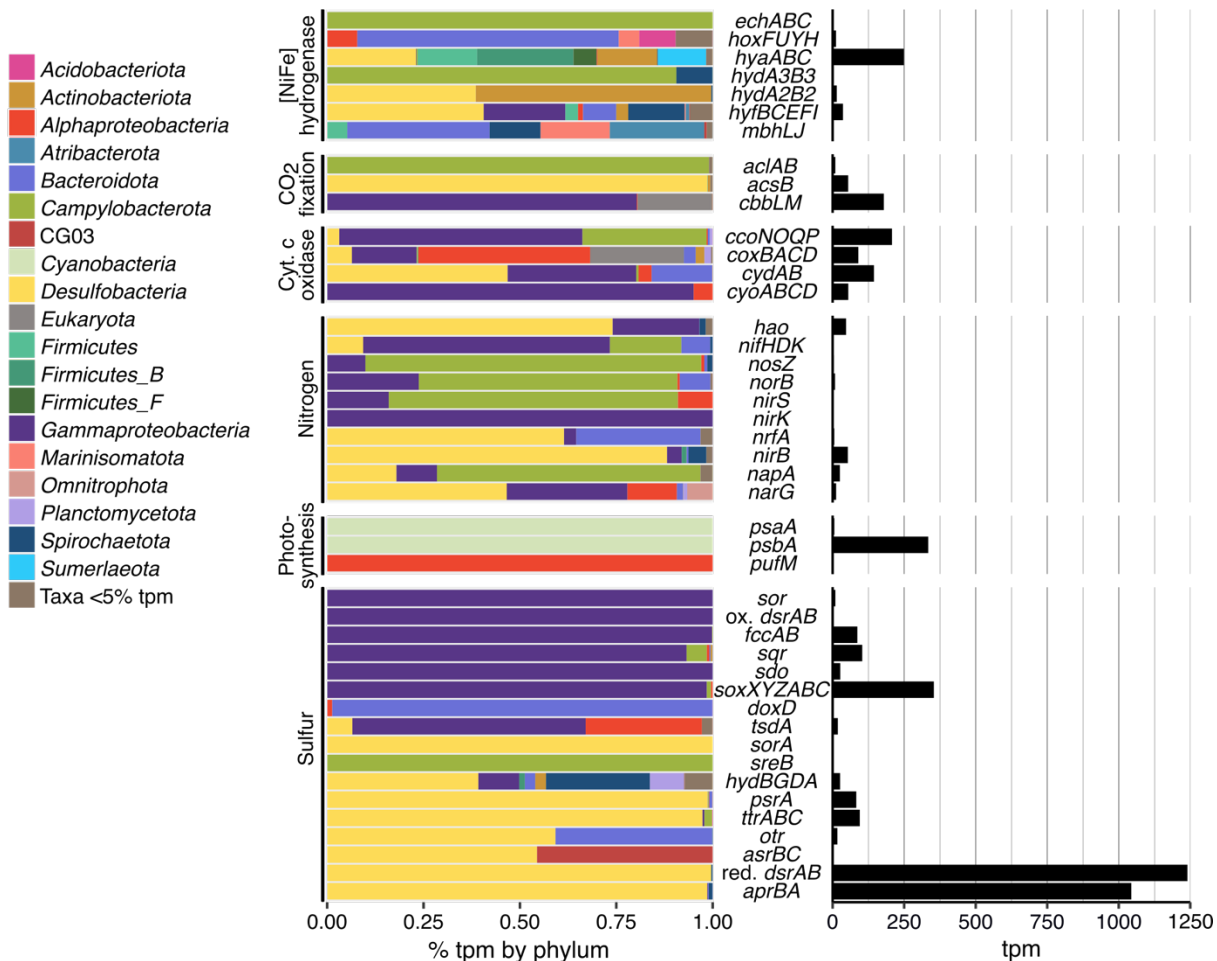


Figure 3.2. Metabolic gene relative expression and distribution of gene relative expression by phylum. Relative expression by phylum is based on the presence of expressed genes in MAGs and phylogenetic classification of unbinned genes in JGI. Complete phylogenetic distribution of depicted genes in MAGs is located in Table S3.8.

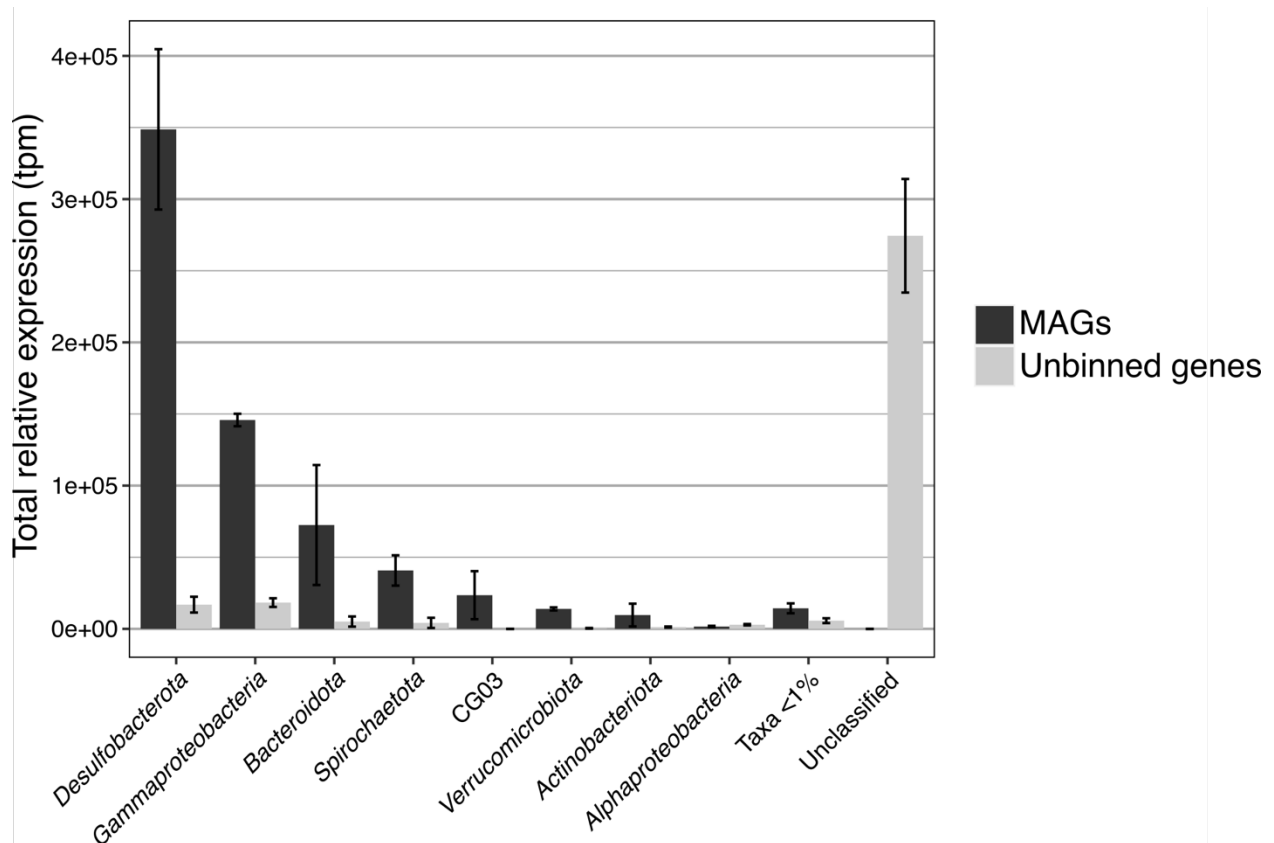


Figure 3.3. Total relative expression (tpm) of MAGs and unbinned genes in phyla or classes >1% relative abundance. Error bars indicate standard deviation between metatranscriptome replicates. Unbinned genes were classified with the JGI Phylo Distribution function.

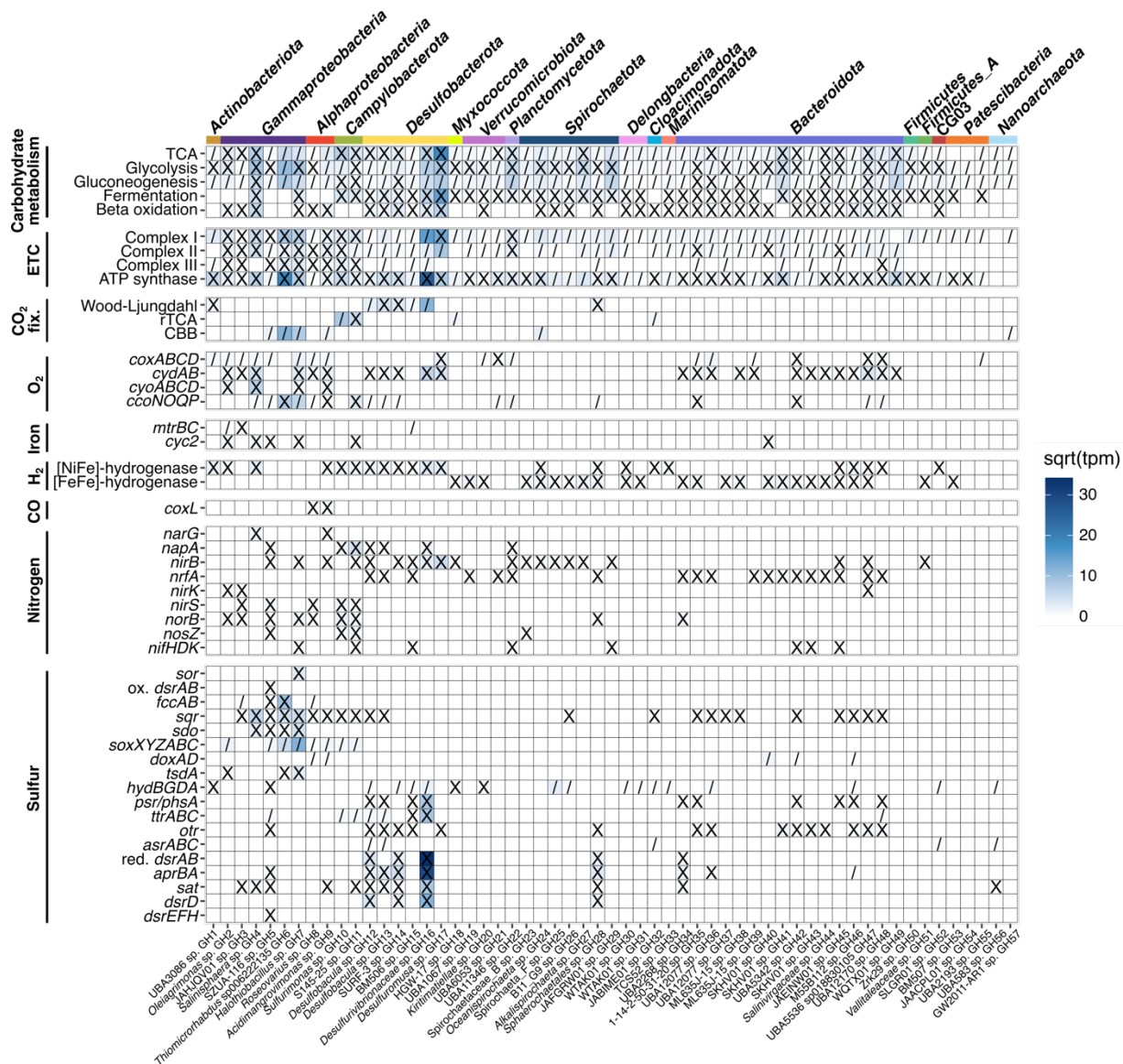


Figure 3.4. Pathway and gene presence in MAGs. Where applicable, ‘X’ indicates presence of a complete pathway and ‘/’ indicates a partial pathway. Heat map indicates square root of relative expression (transcripts per million reads) of genes in each MAG. A complete table of gene IDs and criteria for denoting the presence of a complete or partial pathway is located in Table S3.9; a corresponding table with tpm values is located in Table S3.10.

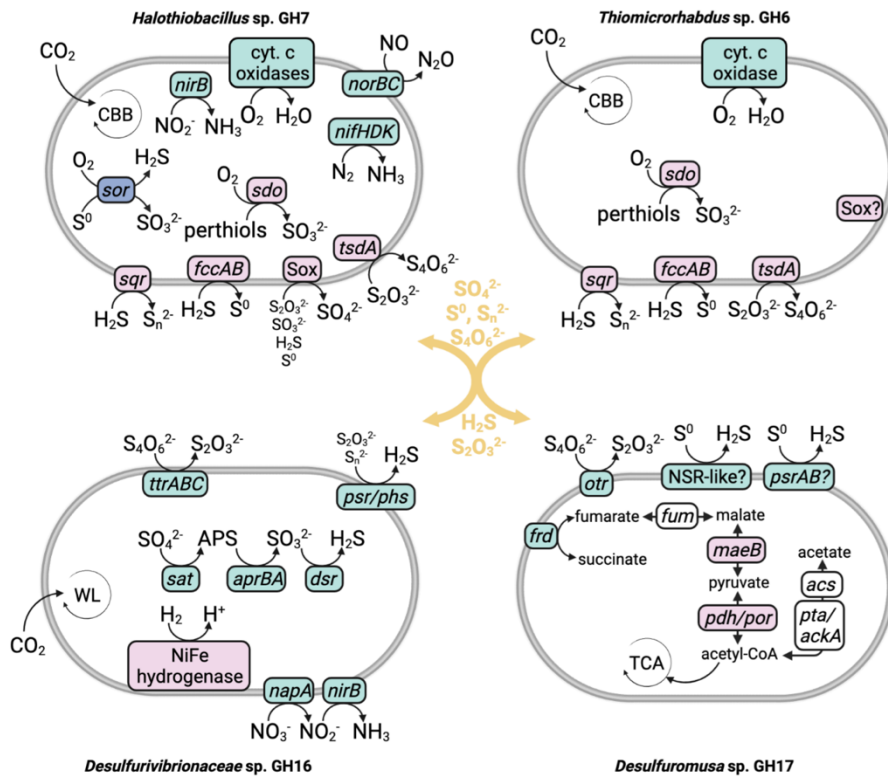


Figure 3.5. Genome content of key sulfur cycling MAGs. Genes involved in oxidation reactions are in pink; reduction in green; disproportionation in blue. Yellow text indicates sulfur species putatively exchanged between S-oxidizing and S-reducing bacteria. Complete gene names and genome content are located in Table S3.10. Abbreviations are as follows: CBB, Calvin Benson Bassham cycle; NSR, NADH-dependent sulfur reductase; TCA, tricarboxylic acid cycle; WL, Wood-Ljungdahl pathway.

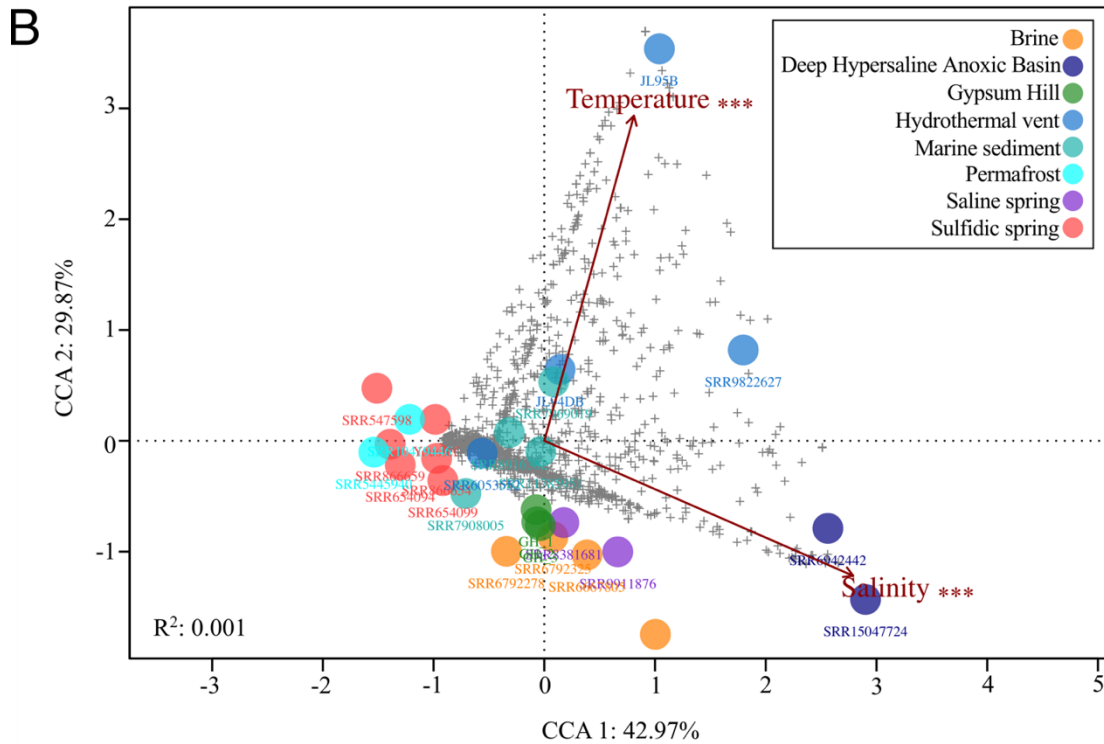
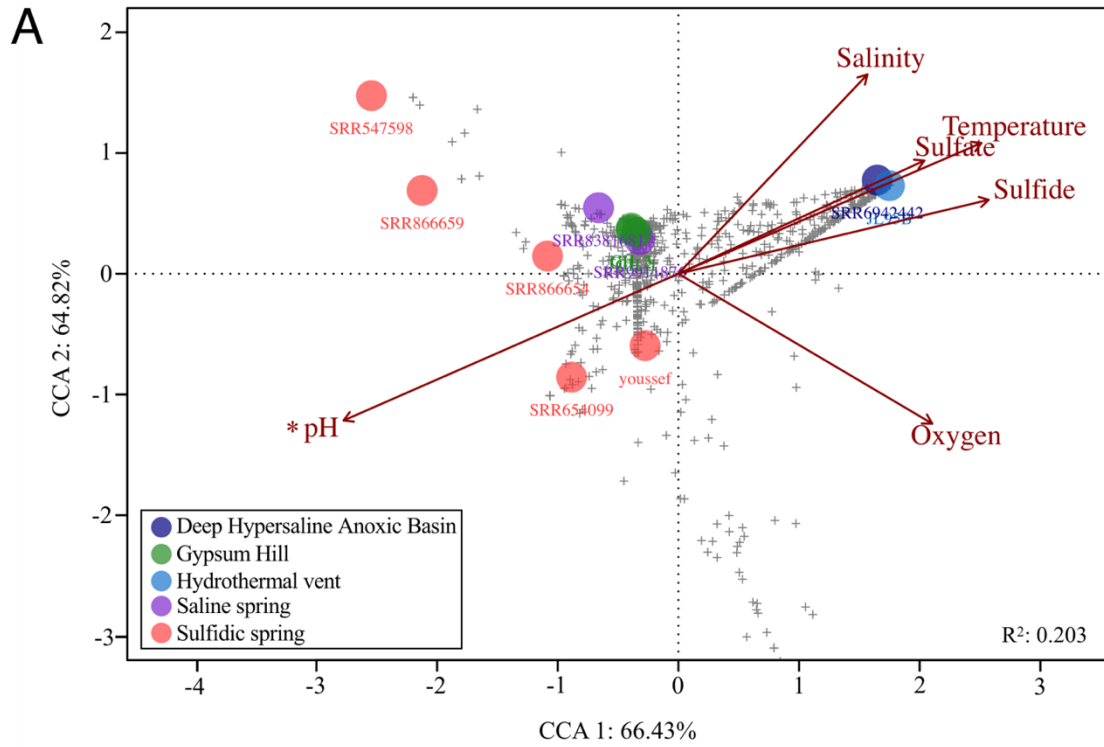


Figure 3.6.A. Plot of canonical correspondence analysis (CCA) of 16S rRNA gene sequencing from GH and cold, saline, and sulfur-rich environments relating environmental variables to

taxonomic composition of the samples (ANOVA $F=1.46$ and $p\text{-value}=0.003$ **). Circles represent total samples, '+' indicates individual taxa, '*' represents statistical significant environmental variables of $p\text{-value} \leq 0.05$. Sample metadata can be found in Table S3.4. **B.** Plot of canonical correspondence analysis (CCA) of 16S rRNA gene sequencing from GH and additional comparable environments relating temperature and salinity to taxonomic composition of the samples (ANOVA $F=1.001$ and $p\text{-value}=0.476$). Circles represent total samples, '+' indicates individual taxa, '***' represents statistically significant environmental variables of $p\text{-value} \leq 0.001$. Sample metadata can be found in Table S3.4.

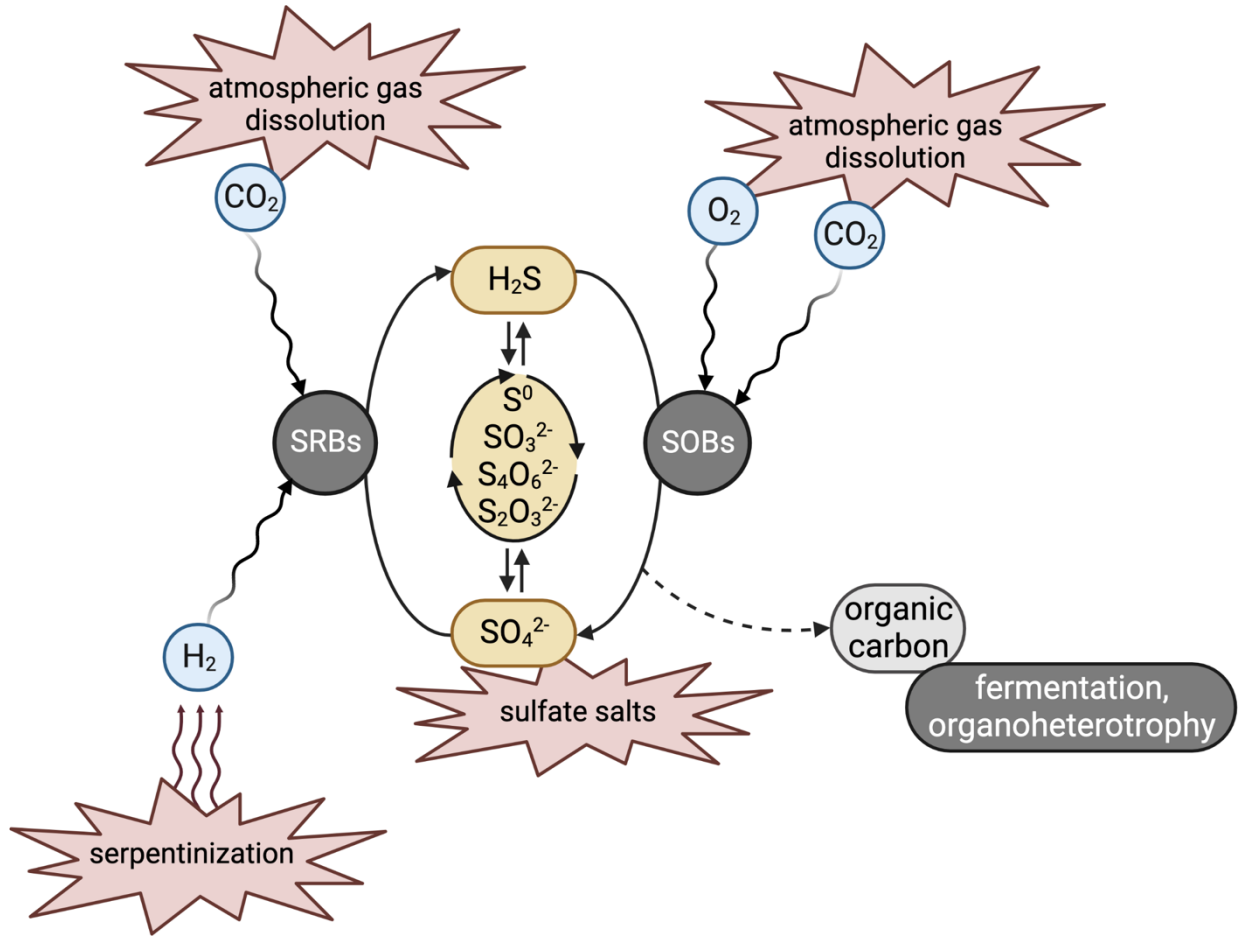


Figure 3.7. Model for a hypothetical sulfur cycling microbial community similar to the GH microbial community in a theoretical Martian environment such as sub-surface sulfate brines. Putative Martian sources of energy and carbon are indicated in red. SRBs refers to S-reducing bacteria and SOBs refers to S-oxidizing bacteria.

3.7 References

1. Andersen DT. Cold springs in permafrost on Earth and Mars. *Journal of Geophysical Research*. 2002;107(E3):4-1-4-7.
2. Pollard W, Omelon C, Andersen D, McKay C. Perennial spring occurrence in the Expedition Fiord area of western Axel Heiberg Island, Canadian High Arctic. *Can J Earth Sci*. 1999;36:105-20.
3. Perreault NN, Andersen DT, Pollard WH, Greer CW, Whyte LG. Characterization of the prokaryotic diversity in cold saline perennial springs of the Canadian high Arctic. *Appl Environ Microbiol*. 2007;73(5):1532-43.
4. Perreault NN, Greer CW, Andersen DT, Tille S, Lacrampe-Couloume G, Lollar BS, et al. Heterotrophic and autotrophic microbial populations in cold perennial springs of the high arctic. *Appl Environ Microbiol*. 2008;74(22):6898-907.
5. Battler MM, Osinski GR, Banerjee NR. Mineralogy of saline perennial cold springs on Axel Heiberg Island, Nunavut, Canada and implications for spring deposits on Mars. *Icarus*. 2013;224(2):364-81.
6. Macey MC, Fox-Powell M, Ramkissoon NK, Stephens BP, Barton T, Schwenzer SP, et al. The identification of sulfide oxidation as a potential metabolism driving primary production on late Noachian Mars. *Sci Rep*. 2020;10(1):10941.
7. Moreras-Marti A, Fox-Powell M, Stueeken E, Di Rocco T, Galloway T, Osinski GR, et al. Quadruple sulfur isotope biosignatures from terrestrial Mars analogue systems. *Geochimica et Cosmochimica Acta*. 2021;308:157-72.

8. Leask EK, Ehlmann BL. Evidence for Deposition of Chloride on Mars From Small-Volume Surface Water Events Into the Late Hesperian-Early Amazonian. *AGU Advances*. 2022;3(1):1-19.
9. Rapin W, Ehlmann BL, Dromart G, Schieber J, Thomas NH, Fischer WW, et al. An interval of high salinity in ancient Gale crater lake on Mars. *Nature Geoscience*. 2019;12(11):889-95.
10. King PL, McLennan SM. Sulfur on Mars. *Elements*. 2010;6(2):107-12.
11. Orosei R, Lauro SE, Pettinelli E, Cicchetti A, Coradini M, Cosciotti B, et al. Radar evidence of subglacial liquid water on Mars. *Science*. 2018;361(6401):490-3.
12. Bishop JL, Yesilbas M, Hinman NW, Burton ZFM, Englert PAJ, Toner JD, et al. Martian subsurface cryosalt expansion and collapse as trigger for landslides. *Science Advances*. 2021;7(6).
13. Malin MC, Edgett KS. Evidence for recent groundwater seepage and surface runoff on Mars. *Science*. 2000;288(5475):2330-5.
14. Hoffman N. Ideas About the Surface Runoff Features on Mars. *Science*. 2000;290(5492):711-4.
15. Brazelton WJ, Schrenk MO, Kelley DS, Baross JA. Methane- and sulfur-metabolizing microbial communities dominate the Lost City hydrothermal field ecosystem. *Appl Environ Microbiol*. 2006;72(9):6257-70.
16. McNichol J, Dyksma S, Mussmann M, Seewald J, Sylva SP, Sievert SM. Genus-Specific Carbon Fixation Activity Measurements Reveal Distinct Responses to Oxygen among Hydrothermal Vent Campylobacteria. *Applied and Environmental Microbiology*. 2022;88(2):e02083-21.

17. Wasmund K, Mussmann M, Loy A. The life sulfuric: microbial ecology of sulfur cycling in marine sediments. *Environ Microbiol Rep.* 2017;9(4):323-44.
18. Meziti A, Nikouli E, Hatt JK, Konstantinidis KT, Kormas KA. Time series metagenomic sampling of the Thermopyles, Greece, geothermal springs reveals stable microbial communities dominated by novel sulfur-oxidizing chemoautotrophs. *Environ Microbiol.* 2021;23(7):3710-26.
19. Engel AS, Porter ML, Stern LA, Quinlan S, Bennett PC. Bacterial diversity and ecosystem function of filamentous microbial mats from aphotic (cave) sulfidic springs dominated by chemolithoautotrophic "Epsilonproteobacteria". *FEMS Microbiol Ecol.* 2004;51(1):31-53.
20. Kubo K, Knittel K, Amann R, Fukui M, Matsuura K. Sulfur-metabolizing bacterial populations in microbial mats of the Nakabusa hot spring, Japan. *Syst Appl Microbiol.* 2011;34(4):293-302.
21. Di Nezio F, Beney C, Roman S, Danza F, Buetti-Dinh A, Tonolla M, et al. Anoxygenic photo- and chemo-synthesis of phototrophic sulfur bacteria from an alpine meromictic lake. *FEMS Microbiol Ecol.* 2021;97(3).
22. Wright KE, Williamson C, Grasby SE, Spear JR, Templeton AS. Metagenomic evidence for sulfur lithotrophy by Epsilonproteobacteria as the major energy source for primary productivity in a sub-aerial arctic glacial deposit, Borup Fiord Pass. *Front Microbiol.* 2013;4:63.
23. Reigstad LJ, Jorgensen SL, Lauritzen SE, Schleper C, Urich T. Sulfur-oxidizing chemolithotrophic proteobacteria dominate the microbiota in high arctic thermal springs on Svalbard. *Astrobiology.* 2011;11(7):665-78.
24. Mikucki JA, Pearson, A., Johnston, D.T., Turchyn, A.V., Farquhar, J., Schrag, D.P., Anbar, A.D., Priscu, J.C., Lee, P.A. A contemporary microbially maintained subglacial ferrous "ocean". *Science.* 2009;324:397-400.

25. Gilichinsky D, Rivkina E, Bakermans C, Shcherbakova V, Petrovskaya L, Ozerskaya S, et al. Biodiversity of cryopegs in permafrost. *FEMS Microbiol Ecol.* 2005;53(1):117-28.
26. Papale M, Lo Giudice A, Conte A, Rizzo C, Rappazzo AC, Maimone G, et al. Microbial Assemblages in Pressurized Antarctic Brine Pockets (Tarn Flat, Northern Victoria Land): A Hotspot of Biodiversity and Activity. *Microorganisms.* 2019;7(9).
27. Magnuson E, Altshuler I, Fernandez-Martinez MA, Chen YJ, Maggiori C, Goordial J, et al. Active lithoautotrophic and methane-oxidizing microbial community in an anoxic, sub-zero, and hypersaline High Arctic spring. *ISME J.* 2022;16(7):1798-808.
28. Lamarche-Gagnon G, Comery R, Greer CW, Whyte LG. Evidence of in situ microbial activity and sulphidogenesis in perennially sub-0 degrees C and hypersaline sediments of a high Arctic permafrost spring. *Extremophiles.* 2015;19(1):1-15.
29. Colangelo-Lillis J, Wing BA, Raymond-Bouchard I, Whyte LG. Viral Induced Microbial Mortality in Arctic Hypersaline Spring Sediments. *Front Microbiol.* 2016;7:2158.
30. Sapers HM, Ronholm J, Raymond-Bouchard I, Comrey R, Osinski GR, Whyte LG. Biological Characterization of Microenvironments in a Hypersaline Cold Spring Mars Analog. *Front Microbiol.* 2017;8:2527.
31. Colangelo-Lillis J, Pelikan C, Herbold CW, Altshuler I, Loy A, Whyte LG, et al. Diversity decoupled from sulfur isotope fractionation in a sulfate-reducing microbial community. *Geobiology.* 2019;17(6):660-75.
32. Magnuson E, Mykytczuk NCS, Pellerin A, Goordial J, Twine SM, Wing B, et al. Thiomicrorhabdus streamers and sulfur cycling in perennial hypersaline cold springs in the Canadian high Arctic. *Environ Microbiol.* 2020.

33. Andersen D. Perennial Springs in the Canadian High Arctic: Analogues of Martian hydrothermal systems. 2004.
34. Menzel P, Ng KL, Krogh A. Fast and sensitive taxonomic classification for metagenomics with Kaiju. *Nat Commun.* 2016;7(1):1-9.
35. Gruber-Vodicka HR, Seah BKB, Pruesse E. phyloFlash: rapid small-subunit rRNA profiling and targeted assembly from metagenomes. *mSystems.* 2020;5(5):1-16.
36. Li D, Liu CM, Luo R, Sadakane K, Lam TW. MEGAHIT: an ultra-fast single-node solution for large and complex metagenomics assembly via succinct de Bruijn graph. *Bioinformatics.* 2015;31(10):1674-6.
37. Mikheenko A, Saveliev V, Gurevich A. MetaQUAST: evaluation of metagenome assemblies. *Bioinformatics.* 2016;32(7):1088-90.
38. Chen IA, Chu K, Palaniappan K, Ratner A, Huang J, Huntemann M, et al. The IMG/M data management and analysis system v.6.0: new tools and advanced capabilities. *Nucleic Acids Res.* 2020;49(D1):D751–D63.
39. Mukherjee S, Stamatis D, Bertsch J, Ovchinnikova G, Sundaramurthi JC, Lee J, et al. Genomes OnLine Database (GOLD) v.8: overview and updates. *Nucleic Acids Res.* 2020;49(D1):D723-D33.
40. Langmead B, Salzberg SL. Fast gapped-read alignment with Bowtie 2. *Nat Methods.* 2012;9(4):357-9.
41. Kang DD, Froula J, Egan R, Wang Z. MetaBAT, an efficient tool for accurately reconstructing single genomes from complex microbial communities. *PeerJ.* 2015;3:e1165.
42. Wu YW, Simmons BA, Singer SW. MaxBin 2.0: an automated binning algorithm to recover genomes from multiple metagenomic datasets. *Bioinformatics.* 2016;32(4):605-7.

43. Parks DH, Imelfort M, Skennerton CT, Hugenholtz P, Tyson GW. CheckM: assessing the quality of microbial genomes recovered from isolates, single cells, and metagenomes. *Genome Res.* 2015;25(7):1043-55.
44. Chaumeil PA, Mussig AJ, Hugenholtz P, Parks DH. GTDB-Tk: a toolkit to classify genomes with the Genome Taxonomy Database. *Bioinformatics.* 2019;36(6):1925–7.
45. Alneberg J, Bjarnason BS, de Bruijn I, Schirmer M, Quick J, Ijaz UZ, et al. Binning metagenomic contigs by coverage and composition. *Nat Methods.* 2014;11(11):1144-6.
46. Sieber CMK, Probst AJ, Sharrar A, Thomas BC, Hess M, Tringe SG, et al. Recovery of genomes from metagenomes via a dereplication, aggregation and scoring strategy. *Nat Microbiol.* 2018;3(7):836-43.
47. Parks DH, Rinke C, Chuvochina M, Chaumeil PA, Woodcroft BJ, Evans PN, et al. Recovery of nearly 8,000 metagenome-assembled genomes substantially expands the tree of life. *Nat Microbiol.* 2017;2(11):1533-42.
48. Chen YJ, Leung PM, Cook PLM, Wong WW, Hutchinson T, Eate V, et al. Hydrodynamic disturbance controls microbial community assembly and biogeochemical processes in coastal sediments. *ISME J.* 2022;16(3):750-63.
49. Olm MR, Brown CT, Brooks B, Banfield JF. dRep: a tool for fast and accurate genomic comparisons that enables improved genome recovery from metagenomes through de-replication. *ISME J.* 2017;11(12):2864-8.
50. Eren AM, Esen OC, Quince C, Vineis JH, Morrison HG, Sogin ML, et al. Anvi'o: an advanced analysis and visualization platform for 'omics data. *PeerJ.* 2015;3:e1319.
51. Price MN, Dehal PS, Arkin AP. FastTree 2 – Approximately Maximum-Likelihood Trees for Large Alignments. *PLoS One.* 2010;5(3):e9490.

52. Garber AI, Nealson KH, Okamoto A, McAllister SM, Chan CS, Barco RA, et al. FeGenie: A comprehensive tool for the identification of iron genes and iron gene neighborhoods in genome and metagenome assemblies. *Front Microbiol.* 2020;11:37.
53. Sondergaard D, Pedersen CN, Greening C. HydDB: A web tool for hydrogenase classification and analysis. *Sci Rep.* 2016;6:34212.
54. Muller AL, Kjeldsen KU, Rattei T, Pester M, Loy A. Phylogenetic and environmental diversity of DsrAB-type dissimilatory (bi)sulfite reductases. *ISME J.* 2015;9(5):1152-65.
55. Edgar RC. MUSCLE: multiple sequence alignment with high accuracy and high throughput. *Nucleic Acids Res.* 2004;32(5):1792-7.
56. Anantharaman K, Hausmann B, Jungbluth SP, Kantor RS, Lavy A, Warren LA, et al. Expanded diversity of microbial groups that shape the dissimilatory sulfur cycle. *ISME J.* 2018;12(7):1715-28.
57. Frank JA, Reich CI, Sharma S, Weisbaum JS, Wilson BA, Olsen GJ. Critical evaluation of two primers commonly used for amplification of bacterial 16S rRNA genes. *Appl Environ Microbiol.* 2008;74(8):2461-70.
58. Turner S, Pryer KM, Miao VP, Palmer JD. Investigating deep phylogenetic relationships among cyanobacteria and plastids by small subunit rRNA sequence analysis. *J Eukaryot Microbiol.* 1999;46(4):327-38.
59. Kopylova E, Noe L, Touzet H. SortMeRNA: fast and accurate filtering of ribosomal RNAs in metatranscriptomic data. *Bioinformatics.* 2012;28(24):3211-7.
60. Parada AE, Needham DM, Fuhrman JA. Every base matters: assessing small subunit rRNA primers for marine microbiomes with mock communities, time series and global field samples. *Environ Microbiol.* 2016;18(5):1403-14.

61. Illumina. 16S metagenomic sequencing library preparation. 2013.
62. Callahan BJ, McMurdie PJ, Rosen MJ, Han AW, Johnson AJ, Holmes SP. DADA2: High-resolution sample inference from Illumina amplicon data. *Nat Methods*. 2016;13(7):581-3.
63. Quast C, Pruesse E, Yilmaz P, Gerken J, Schweer T, Yarza P, et al. The SILVA ribosomal RNA gene database project: improved data processing and web-based tools. *Nucleic Acids Res*. 2013;41(Database issue):D590-6.
64. Leng H, Zhao W, Xiao X. Cultivation and metabolic insights of an uncultured clade, *Bacteroidetes* VC2.1 Bac22 (*Candidatus* Sulfidibacteriales ord. nov.), from deep-sea hydrothermal vents. *Environ Microbiol*. 2022;24(5):2484-501.
65. Youssef NH, Farag IF, Hahn CR, Jarett J, Becraft E, Eloë-Fadrosh E, et al. Genomic Characterization of Candidate Division LCP-89 Reveals an Atypical Cell Wall Structure, Microcompartment Production, and Dual Respiratory and Fermentative Capacities. *Appl Environ Microbiol*. 2019;85(10).
66. Schut GJ, Bridger SL, Adams MW. Insights into the metabolism of elemental sulfur by the hyperthermophilic archaeon *Pyrococcus furiosus*: characterization of a coenzyme A- dependent NAD(P)H sulfur oxidoreductase. *J Bacteriol*. 2007;189(12):4431-41.
67. Schut GJ, Nixon WJ, Lipscomb GL, Scott RA, Adams MW. Mutational analyses of the enzymes involved in the metabolism of hydrogen by the hyperthermophilic archaeon *Pyrococcus furiosus*. *Front Microbiol*. 2012;3:1-6.
68. Paster BJ. Spirochaetes. *Bergey's Manual of Systematics of Archaea and Bacteria* 2015. p. 1- .
69. Minegishi H. Halophilic, Acidophilic, and Haloacidophilic Prokaryotes. In: Seckbach J, Oren A, Stan-Lotter H, editors. *Polyextremophiles*. New York: Springer; 2013. p. 203-13.

70. Murray AE, Kenig F, Fritsen CH, McKay CP, Cawley KM, Edwards R, et al. Microbial life at -13 degrees C in the brine of an ice-sealed Antarctic lake. *Proc Natl Acad Sci U S A*. 2012;109(50):20626-31.
71. Hahn CR, Farag IF, Murphy CL, Podar M, Elshahed MS, Youssef NH. Microbial diversity and sulfur cycling in an early earth analogue: From ancient novelty to modern commonality. 2021.
72. Neukirchen S, Sousa FL. DiSCo: a sequence-based type-specific predictor of Dsr-dependent dissimilatory sulphur metabolism in microbial data. *Microb Genom*. 2021;7(7).
73. Thiel V, Garcia Costas AM, Fortney NW, Martinez JN, Tank M, Roden EE, et al. "Candidatus *Thermonerobacter thiotrophicus*," A Non-phototrophic Member of the Bacteroidetes/Chlorobi With Dissimilatory Sulfur Metabolism in Hot Spring Mat Communities. *Front Microbiol*. 2018;9:3159.
74. Kadnikov VV, Mardanov AV, Beletsky AV, Karnachuk OV, Ravin NV. Microbial Life in the Deep Subsurface Aquifer Illuminated by Metagenomics. *Front Microbiol*. 2020;11:572252.
75. Liesack W, Finster K. Phylogenetic analysis of five strains of gram-negative, obligately anaerobic, sulfur-reducing bacteria and description of *Desulfuromusa* gen. nov., including *Desulfuromusa kysingii* sp. nov., *Desulfuromusa bakii* sp. nov., and *Desulfuromusa succinoxidans* sp. nov. *International Journal of Systematic Bacteriology*. 1994;44(4):753-8.
76. Vandieken V, Musmann M, Niemann H, Jorgensen BB. *Desulfuromonas svalbardensis* sp. nov. and *Desulfuromusa ferrireducens* sp. nov., psychrophilic, Fe(III)-reducing bacteria isolated from Arctic sediments, Svalbard. *Int J Syst Evol Microbiol*. 2006;56(Pt 5):1133-9.

77. Reysenbach AL, St John E, Meneghin J, Flores GE, Podar M, Dombrowski N, et al. Complex subsurface hydrothermal fluid mixing at a submarine arc volcano supports distinct and highly diverse microbial communities. *Proc Natl Acad Sci U S A*. 2020;117(51):32627-38.
78. Bowman JP, Rea SM, McCammon SA, McMeekin TA. Diversity and community structure within anoxic sediment from marine salinity meromictic lakes and a coastal meromictic marine basin, Vestfold Hills, Eastern Antarctica. *Environ Microbiol*. 2000;2(2):227-37.
79. Niederberger TD, Perreault NN, Lawrence JR, Nadeau JL, Mielke RE, Greer CW, et al. Novel sulfur-oxidizing streamers thriving in perennial cold saline springs of the Canadian high Arctic. *Environ Microbiol*. 2009;11(3):616-29.
80. Jelen B, Giovannelli D, Falkowski PG, Vetriani C. Elemental sulfur reduction in the deep-sea vent thermophile, *Thermovibrio ammonificans*. *Environ Microbiol*. 2018;20(6):2301-16.
81. Kletzin A, Urich T, Muller F, Bandejas TM, Gomes CM. Dissimilatory oxidation and reduction of elemental sulfur in thermophilic archaea. *Journal of Bioenergetics and Biomembranes*. 2004;36(1):77-91.
82. Ellis JC. P finder: genomic and metagenomic annotation of RNase P RNA gene (*rnpB*). *BMC Genomics*. 2020;21(1):334.
83. Steuten B, Hoch PG, Damm K, Schneider S, Kohler K, Wagner R, et al. Regulation of transcription by 6S RNAs: insights from the *Escherichia coli* and *Bacillus subtilis* model systems. *RNA Biol*. 2014;11(5):508-21.
84. Trojan D, Garcia-Robledo E, Meier DV, Hausmann B, Revsbech NP, Eichorst SA, et al. Microaerobic Lifestyle at Nanomolar O₂ Concentrations Mediated by Low-Affinity Terminal Oxidases in Abundant Soil Bacteria. *mSystems*. 2021;6(4):e0025021.

85. Ghosh W, Mallick S, DasGupta SK. Origin of the Sox multienzyme complex system in ancient thermophilic bacteria and coevolution of its constituent proteins. *Res Microbiol.* 2009;160(6):409-20.
86. Knittel K, Kuever J, Meyerdierks A, Meinke R, Amann R, Brinkhoff T. *Thiomicrospira arctica* sp. nov. and *Thiomicrospira psychrophila* sp. nov., psychrophilic, obligately chemolithoautotrophic, sulfur-oxidizing bacteria isolated from marine Arctic sediments. *Int J Syst Evol Microbiol.* 2005;55(Pt 2):781-6.
87. Mikucki JA, Priscu JC. Bacterial diversity associated with Blood Falls, a subglacial outflow from the Taylor Glacier, Antarctica. *Appl Environ Microbiol.* 2007;73(12):4029-39.
88. Wood AP, Woodall CA, Kelly DP. *Halothiobacillus neapolitanus* strain OSWA isolated from "The Old Sulphur Well" at Harrogate (Yorkshire, England). *Syst Appl Microbiol.* 2005;28(8):746-8.
89. Sievert SM, Heidorn T, Kuever J. *Halothiobacillus kellyi* sp. nov., a mesophilic, obligately chemolithoautotrophic, sulfur-oxidizing bacterium isolated from a shallow-water hydrothermal vent in the Aegean Sea, and emended description of the genus *Halothiobacillus*. *Journal of Systematic and Evolutionary Microbiology.* 2000;50:1229–37.
90. Kelly DP, Wood AP. Reclassification of some species of *Thiobacillus* to the newly designated genera *Acidithiobacillus* gen. nov., *Halothiobacillus* gen. nov. and *Thermithiobacillus* gen. nov. *International Journal of Systematic Bacteriology.* 2000;50:511–6.
91. Sorokin DY, Tourova TP, Lysenko AM, Muyzer G. Diversity of culturable halophilic sulfur-oxidizing bacteria in hypersaline habitats. *Microbiology (Reading).* 2006;152(Pt 10):3013-23.

92. Liu S. Archaeal and Bacterial Sulfur Oxygenase-Reductases: Genetic Diversity and Physiological Function. In: Dahl C, Friedrich CG, editors. *Microbial Sulfur Metabolism*. Heidelberg: Springer-Verlag; 2008. p. 217-23.
93. Daffonchio D, Borin S, Brusa T, Brusetti L, van der Wielen PW, Bolhuis H, et al. Stratified prokaryote network in the oxic-anoxic transition of a deep-sea halocline. *Nature*. 2006;440(7081):203-7.
94. Whaley-Martin KJ, Chen L-X, Nelson TC, Gordon J, Kantor R, Twible LE, et al. Acidity and sulfur oxidation intermediate concentrations controlled by O₂-driven partitioning of sulfur oxidizing bacteria in a mine tailings impoundment. *biorRxiv*. 2021.
95. Boden R. Reclassification of *Halothiobacillus hydrothermalis* and *Halothiobacillus halophilus* to *Guyarkeria* gen. nov. in the Thioalkalibacteraceae fam. nov., with emended descriptions of the genus *Halothiobacillus* and family Halothiobacillaceae. *Int J Syst Evol Microbiol*. 2017;67(10):3919-28.
96. Aletsee L, Jahnke J. Growth and productivity of the psychrophilic marine diatoms *Thalassiosira antarctica* Comber and *Nitzschia frigida* Grunow in batch cultures at temperatures below the freezing point of sea water. *Polar Biology*. 1992;11.
97. Zhang Q, Liu G-X, Hu Z-Y. *Durinskia baltica* (Dinophyceae), a newly recorded species and genus from China, and its systematics. *Journal of Systematics and Evolution*. 2011;49(5):476-85.
98. George DM, Vincent AS, Mackey HR. An overview of anoxygenic phototrophic bacteria and their applications in environmental biotechnology for sustainable Resource recovery. *Biotechnol Rep (Amst)*. 2020;28:e00563.
99. Yamamoto M, Takai K. Sulfur metabolisms in epsilon- and gamma-proteobacteria in deep-sea hydrothermal fields. *Front Microbiol*. 2011;2:192.

100. Boetius A, Anesio AM, Deming JW, Mikucki JA, Rapp JZ. Microbial ecology of the cryosphere: sea ice and glacial habitats. *Nat Rev Microbiol.* 2015;13(11):677-90.
101. Ding J, Zhang Y, Wang H, Jian H, Leng H, Xiao X. Microbial Community Structure of Deep-sea Hydrothermal Vents on the Ultraslow Spreading Southwest Indian Ridge. *Front Microbiol.* 2017;8:1012.
102. Nigro LM, Elling FJ, Hinrichs KU, Joye SB, Teske A. Microbial ecology and biogeochemistry of hypersaline sediments in Orca Basin. *PLoS One.* 2020;15(4):e0231676.
103. Rummel JD, Beaty DW, Jones MA, Bakermans C, Barlow NG, Boston PJ, et al. A new analysis of Mars "Special Regions": findings of the second MEPAG Special Regions Science Analysis Group (SR-SAG2). *Astrobiology.* 2014;14(11):887-968.
104. Berg J, Ahmerkamp S, Pjevac P, Hausmann B, Milucka J, Kuypers MMM. How low can they go? Aerobic respiration by microorganisms under apparent anoxia. *FEMS Microbiol Rev.* 2022:1-37.
105. Oren A. Thermodynamic limits to microbial life at high salt concentrations. *Environ Microbiol.* 2011;13(8):1908-23.
106. Stamenković V, Ward LM, Mischna M, Fischer WW. O₂ solubility in Martian near-surface environments and implications for aerobic life. *Nature Geoscience.* 2018;11(12):905-9.
107. Franz HB, McAdam AC, Ming DW, Freissinet C, Mahaffy PR, Eldridge DL, et al. Large sulfur isotope fractionations in Martian sediments at Gale crater. *Nature Geoscience.* 2017;10(9):658-62.
108. Westall F, Foucher F, Bost N, Bertrand M, Loizeau D, Vago JL, et al. Biosignatures on Mars: What, Where, and How? Implications for the Search for Martian Life. *Astrobiology.* 2015;15(11):998-1029.

109. Banfield JF, Moreau JW, Chan CS, Welch SA, Little B. Mineralogical Biosignatures and the Search for Life on Mars. *Astrobiology*. 2001;1(4):447-65.

Connecting Text

The previous chapters described the active microbial communities inhabiting cold, hypersaline spring sediments utilizing a combination of meta'omics methods. In this chapter, I utilized metagenomics, metatranscriptomics, and metaproteomics to describe the genome and in situ gene and protein expression of a sulfide-oxidizing chemolithoautotrophic bacterium capable of forming biofilm 'streamers' under cold and hypersaline conditions in the Gypsum Hill Spring channels. I additionally described the stress response capabilities putatively enabling its survival and allowing for the formation of these unique biofilms under extreme conditions.

This manuscript appears in:

Magnuson E, Mykytczuk NCS, Pellerin A, Goordial J, Twine SM, Wing B, et al.

Thiomicrothrix streamers and sulfur cycling in perennial hypersaline cold springs in the Canadian high Arctic. *Environ Microbiol.* 2021;23(7):3384-3400. doi: 10.1111/1462-2920.14916.

File S1 is available as supplemental material.

Chapter 4. *Thiomicrohabdus* streamers and sulfur cycling in perennial hypersaline cold springs in the Canadian high Arctic

Elisse Magnuson¹, Nadia C.S. Mykytczuk², Andre Pellerin³, Jacqueline Goordial^{1,4}, Susan M. Twine⁵, Boswell Wing⁶, Simon J. Foote⁵, Kelly Fulton⁵, Lyle G. Whyte¹

¹Natural Resource Sciences, McGill University, Montreal, QC

²Vale Living with Lakes Centre, Laurentian University, Sudbury, ON

³Centre for Geomicrobiology, Aarhus University, Aarhus, Denmark

⁴Bigelow Laboratory for Ocean Sciences, East Boothbay, USA

⁵Institute for Biological Sciences, National Research Council, Ottawa, ON

⁶Earth and Planetary Sciences, McGill University, Montreal, QC

4.1 Originality-Significance Statement

The high Arctic Gypsum Hill springs flow perennially despite temperatures that drop below -40°C during the winter and discharge oligotrophic brines transported through ~600 m of permafrost that are rich in inorganic sulfur compounds. In this study, the activity and adaptation of microbial streamers formed in the springs' outflow channels during the winter were investigated through metagenomic, metatranscriptomic, and metaproteomic analyses. A 96% complete *Thiomicrobacterium* sp. metagenome-assembled genome was recovered and characterized. The -omic data in combination with multiple sulfur isotope fractionation data from the spring system revealed a halo- and cryo-tolerant community cycling abiotic and biogenic sulfur species in a unique cryoenvironment.

4.2 Summary

The Gypsum Hill (GH) springs on Axel Heiberg Island in the Canadian high Arctic are host to chemolithoautotrophic, sulfur-oxidizing streamers that flourish in the high Arctic winter in water temperatures from -1.3 to 7°C with ~8% salinity in a high Arctic winter environment with air temperatures commonly less than -40°C and an average annual air temperature of -15°C.

Metagenome sequencing and binning of streamer samples produced a 96% complete *Thiomicrobacterium* sp. metagenome-assembled genome representing a possible new species or subspecies. This is the most cold- and salt-extreme source environment for a *Thiomicrobacterium* genome yet described. Metaproteomic and metatranscriptomic analysis attributed nearly all gene expression in the streamers to the *Thiomicrobacterium* sp. and suggested that it is active in CO₂ fixation and oxidation of sulfide to elemental sulfur. In situ geochemical and isotopic analyses of the fractionation of multiple sulfur isotopes determined the biogeochemical transformation of

sulfur from its source in Carboniferous evaporites to biotic processes occurring in the sediment and streamers. These complementary molecular tools provided a functional link between the geochemical substrates and the collective traits and activity that define the microbial community's interactions within a unique polar saline habitat where *Thiomicrothrix*-dominated streamers form and flourish.

4.3 Introduction

Perennial springs in the Canadian high Arctic are rare examples of deep saline groundwater springs underlain by continuous permafrost. Such springs are of interest as analogs to the recurring slope lineae (RSL) observed on Mars (1), where chemolithoautotrophic metabolism might have left biosignatures of extinct or possibly extant life (2). The network of perennial springs found at Gypsum Hill (GH) on west-central Axel Heiberg Island, Nunavut, surface through 600 m thick continuous permafrost in a region with a mean annual temperature of -15°C (3, 4). They discharge oligotrophic brines (7.5-7.9% salt) that are rich in inorganic sulfur compounds (1-100ppm total sulfides), saturated with dissolved gases (primarily N_2), anoxic (mean Oxidation Reduction Potential of -325 mV), near neutral (pH 6.9–7.5), high in sulfate (23.9-38.8 mM), low in dissolved inorganic carbon (13.1–17.2 mg/L), and maintain a constant temperature (-1.3°C to 6.9°C) throughout the year despite air temperatures that drop below -40°C during the winter (3, 5). The springs are located at nearly 80°N and experience distinct seasonal illumination with continuous sun during the Arctic summer and total darkness in the winter.

Previous studies found the GH spring source sediments harbour a diverse community of bacterial heterotrophic and autotrophic populations including bacterial species from *Actinobacteria*, *Bacteroidetes*, *Firmicutes*, *Gemmatimonadetes*, *Proteobacteria*, *Spirochaetes*, and *Verrucomicrobia*, and a lower abundance of archaeal species from the *Crenarchaeota* and *Euryarchaeota* (5, 6). The spring's primary outflow community contained a significant proportion of clones (19%) most closely related to *Thiomicrothabodus psychrophila* (initially referred to as *Thiomicrospira* sp. in our previous study (7)) that form and dominate greyish streamers flowing in the runoff channels (Figure 4.1). These streamers are observed in dense clusters in the dark winter months while the springs' runoff channels are covered in snow, trapping hydrogen sulfide gas, followed by dissipation in the continuous sun of the summer months (7). The streamers were found to flourish via chemolithoautotrophic, phototrophic-independent metabolism. In situ activity measurements identified sulfide and thiosulfate oxidation and CO₂ fixation by the streamers in the high Arctic winter environment. The streamers were also found to contain unusual cigar-shaped minerals within the biofilm exopolymeric substances (EPS) consisting of elemental sulfur and gypsum minerals potentially of biogenic origin.

Microbial sulfur cycling has been described in a variety of environments where sulfur compounds are in abundance and is often linked to volcanic activity, including hydrothermal vents (8, 9), hot springs (10, 11), and cold springs (12). Sulfur is also a primary driver of microbial metabolism in oligotrophic anoxic and aphotic systems such as caves (13-16), subglacial environments (17), and even as cryptic cycles in marine oxygen minimum zones (18). Microbial species among *Gamma*- and *Epsilon*proteobacteria, *Bacteroidetes*, and *Chlorobi*

(green sulfur bacteria) are most commonly involved in sulfur oxidation (15, 19, 20), while sulfate reduction is driven by sulfate-reducing bacteria (SRB) species among the *Deltaproteobacteria*, *Nitrospirae*, *Clostridia*, and *Thermodesulfobacteria* and several Archaeal genera (19) Recent surveys have also identified the capacity for sulfate reduction in genomes from many additional phyla (21).

Thiomicrohabdus spp. are chemolithoautotrophic sulfur oxidizers that have primarily been isolated from and found in sulfidic marine sediments and hydrothermal vents (22). This genus was previously part of *Thiomicrospira*, which was split into the *Thiomicrospira*, *Thiomicrohabdus*, and *Hydrogenovibrio* genera (23). The majority of *Thiomicrohabdus* spp. have been found in environments warmer than GH, but a few isolates have been obtained from comparably cold and salty conditions, including *T. arctica* (Arctic coastal sediments) and *T. sp.* HaS4 (cold saline lake) (24, 25). *Thiomicrohabdus arctica* dominated a sulfate-rich subglacial brine in Antarctica, indicating the cold and salt adaptability of the genus (17). However, the contributions of sulfur oxidizers such as *Thiomicrohabdus* spp. to sulfur cycling in polar environments have not yet been fully described. In a subaerial glacial deposit in Borup fjord in the Canadian high Arctic, not far from our study site, a metagenomic analysis revealed the sulfur oxidation in the glacial system was dominated by *Sulfurovum* and *Sulfuricurvum* species, while sequences related to *Thiomicrohabdus* (previously identified as *Thiomicrospira*) and the sulfur-reducing community were in low abundance (26). Other metagenomic studies of cold sulfur-cycling ecosystems such as the Southwest Indian Ridge were able to map the functional link between the SRB and sulfur-oxidizing (S-ox) communities, including sequences attributed to *Thiomicrospira* (prior to reorganization of the genus), providing stronger genomic evidence for

complete sulfur cycles in these limiting systems (27). Although SRB have been identified as drivers of S-ox communities, the diversity of metabolic pathways and shuffling of sulfur between microbial species in cryoenvironments is not entirely clear.

S-isotopes are useful in deciphering biogeochemical S pathways in studies of bacterial sulfur cycling. Microbial sulfate reduction, sulfide oxidation, and S disproportionation all produce characteristic relationships between ^{33}S – ^{32}S and ^{34}S – ^{32}S ratios of their respective products and reactants (28-30). Multiple sulfur isotope approaches have been applied in a variety of aquatic systems where sulfate reduction dominates the S-isotope cycling, such as euxinic Lake Cadagno, Switzerland (18). For example, by comparing the multiple sulfur isotope signatures produced by pure cultures of sulfate-reducing bacteria, sulfide-oxidizing bacteria, and sulfur disproportionators to the porewater sulfate multiple sulfur isotope signature in Mangrove Lake, Bermuda, the fraction of reduced sulfate that is re-oxidized was estimated (31).

The GH spring streamers dominated by *Thiomicrothrix* sp. are an excellent model for deciphering sulfur cycling with potential for mapping biosignatures between sulfur compounds of different redox states in a cold spring system. The objectives of this study were to provide a comprehensive meta-genomic, -proteomic, and -transcriptomic analysis of the functional potential and expressed metabolism of the streamers and to link the S-isotopic signatures of sulfur cycling in the spring channel environment.

4.4 Results

4.4.1 Phylogenetic classification

Streamers were sampled in May, when the GH outflow channels are partially snow-covered and streamers are most abundant. Pyrosequencing of 16S rRNA identified *Proteobacteria* as the most abundant phylum in the streamers, with *Actinobacteria*, *Bacteroidetes*, and *Cyanobacteria* constituting the rest of the community (Figure 4.2). Within *Proteobacteria*, *Gammaproteobacteria* were the most abundant, with *Thiomicrohabdus* the most abundant genus in the total population at 27% relative abundance. *Pseudomonas*, *Methylococcaceae*, and *Marinobacter* were also identified within *Gammaproteobacteria*. These results suggest that *Thiomicrohabdus*, while the most abundant genus within the streamers, did not completely dominate the 16S rRNA transcript pool.

4.4.2 Metagenome analyses

MIRA assembly of the metagenome produced 4.9 Mbp of assembled sequence data in 2,653 contigs. MG-RAST analysis attributed 70.5% of contigs to *Thiomicrospira* (using a database that has not been updated to reflect recent changes to the *Thiomicrospira* genus). No other phylum or class was assigned more than 3% of total contigs. Other represented phyla included *Firmicutes*, *Bacteroidetes*, and *Euryarchaeota*. Fifteen partial 16S rRNA sequences were identified in the assembled sequence. Fourteen aligned at >99% identity to *Thiomicrohabdus* sp. NP51 and other *Thiomicrohabdus* spp, most commonly *T. arctica*, while one aligned with 90% identity.

4.4.3 *Thiomicrohabdus* sp. metagenome-assembled genome

Metagenome binning of the MIRA assembly produced a single bin, which was attributed to *Thiomicrohabdus*. The *Thiomicrohabdus* bin represented a near-complete metagenome-assembled genome (MAG) at 2.3 Mbp and was estimated at 96% complete with 3%

contamination and 100% strain heterogeneity by CheckM. Two partial 16S sequences were identified within the MAG, and aligned with 99% identity to *T. arctica* and 100% identity to *Thiomicrospira* sp. NP51 (formerly *Thiomicrospira* sp. NP51) previously isolated from the springs (GenBank: EU196304.1) (6). Amino acid identity (AAI) was calculated against the NCBI RefSeq and Microbial Genomes Atlas Online TypeMat databases. *Thiomicrospira arctica* was identified as the closest species at 86.89% AAI. According to the standards for classification with AAI described in Konstantinidis et al. (32), the *Thiomicrospira* sp. genome can thus be considered a new species in the *Thiomicrospira* genus. Additionally, average nucleotide identity (ANI) was calculated with 10 *Thiomicrospira*, *Thiomicrospira*, and *Hydrogenovibrio* genomes (File S1). The closest genome was *T. arctica* at 84.76%, while the rest were calculated at 75-77%. An ANI below 95% indicates the genome represents novelty at the species level at a minimum (32). As such, the MAG was classified as *Thiomicrospira* sp., possibly representing a new species of *Thiomicrospira*. The MAG will thus be referred to as *Thiomicrospira* sp. GH.

4.4.4 Metatranscriptome results

Following quality control, 7,128 sequences were detected in the metatranscriptome. Of these, 3,106 were annotated in MG-RAST (43.6%) and 2,992 were classified by COG identifiers (41.9%) (File S1). The largest group of sequences were uncharacterized or poorly characterized (COG categories S and R, 544 sequences, 18.2%) (File S1). The majority (89%) of annotated sequences were aligned to *Thiomicrospira* sp. GH contigs (2,767 sequences). Of the remaining 11% (339 sequences), sequences aligned to *Bacteroides* (88, exclusively

transposases), *Escherichia coli* (37), *Nitrosococcus* (4), *Marinobacter* (3), and others in smaller amounts.

4.4.5 Metaproteome results

In the metaproteome, 1,593 unique proteins were identified (File S1). Of these, 95% aligned to predicted peptides in the GH metagenome, and 68% aligned to peptides from *Thiomicrothabodus* sp. GH. The predicted gene phylogeny for peptides annotated in joint genome institute found the closest match of 83% of peptides in *T. arctica*, and the closest match of 93% to be in *Thiomicrothabodus*, *Thiomicrospira*, or *Hydrogenovibrio* spp. In addition, the closest match in the NCBI nr database for nearly all proteins (98%) was *Hydrogenovibrio crunogenus* XCL-2, which is closely related to *Thiomicrothabodus*. Approximately 35 proteins were annotated as other species, including sulfur metabolic proteins and cell envelope modification proteins. The Exponentially Modified Protein Abundance Index (emPAI), which estimates relative protein abundance in proteomic studies, was calculated for each identified protein (File S1). The PAI value is calculated from the ratio of observed peptides per protein to the number of theoretically observable peptides per protein. The emPAI value is calculated as 10 to the power of PAI minus one. Annotated proteins with an emPAI value greater than zero (indicating that they have a relatively high concentration in the proteome compared to those with a score of 0) were primarily ribosomal proteins, which is to be expected in a metaproteome sample. Proteins related to stress response and sulfur metabolism with emPAI values above zero included a cold-shock DNA-binding domain protein, exo-polysaccharide synthesis proteins, and a flavocytochrome c sulfide dehydrogenase.

4.4.6 Sulfur metabolism

The *Thiomicrothrix* sp. GH MAG contained putative genes for approximately half of the Sox pathway, which oxidizes thiosulfate to sulfate. In the MAG, *soxB*, *soxC*, *soxD*, *soxF*, and *soxH* were identified. A *soxX* and partial *soxA* and *soxY* were found in unassembled metagenome reads that were attributed to *Thiomicrothrix*. It is possible that these were not assembled due to microdiversity in the samples. Additionally, SoxB and SoxF were identified in the metaproteome, and both aligned to predicted peptides from *Thiomicrothrix* sp. GH. Given the previous detection of thiosulfate oxidation by the streamers, it seems likely that it is indeed capable of this oxidation despite incomplete identification of the pathway in the assembled MAG. The *Thiomicrothrix* sp. GH MAG and transcriptome and the metaproteome contained the assimilatory sulfate reduction pathway (although adenylylsulfate kinase was not found in the transcriptome and metaproteome), which reduces sulfate to sulfide (33). Only one other *Thiomicrothrix* genome examined here contained these genes (*Thiomicrothrix* sp. Milos-T2), which may indicate unique capabilities within this genus for cysteine biosynthesis in the case of low sulfide concentrations. The metagenome, metatranscriptome, and metaproteome do not contain the dissimilatory sulfate reduction pathway (33) beyond sulfate adenylyltransferase, indicating that *Thiomicrothrix* sp. GH is apparently incapable of this sulfate reduction pathway as well as the reverse pathway proposed as a sulfur oxidizing mechanism for some chemolithoautotrophic sulfur oxidizers (34).

The *Thiomicrothrix* sp. GH MAG, the streamer metatranscriptome, and the metaproteome contained a flavocytochrome c sulfide dehydrogenase (EC 1.8.2.-), which oxidizes sulfide to sulfur and is commonly found in phototrophic bacteria that use reduced sulfur compounds as

electron donors for CO₂ fixation (35). The *Thiomicrobacterium* sp. GH MAG and transcriptome also contained a sulfide:quinone reductase, which catalyzes the oxidation of sulfide to elemental sulfur and deposits sulfur globules outside the cell. Additionally, enzymes catalyzing sulfide oxidation to cysteine and serine are present (cysteine synthase (EC 2.5.1.47) and serine O-acetyltransferase (EC 2.3.1.30)). A single gene (*dsrE*) was identified in the MAG from the Dsr gene cluster, which oxidizes sulfur globules. The *Thiomicrobacterium* sp. GH MAG, streamer metatranscriptome, and the metaproteome also contained rhodanese enzymes, which cleave thiosulfate and have been proposed to be involved in thiosulfate oxidation pathways (36). They did not contain the sulfur oxygenase reductase (SOR), which catalyzes the conversion of sulfur in the presence of molecular oxygen to sulfite, thiosulfate, and hydrogen sulfite (37). With the exception of the assimilatory sulfate reduction pathway, the capability of the *Thiomicrobacterium* sp. GH MAG in the utilization of sulfide and thiosulfate was typical of previous reports of *Thiomicrobacterium* spp. and consistent with in situ activity measurements.

4.4.7 Additional metabolic pathways

A single Form II RuBisCO was identified in the MAG. This is unusual for *Thiomicrobacterium* spp., which typically also contain a Form IAq RuBisCO. While the RuBisCO gene is located near a carbonic anhydrase gene, the MAG lacks a carboxysomal locus and many typical carboxysomal genes like those found in other *Thiomicrobacterium* spp. (38). *Thiomicrobacterium arctica* and Milos-T2 are the only *Thiomicrobacterium*, *Thiomicrospira*, and *Hydrogenovibrio* spp. that lack this locus. It does contain SulP-family transporters that are homologous to those identified on *Thiomicrobacterium* carboxysomal loci and shown to be upregulated in low inorganic carbon conditions (38), and may transport bicarbonate into the cell to compensate for low DIC

concentrations. Additionally, both alpha- and beta-carbonic anhydrases were identified in the MAG. Most genes encoding enzymes in the Calvin-Benson-Bassham cycle were identified in the MAG, with the exception of sedoheptulose-1,7-bisphosphatase (EC 3.1.3.37). This is common in *Thiomicrothabodus*, and it has been proposed that they use the transaldolase version of the cycle (22). No transaldolase was identified in the MAG, transcriptome, or metaproteome.

The genes related to nitrogen metabolism in the *Thiomicrothabodus* sp. GH MAG were typical of *Thiomicrothabodus*, which utilize ammonium as an N source (23). The *Thiomicrothabodus* sp. GH MAG contained Type I glutamine synthetase and glutamate synthase, which convert ammonia to glutamine and glutamate. It also contained several regulators and adenylylators of glutamine synthetase. In the transcriptome and metaproteome, glutamine synthetase (Type I), glutamate synthase, and glutamate-ammonia-ligase adenylyltransferase were identified, as well as nitrite reductase and PII nitrogen regulatory protein. The *Thiomicrothabodus* sp. GH MAG, transcriptome, and proteome also contained ammonia permease, ammonium transporter, and nitrate transporter. In the metagenome, there was additional functional potential, including assimilatory nitrate reduction genes on contigs attributed to *Hahella* (*Gammaproteobacteria*), *Sphingopyxis* (*Alphaproteobacteria*), and *Pseudoalteromonas* (*Gammaproteobacteria*).

The *Thiomicrothabodus* sp. GH MAG contained putative genes for a complete Embden-Meyerhof-Parnas glycolysis pathway. As found in all other *Thiomicrothabodus*, *Thiomicrospira*, and *Hydrogenovibrio* genomes (22), the citric acid cycle was incomplete and lacked NADH malate dehydrogenase (EC 1.1.1.37) and a complete 2-oxoglutarate dehydrogenase complex (EC 1.2.4.2/2.3.1.61/1.8.1.4). Only one of the proposed alternative genes (succinate semialdehyde

dehydrogenase, EC 1.2.1.24) was identified, suggesting that the citric acid cycle is incomplete and functions only in biosynthesis of intermediates. In addition, electron transport chain components previously found in other *Thiomicrohabdus* spp. were identified, including a cytochrome bc1 complex and cbb₃-type cytochrome c oxidase (Figure 4.3) (22).

4.4.8 Stress response

The *Thiomicrohabdus* sp. GH MAG contained a number of genes related to osmotic and temperature stress response. This included ectoine synthesis and regulation genes (*ectABC*) and choline and betaine uptake genes (ProVWX and BetT transporters). While these genes are present in many *Thiomicrohabdus*, *Thiomicrospira*, and *Hydrogenovibrio* spp., the accumulation of compatible solutes has been shown to be an important strategy in cold- and salt-adapted microorganisms, including in the Arctic (39, 40), and is thus likely a survival mechanism for *Thiomicrohabdus* sp. GH survival in 8% salinity and -1.3 to 7°C in the GH springs. The MAG also contained three Na⁺/H⁺ antiporter genes, generally found in higher copies in cold adapted organisms (41). Cold response genes present include cold-induced stress response regulator CspE (42) and a DEAD box helicase that is involved in translation at low temperatures (43).

Presence and copy number of a variety of stress response genes were identified in six *Thiomicrohabdus* genomes as well as the *Thiomicrohabdus* sp. GH MAG, transcriptome, and metaproteome (Table 4.1; extended table in File S1). The genomes were sourced from environments with a range of temperatures and salinities, including hydrothermal vents (*T. sp.* 13-15a, *T. frisia* Kp2, *T. sp.* Milos-T2), marine sediments (*T. chilensis* and *T. arctica*), and a cold

saline lake (*T. HaS4*). Of particular interest were genes in the psychrophilic and closely-related *T. arctica*. It is worth noting here that the *Thiomicrobacterium* sp. GH MAG was estimated to have 100% strain heterogeneity, and thus there exists the possibility that it consists of a co-assembly of multiple strains, which could artificially increase copy number. Given low estimated contamination and the presence of gene copies on separate contigs for the genes discussed below, we will assume that the comparisons remain valid. Gene presence and copy number were largely similar across the stress response genes examined here, suggesting that the ability to respond to various stressors is relatively universal across the genus. The *Thiomicrobacterium* sp. GH MAG contained higher copy numbers of glutathione peroxidase (EC 1.11.1.9) (two copies vs. one copy) and thioredoxin reductase (EC 1.8.1.9) (seven copies vs. one copy) than any other *Thiomicrobacterium* genome, which may suggest an increased ability to respond to oxidative stress. However, it also lacked a catalase found in 5 out of 7 *Thiomicrobacterium* genomes used for comparison. Also present was the general stress response DNA-binding protein Dps (EC 1.16.3.1) which was identified only in the *Thiomicrobacterium* sp. GH MAG, *T. arctica*, and *T. sp. HaS4* (one copy in each), which were all found in cold environments. Most notable, however, is the presence of genes related to exo-polysaccharide biosynthesis in *T. arctica* and the *Thiomicrobacterium* sp. GH MAG. Both contained *epsC-L* biosynthesis and transport genes (between one and 11 copies of each), which were generally not identified in any other genome with the exception of *epsC* (at least one copy in all genomes), *epsF* (one copy in *T. milos*), and *epsG* (one copy in *T. milos*). *Thiomicrobacterium arctica* also contained one copy of *ExoZ*. Most exo-polysaccharide biosynthesis proteins were identified in the transcriptome and metaproteome. In addition, the *Thiomicrobacterium* sp. GH MAG and *T. chilensis* genome contained a capsular polysaccharide export protein and capsule polysaccharide biosynthesis protein (both present in

single copies). The presence of exopolysaccharide biosynthesis genes has previously been noted for *T. arctica* (22).

4.4.9 Sulfur isotope results

Analysis of the sulfur isotope composition of streamers showed that they had the most negative signatures with average $\delta^{34}\text{S}$ of -29.21 ‰ and $\Delta^{33}\text{S}$ of 0.13 ‰ (Table 4.2). The sediment had isotopic compositions which were negative in $\delta^{34}\text{S}$ from a minimum of -25.48 ‰ to a maximum of -11.61 ‰ and appeared to become slightly more negative with depth although the data are scattered. The $\Delta^{33}\text{S}$ ranged between 0.05 and 0.11 ‰. We analyzed the isotopic composition of the sulfate remaining after chromium reducible sulfur (CRS) extraction at 5, 7.5, and 10 cm depth and found that they closely clustered around an average $\delta^{34}\text{S}$ of 20.46 ‰ and $\Delta^{33}\text{S}$ of 0.02 ‰ which is a value closely resembling that of the sulfate in the springs (44) as well as seawater sulfate and Carboniferous evaporites (see (45) for support) which are the likely source of sulfate in the spring.

4.5 Discussion

The *Thiomicrothabodus* sp. GH MAG and transcriptome and the metaproteome suggested sulfide oxidation to sulfur and CO_2 fixation as the primary redox functions occurring in the streamers (Figure 4.3). The metagenome and MAG contained nearly all of the Sox pathway, but the *soxZ* gene was not identified. As it is an essential part of the oxidation pathway, it is unclear if the *soxZ* gene was not detected in the assembly or whether the remaining genes would be functional. Additional mechanisms have been proposed involving truncated versions of the Sox pathway, such as a thiosulfate oxidation pathway excluding the Sox(CD)₂ enzymes (46), but no pathway

has been proposed that excludes the SoxZ protein as found here. Additionally, only SoxB was detected in the metatranscriptome or metaproteome. That the additional Sox proteins were not found suggests that despite their presence in the metagenome, they may not be expressed. Without the SoxY/Z complex with which it interacts, it is unclear what activity the SoxB protein would have. However, the measurement of in situ thiosulfate oxidation activity by the streamers suggests that a thiosulfate oxidation mechanism is likely functional within *Thiomicrobacterium* sp. GH. Thiosulfate scavenging by rhodanese may be occurring as described in *Hydrogenovibrio thermophilus*, which uses acceptor substrates like cyanide and lipoic acid (47).

Both a flavocytochrome c sulfide dehydrogenase and a sulfide:quinone reductase were identified in the metagenome, metatranscriptome, and metaproteome. These proteins oxidize sulfide to elemental sulfur which is then deposited in extracellular globules. The formation of extracellular globules has previously been observed primarily in organisms lacking Sox(CD)₂, which is found in the *Thiomicrobacterium* sp. GH MAG, but it has also been observed in *Thiomicrospira* containing the *soxCD* genes dependent on extracellular pH (47, 48). As such, it is suggested that the *Thiomicrobacterium* sp. GH streamers are oxidizing sulfide to sulfur with extracellular deposition of elemental sulfur, and perhaps oxidizing thiosulfate to sulfate as a secondary activity. These results are consistent with previous in situ measurements of sulfide and thiosulfate oxidation and CO₂ fixation in microcosms of streamer samples (7) that in combination with the -omics results obtained in this study strongly indicate that the *Thiomicrobacterium* sp. GH MAG obtained represents a *Thiomicrobacterium* strain capable of forming streamers embedded with S granules and supporting lithoautotrophic metabolism through S oxidation and carbon fixation under ambient conditions.

Within the metagenome there were a notable number of genes related to exo-polysaccharide biosynthesis and transport. Several of these genes have previously only been identified in *T. arctica* within the genus. Their presence in the *Thiomicrohabdus* sp. GH MAG is thus not surprising given its close relatedness to *T. arctica* and previous identification of EPS structures in the streamers (7). EPS formation has been associated with protection from environmental stressors such as cold and desiccation, as well as mediating adhesion (49, 50). High levels of EPS production have been detected in psychrophiles (39). It is possible that it directly provides environmental protection to these *Thiomicrohabdus* spp., or it may contribute to formation of the GH streamers, which have been theorized to form at sites of increased dissolved oxygen concentration to facilitate survival (7). It is unclear whether aggregate formation would have any impact on *T. arctica*. In addition, *T. chilensis* lacks these genes but has been shown to form aggregates (51). Additional experimentation is required to determine if these genes confer unique capability to *T. arctica* and *Thiomicrohabdus* sp. GH. Regardless, based on the presence of these genes and others related to stress response we conclude that *Thiomicrohabdus* sp. GH is cold and salt tolerant.

The GH spring water is characterized by salinities that are greater than seawater (salinity 7-8%) and sulfate concentrations of 38.5 mM (4). This is the result of the spring being formed from salt diapirs and groundwater originating in Phantom and Astro Lakes flowing through salt layers from Carboniferous evaporites (52). The $\delta^{34}\text{S}$ of sulfates from the spring water, 22.2 ‰ (44), corresponds to that of sulfate deposited in Carboniferous evaporites (45). Thus, the source of the sulfur in the GH spring is probably from Carboniferous evaporites. A portion of this sulfate is

converted in the spring sediment by microbial sulfate reduction to sulfide, which accumulates in the spring water to concentrations of 0.26 mM (5). While sulfate reduction can in principle occur deep in the aquifer and convert a portion of the sulfate to sulfide before entering the discharge area, it is likely that most of the sulfide is produced at the discharge area in the spring source sediments. Sulfide production is mostly a result of sulfate reduction in the uppermost portion of sediments, where the availability of labile organic carbon is at its highest. This is consistent with observations from marine and freshwater sediments which often show a close coupling between the site of sulfide production and the site of sulfide oxidation (53). Based on the analysis of $\delta^{34}\text{S}$ of CRS (which includes reduced inorganic sulfur compounds such as thiosulfate and polysulfides) and sulfate in the sediment, the sulfide is isotopically light relative to the sulfate, consistent with active dissimilatory sulfate reduction occurring in the springs. However, the $\delta^{34}\text{S}$ of sulfate in the spring water and in the sediment are close to the Carboniferous evaporites, suggesting that the consumption of sulfate by dissimilatory sulfate reduction has had little to no effect, from a mass balance perspective on the $\delta^{34}\text{S}$ of sulfate flowing out of the spring and thus is quantitatively unimportant. Moreover, the $\delta^{34}\text{S}$ of CRS in the sediment does not reflect a deep source of sulfide because the most negative $\delta^{34}\text{S}$ is observed in the shallowest sediment. If the sulfide was produced deep in the spring, iron oxides in the sediment would react with this sulfide to produce CRS with a $\delta^{34}\text{S}$ reflecting the deep sulfide (uniform and low) which is not the case. These rule out a significant source of deep sulfide.

Thus, the isotopic difference between CRS and sulfate ($\delta^{34}\text{S}_{\text{H}_2\text{S}} - \delta^{34}\text{S}_{\text{SO}_4}$) reflects the fractionation in an open system and can be taken as a proxy for the net sulfur isotope fractionation induced by the microbial community in the spring ($^{34}\epsilon$). In our study, $^{34}\epsilon$ appears to

be roughly -50 ‰ if the most negative CRS samples (the streamers) are compared with the pore water sulfate (Table 4.2). This fractionation between the reduced sulfur and sulfate are within the range produced by pure cultures of sulfate-reducing bacteria (54) and within the typical range observed in marine sediments dominated by sulfate reduction as the main organic matter mineralization process (e.g. (55)). The CRS extractions performed on the streamers also extracted elemental sulfur, a product of sulfide oxidation. Elemental sulfur and sulfur-containing minerals have previously been identified in the streamers with microscopy (7). In this study the genes responsible for sulfur globule production were identified within the *Thiomicrospira* sp. GH MAG. Interestingly, the microbiological and molecular analysis documented the ability of the streamers in the GH spring to oxidize sulfide and intermediate sulfur oxidation phases while lacking the pathway to oxidize sulfide to sulfate (Figure 4.3). It is therefore possible that additional or unknown sulfur cycling processes are contributing to the observed fractionation between sulfate and CRS.

Multiple sulfur isotopes (the relationship between the isotopic discrimination of $^{34}\text{S}/^{32}\text{S}$ and $^{33}\text{S}/^{32}\text{S}$) in some instances are different between different kinds of metabolic pathway and can provide some independent insight into the sulfur cycling. The relationship between the multiple isotopes of sulfur we define here as

$$\lambda = \frac{\ln\left(\frac{^{33}\epsilon}{1000} + 1\right)}{\ln\left(\frac{^{34}\epsilon}{1000} + 1\right)}$$

where $^{33}\epsilon$ is the net minor sulfur isotope fractionation induced by the microbial community in the spring. For example, sulfate reduction produces a relationship between the $^{34}\text{S}/^{32}\text{S}$ and $^{33}\text{S}/^{32}\text{S}$ which falls in a defined field on a plot of $^{34}\epsilon$ vs λ (Figure 4.5A) whereas re-oxidative sulfur

cycling can produce λ which fall outside of this field (56, 57). The CRS extracted from the streamers are characterized by a large $^{34}\epsilon$ but low λ (Figure 4.5). This means that these sulfur isotope fractionations can be explained by microbial sulfate reduction while re-oxidative cycles that induce large multiple sulfur isotope fractionations like disproportionation are not required to explain the measurements. This being said, at high sulfur isotope fractionations it becomes increasingly difficult to differentiate sulfate reduction from re-oxidative processes (58). The streamers are capable of re-oxidizing sulfide to elemental sulfur but do not seem to be able to oxidize elemental sulfur to sulfate. The multiple sulfur isotopes suggest the re-oxidation of sulfide undergone in the streamers may not be causing significant fractionation and it rules out a re-oxidative pathway like disproportionation processing an important fraction of the sulfur found in the streamers. This also agrees with the suggestion from the metagenomics study that *Thiomicrothabodus* sp. GH does not have the metabolic machinery to disproportionate the intermediates to sulfate (Figure 4.3). Alternatively, in the event that elemental sulfur is disproportionated to sulfate and sulfide, the fractionation induced by this process could be diluted in the large sulfate pool and leave little of the signature evident.

The isotopic $\delta^{34}\text{S}$ of CRS extracted from spring source sediments is lower than the streamers. Compared with the streamers, the sediment has a lower $^{34}\epsilon$ and a higher λ (Figure 4.5A). This trajectory appears to have a slight depth-dependence and is not associated with any known microbial process. Rather, the multiple sulfur isotope signature observed in the core taken from the GH spring can be best explained as a mix between CRS with two unique sources. The first corresponds to the isotopic signature in the CRS pool that was recovered from the streamers, likely microbial sulfate reduction in an open system. The second source of reduced sulfur is

speculative as it has not been measured. One possibility is that the sediments contain detrital sulfides that have survived the weathering process and would typically be composed of an igneous isotopic signature $\delta^{34}\text{S} = 0 \text{ ‰}$, $\Delta^{33}\text{S} = 0 \text{ ‰}$. Mixing these two sources of sulfide reproduces the sulfur isotopes measured in the sediment where between 10 to 60% of the sulfide must be contributed by sulfate reduction and the balance from the detrital source (Figure 4.5B). Alternative possibilities are 1) in the sediment closed system conditions prevail and a significant portion of the sulfate is reduced to sulfide thereby influencing the net isotope fractionation observed in the sediment; 2) our extraction procedure also extracts sulfate from the sediment. The first alternative possibility is less likely because sulfate was extracted from three sediment depths and showed no isotopic enrichment trends that could be associated with sulfate reduction under a closed system. The second alternative possibility is very unlikely because the CRS procedure employed does not make use of a strong enough reductant to reduce sulfate, as is demonstrated by a strong set of controls which are run in parallel with the extractions.

In summary of the isotope results, the sulfur isotope measurements suggest that sulfate reduction occurs in close proximity to the streamers, where the most labile organic matter is present (Figure 4.4). The sulfide produced by sulfate reduction leads to elemental sulfur formation in close proximity to the streamers. The multiple sulfur isotopes did not reveal clear evidence that a microbial re-oxidative cycle is contributing to the isotopic signature that was measured. The sulfur isotopic signature observed in the reduced sulfur in the sediment is likely the result of mixing of two sources of sulfur; first the sulfide which is produced as a result of microbial sulfate reduction in situ, which has a negative $\delta^{34}\text{S}$, and second, detrital sulfide which was deposited along with the sediment and which has a $\delta^{34}\text{S}$ of around 0 ‰ (Figure 4.5).

The study presented here combines -omic and isotopic approaches to characterize microbial streamers and sulfur cycling in an extreme Arctic cold saline spring. We elucidated the biotic and abiotic sources and transformations of sulfur compounds, and identified the contributions of SRB and S-ox microbial populations to sulfur cycling. In addition, we described a novel *Thiomicrothabodus* sp. MAG sequenced from the most cold- and salt-extreme environment thus far with unique features related to sulfur metabolism and stress response, and discussed how *Thiomicrothabodus*-dominated sulfur-oxidizing streamers are able to survive in a unique polar ecosystem. Overall, these results show that a cold hypersaline environment supports significant populations of chemolithotrophic microbes and expands our understanding of how *Thiomicrothabodus* and other sulfur-oxidizing bacteria flourish in extreme cryoenvironments, with implications for the possibility of life existing in analogous Martian habitats or the outer icy moons hypothetically capable of supporting chemolithotrophic, phototrophic independent microbial life.

4.6 Experimental Procedures

4.6.1 Study site and sample collection

The geology, geomorphology, and water chemistry of the network of perennial springs adjacent to Gypsum Hill (GH) (79°24'30"N, 90°43'05"W) are described in detail in previous papers (3, 4, 59). Previous details of the sediment microbial community completed by 16S rRNA clone library construction and metabolic assays are described by Perreault et al. (5, 6). The first descriptions of the streamer community are described in Niederberger et al. (7). The springs from which streamer samples were collected include GH-4, site of the initial investigation by Perreault et al.

(5), and a new spring channel GH-9, adjacent and downstream from GH-4. Temperature, oxidation reduction potential, and total sulfides were measured in the field as described previously to ensure that conditions were consistent with previous characterization. At time of sampling, the dissolved H₂S concentration in the streams was determined to be ~1 ppm (CHEMtrix, Calverton). Daytime air temperatures averaged -15°C in both GH-4 and GH-9 and the water temperature was 7°C.

Streamer samples were collected in May 2010 using sterile tweezers and were subsequently stored in LifeGuard Soil Preservation Solution (MO BIO Laboratories, Carlsbad) for molecular analyses, and in spring water for S-isotopic analyses. Samples were transported and stored at -20°C until further analysis, which was completed within two weeks of sampling. Sediment cores from the GH-4 and GH-9 spring sources were collected using a homemade rubber piston corer using 3.8cm diameter PVC pipe, rinsed with ethanol. Only short cores (<5cm) could be recovered from GH-4, while a 23cm core was recovered from GH-9. A duplicate core was collected at GH-9 for immediate pore-water extraction using Rhizon pore water samplers (Eijkelkamp Agrisearch, the Netherlands) but insufficient pore water was extracted for further analyses. Intact sediment cores were stored at -20°C until processed for isotopic analyses in the lab.

Additional sample collection for the snow-covered channel head-space gas was attempted using a glass vacuum sampler containing zinc acetate (4% w/v). Although ~300 mL of gas was sampled and bubbled through the Zn-acetate solution, insufficient H₂S precipitated as ZnS needed for downstream isotopic analyses.

4.6.2 Metagenome library

All meta-omic analyses were completed on streamer samples stored in LifeGuard Soil Preservation Solution (MO BIO Laboratories, Carlsbad). For metagenomic analyses, total genomic DNA was extracted from 2 x 0.5 g (wet weight) streamers using the Ultra Clean DNA Extraction kit (MO BIO Laboratories, Carlsbad) according to manufacturer's protocols. A total of 1 ug of DNA was sent for whole genome shotgun sequencing using a Roche 454 GS-FLX Titanium sequencer (454 Life Sciences, Branford), located at the Centre for Applied Genomics, Hospital for Sick Children (Toronto, Canada). Quality filtering of raw sequence data was performed using FastQC, followed by de novo assembly using MIRA v2.0 (60). The assembled metagenome totaled 4.9Mbp with 2,653 contigs and was annotated using MetaGenomics Rapid Annotation using Subsystem Technology (MG-RAST) (ID: 4466258.3) (61, 62). Protein annotations were determined using BLAST against M5NR compiled protein database at a cutoff e-value $<1e^{-5}$. Taxonomic and functional classification were compared within the MG-RAST workbench and against COGs and the NCBI non-redundant databases using a basic local alignment search tool for proteins (BLASTp) (63). The metagenome was also uploaded to joint genome institute integrated microbial genomes and microbiomes (JGI IMG)/MER for annotation and additional analysis. CommunityM and barnap were used to identify 16S rRNA sequences in the assembled data. Extracted sequences were aligned against the SILVA database (132 SSU Ref NR 99). The metagenome and metatranscriptome sequence data are available in GenBank under the BioProject accession number VCMH00000000.

Assembled MIRA contigs were binned with MetaBAT (v2.12.1) using standard and sensitive settings (64). A single identical bin with 206 contigs (2.3 Mbp total) was produced with both settings. The output bin was taxonomically identified and analyzed with CheckM (65). Binning was attempted a second time with MIRA contigs after removal of previously-binned contigs, but no additional bins could be produced. Binned contigs were queried against the NCBI nucleotide (nt) and Greengenes (13_5) databases with BLASTn (66-68). Binned contigs were also uploaded to RAST for annotation (69). Amino acid identity was calculated with the Microbial Genomes Atlas Online (70). Average nucleotide identity was calculated with FastANI v1.1 (71).

For gene copy number comparisons, protein-coding genes were predicted in the *Thiomicrothabodus* sp. GH genome with Prodigal v2.6.3. Protein annotations for all reference genomes were downloaded from the NCBI Genome database and used to create a custom BLAST database. The protein-coding genes from all genomes were individually queried against the custom database with BLASTp using a cut-off e-value of 1e-15. Additionally, the reference genomes were queried against the *Thiomicrothabodus* sp. GH protein-coding genes annotated with JGI IMG/MER.

4.6.3 Metatranscriptome library

Total RNA was extracted from 2 x 2.0 g (wet weight) streamer samples using the PowerSoil RNA Extraction kit (MO BIO, Carlsbad, USA) according to manufacturer's protocols with modifications as follows: (i) an additional 1.0 g of 0.1 mm glass beads (MO BIO, Carlsbad, USA) were added to each reaction tube, (ii) bead-beating time was doubled, and (iii) nucleotide precipitation was performed overnight. Extracted RNA was pooled and treated with

amplification grade DNase I (1U/uL, Invitrogen, Carlsbad, USA) at room temperature for 15 minutes following the manufacturer's instructions and then inactivated by the addition of EDTA at 65°C for 20 minutes. The iScript cDNA synthesis kit (Bio-Rad, Hercules) was used for cDNA synthesis from RNA according to the manufacturer's protocols. The cDNA was cleaned using 30 k Amicon Ultra-0.5 mL Centrifugal Filters (Millipore Corporation, Burlington). The cDNA library was sequenced by the Research and Testing Laboratory (Lubbock) using a Roche 454 GSFLX Titanium sequencer (454 Life Sciences, Branford) system with bacterial primers (28F:5'GAGTTTGATCNTGGCTCAG'3, 519R:5' GTNTTACNGCGGCKGCTG'3) following established protocols (72). The sequence library was trimmed, aligned, and dereplicated using the ribosomal database project pyrosequencing pipeline (73) with a minimum quality score of 20 and a minimum sequence length of 150 bp. Trimmed sequences were aligned using the pyrosequencing aligner with Bacteria/Archaea model and clustered using complete-linkage clustering method with a maximum distance of 15% and step size of 1.0. The dereplicated sequences were generated using representative sequence method with 98% similarity and then analyzed via the BLASTn algorithm against the GenBank nr database (63). Phylogenetic trees of selected sequences were generated with MEGA 5 (74), using a bootstrap method with 1,000 replications and a Jukes-Cantor model.

The remaining DNase I-treated RNA (1.5ug) was enriched for mRNA using the MICROBExpress kit (Ambion, Austin) to deplete bacterial 16S and 23S rRNAs, according to the manufacturer's instructions. The total mRNA yield was used in cDNA synthesis using the iScript cDNA synthesis kit (Bio-Rad, Hercules) as earlier. The cDNA was cleaned to remove oligos and amplification reagents using 30 k Amicon Ultra-0.5 mL Centrifugal Filters (Millipore

Corporation, Burlington) to a final amount of 2.3 µg. The cDNA was then treated with RNase H (Invitrogen, Carlsbad) according to manufacturer's protocols followed by sample clean-up using the Amicon Ultra filters (as above) yielding 1.8 µg. Whole genome amplification (WGA) was used to increase template yields using the GenomiPhi V2 kit via multiple displacement amplification (MDA) (GE Healthcare, Piscataway, USA) according to manufacturer's protocols. Briefly, 2 µL of cDNA with concentration 867 ng/µL were combined with 9 µL sample buffer and heated at 95 °C for 3 mins, cooled to 4 °C briefly then followed by incubation at 30 °C for 90 min with addition of 10µL of 10:1 enzyme:reaction buffer. To terminate the reaction, the sample was heated at 65°C for 10 mins yielding 6.5 µg templates ranging from 200bp-1kb. The transcriptome library was generated using paired-end 2x 100bp sequencing on the Illumina HiSeq 2000 platform by the Centre for Applied Genomics, Hospital for Sick Children (Toronto, ON, Canada) with library preparation completed using standard oligonucleotides designed for multiplexed paired-end sequencing.

The transcriptomic data was quality filtered with removal of duplicate reads and reads with total quality < 20 and assembled using the metagenome as a scaffold using MIRA v2.0 and Newbler for comparison and annotated in MG-RAST, as earlier. Transcripts were aligned using bowtie2 run in the default end-end mode (75) and total counts were generated using HTSeq-count (76).

4.6.4 Metaproteomic analyses

Protein extraction of environmental samples with single or limited extraction methods may neglect proteins with particular characteristics, such as hydrophobic or membrane-bound proteins (77, 78). In order to overcome this extraction bias, streamer samples were processed

using one of two different protein extraction methods (one-step detergent vs. phenol-chloroform) and one of two different purification methods to maximize the total number of surface and intracellular proteins recovered. In all cases, extractions were completed on streamers washed with PBS buffer at environmental salinity (7.5% NaCl) to clear away residual sediments without cell lysis. A subsample of washed streamers were then extracted using standard phenol-chloroform-isoamyl alcohol (25:24:1) extraction. This yielded a protein pellet with a black and white fraction. To promote solubilization, the pellet was first solubilized with formic acid (80% v/v), and any residual pellet was re-suspended in twelve times the pellet volume of lysis solution (5 M urea, 2 M thiourea, 1% DTT, 4% CHAPS, 0.5% ASB-14). In a second method, the washed streamers were extracted directly into the lysis solution and cells were disrupted by sonication (Fisher Scientific, Ontario, Canada) using 0.5 s bursts for three cycles of 30 s and incubated for 1.5 h at room temperature with agitation. Extracts were separated with centrifugation at 14,000 × g for 10 min. As in the first method, any residual pellet was re-extracted using the lysis solution. These extractions yielded four separate fractions, on which two purification steps were completed on the heterogeneous protein extract to remove remaining contaminants: (i) The aqueous fraction of the protein extracts was processed using the Wessel and Flugge protocol (79) which uses methanol-chloroform to pellet protein, or (ii) the aqueous fraction was treated with cold-acetone (20% v/v) addition to precipitate the proteins from the cloudy supernatant. In total, eight different protein fractions were collected, including all possible combinations of the two extraction methods and two purification methods, and quantified individually using a modified Bradford assay (80). Yields ranged between 2.5 and 30.9 µg/µL.

All protein extracts were separated in 1D SDS-PAGE (12% acrylamide) gels run at 175V for 45min. Gels were subsequently stained with silver nitrate and imaged on a FluorS (Bio-Rad, Hercules) gel scanner. Each lane was cut into ~25 gel slices and destained with 15 mM potassium hexacyanoferrate, 50 mM sodium thiosulfate. Proteins were digested with 10 ng/ μ L trypsin in 50 mM ammonium bicarbonate at 37°C for 16 h and final volumes were concentrated. The resulting peptides were analyzed by nano-liquid chromatography MS/MS (nLC-MS/MS) using an LTQ XL orbitrap MS (Thermo Fisher Scientific, Ottawa, Canada) coupled to a nanoAcquity ultrahigh-pressure liquid chromatography system (Waters, Milford). Peak lists were automatically generated by Proteinlynx software (Waters, Milford) with the following parameters: smoothing—four channels, two smooths, Savitzky-Golay mode; centroid—minimum peak width at half height of four channels, centroid top 80%. Peptide spectra were searched against the National Centre for Biotechnology nonredundant database and using Mascot 2.0.6 (Matrix Science, London, UK). A peptide score of 30 and above for a top-ranked hit was taken as positive identification, with each MS/MS spectrum verified by manual inspection. Annotated proteins were matched with COG assignments as above. Protein abundance was quantified within each of the 8 extracted fractions using emPAI (exponentially modified protein abundance index) (81).

4.6.5 Sediment mineralogy via XRD

The 23cm core from GH-9 was divided into 2.5 cm sections and subsamples were sent for X-ray diffraction (XRD) analysis. Sediments were air dried at room temperature and crushed by hand with a mortar and pestle, then prepared in back-packed powder mounts, to decrease preferred orientation of the crystallites. Detailed mineral determination was performed via XRD (Co K-

alpha radiation $\lambda=1.7902 \text{ \AA}$, Rigaku Rotaflex, 45kV, 160 mA) at the Laboratory for Stable Isotope Science at the University of Western Ontario (London, Canada). Data were collected with an effective step size of 0.02° from 2° - 82° 2θ . Crystalline mineral phases were identified using the International Center for Diffraction Data Powder Diffraction File (ICDD PDF-4) and the BrukerAXS Eva software package at the micro-XRD facility at the University of Western Ontario. Qualitative relative abundances of minerals observed were determined based on visual inspection of peak height intensities.

4.6.6 S-isotopic analyses

Total sulfur pools were measured in the streamers, the GH spring source sediments (core GH-8), core porewaters, and GH spring water. Several attempts to concentrate porewaters and strip sufficient dissolved sulfides from the GH spring waters were unsuccessful and were processed for sulfate only.

Sequential extractions were completed following Bruchert and Pratt (82) and Pellerin *et al.* (58). Briefly, the 23 cm sediment core from GH-9 was divided into 2.5 cm sections and ~ 1.0 g of each fraction was transferred to boiling flasks and reacted with 15 mL 6 N HCl to produce acid volatile H_2S (AVS). This was carried by N_2 gas through a cold-water distillation column, a water trap, and bubbled through an acidic zinc acetate trap, which precipitated the evolved H_2S as a purified ZnS. Subsequently, 20 mL of 1 M CrCl_3 and 15 mL of 12 N HCl was injected into the boiling flasks to release any CRS into the distillation column and precipitate the H_2S as a purified ZnS. A few drops of silver nitrate (0.1 N) were added to the zinc acetate solution to convert the ZnS to Ag_2S . This reaction was carried out for several days in the dark. The Ag_2S

was then separated from the solution by filtration on a 0.22 µm membrane filter, rinsed with 1 N NH₃OH and three times with Milli-Q water, scraped from the filter, and dried for a minimum of 3 h at 50°C. The remaining sediment residues following CRS extraction were centrifuged to remove CRS solution, washed with Milli-Q water, dried overnight at 50°C, and weighed and re-extracted for total sulfate using 15 mL of Thode solution containing a mixture of (32:15:53) HI, H₃PO₂ and HCl) at 100 °C under a stream of pure N₂ for 90 min (83) using the same trapping method as described earlier. The same series of extractions was repeated with 0.1 g of lyophilized streamers and 0.7 g of wet streamer sample. All precipitated residues were weighed and 3-4 mg of sample were retained for isotopic analyses.

The samples were subsequently converted to sulfur hexafluoride and the gas purified using the procedure outlined in Pellerin *et al.* (58) before analysis of the sample with a MAT 253 gas-source MS running in dual inlet mode in the Stable Isotope Laboratory of the Earth and Planetary Sciences Department (McGill University, Montreal, Canada). Isotopic compositions are reported using δ notation

$$\delta^{3iS} = \left(\frac{{}^{3i}R \text{ sample}}{{}^{3i}R \text{ V-CDT}} \right) - 1 \times 1000$$

where ${}^{3i}R = {}^{3i}S/{}^{32}S$, i is 3 or 4, and V-CDT refers to the Vienna-Cañon Diablo Troilite international reference scale. The measurement of multiple sulfur isotope is reported in ‘cap’ notation and expressed as

$$\Delta^{33S} = \delta^{33S} - 1000 \times \left(\left(1 + \frac{\delta^{34S}}{1000} \right)^{0.515} - 1 \right)$$

Δ^{33S} is the measured degree to which the δ^{33S} fractionation differs from the value expected from a reference near mass-dependence (56). All sulfur isotope data reported relative to Vienna Cañon

Diablo Troilite (V-CDT), against which the international reference material IAEA-S-1 is taken to have the following isotopic composition: $\Delta^{33}\text{S} = -0.061\text{‰}$ and $\delta^{34}\text{S} \equiv -0.3\text{‰}$. The mass spectrometric uncertainty is described in Pellerin et al. (31).

4.7 Acknowledgments

This work was supported by a Polar Continental Shelf Project, NSERC Discovery Grant, and Canada Research Chair Program to LGW. NM was supported by an NSERC CREATE Postdoctoral Fellowship. JG was supported by a McGill Space Institute Postdoctoral Fellowship and the Northern Scientific Training Program. EM was supported by an NSERC Alexander Graham Bell Canada Graduate Scholarship. AP acknowledges the Danish National Research Foundation (DNRF104), the Danish Council for Independent Research (DFF-7014-00196) and the European Research Council (ERC Advanced Grant #294200).



Figure 4.1. Field photograph of the streamers in the GH springs. The arrow indicates the location of the streamers.

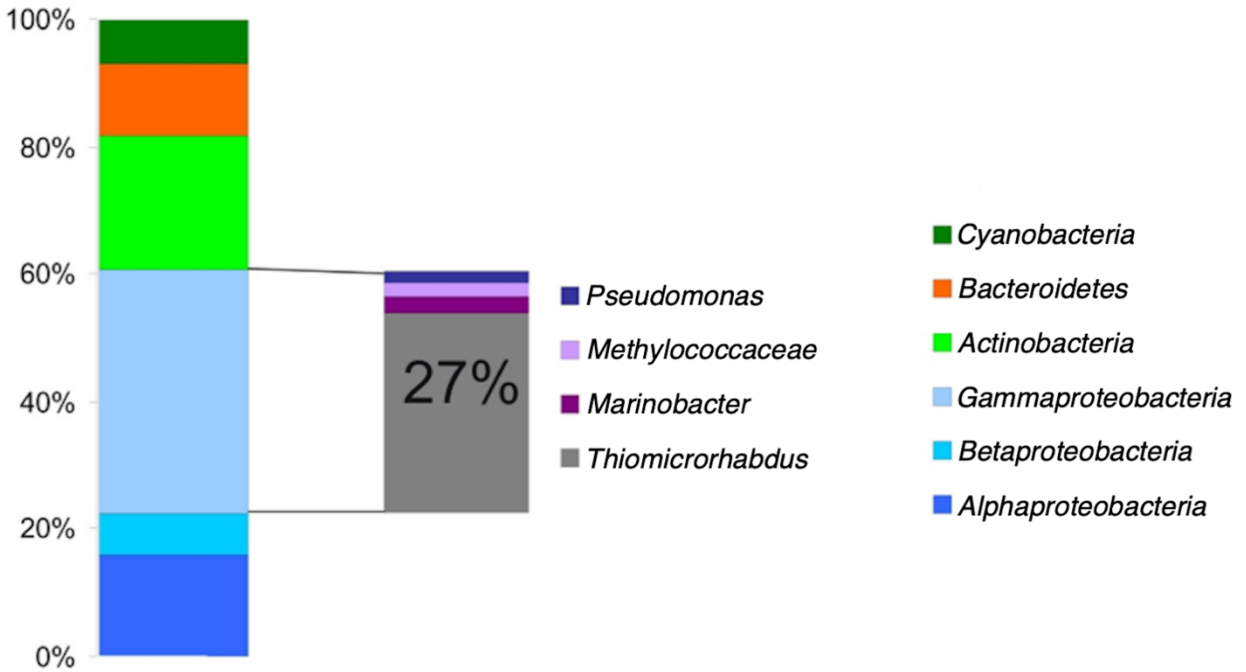


Figure 4.2. Phylogenetic classification of streamers from Gypsum Hill springs based on 16S rRNA pyrosequencing and showing reads > 1% relative abundance.

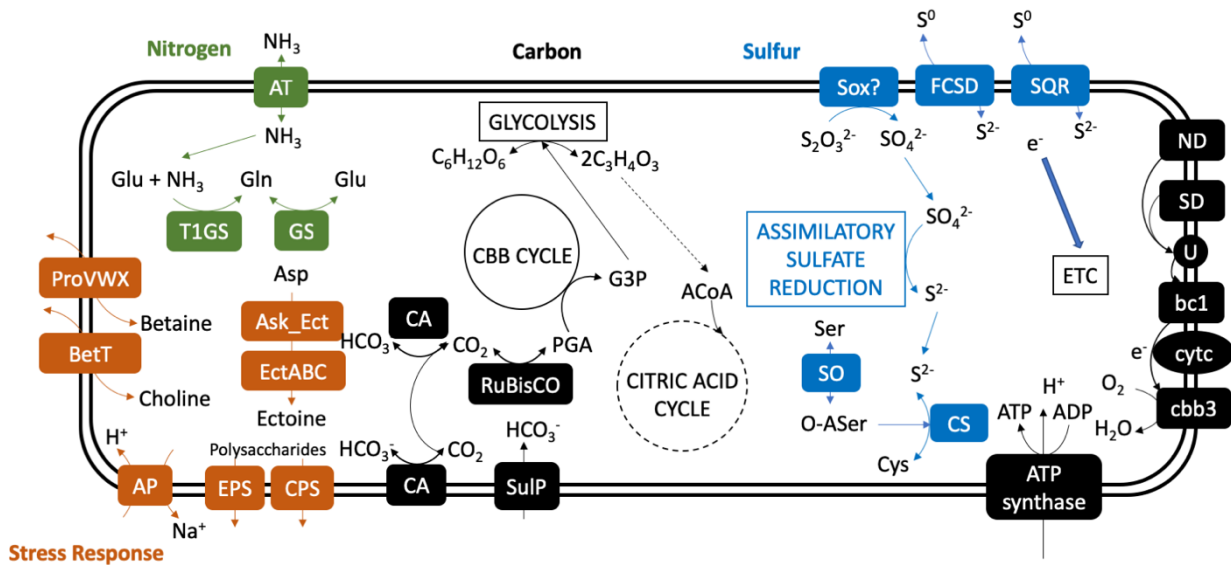


Figure 4.3. Model of *Thiomicrobacterium* sp. GH partial genome cellular systems. Enzymes related to carbon, sulfur, and nitrogen metabolism are presented based on genomic, transcriptomic, and proteomic analysis. Stress response enzymes are also presented. Abbreviations are as follows: ACoA, acetyl-CoA; AP, antiporter; Asp, aspartic acid; AT, ammonium transporter; bc1, cytochrome bc1; CA, carbonic anhydrase; CBB cycle, Calvin-Benson-Bassham cycle; cbb3, cbb3-type cytochrome oxidase; CS, cysteine synthase; Cys, cysteine; cytc, cytochrome c; ETC, electron transport chain; FCSD, flavocytochrome c sulfide dehydrogenase; G3P, glyceraldehyde-3-phosphate; Gln, glutamine; Glu, glutamate; ND, NADH dehydrogenase; O-A-Ser, o-acetylserine; PGA, 3-phosphoglyceric acid; SD, succinate dehydrogenase; Ser, serine; SO, serine o-acetyltransferase; Sox, sulfur oxidation pathway; SQR, sulfide:quinone reductase; SulP, SulP-family transporter; U, ubiquinone.

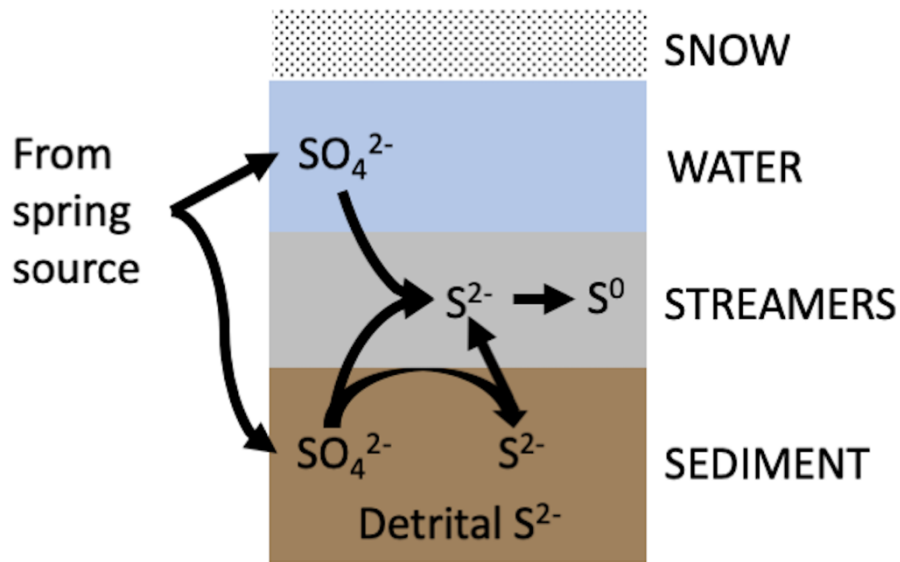


Figure 4.4. Model of sulfur compounds in GH spring environment based on isotopic analysis.

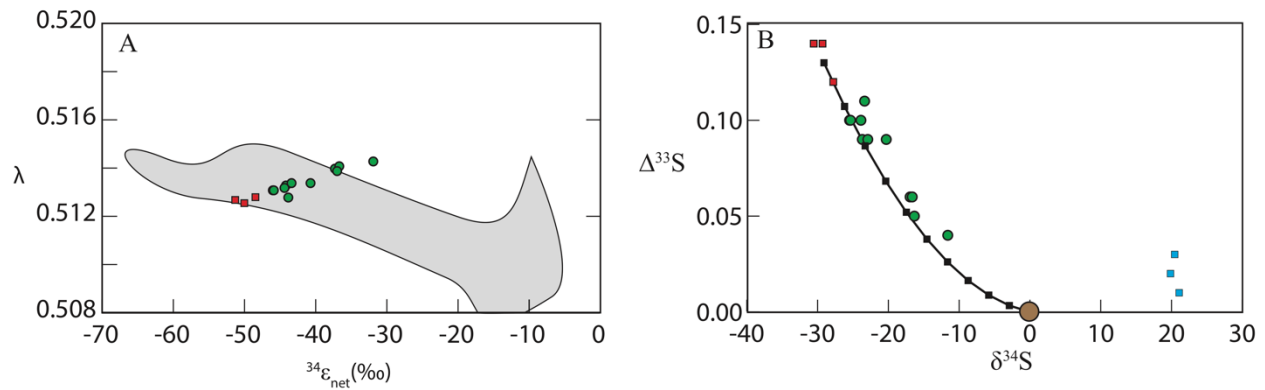


Figure 4.5. Summary of multiple sulfur isotope results. **A.** The measurements of multiple sulfur isotope as fractionations relative to the sulfate in the stream. Red squares correspond to the streamers, green circles correspond to the sediment, grey background corresponds to the field associated with pure cultures of sulfate reducing bacteria. **B.** The measurements of multiple sulfur isotope and a mixing model. Red squares and green circles are same as A, blue squares are measurements of porewater sulfate and brown circle is an igneous endmember (see text for details). Black line corresponds to the mixing line between the streamers end member and the igneous end member. Black squares correspond to changes in fractions of 10% of each end member.

Table 4.1. Stress response genes in *Thiomicrohabdus* genomes. Extended table in File S1. The ‘present in MT/MP’ column indicates if the gene is present in the metatranscriptome and/or metaproteome.

	Name	<i>T. sp.</i> GH	<i>T. arctica</i>	<i>T.</i> <i>chilensis</i>	<i>T.</i> Milos- T2	<i>T.</i> 13- 15A	<i>T.</i> <i>frisia</i> Kp2	<i>T.</i> HaS4	Present in MT/MP
Osmotic stress	L-ectoine synthase (EC 4.2.1.-)	1	1	1	1	1	1	1	✓
	L-2,4-diaminobutyric acid acetyltransferase (ectA) (EC 2.3.1.-)	1	1	1	1	1	1	1	
	diaminobutyrate-2-oxoglutarate transaminase (ectB) (EC 2.6.1.76)	2	2	5	4	5	4	3	✓
	L-proline glycine betaine ABC transport system permease (ProV) (EC 7.6.2.9)	19	21	19	16	20	20	18	✓
	L-proline glycine betaine binding ABC transporter protein (ProX) (EC 7.6.2.9)	2	1	0	1	1	0	0	✓
	L-proline glycine betaine ABC transport system permease protein (ProW) (EC 7.6.2.9)	1	1	0	1	1	0	0	
	High-affinity choline uptake protein (BetT)	1	1	2	1	1	1	0	
	Na ⁺ /H ⁺ antiporter	3	3	3	1	4	3	3	
	Oxidative stress	Superoxide dismutase (EC 1.15.1.1)	1	1	1	1	1	1	1
Catalase (EC 1.11.1.6)	0	1	1	1	1	0	1		
Peroxiredoxin (EC 1.11.1.15)	6	6	6	5	6	7	5		
Glutathione peroxidase (EC 1.11.1.9)	2	1	1	1	1	1	1		
Thioredoxin reductase (EC 1.8.1.9)	7	1	1	1	1	1	1	✓	

Cold shock	Cold shock proteins	3	3	2	5	4	4	2	✓
Heat shock	Chaperone protein DnaK	1	1	1	1	1	1	1	
	Chaperone protein DnaJ	4	4	4	1	4	4	3	✓
	Heat shock protein GrpE	1	1	1	1	1	1	1	✓
	GroES	1	1	1	1	1	1	1	✓
	GroEL	1	1	1	1	1	1	1	✓
	Hsp90	3	0	0	0	0	0	0	✓
General stress response	Stringent starvation protein A	1	1	2	2	1	1	1	
	Universal stress protein A	1	2	4	2	2	2	3	
	General stress protein Ctc	1	1	1	1	1	1	1	✓
	Non-specific DNA-binding protein Dps (EC 1.16.3.1)	1	1	0	0	0	0	1	✓
Periplasmic stress and membrane alteration	Outer membrane protein H precursor	4	1	1	1	1	1	1	✓
	Fatty acid desaturase	1	1	1	1	0	2	0	
Capsular and exo-polysaccharides	ExoZ	0	1	0	0	0	0	0	
	EpsC	11	1	1	2	1	1	1	✓
	EpsD	1	1	0	0	0	0	0	✓
	EpsF	2	1	0	1	0	0	0	
	EpsG	1	1	0	1	0	0	0	✓
	EpsI	1	1	0	0	0	0	0	
	EpsL	2	1	0	0	0	0	0	✓
	Capsular polysaccharide export protein	1	0	1	0	0	0	0	✓
Capsule polysaccharide biosynthesis protein	1	0	1	0	0	0	0	✓	

Table 4.2. Characteristics and isotopic compositions of streamers and sediments.

Sample	Depth (cm)	$\delta^{34}\text{S}$	$\Delta^{33}\text{S}$
Streamers	Surface	-27.78	0.12
		-29.31	0.14
		-30.55	0.14
Core (chromium reducible sulfur)	2.5	-16.93	0.06
	5	-11.61	0.04
	7.5	-23.68	0.09
	10	-20.30	0.09
	12.5	-25.48	0.10
	15	-16.33	0.05
	17.5	-23.36	0.11
	20	-23.88	0.10
	22.5	-22.91	0.09
	25	-25.35	0.10
27.5	-16.63	0.06	
Core (SO_4^{2-})	5	21.08	0.01
	7.5	20.45	0.03
	10	19.86	0.02

4.8 References

1. Ojha L, Wilhelm MB, Murchie SL, McEwen AS, Wray JJ, Hanley J, et al. Spectral evidence for hydrated salts in recurring slope lineae on Mars. *Nature Geoscience*. 2015;8(11):829-32.
2. Gleeson DF, Pappalardo RT, Anderson MS, Grasby SE, Mielke RE, Wright KE, et al. Biosignature detection at an Arctic analog to Europa. *Astrobiology*. 2012;12(2):135-50.
3. Pollard W, Omelon C, Andersen D, McKay C. Perennial spring occurrence in the Expedition Fiord area of western Axel Heiberg Island, Canadian High Arctic. *Can J Earth Sci*. 1999;36:105-20.
4. Omelon CR, Pollard WH, Andersen DT. A geochemical evaluation of perennial spring activity and associated mineral precipitates at Expedition Fjord, Axel Heiberg Island, Canadian High Arctic. *Applied Geochemistry*. 2006;21(1):1-15.
5. Perreault NN, Andersen DT, Pollard WH, Greer CW, Whyte LG. Characterization of the prokaryotic diversity in cold saline perennial springs of the Canadian high Arctic. *Appl Environ Microbiol*. 2007;73(5):1532-43.
6. Perreault NN, Greer CW, Andersen DT, Tille S, Lacrampe-Couloume G, Lollar BS, et al. Heterotrophic and autotrophic microbial populations in cold perennial springs of the high arctic. *Appl Environ Microbiol*. 2008;74(22):6898-907.
7. Niederberger TD, Perreault NN, Lawrence JR, Nadeau JL, Mielke RE, Greer CW, et al. Novel sulfur-oxidizing streamers thriving in perennial cold saline springs of the Canadian high Arctic. *Environ Microbiol*. 2009;11(3):616-29.
8. Teske A, Brinkhoff T, Muyzer G, Moser DP, Rethmeier J, Jannasch HW. Diversity of Thiosulfate-Oxidizing Bacteria from Marine Sediments and Hydrothermal Vents. *Appl Environ Microbiol*. 2000;66(8):3125-33.

9. Brazelton WJ, Schrenk MO, Kelley DS, Baross JA. Methane- and sulfur-metabolizing microbial communities dominate the Lost City hydrothermal field ecosystem. *Appl Environ Microbiol.* 2006;72(9):6257-70.
10. Yamamoto H, Hiraishi A, Kato K, Chiura HX, Maki Y, Shimizu A. Phylogenetic Evidence for the Existence of Novel Thermophilic Bacteria in Hot Spring Sulfur-Turf Microbial Mats in Japan. *Appl Environ Microbiol.* 1998;64(5):1680-7.
11. Dillon JG, Fishbain S, Miller SR, Bebout BM, Habicht KS, Webb SM, et al. High rates of sulfate reduction in a low-sulfate hot spring microbial mat are driven by a low level of diversity of sulfate-respiring microorganisms. *Appl Environ Microbiol.* 2007;73(16):5218-26.
12. Rudolph C, Wanner G, Huber R. Natural communities of novel archaea and bacteria growing in cold sulfurous springs with a string-of-pearls-like morphology. *Appl Environ Microbiol.* 2001;67(5):2336-44.
13. Angert ER, Northup DE, Reysenbach A, Peek AS, Goebel BM, Pace NR. Molecular phylogenetic analysis of a bacterial community in Sulphur River, Parker Cave, Kentucky. *American Mineralogist.* 1998;83:1583-92.
14. Engel AS, Lee N, Porter ML, Stern LA, Bennett PC, Wagner M. Filamentous "Epsilonproteobacteria" Dominate Microbial Mats from Sulfidic Cave Springs. *Applied and Environmental Microbiology.* 2003;69(9):5503-11.
15. Engel AS, Porter ML, Stern LA, Quinlan S, Bennett PC. Bacterial diversity and ecosystem function of filamentous microbial mats from aphotic (cave) sulfidic springs dominated by chemolithoautotrophic "Epsilonproteobacteria". *FEMS Microbiol Ecol.* 2004;51(1):31-53.

16. Macalady JL, Lyon EH, Koffman B, Albertson LK, Meyer K, Galdenzi S, et al. Dominant microbial populations in limestone-corroding stream biofilms, Frasassi cave system, Italy. *Appl Environ Microbiol.* 2006;72(8):5596-609.
17. Mikucki JA, Priscu JC. Bacterial diversity associated with Blood Falls, a subglacial outflow from the Taylor Glacier, Antarctica. *Appl Environ Microbiol.* 2007;73(12):4029-39.
18. Canfield DE, Stewart FJ, Thamdrup B, de Brabandere L, Dalsgaard T, DeLong EF, et al. A Cryptic Sulfur Cycle in Oxygen-Minimum-Zone Waters off the Chilean Coast. *Science.* 2010;330:1375-8.
19. Friedrich CG, Rother D, Bardischewsky F, Quentmeier A, Fischer J. Oxidation of reduced inorganic sulfur compounds by bacteria: emergence of a common mechanism? *Appl Environ Microbiol.* 2001;67(7):2873-82.
20. Campbell BJ, Engel AS, Porter ML, Takai K. The versatile ϵ -proteobacteria: key players in sulphidic habitats. *Nature Reviews Microbiology.* 2006;4(6):458-68.
21. Anantharaman K, Hausmann B, Jungbluth SP, Kantor RS, Lavy A, Warren LA, et al. Expanded diversity of microbial groups that shape the dissimilatory sulfur cycle. *ISME J.* 2018;12(7):1715-28.
22. Scott KM, Williams J, Porter CMB, Russel S, Harmer TL, Paul JH, et al. Genomes of ubiquitous marine and hypersaline *Hydrogenovibrio*, *Thiomicrothrix* and *Thiomicrospira* spp. encode a diversity of mechanisms to sustain chemolithoautotrophy in heterogeneous environments. *Environ Microbiol.* 2018;20(8):2686-708.
23. Boden R, Scott KM, Williams J, Russel S, Antonen K, Rae AW, et al. An evaluation of *Thiomicrospira*, *Hydrogenovibrio* and *Thioalkalimicrobium*: reclassification of four species of *Thiomicrospira* to each *Thiomicrothrix* gen. nov. and *Hydrogenovibrio*, and reclassification

- of all four species of Thioalkalimicrobium to Thiomicrospira. *Int J Syst Evol Microbiol.* 2017;67(5):1140-51.
24. Knittel K, Kuever J, Meyerdierks A, Meinke R, Amann R, Brinkhoff T. *Thiomicrospira arctica* sp. nov. and *Thiomicrospira psychrophila* sp. nov., psychrophilic, obligately chemolithoautotrophic, sulfur-oxidizing bacteria isolated from marine Arctic sediments. *Int J Syst Evol Microbiol.* 2005;55(Pt 2):781-6.
25. Watanabe T, Kojima H, Umezawa K, Hori C, Takasuka TE, Kato Y, et al. Genomes of Neutrophilic Sulfur-Oxidizing Chemolithoautotrophs Representing 9 Proteobacterial Species From 8 Genera. *Front Microbiol.* 2019;10:316.
26. Wright KE, Williamson C, Grasby SE, Spear JR, Templeton AS. Metagenomic evidence for sulfur lithotrophy by Epsilonproteobacteria as the major energy source for primary productivity in a sub-aerial arctic glacial deposit, Borup Fiord Pass. *Front Microbiol.* 2013;4:63.
27. Cao H, Wang Y, Lee OO, Zeng X, Shao Z, Qian PY. Microbial sulfur cycle in two hydrothermal chimneys on the Southwest Indian Ridge. *MBio.* 2014;5(1):e00980-13.
28. Johnston DT, Farquhar J, Wing BA, Kaufman AJ, Canfield DE, Habicht KS. Multiple sulfur isotope fractionations in biological systems: A case study with sulfate reducers and sulfur disproportionators. *American Journal of Science.* 2005;305:645-60.
29. Farquhar J, Johnston DT, Wing BA. Implications of conservation of mass effects on mass-dependent isotope fractionations: Influence of network structure on sulfur isotope phase space of dissimilatory sulfate reduction. *Geochimica et Cosmochimica Acta.* 2007;71(24):5862-75.
30. Zerkle AL, Farquhar J, Johnston DT, Cox RP, Canfield DE. Fractionation of multiple sulfur isotopes during phototrophic oxidation of sulfide and elemental sulfur by a green sulfur bacterium. *Geochimica et Cosmochimica Acta.* 2009;73(2):291-306.

31. Pellerin A, Anderson-Trocme L, Whyte LG, Zane GM, Wall JD, Wing BA. Sulfur isotope fractionation during the evolutionary adaptation of a sulfate-reducing bacterium. *Appl Environ Microbiol.* 2015;81(8):2676-89.
32. Konstantinidis KT, Rossello-Mora R, Amann R. Uncultivated microbes in need of their own taxonomy. *ISME J.* 2017;11(11):2399-406.
33. Grein F, Ramos AR, Venceslau SS, Pereira IA. Unifying concepts in anaerobic respiration: insights from dissimilatory sulfur metabolism. *Biochim Biophys Acta.* 2013;1827(2):145-60.
34. Nelson DC, Hagen KD. Physiology and Biochemistry of Symbiotic and Free-Living Chemoautotrophic Sulfur Bacteria. *American Zoologist.* 1995;35(2):91-101.
35. Kostanjevecki V, Brige A, Meyer TE, Cusanovich MA, Guisez Y, van Beeumen J. A Membrane-Bound Flavocytochrome c-Sulfide Dehydrogenase from the Purple Phototrophic Sulfur Bacterium *Ectothiorhodospira vacuolata*. *Journal of Bacteriology.* 2000;182(11):3097-103.
36. Meyer B, Imhoff JF, Kuever J. Molecular analysis of the distribution and phylogeny of the *soxB* gene among sulfur-oxidizing bacteria - evolution of the Sox sulfur oxidation enzyme system. *Environ Microbiol.* 2007;9(12):2957-77.
37. Friedrich CG, Bardischewsky F, Rother D, Quentmeier A, Fischer J. Prokaryotic sulfur oxidation. *Current Opinion in Microbiology.* 2005;8(3):253-9.
38. Scott KM, Leonard JM, Boden R, Chaput D, Dennison C, Haller E, et al. Diversity in CO₂-Concentrating Mechanisms among Chemolithoautotrophs from the Genera *Hydrogenovibrio*, *Thiomicrothabodus*, and *Thiomicrospira*, Ubiquitous in Sulfidic Habitats Worldwide. *Appl Environ Microbiol.* 2019;85(3).

39. De Maayer P, Anderson D, Cary C, Cowan DA. Some like it cold: understanding the survival strategies of psychrophiles. *EMBO reports*. 2014;15(5):508-17.
40. Raymond-Bouchard I, Chourey K, Altshuler I, Iyer R, Hettich RL, Whyte L. Mechanisms of subzero growth in the cryophile *Planococcus halocryophilus* determined through proteomic analysis. *Environ Microbiol*. 2017.
41. Raymond-Bouchard I, Goordial J, Zolotarov Y, Ronholm J, Stromvik M, Bakermans C, et al. Conserved genomic and amino acid traits of cold adaptation in subzero-growing Arctic permafrost bacteria. *FEMS Microbiology Ecology*. 2018;94(4).
42. Keto-Timonen R, Hietala N, Palonen E, Hakakorpi A, Lindstrom M, Korkeala H. Cold Shock Proteins: A Minireview with Special Emphasis on Csp-family of Enteropathogenic *Yersinia*. *Front Microbiol*. 2016;7:1151.
43. Kuhn E. Toward understanding life under subzero conditions: the significance of exploring psychrophilic "cold-shock" proteins. *Astrobiology*. 2012;12(11):1078-86.
44. Comery R. Characterization of sulfur metabolizing microbes in a cold saline microbial mat of the Canadian High Arctic. 2015.
45. Wu N, Farquhar J, Strauss H, Kim S-T, Canfield DE. Evaluating the S-isotope fractionation associated with Phanerozoic pyrite burial. *Geochimica et Cosmochimica Acta*. 2010;74(7):2053-71.
46. Ghosh W, Dam B. Biochemistry and molecular biology of lithotrophic sulfur oxidation by taxonomically and ecologically diverse bacteria and archaea. *FEMS Microbiol Rev*. 2009;33(6):999-1043.

47. Houghton JL, Foustoukos DI, Flynn TM, Vetriani C, Bradley AS, Fike DA. Thiosulfate oxidation by *Thiomicrospira thermophila*: metabolic flexibility in response to ambient geochemistry. *Environ Microbiol.* 2016;18(9):3057-72.
48. Javor BJ, Wilmot DB, Vetter RD. pH-Dependent metabolism of thiosulfate and sulfur globules in the chemolithotrophic marine bacterium *Thiomicrospira crunogena*. *Arch Microbiol.* 1990;154:231-8.
49. Ophir T, Gutnick DL. A Role for Exopolysaccharides in the Protection of Microorganisms from Desiccation. *Appl Environ Microbiol.* 1994;60(2):740-5.
50. Vuong C, Kocianova S, Voyich JM, Yao Y, Fischer ER, DeLeo FR, et al. A crucial role for exopolysaccharide modification in bacterial biofilm formation, immune evasion, and virulence. *J Biol Chem.* 2004;279(52):54881-6.
51. Brinkhoff T, Muyzer G, Wirsén CO, Kuever J. *Thiomicrospira chilensis* sp. nov., a mesophilic obligately chemolithoautotrophic sulfur-oxidizing bacterium isolated from a Thioploca mat. *International Journal of Systematic Bacteriology.* 1999;49:875-9.
52. Andersen DT. Cold springs in permafrost on Earth and Mars. *Journal of Geophysical Research.* 2002;107(E3):4-1-4-7.
53. van de Velde S, Meysman FJR. The Influence of Bioturbation on Iron and Sulphur Cycling in Marine Sediments: A Model Analysis. *Aquatic Geochemistry.* 2016;22(5-6):469-504.
54. Sim MS, Bosak T, Ono S. Large Sulfur Isotope Fractionation Does Not Require Disproportionation. *Science.* 2011;333(6038):74-7.
55. Goldhaber MB, Kaplan IR. Mechanisms of sulfur incorporation and isotope fractionation during early diagenesis in sediments of the gulf of California. *Marine Chemistry.* 1980;9:95-143.

56. Farquhar J, Johnston DT, Wing BA, Habicht KS, Canfield DE, Airieau S, et al. Multiple sulphur isotopic interpretations of biosynthetic pathways: Implications for biological signatures in the sulphur isotope record. *Geobiology*. 2003;1:27-36.
57. Johnston DT, Farquhar J, Wing BA, Kaufman AJ, Canfield DE, Habicht KS. Multiple sulfur isotope fractionations in biological systems: A case study with sulfate reducers and sulfur disproportionators. *Am J Sci*. 2005;305(6-8):645-60.
58. Pellerin A, Bui TH, Rough M, Mucci A, Canfield DE, Wing BA. Mass-dependent sulfur isotope fractionation during reoxidative sulfur cycling: A case study from Mangrove Lake, Bermuda. *Geochimica et Cosmochimica Acta*. 2015;149:152-64.
59. Andersen D. Perennial Springs in the Canadian High Arctic: Analogues of Martian hydrothermal systems. 2004.
60. Chevreur B, Pfisterer T, Drescher B, Driesel AJ, Muller WEG, Wetter T, et al. Using the miraEST Assembler for Reliable and Automated mRNA Transcript Assembly and SNP Detection in Sequenced ESTs. *Genome Res*. 2004;14:1147-59.
61. Wilke A, Bischof J, Gerlach W, Glass E, Harrison T, Keegan KP, et al. The MG-RAST metagenomics database and portal in 2015. *Nucleic Acids Res*. 2016;44(D1):D590-4.
62. Overbeek R, Olson R, Pusch GD, Olsen GJ, Davis JJ, Disz T, et al. The SEED and the Rapid Annotation of microbial genomes using Subsystems Technology (RAST). *Nucleic Acids Res*. 2014;42(Database issue):D206-14.
63. Altschul SF, Madden TL, Schaffer AA, Zhang J, Zhang Z, Miller W, et al. Gapped BLAST and PSI-BLAST: a new generation of protein database search programs. *Nucleic Acids Res*. 1997;25(17):3389-402.

64. Kang DD, Froula J, Egan R, Wang Z. MetaBAT, an efficient tool for accurately reconstructing single genomes from complex microbial communities. *PeerJ*. 2015;3:e1165.
65. Parks DH, Imelfort M, Skennerton CT, Hugenholtz P, Tyson GW. CheckM: assessing the quality of microbial genomes recovered from isolates, single cells, and metagenomes. *Genome Res*. 2015;25(7):1043-55.
66. Coordinators NR. Database resources of the National Center for Biotechnology Information. *Nucleic Acids Res*. 2016;44(D1):D7-19.
67. McDonald D, Price MN, Goodrich J, Nawrocki EP, DeSantis TZ, Probst A, et al. An improved Greengenes taxonomy with explicit ranks for ecological and evolutionary analyses of bacteria and archaea. *ISME J*. 2012;6(3):610-8.
68. Altschul SF, Gish W, Miller W, Myers EW, Lipman DJ. Basic Local Alignment Search Tool. *J Mol Biol*. 1990;215:403-10.
69. Aziz RK, Bartels D, Best AA, DeJongh M, Disz T, Edwards RA, et al. The RAST Server: rapid annotations using subsystems technology. *BMC Genomics*. 2008;9:75.
70. Rodriguez RL, Gunturu S, Harvey WT, Rossello-Mora R, Tiedje JM, Cole JR, et al. The Microbial Genomes Atlas (MiGA) webserver: taxonomic and gene diversity analysis of Archaea and Bacteria at the whole genome level. *Nucleic Acids Res*. 2018;46(W1):W282-W8.
71. Jain C, Rodriguez RL, Phillippy AM, Konstantinidis KT, Aluru S. High throughput ANI analysis of 90K prokaryotic genomes reveals clear species boundaries. *Nat Commun*. 2018;9(1):5114.
72. Handl S, Dowd SE, Garcia-Mazcorro JF, Steiner JM, Suchodolski JS. Massive parallel 16S rRNA gene pyrosequencing reveals highly diverse fecal bacterial and fungal communities in healthy dogs and cats. *FEMS Microbiol Ecol*. 2011;76(2):301-10.

73. Cole JR, Wang Q, Cardenas E, Fish J, Chai B, Farris RJ, et al. The Ribosomal Database Project: improved alignments and new tools for rRNA analysis. *Nucleic Acids Res.* 2009;37(Database issue):D141-5.
74. Tamura K, Peterson D, Peterson N, Stecher G, Nei M, Kumar S. MEGA5: molecular evolutionary genetics analysis using maximum likelihood, evolutionary distance, and maximum parsimony methods. *Mol Biol Evol.* 2011;28(10):2731-9.
75. Langmead B, Trapnell C, Pop M, Salzberg SL. Ultrafast and memory-efficient alignment of short DNA sequences to the human genome. *Genome Biol.* 2009;10(3):R25.
76. Anders S, Pyl PT, Huber W. HTSeq--a Python framework to work with high-throughput sequencing data. *Bioinformatics.* 2015;31(2):166-9.
77. Schneider T, Riedel K. Environmental proteomics: analysis of structure and function of microbial communities. *Proteomics.* 2010;10(4):785-98.
78. Wang DZ, Kong LF, Li YY, Xie ZX. Environmental Microbial Community Proteomics: Status, Challenges and Perspectives. *Int J Mol Sci.* 2016;17(8).
79. Wessel D, Flugge UI. A Method for the Quantitative Recovery of Protein in Dilute Solution in the Presence of Detergents and Lipids. *Analytical Biochemistry.* 1984;138:141-3.
80. Ramagli LS. Quantifying Protein in 2-D PAGE Solubilization Buffers. *Methods in Molecular Biology.* 1999;112:99-103.
81. Ishihama Y, Oda Y, Tabata T, Sato T, Nagasu T, Rappsilber J, et al. Exponentially Modified Protein Abundance Index (emPAI) for Estimation of Absolute Protein Amount in Proteomics by the Number of Sequenced Peptides per Protein. *Molecular and Cellular Proteomics.* 2005;4(9):1265-72.

82. Bruchert V, Pratt LM. Contemporaneous early diagenetic formation of organic and inorganic sulfur in estuarine sediments from St. Andrew Bay, Florida, USA. *Geochimica et Cosmochimica Acta*. 1996;60(13):2325-32.

83. Thode HG, Monster J, Dunford HB. Sulphur isotope geochemistry. *Geochimica et Cosmochimica Acta*. 1961;25:159-74.

Chapter 5. Discussion

Cold saline springs such as Lost Hammer and Gypsum Hill host microbial communities that are actively metabolizing and reproducing under polyextreme conditions. This thesis contains the first in-depth study of microbial genomes and in situ gene expression in these springs in order to further our understanding of how microbial life is sustained under extreme cold and salinity.

5.1 Identifying the microbial community inhabiting the springs

Previous studies of the LH and GH springs utilized methods including CARD-FISH and 16S rRNA gene sequencing to characterize the microbial community, as well as a 454-pyrosequencing metagenome for LH (176, 180, 181). Estimates of sequencing depth and bacterial rarefaction curves indicated that these surveys did not capture the complete microbial diversity present in the springs but indicated a high degree of taxonomic novelty (178, 181). In Lost Hammer, microbial community structure varied significantly between studies, likely due to the low biomass and use of DNA amplification prior to sequencing (178, 181). Additionally, previous analysis of isolates from GH and LH described their growth conditions and screened for select marker genes, but did not fully sequence and characterize their genomes through whole-genome sequencing (132, 180).

This study utilized a combination of genome-resolved metagenomics, single-cell genomics, and 16S rRNA gene amplicon sequencing to describe the microbial community in the spring sediments. Over 160 MAGs and SAGs were assembled from LH and GH, nearly all of which were novel in comparison with the GTDB database. In both springs, the microbial communities were primarily bacterial, with <2% of archaeal and eukaryotic reads. *Bacteroidota*,

Proteobacteria (*Alpha*- and/or *Gammaproteobacteria*), and *Desulfobacterota* were among the most abundant phyla in both springs. In Lost Hammer, *Campylobacterota* were also relatively abundant, and within these phyla the most abundant orders included *Flavobacteriales* (*Bacteroidota*) and the sulfur cycling taxa *Desulfobulbales* (*Desulfobacterota*), *Campylobacterales* (*Campylobacterota*), and *Halothiobacillales* (*Gammaproteobacteria*). In Gypsum Hill, *Spirochaetota* were also relatively abundant, and the most abundant orders included *Bacteroidales* (*Bacteroidota*); *Desulfuromonadales*, *Desulfobacterales*, and *Desulfobulbales* (*Desulfobacterota*); and *Thiomicrospirales* (*Gammaproteobacteria*).

Comparison of the MAGs in Gypsum Hill and Lost Hammer identified significant overlap at the family level (72% of MAGs in GH belonging to the same family as LH MAGs), but relatively few MAGs at the genus or species level (<15%), suggesting that factors such as physicochemical parameters and nutrient availability likely have a significant influence on community structure. Differences in abundant sulfur-oxidizing *Gammaproteobacteria* were potentially due to the much higher salinity in LH (24%) compared to GH (7-8%). *Halothiobacillales* (*Guyparkeria*) abundant in LH are halophilic and typically have a much higher optimal and maximum salt concentration for growth than *Thiomicrospirales* (*Thiomicrosporhabdus*) abundant in GH (187, 188), which may enable them to outcompete *Thiomicrospirales* in highly saline LH. Sulfate-reducing *Desulfobulbales* (BM506 sp. and *Desulfurivibrionaceae*) related at the genus level were abundant in both springs, indicating this genus is highly adapted to the range of cold and saline conditions across the springs. Other differences in sulfate-reducing *Desulfobacterota* between the springs, such as the high abundance of *Desulfuromonadales* (*Desulfuromusa*) in GH in comparison to LH, potentially result from the differences in abundant S-oxidizing bacteria in

each spring, e.g. production of elemental sulfur by *Thiomicrothabodus* in GH that is subsequently reduced by *Desulfuromonadales*.

Other differences could not be readily posited to result from environmental factors or community interactions, such as the relative absence of *Spirochaetota* in LH compared to GH (0.1% and 5%, respectively). The *Spirochaetota* phylum includes halophiles (189) and has been detected in environments more extreme than LH such as Lake Vida (-13°C) (26). While *Spirochaetota* are typically chemoorganotrophs (190), the GH *Sphaerochaetales* sp. MAG contains the Wood-Ljungdahl pathway for CO₂ fixation and an [NiFe] hydrogenase involved in hydrogenotrophic respiration, indicating it could potentially utilize the H₂ and CO₂ present in LH. Sulfate-reducing *Spirochaetota* have only recently been identified through MAG-based studies (166, 191), and the GH *Sphaerochaetales* sp. would thus be an interesting target for future study, e.g. cultivation or enrichment of isolates, to characterize its capabilities and stress tolerance and determine potential factors for its variable abundance in the springs and similar environments. Additionally, in-depth comparisons could be made in future between metagenomes, MAGs, and SAGs from GH and LH in order to identify shared or divergent traits in correlation with physicochemical parameters, such as in previous comparisons between sea ice and cryopeg environments (14, 15). This could better elucidate the effects of these parameters on spring community structure and function.

In GH, taxonomic characterization was largely consistent with previous 16S rRNA gene sequencing surveys, which primarily identified abundant *Proteobacteria* including *Alpha*-, *Gamma*-, and *Deltaproteobacteria* (*Desulfobacterota*) (132, 176, 177). Sulfur-oxidizing and sulfate-reducing clades detected in this study, including *Thiomicrothabodus* (*Thiomicrospira*),

Halothiobacillus, *Desulfobacteraceae*, and *Desulfuromonadaceae*, have been consistently identified in the spring sediments since their initial characterization in 2007 (176). Additionally, the *Thiomicrohabdus* sp. GH detected in the microbial streamers belonged to the same species (by 16S rRNA gene alignment) as the *Thiomicrohabdus* previously identified in 2009, corroborating the results of this study.

LH microbial community structure has been largely inconsistent between studies despite highly stable conditions in the spring sediments. Previous metagenomic sequencing identified ~40% of reads belonging to *Cyanobacteria* (181), while another study utilizing 16S rRNA gene sequencing identified *Chloroflexi* comprising up to 55% of relative abundance (178). Both of these phyla were found at <1% abundance in the metagenome reported in this study.

Synergistetes previously identified at up to 10% of relative abundance (178) were present at ~0.01% in the metagenome in this study. Conversely, *Desulfobacterota* (*Deltaproteobacteria*), which comprised ~20% of metagenome relative abundance in this study, were either not detected (180) or present in relatively low abundance (1-5%) in previous studies (178, 181). These differences are potentially due to the low spring biomass and usage of multiple displacement amplification methods in previous studies, resulting in outside impacts from sequencing and sampling bias. Metagenome and SAG sequencing in this study additionally identified taxa previously undetected in LH, including DPANN archaea, *Patescibacteria*, CG03, and *Campylobacterota*. Despite these differences, there has been some consistency in detected taxa between studies. *Gammaproteobacteria* have been relatively abundant in all studies, and Gammaproteobacterial genera detected in previous studies including *Halomonas*, *Marinobacter*, *Thiomicrohabdus* (*Thiomicrospira*), and *Thiobacillus* (180, 181) were recovered in the MAGs

and SAGs reported here. Additionally, ANME-1 identified by SAG sequencing in this study were previously detected in 16S rRNA gene clone libraries in 2010 (180).

These results demonstrate the necessity for high-coverage sequencing and avoidance of DNA amplification in studies of low-biomass, high-salinity environments such as LH. One limitation of this study in characterization of the microbial community was in sampling of a single time point for metagenomic or 16S rRNA sequencing in GH and LH as a result of logistical constraints. While biological replicates were utilized to minimize sampling bias, a multi-year sampling campaign would add robustness to the observed community structure and resulting conclusions. Relative similarity between the metagenome (sampled in 2019) and 16S rRNA gene profiling (sampled in 2021), as well as consistency with previous studies, suggests the GH metagenome was not significantly impacted by sequencing or sampling bias. However, potential bias in the LH community described here cannot be conclusively determined based on the available data.

The predominance of *Bacteroidota* and *Proteobacteria* (primarily *Gammaproteobacteria*) in the GH and LH sediments is consistent with other cold, hypersaline environments such as Antarctic lake brine pockets (17), cryopegs (15), and sea ice (15). Genomes from halophilic genera common to these environments such as *Marinobacter* and *Halomonas* were additionally recovered by MAG assembly in LH. Some sulfur-cycling taxa present in GH and LH have also been found in other cold, hypersaline, and sulfate-rich environments including Blood Falls subglacial brines (*Thiomicrothabodus*, *Desulfocapsaceae*) (28) and the nearby AHI spring Colour Peak (*Desulfuromonas*, *Desulfobulbus*, *Halothiobacillus*, *Thiomicrothabodus*) (176, 192),

indicating that these taxa are adapted and common to these polyextreme environments. In comparison of the GH microbial community with other cold, saline, or sulfur-rich environments by NMDS ordination, GH clustered most closely with Blood Falls compared to other brine environments, reflecting this similarity. Other taxa present in LH were detected for the first time under polyextreme cold and hypersaline conditions, expanding the known range for these microorganisms, including ANME-1 and the candidate phyla DPANN archaea and CG03 bacteria.

5.2 Identifying the active microbial community and metabolisms

Functional gene expression was characterized for over 160 MAGs and SAGs as well as unbinned genes in both LH and GH, providing the most in-depth characterization of in situ microbial activity thus far. Sulfur cycling was a major process in both springs, representing some of the most abundantly expressed metabolic genes in LH and GH. Sulfur cycling gene expression could be attributed to inhabitant microorganisms for the first time, confirming in situ activity of S-cycling *Gammaproteobacteria* and *Desulfobacterota* including *Guyparkeria* and BM506 in LH and *Desulfuromusa*, *Desulfovibrionaceae*, *Halothiobacillus*, and *Thiomicrothabodus* in GH. Other sulfur cycling taxa included *Campylobacterota*, *Alphaproteobacteria*, *Bacteroidota*, and *Spirochaetota*. Other metabolisms were detected for the first time in situ, including expression of methane, nitrogen, and hydrogen cycling genes, as well as gene expression by fermentative and heterotrophic microorganisms. Relative expression and abundance of lithoautotrophic MAGs indicated that primary production in both GH and LH is driven by chemolithoautotrophy rather than photoautotrophy. Additionally, functional gene and protein expression in the

Thiomicrothabodus sp. GH present in the GH streamers indicated that they are sustained by aerobic, chemolithoautotrophic sulfide oxidation.

The majority of sulfide oxidation gene expression was attributed to strict aerobes in both LH and GH despite the low oxygen concentrations in the springs. Microorganisms can utilize aerobic metabolisms, including aerobic sulfide oxidation, down to nanomolar O₂ concentrations (50, 89). It thus not necessarily surprising that aerobic metabolisms are present in LH and GH considering the relative energetic favorability of O₂ as an electron acceptor and the energetic cost of osmotic adaptations (13). However, these results raise additional questions about the nature and spatial organization of sulfur cycling in the spring sediments. Oxygen concentrations are highest at the sediment-water interface (6-30 μM O₂) and quickly decrease with depth down to undetectable (0 μM) or near-nanoxic (1.2 μM) concentrations one centimeter below the surface. Alternate electron acceptors including nitrate and iron are present in the spring sediments in higher concentrations. While there was minimal evidence of iron cycling, expression of dissimilatory nitrate reduction genes was detected in both springs, including by facultatively anaerobic SOB. Given these conditions it remains unclear why strictly aerobic SOB are more abundant and have higher gene expression than facultatively anaerobic SOB. Potential reasons for outcompetition by aerobes include energy conservation or nutrient uptake efficiency, or more energetically efficient osmotic adaptations given that the aerobic SOB (*Halothiobacillus*, *Thiomicrothabodus*, *Guyarkeria*) are commonly identified in hypersaline environments (187, 188). Putatively facultatively anaerobic SOB present in the springs include uncultured *Gammaproteobacteria* (SZUA-116) and *Bacteroidales* (UBA5536, ML635J-15), halotolerant and halophilic *Gamma-* and *Alphaproteobacteria* typically found in marine environments (*Oleigrimonas*, *Salinisphaera*,

Roseovarius, *Acidimangrovimonas*) (193-196), and *Campylobacterota* (*Sulfurimonadaceae*, *Sulfurimonas*) globally ubiquitous in diverse S-rich environments (197). In environments occupied by both S-oxidizing *Campylobacterota* and *Gammaproteobacteria* such as hydrothermal vents, they are suggested to occupy different ecophysiological niches based on factors including preferential adaptation to differing sulfide concentrations (198) or kinetically advantageous biochemical pathways in *Gammaproteobacteria* occupying oxic zones (199). Further genomic analysis and/or cultivation of spring SOB for physiological analysis could help elucidate differences in energetic pathway efficiency, osmotic and cold tolerance, nutrient uptake, etc. that influence spring SOB activity and abundance.

Given the oxygen gradient present in the spring sediment and water column, future comparisons over depth across this gradient to correlate oxygen, nitrogen, and sulfur cycling gene expression and taxa abundance with nutrient profiles would be informative. For example, in marine environments, optimal oxygen, sulfide, and nitrate concentrations typically do not overlap, and S-oxidizing bacteria may contain adaptations to bridge this gradient such as nutrient storage or motility (86). Nutrient and microbial community depth analyses in GH and LH could help identify whether similar niches or adaptations influence community structure and function. Previous measurements of S oxidation in sediment microcosms suggest that reduced sulfur compounds are non-limiting in GH (132). Thus, highly active aerobic S-oxidizers may occupy only a narrow oxic zone, with lower rates of S oxidation by facultative anaerobes and anaerobes at depth.

Expression of anaerobic methane oxidation (AOM) genes by ANME-1 archaea and bacterial methanotrophy genes by *Methylobacter* provided the first in situ evidence of active methane metabolism in LH, and is the coldest ambient temperature at which ANME-1 activity has been detected. Despite this detected activity, both ANME-1 and *Methylobacter* were present in low abundance in the sediment (<1%) despite the high concentrations of methane (40-50% ppmv). Future cultivation of isolates or enrichment cultures would be useful in identifying potential energetic or physiological constraints on these microorganisms. Additionally, genomic analysis in this study was insufficient to determine electron acceptor utilization or potential syntrophic interactions in the LH ANME-1, but suggested potential alternate electron donors. Due to the low abundance of LH ANME-1, cultivation of enrichment cultures may be necessary for further elucidation of their activity, e.g. through amendment of microcosms with potential electron donors and acceptors. Single-cell transcriptomics or proteomics could also provide higher-coverage and more thorough detection of ANME-1 gene expression than achieved in this study.

5.3 Identifying microbial stress response capabilities and adaptations

Thiomicrobacter sp. GH present in streamers in the GH outflow channels contained response genes for cold, osmotic, and oxidative stress. Gene expression of ectoine synthesis and betaine uptake suggested accumulation of organic compatible solutes as a strategy for osmoregulation. Most notably, it contained and expressed genes for production and export of exopolysaccharides (EPS), which are associated with cold stress response in psychrophiles (200). Comparison of these stress response genes in *Thiomicrobacter* sp. GH to other *Thiomicrobacter* spp. showed these exopolysaccharide-related genes were primarily present in only *Thiomicrobacter* sp. GH and the closely-related psychrophilic *T. arctica*. *Thiomicrobacter* sp. GH contained additional

genomic redundancy (higher gene copy number) of EPS-related genes, which is associated with cold adaptation (higher protein production to overcome low kinetic energy) (201). These results suggested that *Thiomicrohabdus* sp. GH utilize EPS production for cold stress protection, resulting in formation of the microbial streamers present in the GH channels. Aggregate formation has been observed in *Thiomicrohabdus* spp. in culture (202), but they have not previously been observed forming biofilms or aggregates in the environment. As previously noted, the streamers primarily form at sites of higher oxygen concentration (1 ppm O₂) in the channels (139), suggesting that increased *Thiomicrohabdus* abundance due to relatively available oxygen may incidentally result in streamer formation rather than EPS production due to cold stress alone. Co-occurrence of relatively high oxygen and sulfide concentrations and cold temperatures may explain the presence of *Thiomicrohabdus* streamers in GH outflow channels compared with the source sediments or cold marine sediments inhabited by *T. arctica* (203). Examination of streamer formation in microcosms under varying substrate concentrations and temperature could better constrain the influence of these parameters.

Stress-response genes were also identified in ANME-1 and DPANN archaea and CG03 bacterial genomes. All genomes contained genes related to ‘salt-in’ strategies for osmoregulation, in which K⁺ ions are accumulated to achieve osmotic balance. This strategy is less energetically expensive than compatible solute synthesis (11) and thus may be preferable in the relatively oligotrophic LH spring sediment, particularly in the putatively heterotrophic DPANN and CG03. No genomes examined (ANME-1 or CG03) contained the signature acidic amino acid enrichment typical of salt-in halophiles; however, this is not a universal trait and thus does not rule out this strategy (11). ANME-1 and QMZS01 (DPANN) archaea additionally contained

genes for compatible solute synthesis and uptake, indicating multiple strategies for osmotic stress response may be available to these organisms based on energy or carbon availability. Compatible solute synthesis is also associated with cold adaptation by lowering the freezing point of the cytoplasm (8) and may additionally be utilized for that purpose.

Due to the lack of cultured representatives for these clades, their osmoregulation or cold adaptation mechanisms have not previously been conclusively determined. Other DPANN phyla (*Nanohaloarchaeota*) present in hypersaline environments utilize salt-in strategies (204), and ANME-1 have previously been suggested to utilize compatible solutes based on the presence of synthesis genes (122). While this study identified stress response capabilities in these genomes, their expression and function in situ was largely inconclusive due to low metatranscriptomic coverage and low taxon abundance. Comparative single-cell or meta-transcriptomics in microcosms under varying salt or cold stress could potentially be utilized to identify adaptation mechanisms in these microorganisms. The high energy cost of osmoregulation has been suggested as a reason for the absence or inhibition of AOM in other hypersaline environments (122). Thus, a better understanding of the mechanisms of the cold and salt stress response and adaptation in LH ANME-1 would be useful in constraining AOM favorability in extreme environments globally and in extraterrestrial habitats.

5.4 Future work

This study reported the first in-depth characterization and analysis of over 160 bacterial and archaeal genomes and survey of functional gene expression in unique cold, hypersaline Arctic springs. While providing the most complete survey thus far of microbial diversity and function, it

raises additional questions regarding community structure, interactions, and energetics.

Suggested avenues for future investigation have been included throughout this discussion, and will be summarized briefly here.

This study's conclusions were limited by single time points and bulk sediment sampling due to logistical and time constraints. The influence of physicochemical parameters and nutrient and oxygen gradients on microbial community structure and function could be investigated in future by depth profiling of the spring waters and sediments, as well as comparison between AHI springs. Due to low spring biomass and high salinity, relatively large sample inputs are required for DNA and RNA extraction, making fine-scale sampling and sequencing of sediments technically challenging. This could be addressed by comparison of larger-scale sediment sections or usage of 16S rRNA gene profiling, amplicon sequencing, or reverse transcription quantitative PCR in place of metagenomic and metatranscriptomic sequencing. Depth profiling of the 16S rRNA gene and cDNA in Lost Hammer has previously been described (178); however, the identified microbial community differed significantly from this study and thus it would be useful to re-attempt this experiment with high-throughput shotgun and metatranscriptomic sequencing if possible.

MAG and SAG assembly and analysis in combination with functional gene expression linked metabolic activity to microbial diversity, and described functional capabilities and stress adaptations in novel microbial genomes. Cultivation of isolates or enrichment cultures is necessary for confirmation of predicted functions and to further characterize physiological and functional capabilities. Potential targets include the highly active SRBs and SOB, uncultured

phyla such as CG03, and taxa with high relevance to astrobiology such as ANME-1. Previous culturing attempts have recovered some SRBs and SOBs in the springs, such as *Thiomicrothabodus* (132). These could likely be targeted using traditional culturing methods. For taxa more recalcitrant to culturing, recent methodological innovations to culturing including use of cell sorting or microfluidics to isolate cells may be necessary (135). MAG and SAG data may be utilized in ‘reverse genomics’ methods to identify specific genes for use in targeted cell isolation or for development of specialized media based on predicted nutrient requirements (205).

This study demonstrated the presence of active chemolithoautotrophic microbial communities in briny environments analogous to putative habitats on worlds such as Mars, Europa, and Enceladus. Future studies of gene expression or metabolic activity in microcosms or cultivated isolates under more highly extreme cold, salt, and anoxic conditions could better inform the favorability and response of microbial community function to predicted extraterrestrial conditions. For example, hydrogen-dependent sulfate reduction was previously measured in LH sediment microcosms down to -20°C, the coldest temperature recorded, indicating that these communities are highly adapted to extreme cold and salinity (178). Including comparative community profiling and gene expression in similar studies would enable better understanding of the influence of these conditions on the total microbial community. Additionally, the *Thiomicrothabodus* sp. GH streamers demonstrate the accumulation of significant biomass by a chemolithoautotrophic SOB under cold and hypersaline conditions. Biofilms and similar biomass accumulations can result in morphological and mineralogical (e.g. elemental sulfur deposition) biosignatures (206). Thus, further constraining the conditions required for streamer formation

under cold and hypersaline conditions would be informative for prediction of similar accumulations on extraterrestrial worlds.

Final Conclusion and Summary

The study of microbial life in the cryosphere expands our understanding of the cold and saline limits of life on Earth and other worlds. The cold saline springs on Axel Heiberg Island are some of the most northern springs on Earth, and they host unique microbial communities adapted to life under extreme conditions. This study utilized meta'omics to further our understanding of the limits and capabilities of microbial diversity and activity under the cold and hypersaline conditions in Lost Hammer and Gypsum Hill Springs.

In Chapter 2, I characterized microbial diversity and activity in sub-zero, hypersaline Lost Hammer Spring. Using genome-resolved metatranscriptomics, I identified a microbial community predominantly driven by chemolithoautotrophic microorganisms, including highly active aerobic sulfide-oxidizing *Guyparkeria* spp. utilizing trace oxygen. Additional aerobic and anaerobic sulfur, nitrogen, hydrogen, and carbon cycling microorganisms and metabolisms were detected, including anaerobic methane-oxidizing archaea active under some of the most extreme temperature and salinity conditions recorded thus far.

In Chapter 3, I characterized active sulfur cycling microorganisms sustaining a primarily chemolithoautotrophic microbial community inhabiting the cold and hypersaline Gypsum Hill Spring sediment. A hydrogenotrophic, sulfate-reducing novel *Desulfovibrionaceae* sp. largely drives primary production and, as in Lost Hammer, aerobic sulfide-oxidizing metabolisms in *Halothiobacillus* and *Thiomicrothabodus* predominated despite low oxygen concentrations. Elemental sulfur is likely a significant intermediate in the spring sulfur cycle, sustaining an abundant and highly active sulfur-reducing *Desulfuromusa* sp.

In Chapter 4, I describe the aerobic, sulfide-oxidizing, chemolithoautotrophic *Thiomicrothrix* sp. GH that comprise and form unique microbial streamers in the Gypsum Hill outflow channels. I identified in situ expression of exopolysaccharides (EPS) that result in formation of these streamers, putatively in response to cold and salt stress.

This study demonstrates that the AHI springs sustain active chemolithoautotrophic microbial communities under cold and hypersaline conditions. It expands the known temperature and salinity range for microbial metabolisms such as AOM and microorganisms such as ANME-1 and DPANN archaea. Finally, it demonstrates the potential for microbial life in analogous sulfate-rich, sub-zero brines on Mars, Europa, Enceladus, and beyond.

References

1. Boetius A, Anesio AM, Deming JW, Mikucki JA, Rapp JZ. Microbial ecology of the cryosphere: sea ice and glacial habitats. *Nat Rev Microbiol.* 2015;13(11):677-90.
2. Margesin R, Collins T. Microbial ecology of the cryosphere (glacial and permafrost habitats): current knowledge. *Appl Microbiol Biotechnol.* 2019;103(6):2537-49.
3. Altshuler I, Goordial J, Whyte LG. Microbial Life in Permafrost. *Psychrophiles: From Biodiversity to Biotechnology* 2017. p. 153-79.
4. Maccario L, Sanguino L, Vogel TM, Larose C. Snow and ice ecosystems: not so extreme. *Res Microbiol.* 2015;166(10):782-95.
5. Hotaling S, Hood E, Hamilton TL. Microbial ecology of mountain glacier ecosystems: biodiversity, ecological connections and implications of a warming climate. *Environ Microbiol.* 2017;19(8):2935-48.
6. Bakermans C, Skidmore M. Microbial respiration in ice at subzero temperatures (-4 degrees C to -33 degrees C). *Environ Microbiol Rep.* 2011;3(6):774-82.
7. Mykytczuk NC, Foote SJ, Omelon CR, Southam G, Greer CW, Whyte LG. Bacterial growth at -15 degrees C; molecular insights from the permafrost bacterium *Planococcus halocryophilus* Or1. *ISME J.* 2013;7(6):1211-26.
8. De Maayer P, Anderson D, Cary C, Cowan DA. Some like it cold: understanding the survival strategies of psychrophiles. *EMBO reports.* 2014;15(5):508-17.
9. Sacco M, White NE, Harrod C, Salazar G, Aguilar P, Cubillos CF, et al. Salt to conserve: a review on the ecology and preservation of hypersaline ecosystems. *Biol Rev Camb Philos Soc.* 2021;96(6):2828-50.

10. Doyle S, Dieser M, Broemson E, Christner B. General Characteristics of Cold-Adapted Microorganisms. In: Miller RV, Whyte LG, editors. Polar microbiology. Washington, D.C. : ASM Press; 2011. p. 103-25.
11. Gunde-Cimerman N, Plemenitas A, Oren A. Strategies of adaptation of microorganisms of the three domains of life to high salt concentrations. *FEMS Microbiol Rev.* 2018;42(3):353-75.
12. Hoehler TM, Jorgensen BB. Microbial life under extreme energy limitation. *Nat Rev Microbiol.* 2013;11(2):83-94.
13. Oren A. Thermodynamic limits to microbial life at high salt concentrations. *Environ Microbiol.* 2011;13(8):1908-23.
14. Rapp JZ, Sullivan, Deming, J.W. Divergent genomic adaptations in the microbiomes of Arctic subzero sea-ice and cryopeg brines. *Front Microbiol.* 2021.
15. Cooper ZS, Rapp JZ, Carpenter SD, Iwahana G, Eicken H, Deming JW. Distinctive microbial communities in subzero hypersaline brines from Arctic coastal sea ice and rarely sampled cryopegs. *FEMS Microbiol Ecol.* 2019;95(12).
16. Lo Giudice A, Conte A, Papale M, Rizzo C, Azzaro M, Guglielmin M. Prokaryotic Diversity and Metabolically Active Communities in Brines from Two Perennially Ice-Covered Antarctic Lakes. *Astrobiology.* 2021;21(5):551-65.
17. Papale M, Lo Giudice A, Conte A, Rizzo C, Rappazzo AC, Maimone G, et al. Microbial Assemblages in Pressurized Antarctic Brine Pockets (Tarn Flat, Northern Victoria Land): A Hotspot of Biodiversity and Activity. *Microorganisms.* 2019;7(9).
18. Bowman JP, Rea SM, McCammon SA, McMeekin TA. Diversity and community structure within anoxic sediment from marine salinity meromictic lakes and a coastal meromictic marine basin, Vestfold Hills, Eastern Antarctica. *Environ Microbiol.* 2000;2(2):227-37.

19. Samarkin VA, Madigan MT, Bowles MW, Casciotti KL, Priscu JC, McKay CP, et al. Abiotic nitrous oxide emission from the hypersaline Don Juan Pond in Antarctica. *Nature Geoscience*. 2010;3(5):341-4.
20. Kwon M, Kim M, Takacs-Vesbach C, Lee J, Hong SG, Kim SJ, et al. Niche specialization of bacteria in permanently ice-covered lakes of the McMurdo Dry Valleys, Antarctica. *Environ Microbiol*. 2017;19(6):2258-71.
21. Yau S, Lauro FM, Williams TJ, Demaere MZ, Brown MV, Rich J, et al. Metagenomic insights into strategies of carbon conservation and unusual sulfur biogeochemistry in a hypersaline Antarctic lake. *ISME J*. 2013;7(10):1944-61.
22. Roudier P. Don Juan Pond [photograph]. 2016. Located at: <https://www.flickr.com/photos/10050552@N05/24427085463>. Licensed under Creative Commons Attribution 2.0 Generic.
23. European Space Agency. Lake Vida, Antarctica [photograph]. 2022. Located at: <https://apps.sentinel-hub.com/eo-browser>. Contains modified Copernicus Sentinel data 2022.
24. Mikucki J. “Crime Scene” at Blood Falls [photograph]. 2014. Located at: https://www.flickr.com/photos/dlr_de/16293969810. Licensed under Creative Commons Attribution 2.0 Generic.
25. DeMaere MZ, Williams TJ, Allen MA, Brown MV, Gibson JA, Rich J, et al. High level of intergenera gene exchange shapes the evolution of haloarchaea in an isolated Antarctic lake. *Proc Natl Acad Sci U S A*. 2013;110(42):16939-44.
26. Murray AE, Kenig F, Fritsen CH, McKay CP, Cawley KM, Edwards R, et al. Microbial life at -13 degrees C in the brine of an ice-sealed Antarctic lake. *Proc Natl Acad Sci U S A*. 2012;109(50):20626-31.

27. Guglielmin M, Azzaro M, Buzzini P, Battistel D, Roman M, Ponti S, et al. A possible unique ecosystem in the endoglacial hypersaline brines in Antarctica. *Sci Rep.* 2023;13(1):177.
28. Mikucki JA, Priscu JC. Bacterial diversity associated with Blood Falls, a subglacial outflow from the Taylor Glacier, Antarctica. *Appl Environ Microbiol.* 2007;73(12):4029-39.
29. Campen R, Kowalski J, Lyons WB, Tulaczyk S, Dachwald B, Pettit E, et al. Microbial diversity of an Antarctic subglacial community and high-resolution replicate sampling inform hydrological connectivity in a polar desert. *Environ Microbiol.* 2019;21(7):2290-306.
30. Mikucki JA, Pearson, A., Johnston, D.T., Turchyn, A.V., Farquhar, J., Schrag, D.P., Anbar, A.D., Priscu, J.C., Lee, P.A. A contemporary microbially maintained subglacial ferrous “ocean”. *Science.* 2009;324:397-400.
31. Gilichinsky D, Rivkina E, Bakermans C, Shcherbakova V, Petrovskaya L, Ozerskaya S, et al. Biodiversity of cryopegs in permafrost. *FEMS Microbiol Ecol.* 2005;53(1):117-28.
32. Spirina EV, Durdenko EV, Demidov NE, Abramov AA, Romanovsky VE, Rivkina EM. Halophilic-psychrotrophic bacteria of an Alaskan cryopeg—a model for astrobiology. *Paleontological Journal.* 2018;51(13):1440-52.
33. Pecheritsyna SA, Shcherbakova VA, Kholodov AL, Akimov VN, Abashina TN, Suzina NE, et al. Microbiological analysis of cryopegs from the Varandei Peninsula, Barents Sea. *Microbiology.* 2007;76(5):614-20.
34. Brown MV, Bowman JP. A molecular phylogenetic survey of sea-ice microbial communities (SIMCO). *FEMS Microbiol Ecol.* 2001;35:267-75.
35. Junge K, Eicken H, Deming JW. Bacterial Activity at -2 to -20 degrees C in Arctic wintertime sea ice. *Appl Environ Microbiol.* 2004;70(1):550-7.

36. Eronen-Rasimus E, Piiparinen J, Karkman A, Lyra C, Gerland S, Kaartokallio H. Bacterial communities in Arctic first-year drift ice during the winter/spring transition. *Environ Microbiol Rep.* 2016;8(4):527-35.
37. Cockell CS, Wordsworth R, Whiteford N, Higgins PM. Minimum Units of Habitability and Their Abundance in the Universe. *Astrobiology.* 2021;21(4):481-9.
38. Rummel JD, Beaty DW, Jones MA, Bakermans C, Barlow NG, Boston PJ, et al. A new analysis of Mars "Special Regions": findings of the second MEPAG Special Regions Science Analysis Group (SR-SAG2). *Astrobiology.* 2014;14(11):887-968.
39. Wordsworth RD. The Climate of Early Mars. *Annual Review of Earth and Planetary Sciences.* 2016;44(1):381-408.
40. Allen CC, Oehler, D.Z. A case for ancient springs in Arabia Terra, Mars. *Astrobiology.* 2008;8(6):1093-112.
41. Jakosky BM, Phillips RJ. Mars' volatile and climate history. *Nature.* 2001;412:237-44.
42. Leask EK, Ehlmann BL. Evidence for Deposition of Chloride on Mars From Small-Volume Surface Water Events Into the Late Hesperian-Early Amazonian. *AGU Advances.* 2022;3(1):1-19.
43. Ojha L, Wilhelm MB, Murchie SL, McEwen AS, Wray JJ, Hanley J, et al. Spectral evidence for hydrated salts in recurring slope lineae on Mars. *Nature Geoscience.* 2015;8(11):829-32.
44. Bishop JL, Yesilbas M, Hinman NW, Burton ZFM, Englert PAJ, Toner JD, et al. Martian subsurface cryosalt expansion and collapse as trigger for landslides. *Science Advances.* 2021;7(6).
45. Orosei R, Lauro SE, Pettinelli E, Cicchetti A, Coradini M, Cosciotti B, et al. Radar evidence of subglacial liquid water on Mars. *Science.* 2018;361(6401):490-3.

46. Lauro SE, Pettinelli E, Caprarelli G, Guallini L, Pio Rossi A, Mattei E, et al. Multiple subglacial water bodies below the south pole of Mars unveiled by new MARSIS data. *Nature Astronomy*. 2021;5:63-70.
47. Jakosky BM, Nealson KH, Bakermans C, Ley RE, Mellon MT. Subfreezing Activity of Microorganisms and the Potential Habitability of Mars' Polar Regions. *Astrobiology*. 2003;3(2).
48. King PL, McLennan SM. Sulfur on Mars. *Elements*. 2010;6(2):107-12.
49. Mahaffy PR, Webster CR, Atreya SK, Franz H, Wong M, Conrad PG, et al. Abundance and Isotopic Composition of Gases in the Martian Atmosphere from the Curiosity Rover. 2013.
50. Berg J, Ahmerkamp S, Pjevac P, Hausmann B, Milucka J, Kuypers MMM. How low can they go? Aerobic respiration by microorganisms under apparent anoxia. *FEMS Microbiol Rev*. 2022;1-37.
51. Stamenković V, Ward LM, Mischna M, Fischer WW. O₂ solubility in Martian near-surface environments and implications for aerobic life. *Nature Geoscience*. 2018;11(12):905-9.
52. Eigenbrode JL, Summons RE, Steele A, Freissinet C, Millan M, Navarro-Gonzalez R, et al. Organic matter preserved in 3-billion-year-old mudstones at Gale crater, Mars. *Science*. 2018;360(1096-1101).
53. Webster CR, Mahaffy PR, Atreya SK, Moores JE, Flesch GJ, Malespin C, et al. Background levels of methane in Mars' atmosphere show strong seasonal variations. *Science*. 2018;360:1093-6.
54. Schulte M, Blake D, Hoehler T, McCollom T. Serpentinization and Its Implications for Life on the Early Earth and Mars. *Astrobiology*. 2006;6(2):364-76.
55. McCollom TM. Abiotic methane formation during experimental serpentinization of olivine. *Proceedings of the National Academy of Sciences*. 2016;113(49):13965-70.

56. Kargel JS, Kaye JZ, Head JW, Marion GM, Sassen R, Crowley JK, et al. Europa's crust and ocean: Origin, composition, and the prospects for life. *Icarus*. 2000;148(1):226-65.
57. Hand KP, Chyba CF, Priscu JC, Carlson RW, Nealson KH. *Astrobiology and the Potential for Life on Europa*. 2009.
58. Porco CC, Helfenstein P, Thomas PC, Ingersoll AP, Wisdom J, West R, et al. Cassini observes the active south pole of Enceladus. *Science*. 2006;311(5766):1393-401.
59. Waite Jr. JH, Combi MR, Ip W, Cravens TE, McNutt Jr. RL, Kasprzak W, et al. Cassini Ion and Neutral Mass Spectrometer: Enceladus Plume Composition and Structure. *Science*. 2006;311(5766):1419-22.
60. Hsu HW, Postberg F, Sekine Y, Shibuya T, Kempf S, Horanyi M, et al. Ongoing hydrothermal activities within Enceladus. *Nature*. 2015;519(7542):207-10.
61. Merino N, Aronson HS, Bojanova DP, Feyhl-Buska J, Wong ML, Zhang S, et al. Living at the Extremes: Extremophiles and the Limits of Life in a Planetary Context. *Front Microbiol*. 2019;10:780.
62. Andersen DT. Cold springs in permafrost on Earth and Mars. *Journal of Geophysical Research*. 2002;107(E3):4-1-4-7.
63. Fox-Powell M, Osinski GR, Applin D, Stromberg JM, Gazquez F, Cloutis E, et al. Natural Analogue Constraints on Europa's Non-ice Surface Material. *Geophys Res Lett*. 2019;46:5759-67.
64. Ghosh W, Dam B. Biochemistry and molecular biology of lithotrophic sulfur oxidation by taxonomically and ecologically diverse bacteria and archaea. *FEMS Microbiol Rev*. 2009;33(6):999-1043.

65. Finster K. Microbiological disproportionation of inorganic sulfur compounds. *Journal of Sulfur Chemistry*. 2008;29(3-4):281-92.
66. Muyzer G, Stams AJ. The ecology and biotechnology of sulphate-reducing bacteria. *Nat Rev Microbiol*. 2008;6(6):441-54.
67. Jorgensen BB, Findlay AJ, Pellerin A. The Biogeochemical Sulfur Cycle of Marine Sediments. *Front Microbiol*. 2019;10:849.
68. van Vliet DM, von Meijnenfeldt FAB, Dutilh BE, Villanueva L, Sinninghe Damste JS, Stams AJM, et al. The bacterial sulfur cycle in expanding dysoxic and euxinic marine waters. *Environ Microbiol*. 2021;23(6):2834-57.
69. Dyksma S, Bischof K, Fuchs BM, Hoffmann K, Meier D, Meyerdierks A, et al. Ubiquitous Gammaproteobacteria dominate dark carbon fixation in coastal sediments. *ISME J*. 2016;10(8):1939-53.
70. Reveillaud J, Reddington E, McDermott J, Algar C, Meyer JL, Sylva S, et al. Subseafloor microbial communities in hydrogen-rich vent fluids from hydrothermal systems along the Mid-Cayman Rise. *Environ Microbiol*. 2016;18(6):1970-87.
71. Osburn MR, LaRowe DE, Momper LM, Amend JP. Chemolithotrophy in the continental deep subsurface: Sanford Underground Research Facility (SURF), USA. *Front Microbiol*. 2014;5:610.
72. Engel AS, Lee N, Porter ML, Stern LA, Bennett PC, Wagner M. Filamentous "Epsilonproteobacteria" Dominate Microbial Mats from Sulfidic Cave Springs. *Applied and Environmental Microbiology*. 2003;69(9):5503-11.

73. Bowles MW, Mogollón JM, Kasten S, Zabel M, Hinrichs K. Global rates of marine sulfate reduction and implications for sub-sea-floor metabolic activities. *Science*. 2014;344(6186):889-91.
74. Pester M, Knorr KH, Friedrich MW, Wagner M, Loy A. Sulfate-reducing microorganisms in wetlands - fameless actors in carbon cycling and climate change. *Front Microbiol*. 2012;3:72.
75. Anantharaman K, Hausmann B, Jungbluth SP, Kantor RS, Lavy A, Warren LA, et al. Expanded diversity of microbial groups that shape the dissimilatory sulfur cycle. *ISME J*. 2018;12(7):1715-28.
76. Muller AL, Kjeldsen KU, Rattei T, Pester M, Loy A. Phylogenetic and environmental diversity of DsrAB-type dissimilatory (bi)sulfite reductases. *ISME J*. 2015;9(5):1152-65.
77. Brysch K, Schneider C, Fuchs G, Widdel F. Lithoautotrophic growth of sulfate-reducing bacteria, and description of *Desulfobacterium autotrophicum* gen. nov., sp. nov. *Arch Microbiol*. 1987;148:264-74.
78. Plugge CM, Zhang W, Scholten JC, Stams AJ. Metabolic flexibility of sulfate-reducing bacteria. *Front Microbiol*. 2011;2:81.
79. Rabus R, Venceslau SS, Wohlbrand L, Voordouw G, Wall JD, Pereira IA. A Post-Genomic View of the Ecophysiology, Catabolism and Biotechnological Relevance of Sulphate-Reducing Prokaryotes. *Adv Microb Physiol*. 2015;66:55-321.
80. Dilling W, Cypionka H. Aerobic respiration in sulfate-reducing bacteria. *FEMS Microbiology Letters*. 1990;71:123-8.
81. Simon J, Kroneck PM. Microbial sulfite respiration. *Adv Microb Physiol*. 2013;62:45-117.

82. Hedderich R, Klimmek O, Kroger A, Dirmeier R, Keller M, Stetter KO. Anaerobic respiration with elemental sulfur and with disulfides. *FEMS Microbiology Reviews*. 1999;22:353-81.
83. Findlay AJ, Kamyshny A. Turnover Rates of Intermediate Sulfur Species ($S_x(2-)$, $S(0)$, $S_2O_3(2-)$, $S_4O_6(2-)$, $SO_3(2-)$) in Anoxic Freshwater and Sediments. *Front Microbiol*. 2017;8:2551.
84. Zopfi J, Ferdelman TG, Fossing H. Distribution and fate of sulfur intermediates—sulfite, tetrathionate, thiosulfate, and elemental sulfur—in marine sediments. 2004.
85. Jelen B, Giovannelli D, Falkowski PG, Vetriani C. Elemental sulfur reduction in the deep-sea vent thermophile, *Thermovibrio ammonificans*. *Environ Microbiol*. 2018;20(6):2301-16.
86. Wasmund K, Mussmann M, Loy A. The life sulfuric: microbial ecology of sulfur cycling in marine sediments. *Environ Microbiol Rep*. 2017;9(4):323-44.
87. Poser A, Lohmayer R, Vogt C, Knoeller K, Planer-Friedrich B, Sorokin D, et al. Disproportionation of elemental sulfur by haloalkaliphilic bacteria from soda lakes. *Extremophiles*. 2013;17(6):1003-12.
88. Thamdrup B, Finster K, Hansen JW, Bak F. Bacterial Disproportionation of Elemental Sulfur Coupled to Chemical Reduction of Iron or Manganese. *Appl Environ Microbiol*. 1993;59(1):101-8.
89. Berg JS, Pjevac P, Sommer T, Buckner CRT, Philippi M, Hach PF, et al. Dark aerobic sulfide oxidation by anoxygenic phototrophs in anoxic waters. *Environ Microbiol*. 2019;21(5):1611-26.

90. Di Nezio F, Beney C, Roman S, Danza F, Buetti-Dinh A, Tonolla M, et al. Anoxygenic photo- and chemo-synthesis of phototrophic sulfur bacteria from an alpine meromictic lake. *FEMS Microbiol Ecol.* 2021;97(3).
91. Meier DV, Pjevac P, Bach W, Hourdez S, Girguis PR, Vidoudez C, et al. Niche partitioning of diverse sulfur-oxidizing bacteria at hydrothermal vents. *ISME J.* 2017;11(7):1545-58.
92. Kubo K, Knittel K, Amann R, Fukui M, Matsuura K. Sulfur-metabolizing bacterial populations in microbial mats of the Nakabusa hot spring, Japan. *Syst Appl Microbiol.* 2011;34(4):293-302.
93. Xia Y, Lu C, Hou N, Xin Y, Liu J, Liu H, et al. Sulfide production and oxidation by heterotrophic bacteria under aerobic conditions. *ISME J.* 2017;11(12):2754-66.
94. Swingley WD, Sadekar S, Mastrian SD, Matthies HJ, Hao J, Ramos H, et al. The complete genome sequence of *Roseobacter denitrificans* reveals a mixotrophic rather than photosynthetic metabolism. *J Bacteriol.* 2007;189(3):683-90.
95. Ghosh W, Mallick S, DasGupta SK. Origin of the Sox multienzyme complex system in ancient thermophilic bacteria and coevolution of its constituent proteins. *Res Microbiol.* 2009;160(6):409-20.
96. Meyer B, Imhoff JF, Kuever J. Molecular analysis of the distribution and phylogeny of the *soxB* gene among sulfur-oxidizing bacteria - evolution of the Sox sulfur oxidation enzyme system. *Environ Microbiol.* 2007;9(12):2957-77.
97. Houghton JL, Foustoukos DI, Flynn TM, Vetriani C, Bradley AS, Fike DA. Thiosulfate oxidation by *Thiomicrospira thermophila*: metabolic flexibility in response to ambient geochemistry. *Environ Microbiol.* 2016;18(9):3057-72.

98. Loy A, Duller S, Baranyi C, Mussmann M, Ott J, Sharon I, et al. Reverse dissimilatory sulfite reductase as phylogenetic marker for a subgroup of sulfur-oxidizing prokaryotes. *Environ Microbiol.* 2009;11(2):289-99.
99. Kletzin A, Urich T, Muller F, Bandejas TM, Gomes CM. Dissimilatory oxidation and reduction of elemental sulfur in thermophilic archaea. *Journal of Bioenergetics and Biomembranes.* 2004;36(1):77-91.
100. Liu Y, Beer LL, Whitman WB. Sulfur metabolism in archaea reveals novel processes. *Environ Microbiol.* 2012;14(10):2632-44.
101. Trivedi CB, Lau GE, Grasby SE, Templeton AS, Spear JR. Low-Temperature Sulfidic-Ice Microbial Communities, Borup Fiord Pass, Canadian High Arctic. *Front Microbiol.* 2018;9:1622.
102. Wright KE, Williamson C, Grasby SE, Spear JR, Templeton AS. Metagenomic evidence for sulfur lithotrophy by Epsilonproteobacteria as the major energy source for primary productivity in a sub-aerial arctic glacial deposit, Borup Fiord Pass. *Front Microbiol.* 2013;4:63.
103. Reigstad LJ, Jørgensen SL, Lauritzen SE, Schleper C, Urich T. Sulfur-oxidizing chemolithotrophic proteobacteria dominate the microbiota in high arctic thermal springs on Svalbard. *Astrobiology.* 2011;11(7):665-78.
104. Buongiorno J, Herbert LC, Wehrmann LM, Michaud AB, Laufer K, Røy H, et al. Complex Microbial Communities Drive Iron and Sulfur Cycling in Arctic Fjord Sediments. *Appl Environ Microbiol.* 2019;85(14).
105. Scholze C, Jørgensen BB, Røy H. Psychrophilic properties of sulfate-reducing bacteria in Arctic marine sediments. *Limnology and Oceanography.* 2020;66(S1).

106. Foti M, Sorokin DY, Lomans B, Mussman M, Zacharova EE, Pimenov NV, et al. Diversity, activity, and abundance of sulfate-reducing bacteria in saline and hypersaline soda lakes. *Appl Environ Microbiol.* 2007;73(7):2093-100.
107. Pontefract A, Zhu TF, Walker VK, Hepburn H, Lui C, Zuber MT, et al. Microbial Diversity in a Hypersaline Sulfate Lake: A Terrestrial Analog of Ancient Mars. *Front Microbiol.* 2017;8:1819.
108. Nigro LM, Elling FJ, Hinrichs KU, Joye SB, Teske A. Microbial ecology and biogeochemistry of hypersaline sediments in Orca Basin. *PLoS One.* 2020;15(4):e0231676.
109. Borin S, Brusetti L, Mapelli F, D'Auria G, Brusa T, Marzorati M, et al. Sulfur cycling and methanogenesis primarily drive microbial colonization of the highly sulfidic Urania deep hypersaline basin. *Proc Natl Acad Sci U S A.* 2009;106(23):9151-6.
110. Callbeck CM, Lavik G, Ferdelman TG, Fuchs B, Gruber-Vodicka HR, Hach PF, et al. Oxygen minimum zone cryptic sulfur cycling sustained by offshore transport of key sulfur oxidizing bacteria. *Nat Commun.* 2018;9(1):1729.
111. Plominsky AM, Trefault N, Podell S, Blanton JM, De la Iglesia R, Allen EE, et al. Metabolic potential and in situ transcriptomic profiles of previously uncharacterized key microbial groups involved in coupled carbon, nitrogen and sulfur cycling in anoxic marine zones. *Environ Microbiol.* 2018;20(8):2727-42.
112. Trotsenko YA, Khmelenina VN. Aerobic methanotrophic bacteria of cold ecosystems. *FEMS Microbiol Ecol.* 2005;53(1):15-26.
113. Carrier V, Svenning MM, Grundger F, Niemann H, Dessandier PA, Panieri G, et al. The Impact of Methane on Microbial Communities at Marine Arctic Gas Hydrate Bearing Sediment. *Front Microbiol.* 2020;11:1932.

114. Evans PN, Boyd JA, Leu AO, Woodcroft BJ, Parks DH, Hugenholtz P, et al. An evolving view of methane metabolism in the Archaea. *Nat Rev Microbiol.* 2019;17(4):219-32.
115. Singleton CM, McCalley CK, Woodcroft BJ, Boyd JA, Evans PN, Hodgkins SB, et al. Methanotrophy across a natural permafrost thaw environment. *ISME J.* 2018;12(10):2544-58.
116. Bhattarai S, Cassarini C, Lens PNL. Physiology and distribution of archaeal methanotrophs that couple anaerobic oxidation of methane with sulfate reduction. *Microbiol Mol Biol Rev.* 2019;83(3).
117. Leu AO, Cai C, McIlroy SJ, Southam G, Orphan VJ, Yuan Z, et al. Anaerobic methane oxidation coupled to manganese reduction by members of the Methanoperedenaceae. *ISME J.* 2020;14(4):1030-41.
118. Haroon MF, Hu S, Shi Y, Imelfort M, Keller J, Hugenholtz P, et al. Anaerobic oxidation of methane coupled to nitrate reduction in a novel archaeal lineage. *Nature.* 2013;500(7464):567-70.
119. Cai C, Leu AO, Xie GJ, Guo J, Feng Y, Zhao JX, et al. A methanotrophic archaeon couples anaerobic oxidation of methane to Fe(III) reduction. *ISME J.* 2018;12(8):1929-39.
120. Lloyd KG, Lapham L, Teske A. An anaerobic methane-oxidizing community of ANME-1b archaea in hypersaline Gulf of Mexico sediments. *Appl Environ Microbiol.* 2006;72(11):7218-30.
121. Avrahamov N, Antler G, Yechieli Y, Gavrieli I, Joye SB, Saxton M, et al. Anaerobic oxidation of methane by sulfate in hypersaline groundwater of the Dead Sea aquifer. *Geobiology.* 2014;12(6):511-28.

122. Maignien L, Parkes RJ, Cragg B, Niemann H, Knittel K, Coulon S, et al. Anaerobic oxidation of methane in hypersaline cold seep sediments. *FEMS Microbiol Ecol*. 2013;83(1):214-31.
123. Winkel M, Mitzscherling J, Overduin PP, Horn F, Winterfeld M, Rijkers R, et al. Anaerobic methanotrophic communities thrive in deep submarine permafrost. *Sci Rep*. 2018;8(1):1291.
124. Hanson RE, Hanson TE. Methanotrophic Bacteria. *Microbiological Reviews*. 1996;60(2):439-71.
125. Altshuler I, Raymond-Bouchard I, Magnuson E, Tremblay J, Greer CW, Whyte LG. Unique high Arctic methane metabolizing community revealed through in situ (13)CH(4)-DNA-SIP enrichment in concert with genome binning. *Sci Rep*. 2022;12(1):1160.
126. He Z, Cai C, Wang J, Xu X, Zheng P, Jetten MS, et al. A novel denitrifying methanotroph of the NC10 phylum and its microcolony. *Sci Rep*. 2016;6:32241.
127. Schmitz RA, Peeters SH, Versantvoort W, Picone N, Pol A, Jetten MSM, et al. Verrucomicrobial methanotrophs: ecophysiology of metabolically versatile acidophiles. *FEMS Microbiol Rev*. 2021;45(5).
128. van Grinsven S, Sinnighe Damste JS, Abdala Asbun A, Engelmann JC, Harrison J, Villanueva L. Methane oxidation in anoxic lake water stimulated by nitrate and sulfate addition. *Environ Microbiol*. 2020;22(2):766-82.
129. Cabrol L, Thalasso F, Gandois L, Sepulveda-Jauregui A, Martinez-Cruz K, Teisserenc R, et al. Anaerobic oxidation of methane and associated microbiome in anoxic water of Northwestern Siberian lakes. *Sci Total Environ*. 2020;736:139588.
130. Trotsenko YA, Khmelenina VN. Biology of extremophilic and extremotolerant methanotrophs. *Arch Microbiol*. 2002;177(2):123-31.

131. Lewis WH, Tahon G, Geesink P, Sousa DZ, Ettema TJG. Innovations to culturing the uncultured microbial majority. *Nat Rev Microbiol.* 2021;19(4):225-40.
132. Perreault NN, Greer CW, Andersen DT, Tille S, Lacrampe-Couloume G, Lollar BS, et al. Heterotrophic and autotrophic microbial populations in cold perennial springs of the high arctic. *Appl Environ Microbiol.* 2008;74(22):6898-907.
133. Mudge, MC, Nunn BL, Firth E, Ewert M, Hales K, Fondrie WE, et al. Subzero, saline incubations of *Colwellia psychrerythraea* reveal strategies and biomarkers for sustained life in extreme icy environments. *Environ Microbiol.* 2021;23(7):3840-66.
134. Lee MD, Webb EA, Walworth NG, Fu FX, Held NA, Saito MA, et al. Transcriptional activities of the microbial consortium living with the marine nitrogen-fixing cyanobacterium *Trichodesmium* reveal potential roles in community-level nitrogen cycling. *Appl Environ Microbiol.* 2018;84(1).
135. Amann RI, Ludwig W, Schleifer KH. Phylogenetic Identification and In Situ Detection of Individual Microbial Cells without Cultivation. *Microbiological Reviews.* 1999;59(1):143-69.
136. Lloyd KG, Steen AD, Ladau J, Yin J, Crosby L. Phylogenetically Novel Uncultured Microbial Cells Dominate Earth Microbiomes. *mSystems.* 2018;3(5).
137. Shu WS, Huang LN. Microbial diversity in extreme environments. *Nat Rev Microbiol.* 2022;20(4):219-35.
138. Bowman JS. Identification of Microbial Dark Matter in Antarctic Environments. *Front Microbiol.* 2018;9:3165.
139. Niederberger TD, Perreault NN, Lawrence JR, Nadeau JL, Mielke RE, Greer CW, et al. Novel sulfur-oxidizing streamers thriving in perennial cold saline springs of the Canadian high Arctic. *Environ Microbiol.* 2009;11(3):616-29.

140. Martineau C, Whyte LG, Greer CW. Stable isotope probing analysis of the diversity and activity of methanotrophic bacteria in soils from the Canadian high Arctic. *Appl Environ Microbiol.* 2010;76(17):5773-84.
141. Ayling M, Clark MD, Leggett RM. New approaches for metagenome assembly with short reads. *Brief Bioinform.* 2020;21(2):584-94.
142. Quince C, Walker AW, Simpson JT, Loman NJ, Segata N. Shotgun metagenomics, from sampling to analysis. *Nat Biotechnol.* 2017;35(9):833-44.
143. Yergeau E, Michel C, Tremblay J, Niemi A, King TL, Wyglinski J, et al. Metagenomic survey of the taxonomic and functional microbial communities of seawater and sea ice from the Canadian Arctic. *Sci Rep.* 2017;7:42242.
144. Goordial J, Davila A, Greer CW, Cannam R, DiRuggiero J, McKay CP, et al. Comparative activity and functional ecology of permafrost soils and lithic niches in a hyper-arid polar desert. *Environ Microbiol.* 2017;19(2):443-58.
145. Sangwan N, Xia F, Gilbert JA. Recovering complete and draft population genomes from metagenome datasets. *Microbiome.* 2016;4:8.
146. Rinke C, Schwientek P, Sczyrba A, Ivanova NN, Anderson IJ, Cheng JF, et al. Insights into the phylogeny and coding potential of microbial dark matter. *Nature.* 2013;499(7459):431-7.
147. Nayfach S, Roux S, Seshadri R, Udway D, Varghese N, Schulz F, et al. A genomic catalog of Earth's microbiomes. *Nat Biotechnol.* 2021;39(4):499-509.
148. Bowers RM, Nayfach S, Schulz F, Jungbluth SP, Ruhl IA, Sheremet A, et al. Dissecting the dominant hot spring microbial populations based on community-wide sampling at single-cell genomic resolution. *ISME J.* 2022;16(5):1337-47.

149. Busi SB, Bourquin M, Fodelianakis S, Michoud G, Kohler TJ, Peter H, et al. Genomic and metabolic adaptations of biofilms to ecological windows of opportunity in glacier-fed streams. *Nat Commun.* 2022;13(1):2168.
150. Royo-Llonch M, Sanchez P, Ruiz-Gonzalez C, Salazar G, Pedros-Alio C, Sebastian M, et al. Compendium of 530 metagenome-assembled bacterial and archaeal genomes from the polar Arctic Ocean. *Nat Microbiol.* 2021;6(12):1561-74.
151. Ruuskanen MO, Colby G, St.Pierre KA, St.Louis VL, Aris-Brosou S, Poulain AJ. Microbial genomes retrieved from High Arctic lake sediments encode for adaptation to cold and oligotrophic environments. *Limnol Oceanogr.* 2020;65(S1):S233-S47.
152. Vavourakis CD, Andrei AS, Mehrshad M, Ghai R, Sorokin DY, Muyzer G. A metagenomics roadmap to the uncultured genome diversity in hypersaline soda lake sediments. *Microbiome.* 2018;6(1):168.
153. Alneberg J, Karlsson CMG, Divne AM, Bergin C, Homa F, Lindh MV, et al. Genomes from uncultivated prokaryotes: a comparison of metagenome-assembled and single-amplified genomes. *Microbiome.* 2018;6(1):173.
154. Bowers RM, Kyrpides NC, Stepanauskas R, Harmon-Smith M, Doud D, Reddy TBK, et al. Minimum information about a single amplified genome (MISAG) and a metagenome-assembled genome (MIMAG) of bacteria and archaea. *Nat Biotechnol.* 2017;35(8):725-31.
155. Bowers RM, Doud DFR, Woyke T. Analysis of single-cell genome sequences of bacteria and archaea. *Emerg Top Life Sci.* 2017;1(3):249-55.
156. Uritskiy G, DiRuggiero J. Applying Genome-Resolved Metagenomics to Deconvolute the Halophilic Microbiome. *Genes (Basel).* 2019;10(3).

157. Woyke T, Doud DFR, Schulz F. The trajectory of microbial single-cell sequencing. *Nat Methods*. 2017;14(11):1045-54.
158. Spits C, Le Caignec C, De Rycke M, Van Haute L, Van Steirteghem A, Liebaers I, et al. Whole-genome multiple displacement amplification from single cells. *Nat Protoc*. 2006;1(4):1965-70.
159. Merino N, Kawai M, Boyd ES, Colman DR, McGlynn SE, Nealson KH, et al. Single-Cell Genomics of Novel Actinobacteria With the Wood-Ljungdahl Pathway Discovered in a Serpentinizing System. *Front Microbiol*. 2020;11:1031.
160. Willerslev E, Hansen AJ, Poinar HN. Isolation of nucleic acids and cultures from fossil ice and permafrost. *Trends Ecol Evol*. 2004;19(3):141-7.
161. Borin S, Crotti E, Mapelli F, Tamagnini I, Corselli C, Daffonchio D. DNA is preserved and maintains transforming potential after contact with brines of the deep anoxic hypersaline lakes of the Eastern Mediterranean Sea. *Saline Syst*. 2008;4:10.
162. Rittershaus ES, Baek SH, Sasseti CM. The normalcy of dormancy: common themes in microbial quiescence. *Cell Host Microbe*. 2013;13(6):643-51.
163. Shakya M, Lo CC, Chain PSG. Advances and Challenges in Metatranscriptomic Analysis. *Front Genet*. 2019;10:904.
164. Segata N, Boernigen D, Tickle TL, Morgan XC, Garrett WS, Huttenhower C. Computational meta'omics for microbial community studies. *Mol Syst Biol*. 2013;9:666.
165. Campbell MA, Grice K, Visscher PT, Morris T, Wong HL, White RA, 3rd, et al. Functional Gene Expression in Shark Bay Hypersaline Microbial Mats: Adaptive Responses. *Front Microbiol*. 2020;11:560336.

166. Hahn CR, Farag IF, Murphy CL, Podar M, Elshahed MS, Youssef NH. Microbial diversity and sulfur cycling in an early earth analogue: From ancient novelty to modern commonality. 2021.
167. Schneider T, Riedel K. Environmental proteomics: analysis of structure and function of microbial communities. *Proteomics*. 2010;10(4):785-98.
168. Wang DZ, Kong LF, Li YY, Xie ZX. Environmental Microbial Community Proteomics: Status, Challenges and Perspectives. *Int J Mol Sci*. 2016;17(8).
169. Pollard WH. Icing processes associated with high Arctic perennial springs, Axel Heiberg Island, Nunavut, Canada. *Permafrost and Periglacial Processes*. 2005;16(1):51-68.
170. Grasby SE, Proemse BC, Beauchamp B. Deep groundwater circulation through the High Arctic cryosphere forms Mars-like gullies. *Geology*. 2014;42(8):651-4.
171. Lauritzen SE, Bottrell S. Microbiological activity in thermoglacial karst springs, south spitsbergen. *Geomicrobiology Journal*. 1994;12(3):161-73.
172. Grasby SE, Allen CC, Longazo TG, Lisle JT, Griffin DW, Beauchamp B. Supraglacial Sulfur Springs and Associated Biological Activity in the Canadian High Arctic- Signs of Life Beneath the Ice. *Astrobiology*. 2003;3(3).
173. Pollard W, Omelon C, Andersen D, McKay C. Perennial spring occurrence in the Expedition Fiord area of western Axel Heiberg Island, Canadian High Arctic. *Can J Earth Sci*. 1999;36:105-20.
174. Andersen D. Perennial Springs in the Canadian High Arctic: Analogues of Martian hydrothermal systems. 2004.

175. Sapers HM, Ronholm J, Raymond-Bouchard I, Comrey R, Osinski GR, Whyte LG. Biological Characterization of Microenvironments in a Hypersaline Cold Spring Mars Analog. *Front Microbiol.* 2017;8:2527.
176. Perreault NN, Andersen DT, Pollard WH, Greer CW, Whyte LG. Characterization of the prokaryotic diversity in cold saline perennial springs of the Canadian high Arctic. *Appl Environ Microbiol.* 2007;73(5):1532-43.
177. Colangelo-Lillis J, Pelikan C, Herbold CW, Altshuler I, Loy A, Whyte LG, et al. Diversity decoupled from sulfur isotope fractionation in a sulfate-reducing microbial community. *Geobiology.* 2019;17(6):660-75.
178. Lamarche-Gagnon G, Comery R, Greer CW, Whyte LG. Evidence of in situ microbial activity and sulphidogenesis in perennially sub-0 degrees C and hypersaline sediments of a high Arctic permafrost spring. *Extremophiles.* 2015;19(1):1-15.
179. Battler MM, Osinski GR, Banerjee NR. Mineralogy of saline perennial cold springs on Axel Heiberg Island, Nunavut, Canada and implications for spring deposits on Mars. *Icarus.* 2013;224(2):364-81.
180. Niederberger TD, Perreault NN, Tille S, Lollar BS, Lacrampe-Couloume G, Andersen D, et al. Microbial characterization of a subzero, hypersaline methane seep in the Canadian High Arctic. *ISME J.* 2010;4(10):1326-39.
181. Lay CY, Mykytczuk NC, Yergeau E, Lamarche-Gagnon G, Greer CW, Whyte LG. Defining the functional potential and active community members of a sediment microbial community in a high-arctic hypersaline subzero spring. *Appl Environ Microbiol.* 2013;79(12):3637-48.

182. Heldmann J, Toon O, McKay C, Andersen D, Pollard W. High Arctic saline springs as analogues for springs on Mars. *Permafrost*. 2003.
183. Moreras-Marti A, Fox-Powell M, Stueeken E, Di Rocco T, Galloway T, Osinski GR, et al. Quadruple sulfur isotope biosignatures from terrestrial Mars analogue systems. *Geochimica et Cosmochimica Acta*. 2021;308:157-72.
184. Malin MC, Edgett KS. Evidence for recent groundwater seepage and surface runoff on Mars. *Science*. 2000;288(5475):2330-5.
185. Hoffman N. Ideas About the Surface Runoff Features on Mars. *Science*. 2000;290(5492):711-4.
186. Baioni D, Wezel FC. Morphology and origin of an evaporitic dome in the eastern Tithonium Chasma, Mars. *Planetary and Space Science*. 2010;58(5):847-57.
187. Boden R. Reclassification of *Halothiobacillus hydrothermalis* and *Halothiobacillus halophilus* to *Guyarkeria* gen. nov. in the Thioalkalibacteraceae fam. nov., with emended descriptions of the genus *Halothiobacillus* and family Halothiobacillaceae. *Int J Syst Evol Microbiol*. 2017;67(10):3919-28.
188. Boden R, Scott KM, Williams J, Russel S, Antonen K, Rae AW, et al. An evaluation of *Thiomicrospira*, *Hydrogenovibrio* and *Thioalkalimicrobium*: reclassification of four species of *Thiomicrospira* to each *Thiomicrospira* gen. nov. and *Hydrogenovibrio*, and reclassification of all four species of *Thioalkalimicrobium* to *Thiomicrospira*. *Int J Syst Evol Microbiol*. 2017;67(5):1140-51.
189. Minegishi H. Halophilic, Acidophilic, and Haloacidophilic Prokaryotes. In: Seckbach J, Oren A, Stan-Lotter H, editors. *Polyextremophiles*. New York: Springer; 2013. p. 203-13.

190. Paster BJ. Spirochaetes. *Bergey's Manual of Systematics of Archaea and Bacteria* 2015. p. 1-.
191. Neukirchen S, Sousa FL. DiSCo: a sequence-based type-specific predictor of Dsr-dependent dissimilatory sulphur metabolism in microbial data. *Microb Genom.* 2021;7(7).
192. Macey MC, Fox-Powell M, Ramkissoon NK, Stephens BP, Barton T, Schwenzer SP, et al. The identification of sulfide oxidation as a potential metabolism driving primary production on late Noachian Mars. *Sci Rep.* 2020;10(1):10941.
193. Yang SH, Seo HS, Seong CN, Kwon KK. *Oleigrimonas citrea* sp. nov., a marine bacterium isolated from tidal flat sediment and emended description of the genus *Oleigrimonas* Fang et al. 2015 and *Oleigrimonas soli*. *Int J Syst Evol Microbiol.* 2017;67(6):1672-5.
194. Crespo-Medina M, Chatziefthimiou A, Cruz-Matos R, Perez-Rodriguez I, Barkay T, Lutz RA, et al. *Salinisphaera hydrothermalis* sp. nov., a mesophilic, halotolerant, facultatively autotrophic, thiosulfate-oxidizing gammaproteobacterium from deep-sea hydrothermal vents, and emended description of the genus *Salinisphaera*. *Int J Syst Evol Microbiol.* 2009;59(Pt 6):1497-503.
195. Slobodkina G, Ratnikova N, Merkel A, Kevbrin V, Kuchierskaya A, Slobodkin A. Lithoautotrophic lifestyle of the widespread genus *Roseovarius* revealed by physiological and genomic characterization of *Roseovarius autotrophicus* sp. nov. *FEMS Microbiol Ecol.* 2022;98(10).
196. Ren H, Ma H, Li H, Huang L, Luo Y. *Acidimangrovimonas sediminis* gen. nov., sp. nov., isolated from mangrove sediment and reclassification of *Defluviimonas indica* as *Acidimangrovimonas indica* comb. nov. and *Defluviimonas pyrenivorans* as *Acidimangrovimonas pyrenivorans* comb. nov. *Int J Syst Evol Microbiol.* 2019;69(8):2445-51.

197. Han Y, Perner M. The globally widespread genus *Sulfurimonas*: versatile energy metabolisms and adaptations to redox clines. *Front Microbiol.* 2015;6:989.
198. Patwardhan S, Foustoukos DI, Giovannelli D, Yucel M, Vetriani C. Ecological Succession of Sulfur-Oxidizing Epsilon- and Gammaproteobacteria During Colonization of a Shallow-Water Gas Vent. *Front Microbiol.* 2018;9:2970.
199. Yamamoto M, Takai K. Sulfur metabolisms in epsilon- and gamma-proteobacteria in deep-sea hydrothermal fields. *Front Microbiol.* 2011;2:192.
200. Casillo A, Parrilli E, Sannino F, Mitchell DE, Gibson MI, Marino G, et al. Structure-activity relationship of the exopolysaccharide from a psychrophilic bacterium: A strategy for cryoprotection. *Carbohydr Polym.* 2017;156:364-71.
201. Raymond-Bouchard I, Goordial J, Zolotarov Y, Ronholm J, Stromvik M, Bakermans C, et al. Conserved genomic and amino acid traits of cold adaptation in subzero-growing Arctic permafrost bacteria. *FEMS Microbiology Ecology.* 2018;94(4).
202. Brinkhoff T, Muyzer G, Wirsén CO, Kuever J. *Thiomicrospira kuenenii* sp. nov. and *Thiomicrospira frisia* sp. nov., two mesophilic obligately chemolithoautotrophic sulfur-oxidizing bacteria isolated from an intertidal mud flat. *International Journal of Systematic Bacteriology.* 1999;49(2):385-92.
203. Knittel K, Kuever J, Meyerdierks A, Meinke R, Amann R, Brinkhoff T. *Thiomicrospira arctica* sp. nov. and *Thiomicrospira psychrophila* sp. nov., psychrophilic, obligately chemolithoautotrophic, sulfur-oxidizing bacteria isolated from marine Arctic sediments. *Int J Syst Evol Microbiol.* 2005;55(Pt 2):781-6.

204. Xie YG, Luo ZH, Fang BZ, Jiao JY, Xie QJ, Cao XR, et al. Functional differentiation determines the molecular basis of the symbiotic lifestyle of *Ca. Nanohaloarchaeota*. *Microbiome*. 2022;10(1):172.
205. Liu S, Moon CD, Zheng N, Huws S, Zhao S, Wang J. Opportunities and challenges of using metagenomic data to bring uncultured microbes into cultivation. *Microbiome*. 2022;10(1):76.
206. Knuth J, Potter-McIntyre SL. Chemical, Morphological, and Mineralogical Biosignature Preservation in a Cold Spring System, UT, USA: Insights for Sample Selection on Mars. *Astrobiology*. 2019.

Appendix 1. Supplementary Materials for Chapter 2

Extended Materials and Methods

i. Site description and sample collection

Lost Hammer (LH) spring discharges through a precipitated mineral salt tufa as described in previous publications (1-5) (Figure S2.1). LH emits gases composed of methane (50%), nitrogen (35%), carbon dioxide (10%), and trace hydrogen, helium, and short-chain alkanes (1). The spring sediments and water contain high concentrations of sulfate (100 000 mg/kg) as well as sulfide (<50 mg/kg), ammonia (2.55 mg/kg), nitrate/nitrite (2.87 mg/kg), and iron (13 000 mg/kg) (1). Physical and geochemical parameters in the outlet (Table S2.1) have remained highly stable since 2005, allowing comparison among samples collected in different years.

For this study, sediment samples (top ~10 cm) were collected in July 2017 and July 2019 with an ethanol-sterilized scoop, and stored in sterile Falcon tubes filled to maximum to avoid aerobic headspace. Sediment from July 2017 was used for metagenomic sequencing, and sediment from July 2019 was used for RNA and SAG sequencing. In parallel, sediment for RNA extractions was mixed with Zymo Research DNA/RNA Shield (Irvine, CA, USA). Samples were kept at <math><5^{\circ}\text{C}</math> during transportation to Montreal, after which they were stored at in situ with a YSI Professional Plus Multiparameter instrument (Yellow Springs, OH, USA) and a PyroScience Piccolo2 oxygen meter (Aachen, Germany). Ortho-phosphate and ammonia were measured *in situ* with CHEMetrics Inc. (Midland, VA, USA) test kits.

ii. DNA extraction, metagenome sequencing, and metagenome data analyses

DNA was extracted from two 5 g portions of sediment with a Qiagen DNeasy PowerMax Soil Kit (Hilden, Germany). The resulting DNA from each sediment sample was concentrated with a Thermo Fisher Scientific SpeedVac Vacuum Concentrator (Waltham, MA, USA) and sequenced on a HiSeq2500 (2x126 base reads) (Illumina, San Diego, CA, USA) at The Centre for Applied Genomics (Toronto, ON, Canada). Low-quality reads and bases were trimmed with Trimmomatic (v0.38, settings LEADING:3 TRAILING:3 SLIDINGWINDOW:4:15) (6). Remaining reads were classified with Kaiju (v1.7.3, default settings, nr_euk database) (7) and phyloFlash (v3.4) (8). The reads from the two sediment samples were co-assembled with Megahit (v1.1.3, setting meta-sensitive) (9) as well as assembled separately with metaSPAdes (v3.13.0, default settings) (10). Reads were mapped to each assembly with BMap (v38.26, minid=0.95) and contigs longer than 5000 bp were binned with MetaBAT (v2.12.1) (11). Bin completeness and contamination was estimated with CheckM (v1.0.12) (12). The Megahit co-assembly and resulting bins were selected for downstream analysis based on sequencing statistics as determined by metaQUAST (v5.0.1) (13) and number of high- and medium-quality bins. Sequencing and assembly statistics can be found in Tables S2.2 and S2.3. The metagenome was annotated with the Joint Genome Institute's IMG/M system using KEGG, COG, and pfam databases (14, 15). Bins were classified with the Genome Taxonomy Database Toolkit (v1.3.0, reference data R05-RS95) (16). Phylogenomic trees were constructed with Anvi'o (v6.2) using the Bacteria_71 collection of single copy genes (17). Amino acid sequences for all genes were concatenated, with a total alignment length of 24 451 bp, and approximately-maximum-likelihood trees were constructed in FastTree with default settings within Anvi'o, with midpoint rooting. Additional analyses were as follows: FeGenie was used to identify iron-related genes

(18); *amoA* and *pmoA* were distinguished by HMMer using FunGene Hidden Markov Models (19); hydrogenases were classified with hydDB (20). Reductive and oxidative DsrAB were classified as follows: DsrAB amino acid sequences were aligned against reference sequences from Muller et al. (21) using MUSCLE with default settings (22). Maximum likelihood phylogenetic trees were constructed in CLC Genomics Workbench (v. 12.0.3) using the WAG protein substitution model and 1000 bootstraps (Figure S9). DsrAB were classified as reductive or oxidative based on phylogenetic clustering and the presence of accessory proteins as in Anantharaman et al. (23).

iii. Single cell sorting, genome amplification, sequencing, and data analyses

Sediment was shipped on ice to the Single Cell Genomics Center at the Bigelow Laboratory for Ocean Sciences (East Boothbay, ME, USA) for SYTO-9 fluorescence-activated single-cell sorting (FACS), DNA extraction, and genome amplification with WGA-X (as described in Stepanauskas et al. (24)). The 16S rRNA gene was PCR amplified from the genomes (primers 27F (25) and 1492R (26)) and sequenced at the Centre de Recherche at Université Laval (Quebec City, QC, Canada) on an Applied Biosystems 3730xl DNA Analyzer (Foster City, CA, USA). Obtained 16S rRNA sequences were annotated by BLAST with the SILVA rRNA database (release 138) (27). For whole genome sequencing, libraries were prepared with a Nextera XT DNA Library Prep Kit and sequenced on a MiSeq (Illumina) with MiSeq Reagent Kit v3 (600 cycles, 2x300 base reads). Low quality reads and bases were trimmed with BBDuk (minimum Phred quality score 15, minimum length 30 bp) and contaminant human reads were removed with DeconSeq (28). Genomes were assembled with SPAdes (v3.13.1, settings --sc --careful) (29) and screened for contamination using JGI's Kmer Frequency Analysis tool and by

read classification with Kaiju (v1.7.3) (7). Average nucleotide identity of the SAGs against other SAGs and metagenome bins was calculated with FastANI (v1.3) (30). Genome annotation was done as described for the metagenome.

iv. mRNA extraction, sequencing, and analysis

RNA was extracted in triplicate with a Zymo Research ZymoBIOMICS DNA/RNA Miniprep Kit from approximately 3 g sediment per extraction. Extracted samples were then treated with the Invitrogen Turbo DNA-free kit (Carlsbad, CA, USA) to remove contaminating DNA. The treated samples were then pooled and concentrated with a New England Biolabs Monarch RNA Cleanup Kit (Ipswich, MA, USA). Ribosomal RNA was depleted with a New England BioLabs NEBNext rRNA Depletion Kit (Bacteria) and a sequencing library was prepared with a New England BioLabs Ultra II RNA Library Prep Kit. The generated cDNA library was sequenced at The Center for Applied Genomics at the Hospital for Sick Children (Toronto, ON, Canada) on a NovaSeq 6000 (Illumina) with an S Prime 100-cycle flow cell (2x100 base reads). Reads were trimmed with Trimmomatic (settings LEADING:3 TRAILING:3 SLIDINGWINDOW:4:15 MINLEN 50) and rRNA reads were removed with SortMeRNA (v4.2.0) (31). Human contaminant reads were removed with BBDMap using the BBTools RemoveHuman masked reference genome. Reads were classified with Kaiju (v1.7.3), and reads classified within common sequencing contaminant groups as in Sheik et al. (2018) (32) were removed (~81,500 reads removed representing 77 genera; the genera with the most reads removed were *Pseudomonas* (~12,000 reads), *Streptococcus* (~7000 reads), and *Ralstonia* (~6000 reads)). Remaining reads were aligned to metagenome contigs and SAG scaffolds with bowtie2 (v2.3.5.1, with setting -very-sensitive-local) (33). Reads aligned to CDS regions were counted

with HTSeq (v0.12.4) (34) and transcripts per million reads (tpm) was calculated to normalize expression values for each gene. For comparison of stress response genes in SAGs to those in related genomes, protein-coding genes from reference genomes were queried against LH SAG protein-coding genes with BLASTp using a cut-off e-value of $1e-15$.

v. Sequencing data availability

Sequencing reads, metagenome, MAGs, and SAGs were deposited in NCBI under BioProject PRJNA699472. JGI annotations of the metagenome and SAGs are available under GOLD Study ID Gs0135943. SAGs were also deposited individually in JGI (Table S2.4).

vi. Gibbs free energy calculations

Gibbs free energy values were calculated using the method reported in Jones et al. (2018) (35) with the following parameters based on measurements reported in Table S1: 278.1° K, pH 6.4, 7.39 M ionic strength, 1.02×10^{-7} M CH₄, 3.81×10^{-4} M NH₃, 8.61×10^{-6} M H₂S, 1.57×10^{-5} M O₂, 2.31×10^{-5} M NO₃⁻, 1.04 M SO₄²⁻, 4.11×10^{-5} M CO₂, 3.16×10^{-7} M H⁺, 3.12×10^{-5} M NO₂⁻, and 0.23 M Fe³⁺.

Supplementary Results and Discussion

Discrepancy between recovered MAGs and SAGs

Using the criteria of average nucleotide identity >95%, only one SAG was found to correspond to MAGs. Typically, more overlap between the two datasets would be expected, particularly for those taxa abundant in the microbial community (36); conversely, the SAGs appear to be

enriched for taxa at low abundance in the metagenome. In the following sections we will discuss possible reasons as to why this occurred.

Firstly, multiple selection steps occurred during generation of the SAGs that may have excluded or did exclude genomes from taxa abundant in the metagenome and MAGs. While 365 events (cells) were sorted during single cell sorting, only the 95 wells with the greatest estimated genome amplification (based on fluorescence during the amplification reaction) were selected for further analysis. This may have resulted in a biased selection of cells: for example, selecting for those genomes most responsive to the MDA reaction or those most resistant to environmental fluxes that may have occurred during transportation or sorting. Additionally, after an initial round of 16S rRNA Sanger sequencing, some wells with highly similar (>98%) 16S rRNA sequences were excluded from subsequent genomic sequencing to maximize sequencing coverage on the remaining wells. This included several *Halomonas* and *Desulfobulbaceae* genomes represented by MAGs, therefore potentially reducing the number of SAGs that may have corresponded to MAGs. As a result of these filtering steps, SAGs corresponding to MAGs may have been excluded and low-abundance taxa including archaeal genomes may have been enriched.

Secondly, 20% of reads map to the high- and medium-quality MAGs, due in part to stringent quality control during binning (i.e. only contigs >5000 bp were binned). As a result, while the MAGs broadly represent the taxonomic groups present in the metagenome, they represent only a portion of the sum diversity. Therefore, this restrictive binning process in combination with the

relatively high number of SAGs corresponding to taxa at low abundance in the metagenome may also have contributed to the discrepancy.

Thirdly, the samples collected for metagenomic analysis and for SAG sequencing were collected in different years (2017 vs. 2019, respectively). This was necessitated by the small amount of sediment removed during sampling to avoid disturbing the site in combination with the low biomass of the sediment, requiring relatively high amounts of sample for processing. While the physical and geochemical parameters of the spring have remained stable for the ~15 years that we have studied the spring, including the measurements taken in 2017 and 2019, we can't exclude the possibility of minor changes in the spring that could have affected the microbial community sampled. Additionally, due to the low biomass and high salinity of the sediment, it is difficult to extract DNA. Biases introduced by the differing processing steps during MAG and SAG sequencing (for example, DNA extraction vs. separation of cells from sediment) may therefore have had outsize effects.

To summarize, we suggest several factors potentially contributing to the discrepancy between MAGs and SAGs: 1) Selection during generation of SAGs, 2) Stringent binning criteria, and 3) Differences in input samples and biases introduced by differing experimental procedures. We conclude by noting that although there is a discrepancy between the MAGs and SAGs, there is overlap between the two samples additional to what was discussed in the manuscript. In addition to the corresponding SAG and MAG noted in the manuscript, two additional SAGs had 16S rRNA sequences >98% identical to unbinned 16S rRNA sequences, and nearly all taxonomic groups represented by the SAGs were also present in the metagenome reads and 16S sequences

as classified by kaiju and PhyloFlash (with the sole exception of Iainarchaeota reads). Additionally, comparison of 16S rRNA sequences in the SAGs to previous 16S rRNA sequencing from over ten years ago (1) identified common sequences (>98%) between the two datasets, including sequences for *Halomonas*, ANME-1, and *Iainarchaeota*, suggesting that the discrepancy is more likely due to the potential technical factors discussed above rather than significant changes in the microbial community. The relative abundances of the microbial community represented in the metagenome are consistent with those observed in previous CARD-FISH and 16S rRNA and metagenomic sequencing (1, 2). We therefore suggest that the metagenome and MAGs more accurately represent the taxa abundant in the microbial community, whereas the SAGs are disproportionately enriched in low-abundance bacteria and archaea due to the potential factors discussed above.

Supplementary Figures and Tables

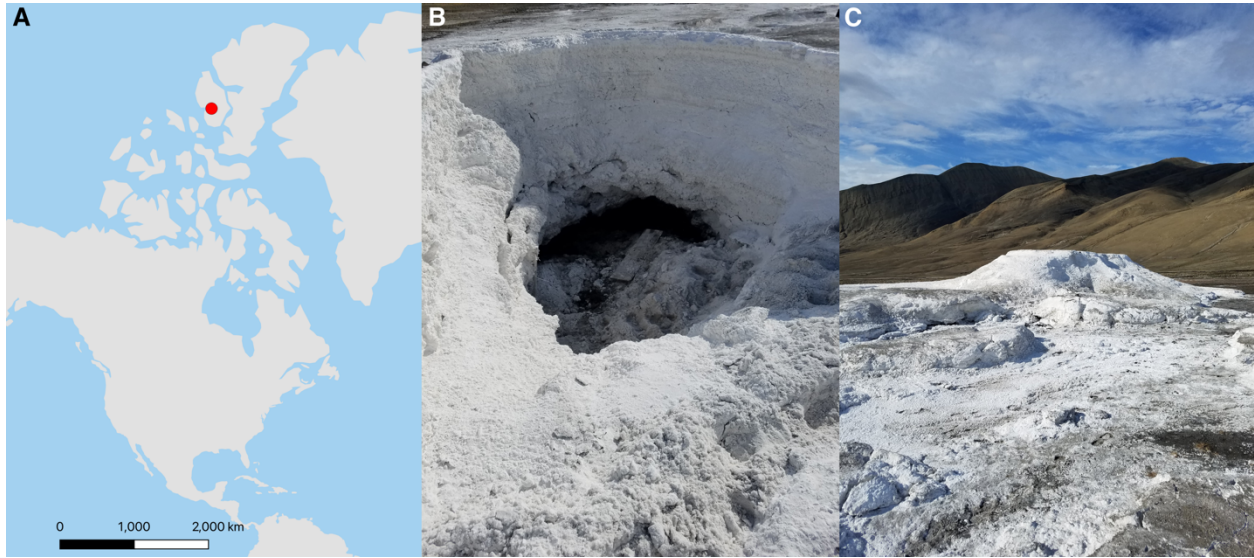


Figure S2.1. A. Location of the LH spring on Axel Heiberg Island in the Canadian High Arctic. Map generated in QGIS with the Natural Earth dataset. B. View looking into the LH salt tufa to the spring source (July 2019). C. View of the LH tufa and outflow channels (July 2019).

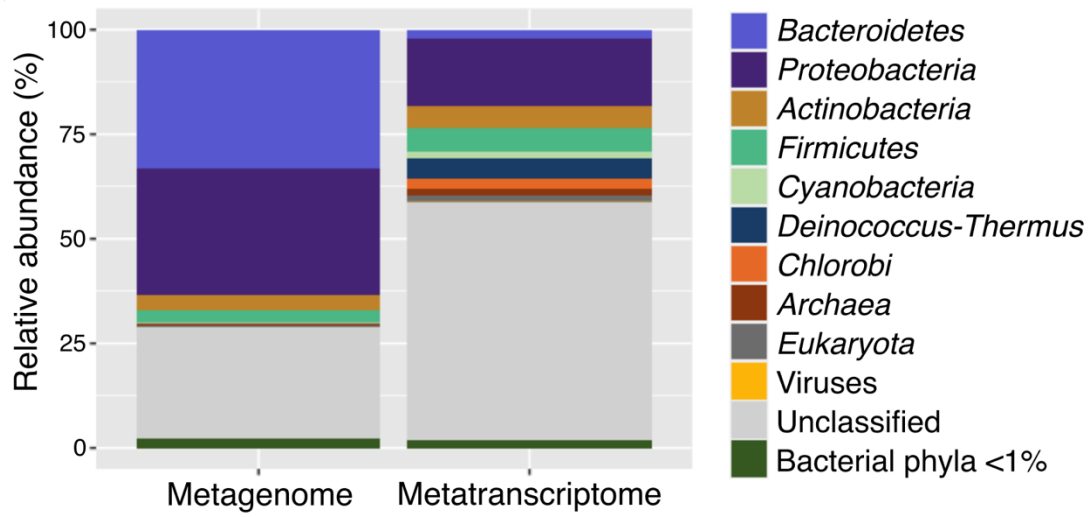


Figure S2.2. Taxonomic classification of metagenome and metatranscriptome reads. Reads were classified by Kaiju using the NCBI non-redundant database. Metagenome reads are an average of the relative abundance in duplicate samples.

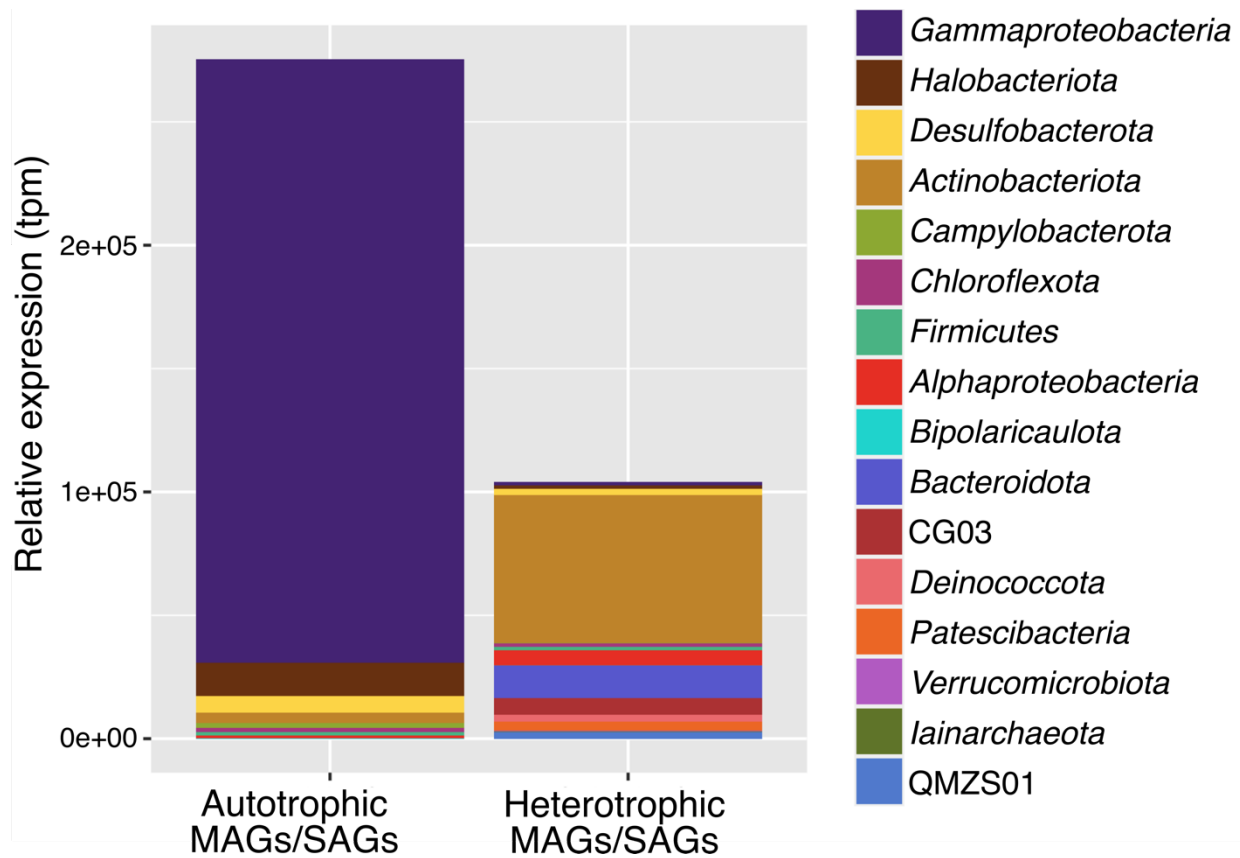


Figure S2.3. Relative expression (tpm) attributed to MAGs and SAGs containing CO₂-fixation genes (autotrophic MAGs/SAGs) and those without (heterotrophic MAGs/SAGs). Unbinned genes with mapped transcripts were omitted from this analysis.

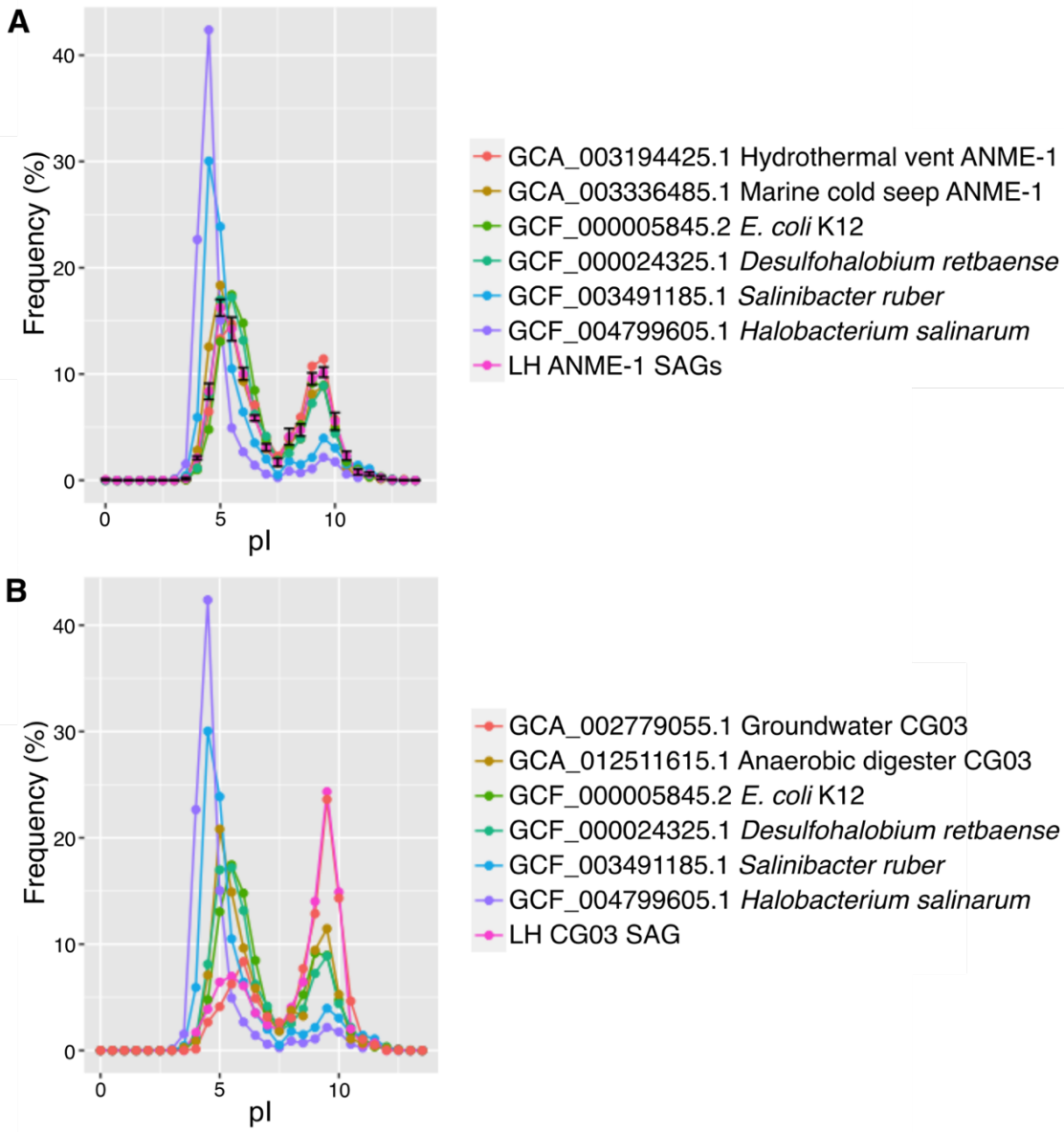


Figure S2.4. Comparison of predicted protein isoelectric points for A. ANME-1 SAGs S10-S14 and B. CG03 SAG S2. Protein isoelectric points were calculated with the ExPASy Compute pI/MW online tool. Genomes for comparison (based on similar analysis in Nigro et al. (37)) include microorganisms known to accumulate salts through the “salting-in” osmoregulation strategy (*Salinibacter ruber* and *Halobacterium salinarum*) and those that do not accumulate salts (*E. coli* K12 and *Desulfohalobium retbaense*).

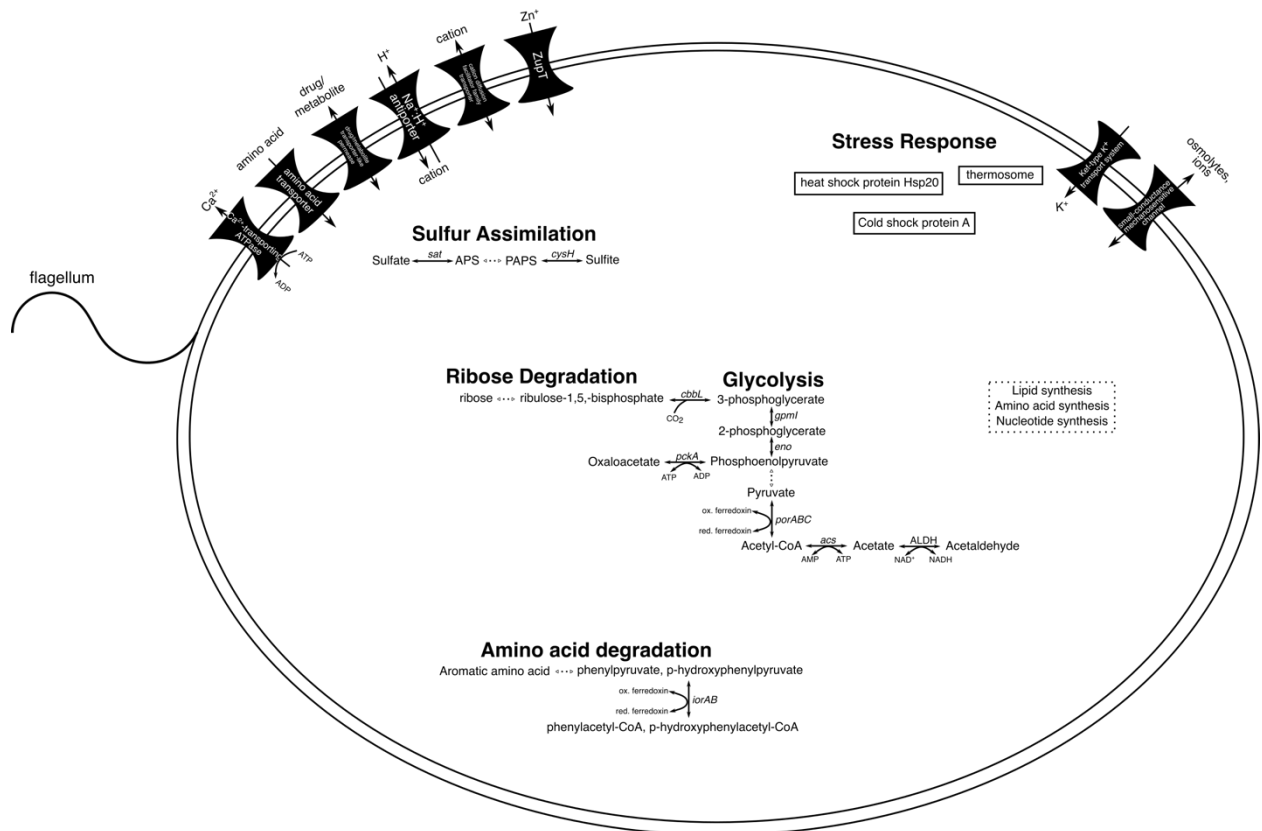


Figure S2.5. Metabolic reconstruction of *Iainarchaeia* SAG S9 (670822 bp, 52.9% completeness, 0% contamination). Solid lines represent genes present within the genome, and dashed lines indicate steps or pathways absent from the genome. Table S2.15 contains a complete list of annotated genes represented in this figure.

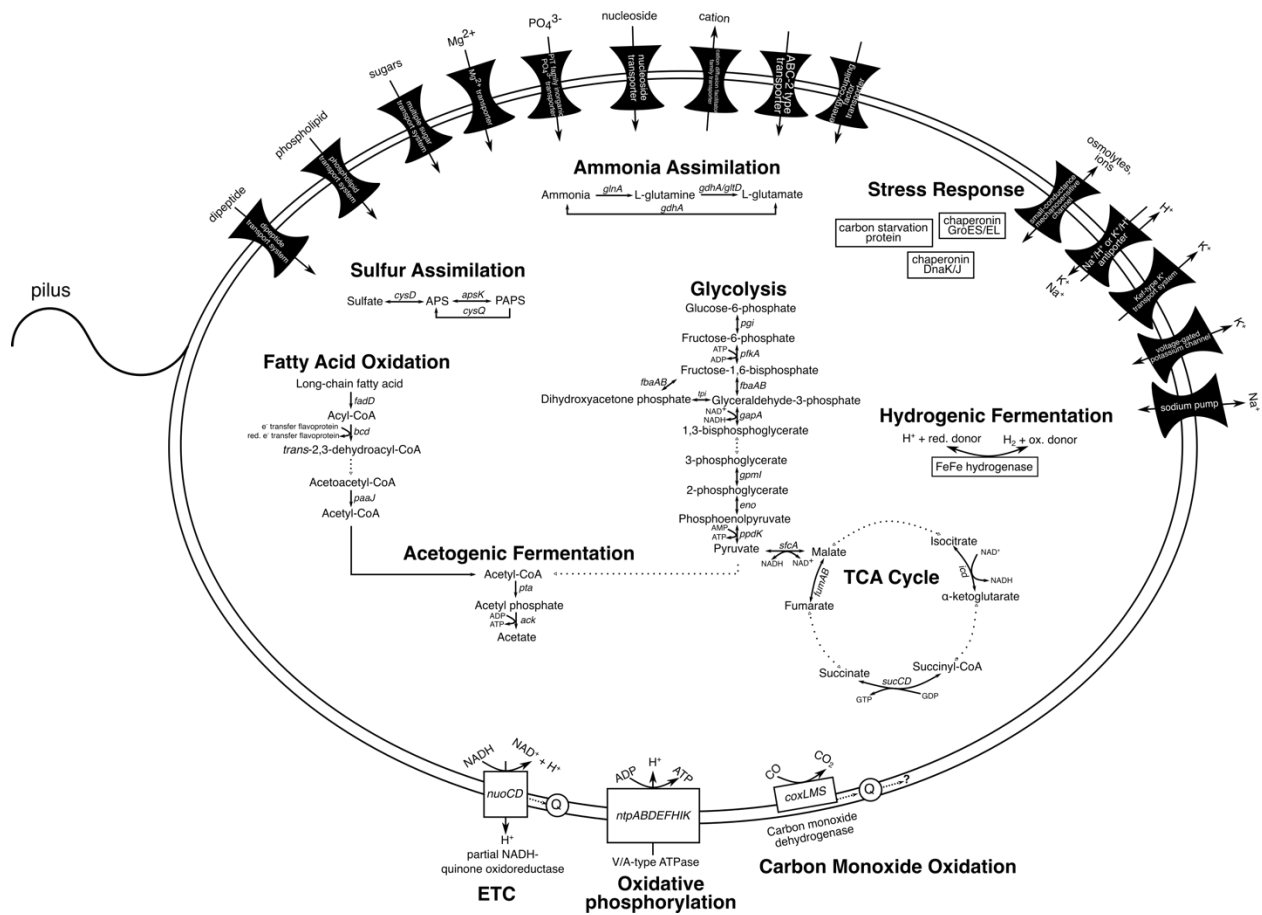


Figure S2.8. Metabolic reconstruction of candidate phylum CG03 SAG S2 (1039757 bp, 62.8% completeness, 0% contamination). Solid lines represent genes present within the genome, and dashed lines indicate steps or pathways absent from the genome. Table S2.17 contains a complete list of annotated genes represented in this figure.

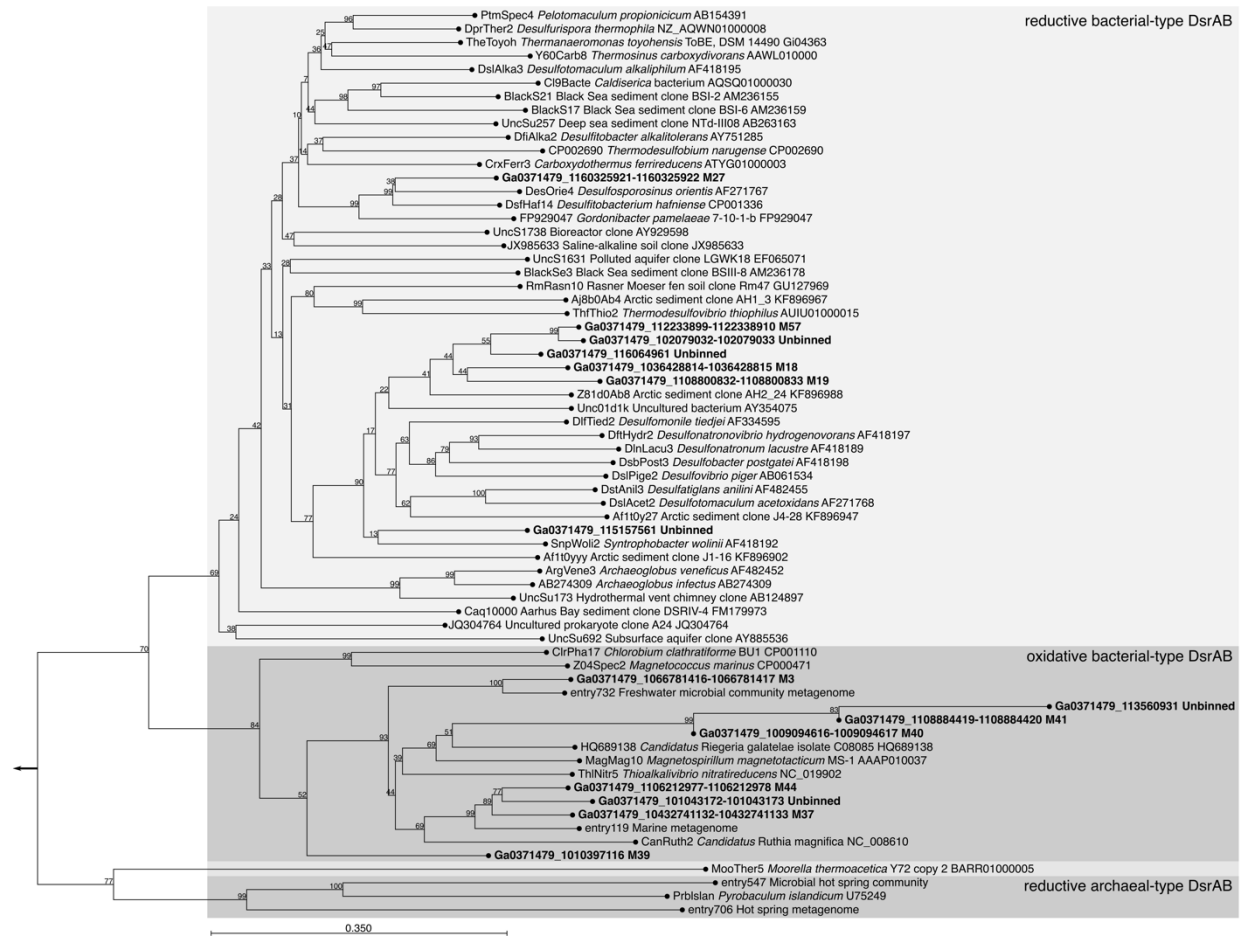


Figure S2.9. Maximum likelihood phylogenetic tree of DsrAB. The tree was constructed in CLC Genomics Workbench with 1000 bootstraps and WAG substitution model using reference sequences from Muller et al. (2015). Sequence names include the gene IDs and MAG number where applicable. A sequence from eggNOG group COG2221 (*Campylobacter ureolyticus* JFJK01000015_gene476) was used as an outgroup (direction indicated by arrow).

Table S2.1 (xlsx). Physical and geochemical parameters of Lost Hammer water and sediment.

Located in Supplementary Tables xlsx file.

Table S2.2. Metagenome and metatranscriptome sequencing statistics.

DNA/RNA	Sample (NCBI ID)	Sequencing platform	Read length	Raw read pairs	Read pairs after quality control
DNA	SRR13628066	Illumina HiSeq2500	2x126	116844950	116746762
DNA	SRR13628065	Illumina HiSeq2500	2x126	107914225	107647735
RNA	SRR13633097	Illumina NovaSeq6000	2x100	9009952	4233149

Table S2.3. Metagenomic assembly statistics.

Assembler	Megahit v1.1.3
# contigs	1620755
# contigs \geq 1000 bp	276578
# contigs \geq 5000 bp	36050
# contigs \geq 10000 bp	14841
# contigs \geq 25000 bp	3946
# contigs \geq 50000 bp	1251
Total length (bp)	1599970111
GC %	51.63
N50	2968
N75	1032
L50	67307
L75	264669
% reads mapping to contigs (average of two samples)	89.7
% reads mapping to contigs $>$ 5000 bp	67.9
Average coverage of metatranscriptome against the metagenome (reads/base)	0.093 ± 59
Average coverage of metatranscriptome against CDS with mapped reads (reads/base)	13 ± 604

Table S2.4 (xlsx). SAG supplemental information. Located in Supplementary Tables xlsx file.

Table S2.5 (xlsx). MAG supplemental information. Located in Supplementary Tables xlsx file.

Table S2.6 (xlsx). Relative expression for KEGG, COG, and pfam IDs. Located in Supplementary Tables xlsx file.

Table S2.7 (xlsx). Taxonomic classification of genes of interest with mapped transcripts. Located in Supplementary Tables xlsx file.

Table S2.8 (xlsx). Gene presence and expression in medium-quality MAGs. Located in Supplementary Tables xlsx file.

Table S2.9 (xlsx). Complete list of genes with mapped transcripts. Located in Supplementary Tables xlsx file.

Table S2.10. Gibbs free energy of redox pairs present in LH. Values were calculated using the methodology in Jones et al. (2018) (35) (additional details in Supplementary Methods). These values should be considered preliminary estimates as some parameter concentrations are based on single-year measurements.

Redox pair	ΔG reaction (kJ/mol electron⁻¹)
H ₂ /O ₂	-111.9
H ₂ /NO ₃ ⁻ (to NH ₃)	-61.3
N ₂ /NO ₃ ⁻ (to NO ₂ ⁻)	-68.1
H ₂ /SO ₄ ²⁻	-3.0
H ₂ /CO ₂	-9.1
H ₂ S/O ₂	-109.0
H ₂ S/NO ₃ ⁻	-93.8
Fe ²⁺ /O ₂	-16.0
NH ₃ /O ₂	-52.9
NH ₃ /NO ₃ ⁻	-90.8
NH ₃ /SO ₄ ²⁻	-56.5
CH ₄ /O ₂	-205.7
CH ₄ /NO ₃ ⁻	-32.4
CH ₄ /SO ₄ ²⁻	6.1

Table S2.11 (xlsx). Stress response gene comparison to related genomes. Located in Supplementary Tables xlsx file.

Table S2.12 (xlsx). Gene content of MAGs. Located in Supplementary Tables xlsx file.

Table S2.13 (xlsx). Gene content of SAGs. Located in Supplementary Tables xlsx file.

Table S2.14 (xlsx). ANME-1 composite genome gene content. Located in Supplementary Tables xlsx file.

Table S2.15 (xlsx). *Iainarchaeia* sp. S9 gene content. Located in Supplementary Tables xlsx file.

Table S2.16 (xlsx). QMZS01 composite genome gene content. Located in Supplementary Tables xlsx file.

Table S2.17 (xlsx). CG03 sp. S2 gene content. Located in Supplementary Tables xlsx file.

Table S2.18 (xlsx). Metagenome copy number and total relative expression of genes of interest. Located in Supplementary Tables xlsx file.

References

1. Niederberger TD, Perreault NN, Tille S, Lollar BS, Lacrampe-Couloume G, Andersen D, et al. Microbial characterization of a subzero, hypersaline methane seep in the Canadian High Arctic. *ISME J.* 2010;4(10):1326-39.
2. Lay CY, Mykytczuk NC, Yergeau E, Lamarche-Gagnon G, Greer CW, Whyte LG. Defining the functional potential and active community members of a sediment microbial community in a high-Arctic hypersaline subzero spring. *Appl Environ Microbiol.* 2013;79(12):3637-48.
3. Lamarche-Gagnon G, Comery R, Greer CW, Whyte LG. Evidence of *in situ* microbial activity and sulphidogenesis in perennially sub-0 degrees C and hypersaline sediments of a high Arctic permafrost spring. *Extremophiles.* 2015;19(1):1-15.
4. Battler MM, Osinski GR, Banerjee NR. Mineralogy of saline perennial cold springs on Axel Heiberg Island, Nunavut, Canada and implications for spring deposits on Mars. *Icarus.* 2013;224(2):364-81.
5. Ward MK, Pollard WH. A hydrohalite spring deposit in the Canadian high Arctic: a potential Mars analogue. *Earth Planet Sci Lett.* 2018;504:126-38.
6. Bolger AM, Lohse M, Usadel B. Trimmomatic: a flexible trimmer for Illumina sequence data. *Bioinformatics.* 2014;30(15):2114-20.
7. Menzel P, Ng KL, Krogh A. Fast and sensitive taxonomic classification for metagenomics with Kaiju. *Nat Commun.* 2016;7(1):1-9.
8. Gruber-Vodicka HR, Seah BKB, Pruesse E. phyloFlash: rapid small-subunit rRNA profiling and targeted assembly from metagenomes. *mSystems.* 2020;5(5):1-16.

9. Li D, Liu CM, Luo R, Sadakane K, Lam TW. MEGAHIT: an ultra-fast single-node solution for large and complex metagenomics assembly via succinct de Bruijn graph. *Bioinformatics*. 2015;31(10):1674-6.
10. Nurk S, Meleshko D, Korobeynikov A, Pevzner PA. metaSPAdes: a new versatile metagenomic assembler. *Genome Res*. 2017;27(5):824-34.
11. Kang DD, Froula J, Egan R, Wang Z. MetaBAT, an efficient tool for accurately reconstructing single genomes from complex microbial communities. *PeerJ*. 2015;3:1-15.
12. Parks DH, Imelfort M, Skennerton CT, Hugenholtz P, Tyson GW. CheckM: assessing the quality of microbial genomes recovered from isolates, single cells, and metagenomes. *Genome Res*. 2015;25(7):1043-55.
13. Mikheenko A, Prjibelski A, Saveliev V, Antipov D, Gurevich A. Versatile genome assembly evaluation with QUAST-LG. *Bioinformatics*. 2018;34(13):i142-i150.
14. Chen IA, Chu K, Palaniappan K, Ratner A, Huang J, Huntemann M, et al. The IMG/M data management and analysis system v.6.0: new tools and advanced capabilities. *Nucleic Acids Res*. 2020;49(D1):D751–D763.
15. Mukherjee S, Stamatis D, Bertsch J, Ovchinnikova G, Sundaramurthi JC, Lee J, et al. Genomes OnLine Database (GOLD) v.8: overview and updates. *Nucleic Acids Res*. 2020;49(D1):D723-D733.
16. Chaumeil PA, Mussig AJ, Hugenholtz P, Parks DH. GTDB-Tk: a toolkit to classify genomes with the Genome Taxonomy Database. *Bioinformatics*. 2019;36(6):1925–7.
17. Eren AM, Esen OC, Quince C, Vineis JH, Morrison HG, Sogin ML, et al. Anvi'o: an advanced analysis and visualization platform for 'omics data. *PeerJ*. 2015;3:1-29.

18. Garber AI, Nealson KH, Okamoto A, McAllister SM, Chan CS, Barco RA, et al. FeGenie: a comprehensive tool for the identification of iron genes and iron gene neighborhoods in genome and metagenome assemblies. *Front Microbiol.* 2020;11:1-23.
19. Fish JA, Chai B, Wang Q, Sun Y, Brown CT, Tiedje JM, et al. FunGene: the functional gene pipeline and repository. *Front Microbiol.* 2013;4:1-14.
20. Sondergaard D, Pedersen CN, Greening C. HydDB: a web tool for hydrogenase classification and analysis. *Sci Rep.* 2016;6:1-8.
21. Muller AL, Kjeldsen KU, Rattei T, Pester M, Loy A. Phylogenetic and environmental diversity of DsrAB-type dissimilatory (bi)sulfite reductases. *ISME J.* 2015;9(5):1152-65.
22. Edgar RC. MUSCLE: multiple sequence alignment with high accuracy and high throughput. *Nucleic Acids Res.* 2004;32(5):1792-7.
23. Anantharaman K, Hausmann B, Jungbluth SP, Kantor RS, Lavy A, Warren LA, et al. Expanded diversity of microbial groups that shape the dissimilatory sulfur cycle. *ISME J.* 2018;12(7):1715-28.
24. Stepanauskas R, Fergusson EA, Brown J, Poulton NJ, Tupper B, Labonte JM, et al. Improved genome recovery and integrated cell-size analyses of individual uncultured microbial cells and viral particles. *Nat Commun.* 2017;8(1):1-10.
25. Kuske CR, Barns SM, Grow CC, Merrill L, Dunbar J. Environmental survey for four pathogenic bacteria and closely related species using phylogenetic and functional genes. *J Forensic Sci.* 2006;51(3):548-58.
26. Miller CS, Handley KM, Wrighton KC, Frischkorn KR, Thomas BC, Banfield JF. Short-read assembly of full-length 16S amplicons reveals bacterial diversity in subsurface sediments. *PLoS One.* 2013;8(2):1-11.

27. Quast C, Pruesse E, Yilmaz P, Gerken J, Schweer T, Yarza P, et al. The SILVA ribosomal RNA gene database project: improved data processing and web-based tools. *Nucleic Acids Res.* 2013;41:D590-596.
28. Schmieder R, Edwards R. Fast identification and removal of sequence contamination from genomic and metagenomic datasets. *PLoS One.* 2011;6(3):1-11.
29. Bankevich A, Nurk S, Antipov D, Gurevich AA, Dvorkin M, Kulikov AS, et al. SPAdes: a new genome assembly algorithm and its applications to single-cell sequencing. *J Comput Biol.* 2012;19(5):455-77.
30. Jain C, Rodriguez RL, Phillippy AM, Konstantinidis KT, Aluru S. High throughput ANI analysis of 90K prokaryotic genomes reveals clear species boundaries. *Nat Commun.* 2018;9(1):1-8.
31. Kopylova E, Noe L, Touzet H. SortMeRNA: fast and accurate filtering of ribosomal RNAs in metatranscriptomic data. *Bioinformatics.* 2012;28(24):3211-7.
32. Sheik CS, Reese BK, Twing KI, Sylvan JB, Grim SL, Schrenk MO, et al. Identification and removal of contaminant sequences from ribosomal gene databases: lessons from the Census of Deep Life. *Front Microbiol.* 2018;9:1-14.
33. Langmead B, Salzberg SL. Fast gapped-read alignment with Bowtie 2. *Nat Methods.* 2012;9(4):357-9.
34. Anders S, Pyl PT, Huber W. HTSeq--a Python framework to work with high-throughput sequencing data. *Bioinformatics.* 2015;31(2):166-9.
35. Jones RM, Goordial JM, Orcutt BN. Low energy subsurface environments as extraterrestrial analogs. *Front Microbiol.* 2018;9:1-18.

36. Alneberg J, Karlsson CMG, Divne AM, Bergin C, Homa F, Lindh MV, et al. Genomes from uncultivated prokaryotes: a comparison of metagenome-assembled and single-amplified genomes. *Microbiome*. 2018;6(1):1-14.
37. Nigro LM, Hyde AS, MacGregor BJ, Teske A. Phylogeography, salinity adaptations and metabolic potential of the candidate division KB1 bacteria based on a partial single cell genome. *Front Microbiol*. 2016;7:1-9.

Appendix 2. Supplementary Materials for Chapter 3

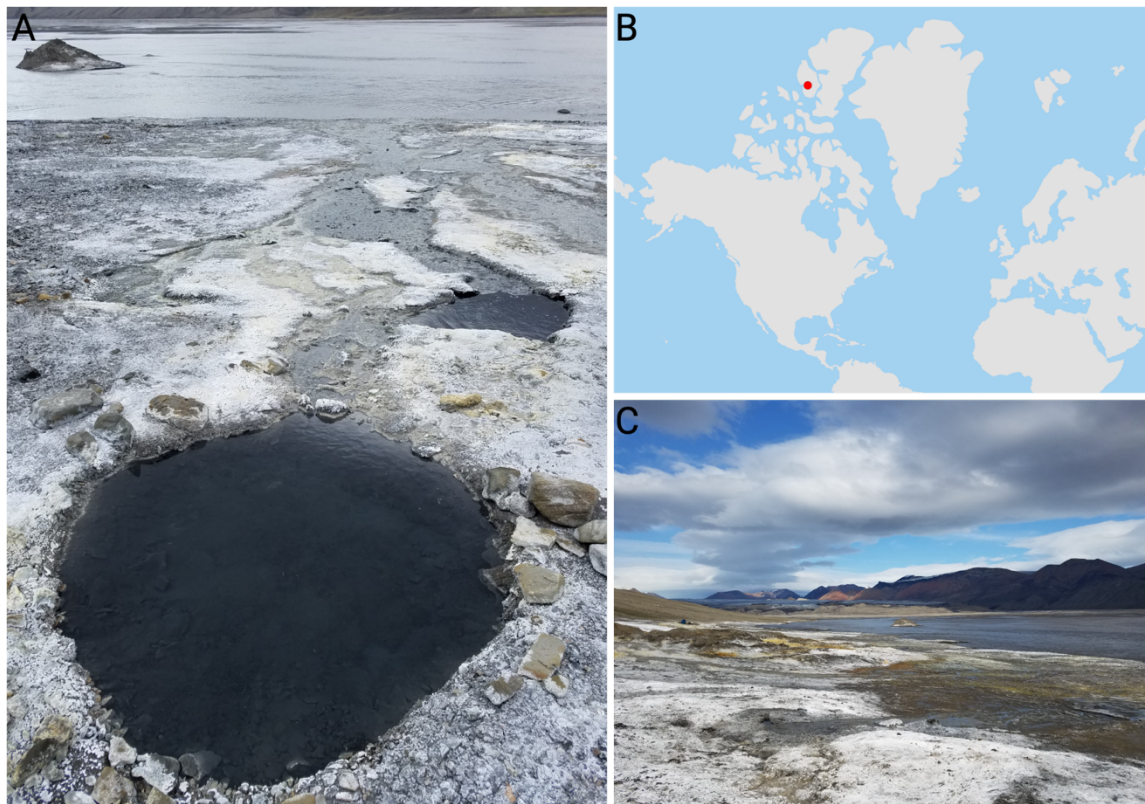


Figure S3.1. a. Photograph of GH-4 primary outlet and downstream channels (July 2019). A fine layer of gypsum coats the area around the springs. **b.** Location of the Gypsum Hill springs on Axel Heiberg Island, Nunavut, Canada (indicated with red dot). Map generated in QGIS with the Natural Earth dataset. **c.** Photograph of the Gypsum Hill springs area in which GH-4 is located. Photos: E. Magnuson.

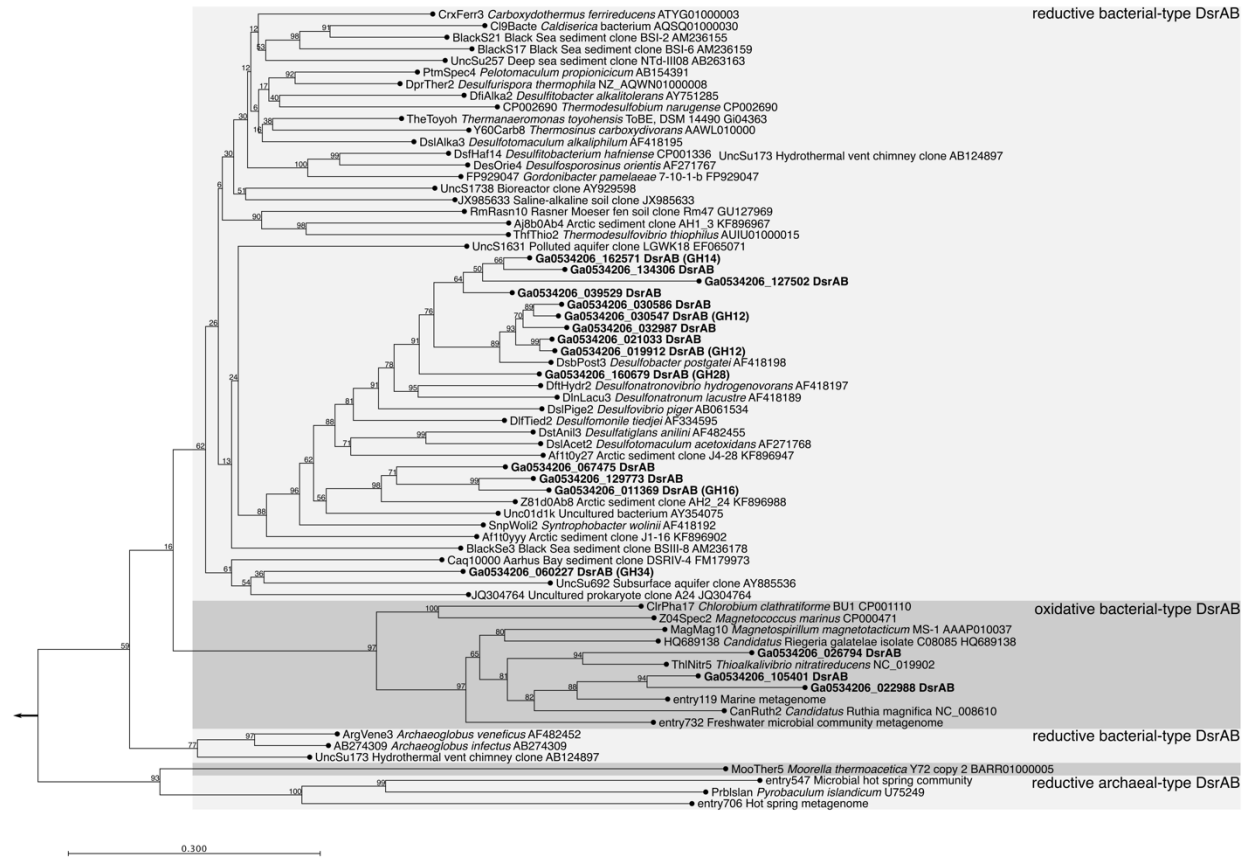


Figure S3.2. Phylogenetic tree of DsrAB sequences. The tree was constructed in CLC Genomics Workbench with 1000 bootstraps and WAG substitution model using reference sequences from Müller *et al.* (2015) (1). Sequence names include the contig IDs and MAG ID where applicable. A sequence from eggNOG group COG2221 (*Campylobacter ureolyticus* JFJK01000015_gene476) was used as an outgroup (direction indicated by arrow).

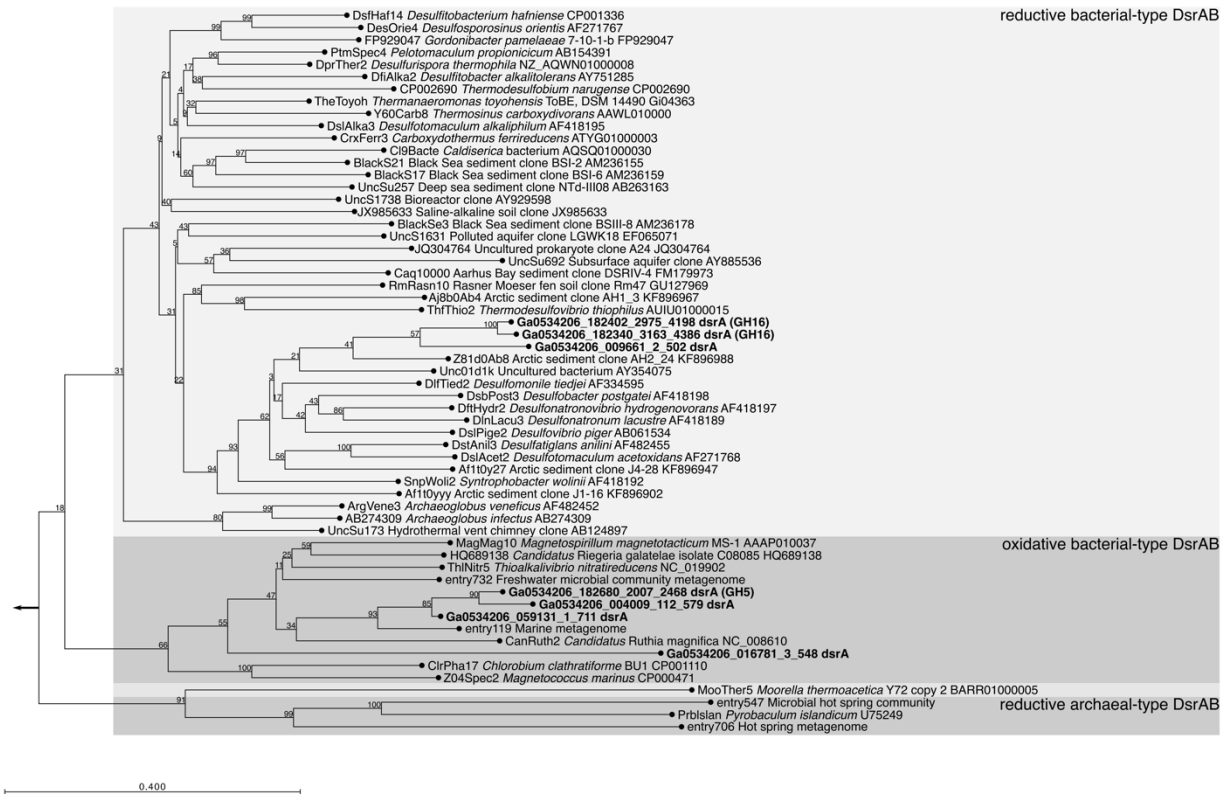


Figure S3.3. Phylogenetic tree of DsrA sequences. The tree was constructed in CLC Genomics Workbench with 1000 bootstraps and WAG substitution model using reference sequences from Müller *et al.* (2015) (1). Sequence names include the contig IDs and MAG ID where applicable. A sequence from eggNOG group COG2221 (*Campylobacter ureolyticus* JFJK01000015_gene476) was used as an outgroup (direction indicated by arrow).

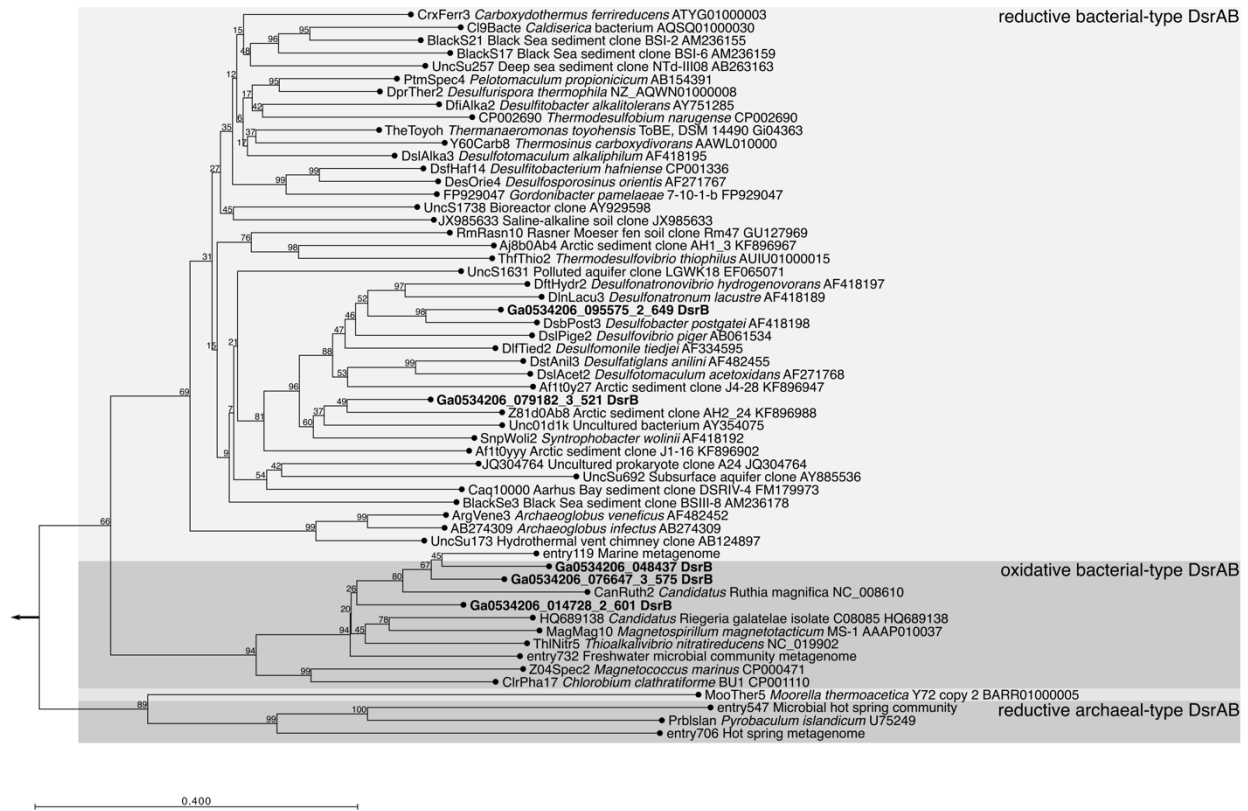


Figure S3.4. Phylogenetic tree of DsrB sequences. The tree was constructed in CLC Genomics Workbench with 1000 bootstraps and WAG substitution model using reference sequences from Müller *et al.* (2015) (1). Sequence names include the contig IDs and MAG ID where applicable. A sequence from eggNOG group COG2221 (*Campylobacter ureolyticus* JFJK01000015_gene476) was used as an outgroup (direction indicated by arrow).

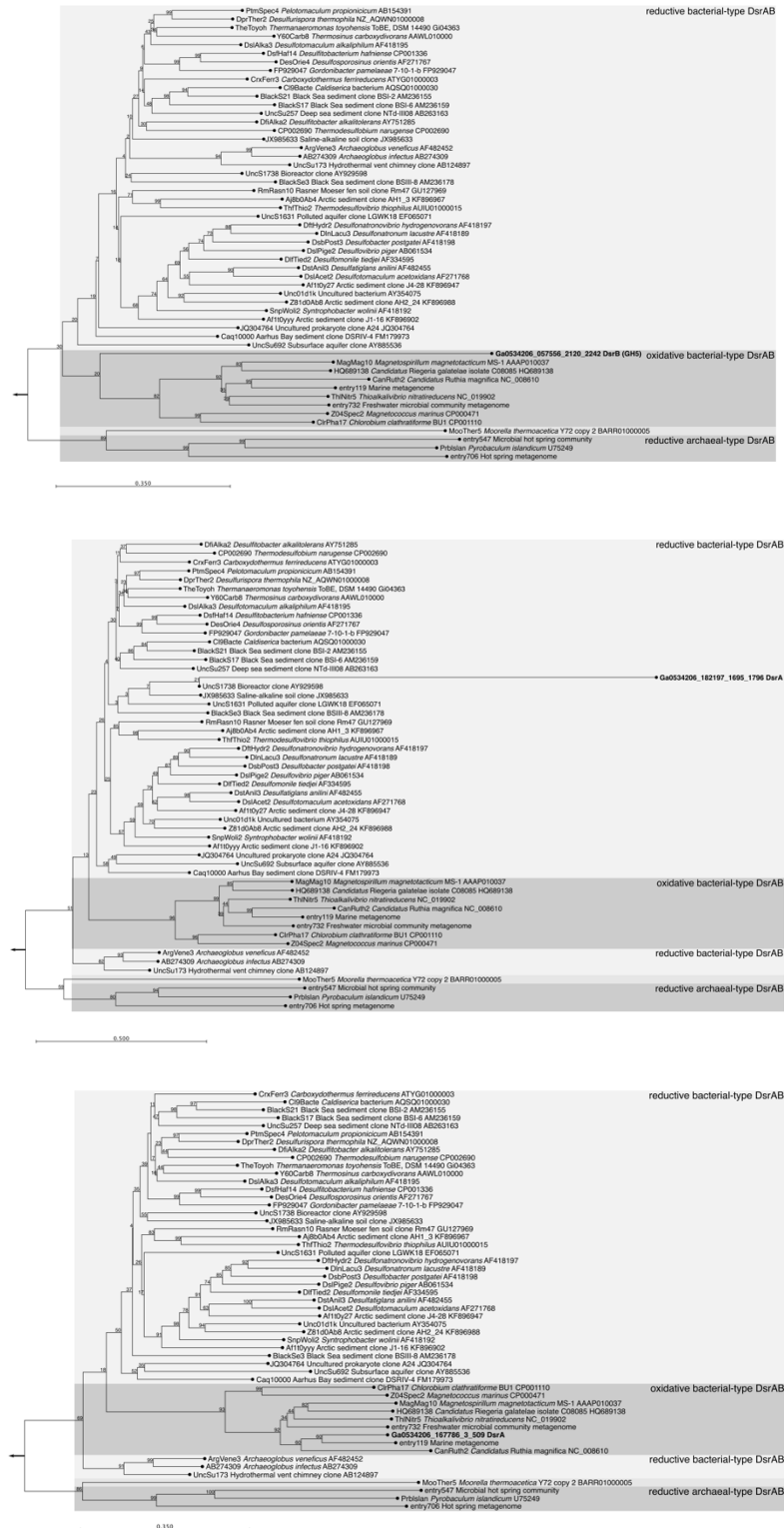


Figure S3.5. Phylogenetic trees of DsrA and DsrB sequences. These sequences were aligned separately due to lack of clustering when included with other DsrAB sequences as in Figures

S3.2-S3.4. The trees were constructed in CLC Genomics Workbench with 1000 bootstraps and WAG substitution model using reference sequences from Müller *et al.* (2015) (1). Sequence names include the contig IDs and MAG ID where applicable. A sequence from eggNOG group COG2221 (*Campylobacter ureolyticus* JFJK01000015_gene476) was used as an outgroup (direction indicated by arrow).

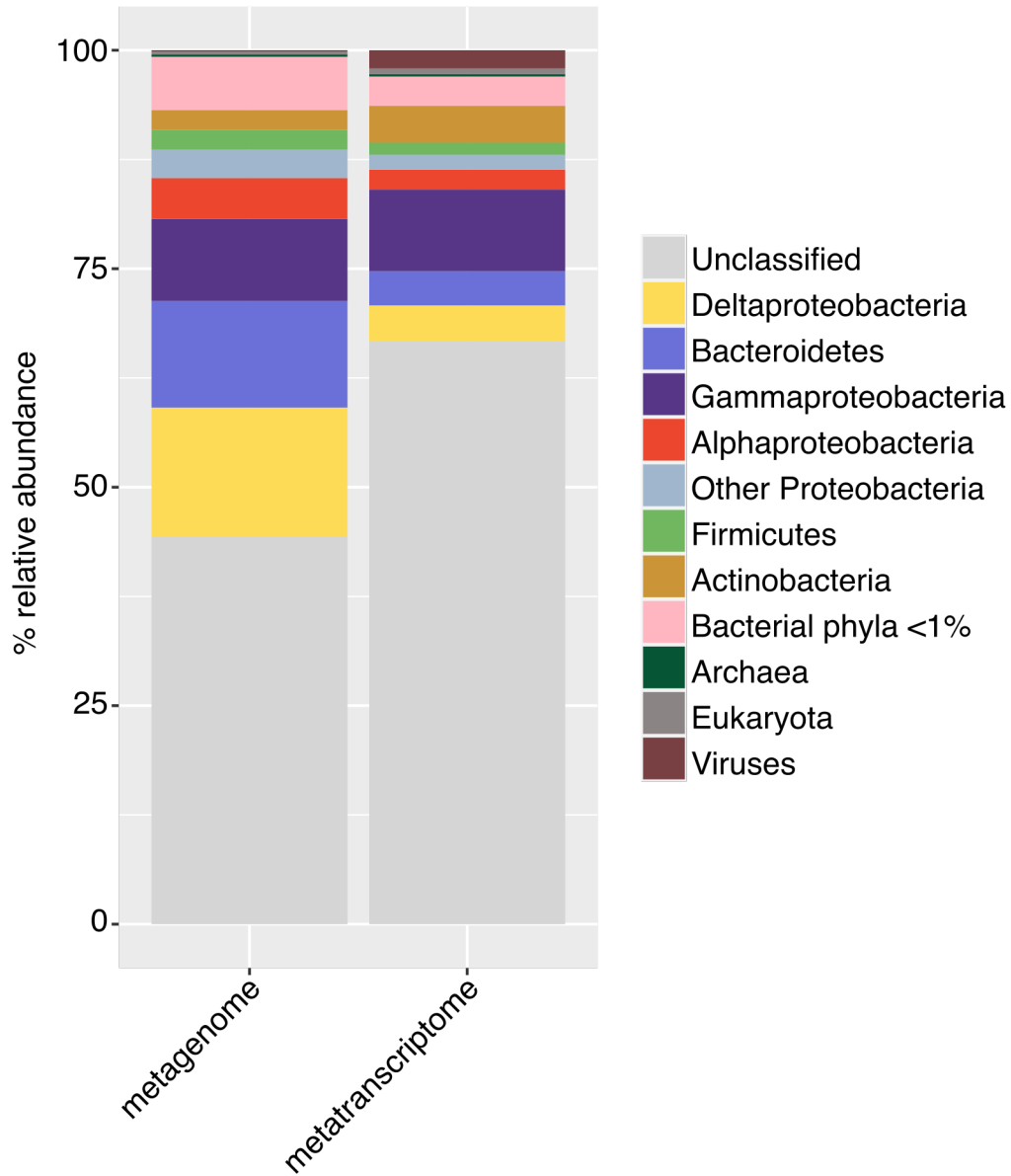


Figure S3.6. Relative abundance of reads in the metagenome and metatranscriptome classified by Kaiju using the NCBI non-redundant database (nr_euk). Relative abundance was averaged between replicates for both the metagenome and metatranscriptome.

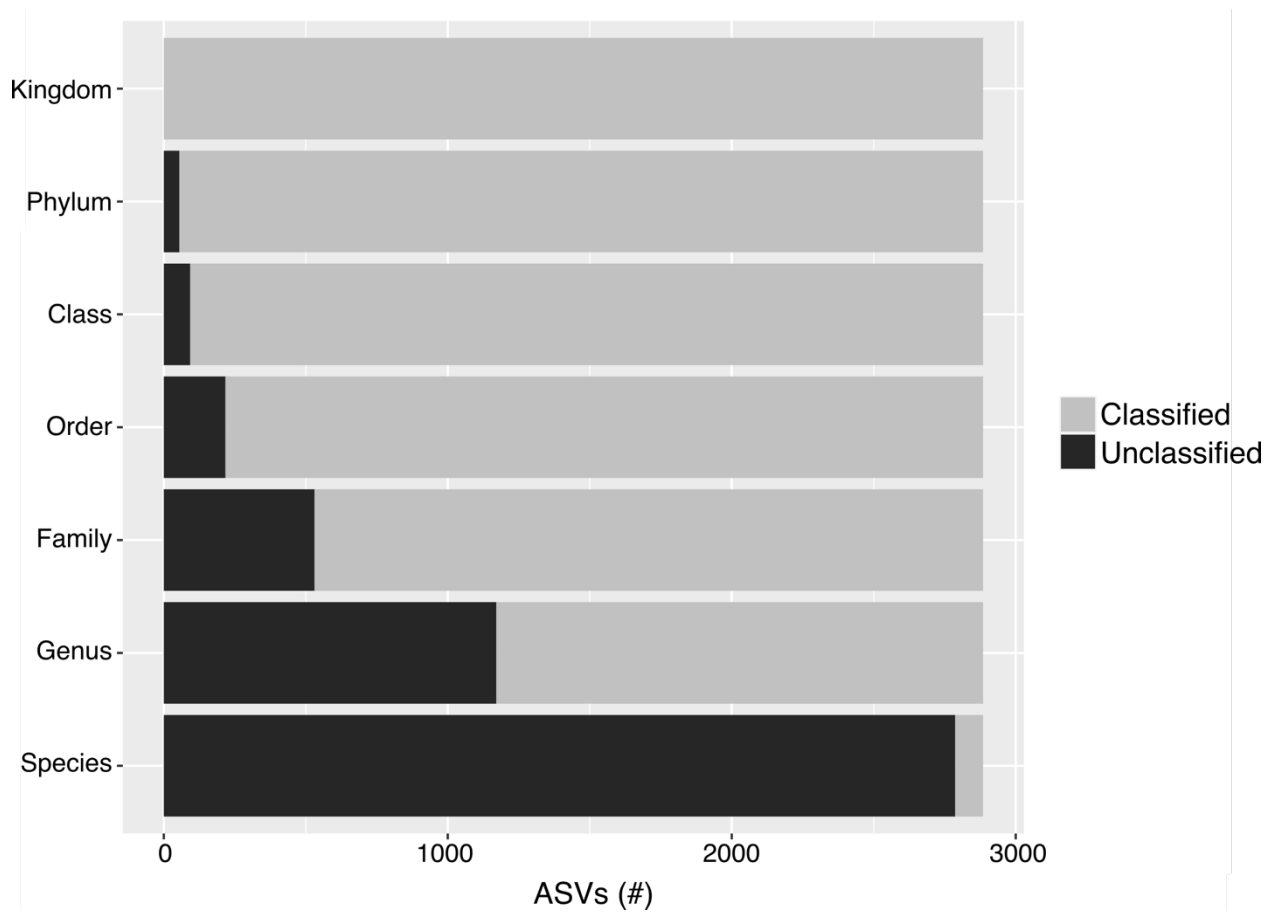


Figure S3.7. Level of taxonomic novelty of ASVs (2,885 ASVs in total). The number of classified and unclassified ASVs at each taxonomic level was determined according to rank assignment and taxonomic classification in DADA2 using the AssignTaxonomy function and the SILVA database.

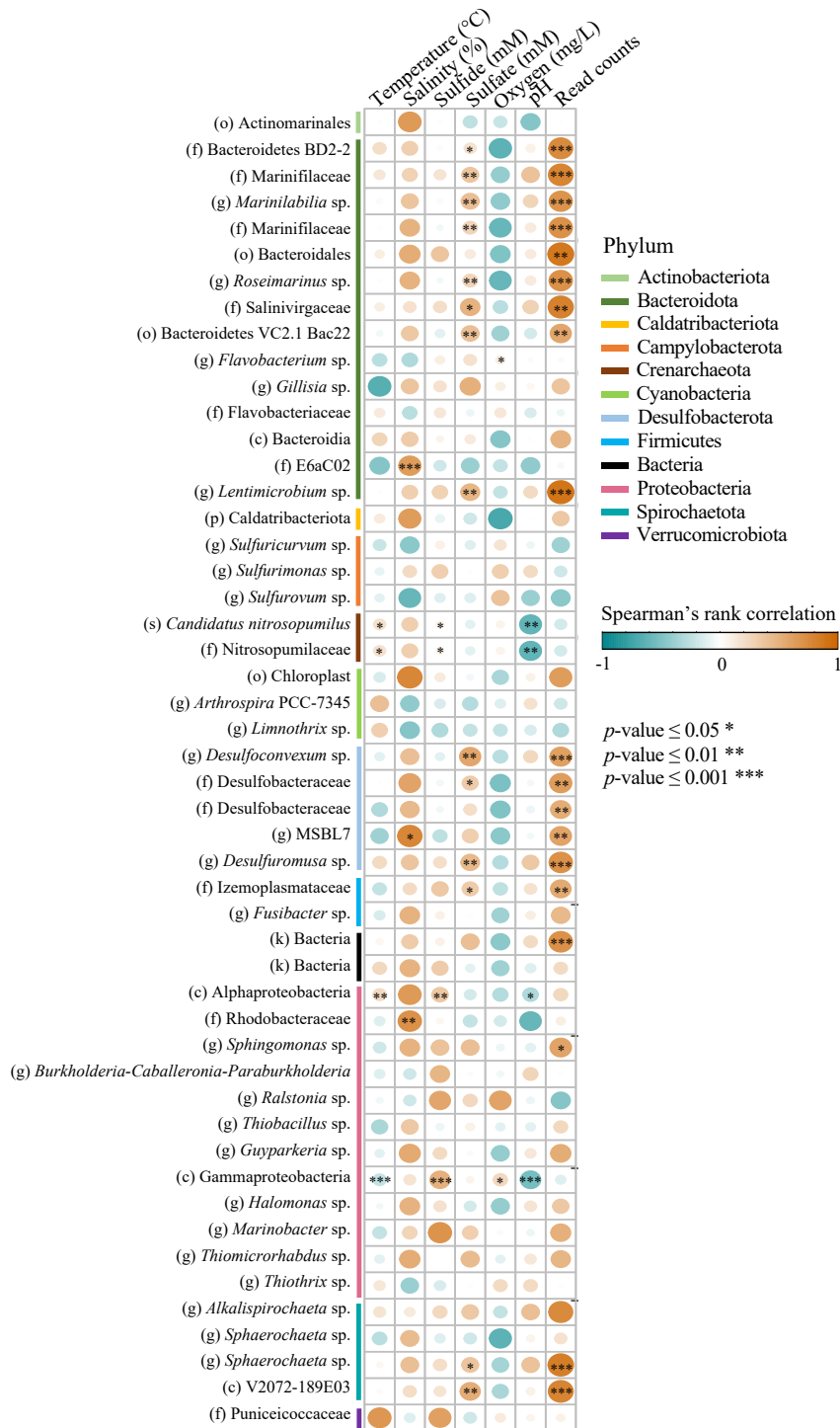


Figure S3.8. Spearman's rank correlation of the top 50 most abundant taxa in the subset of thirteen 16S rRNA gene sequencing data sets with environmental parameters. Metadata for this plot is located in Table S3.4.

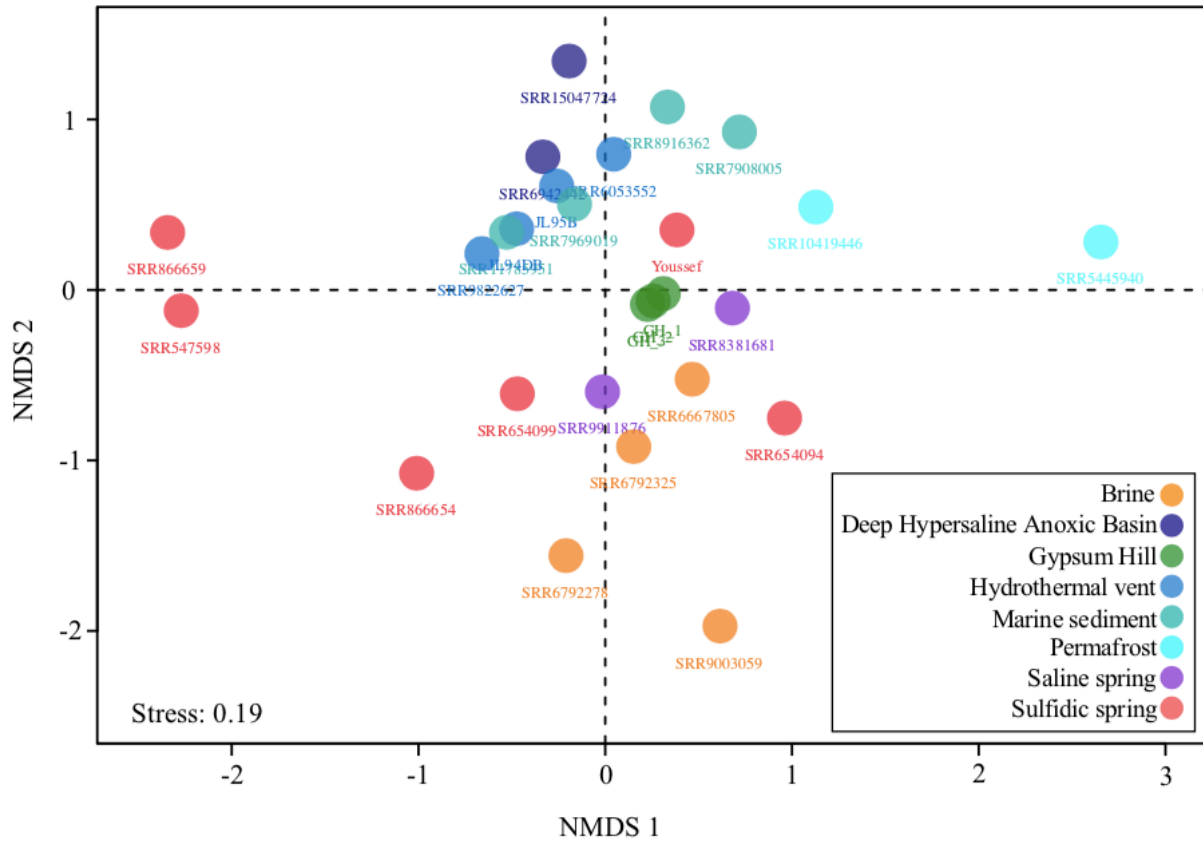


Figure S3.9. NMDS plot with Bray-Curtis dissimilarity matrix for 16S rRNA gene amplicon sequences from GH and comparable environments. Metadata for this plot is located in Table S3.4.

Table S3.1 (xlsx). Physical and chemical parameters in GH-4. Located in Supplementary Tables xlsx file.

Table S3.2. Sequencing library statistics.

Library type	Sample Name	Sample NCBI ID	Read length (base pairs)	Raw read pairs	Read pairs after quality control	Read mapping rate to metagenome co-assembly (%)
Metagenome	Replicate 1 (GH1)	SAMN32378173	2x100	34485105	34483207	71.52
Metagenome	Replicate 2 (GH2)	SAMN32386946	2x100	37844336	37843584	80.54
Metagenome	Replicate 3 (GH3)	SAMN32386947	2x100	36789239	36788071	81.09
Metatranscriptome	Replicate 1 (R2)	SAMN32386639	2x100	59259431	30221082	59.09
Metatranscriptome	Replicate 2 (R5)	SAMN32386637	2x100	29110743	18697235	30.72
Metatranscriptome	Replicate 3 (R6-technical replicate)	SAMN32386638	2x100	48840940	25313326	60.72
Metatranscriptome	Replicate 3 (R9-technical replicate)	SAMN32386638	2x100	48405899	29204507	42.83
Amplicon	Replicate 1 (GH34)	SAMN32406239	2x300	322476	170529	N/A
Amplicon	Replicate 2 (GH35)	SAMN32406240	2x300	256138	130640	N/A
Amplicon	Replicate 3 (GH36)	SAMN32406241	2x300	474775	202598	N/A

Table S3.3. Metagenome co-assembly statistics.

Contigs	464165
Total length (bp)	519632022
Maximum contig length (bp)	874936
Average contig length (bp)	1119
N50 (bp)	2577
Contigs >2 kb	43091
Total length contigs >2 kb	283840215
Metagenome-assembled genomes (#) (>50% complete, <10% contamination)	57
Total length in metagenome-assembled genomes (bp)	182741013

Table S3.4 (xlsx). Metadata for amplicon metagenome libraries used in beta diversity analysis.

Located in Supplementary Tables xlsx file.

Table S3.5 (xlsx). Taxonomic count table used for beta diversity analysis. Located in Supplementary Tables xlsx file.

Table S3.6 (xlsx). List of contigs in each MAG. Located in Supplementary Tables xlsx file.

Table S3.7 (xlsx). MAG supplemental information. Located in Supplementary Tables xlsx file.

Table S3.8 (xlsx). Taxonomic classification of genes of interest with mapped transcripts.

Located in Supplementary Tables xlsx file.

Table S3.9 (xlsx). Gene content of MAGs. Located in Supplementary Tables xlsx file.

Table S3.10 (xlsx). Relative expression of genes of interest in MAGs. Located in Supplementary Tables xlsx file.

Table S3.11 (xlsx). Total tpm per genome feature product ID. Located in Supplementary Tables xlsx file.

Table S3.12 (xlsx). Gene counts and relative expression of genes of interest in the metagenome. Located in Supplementary Tables xlsx file.

Table S3.13 (xlsx). Complete BLAST output of elemental sulfur reduction proteins queried against *Desulfuromusa* sp. GH17. Located in Supplementary Tables xlsx file.

Table S3.14 (xlsx). Relative expression of all genes. Located in Supplementary Tables xlsx file.

References

1. Muller AL, Kjeldsen KU, Rattei T, Pester M, Loy A. Phylogenetic and environmental diversity of DsrAB-type dissimilatory (bi)sulfite reductases. *ISME J.* 2015;9(5):1152-65.

Appendix 3. Supplementary Materials for Chapter 4

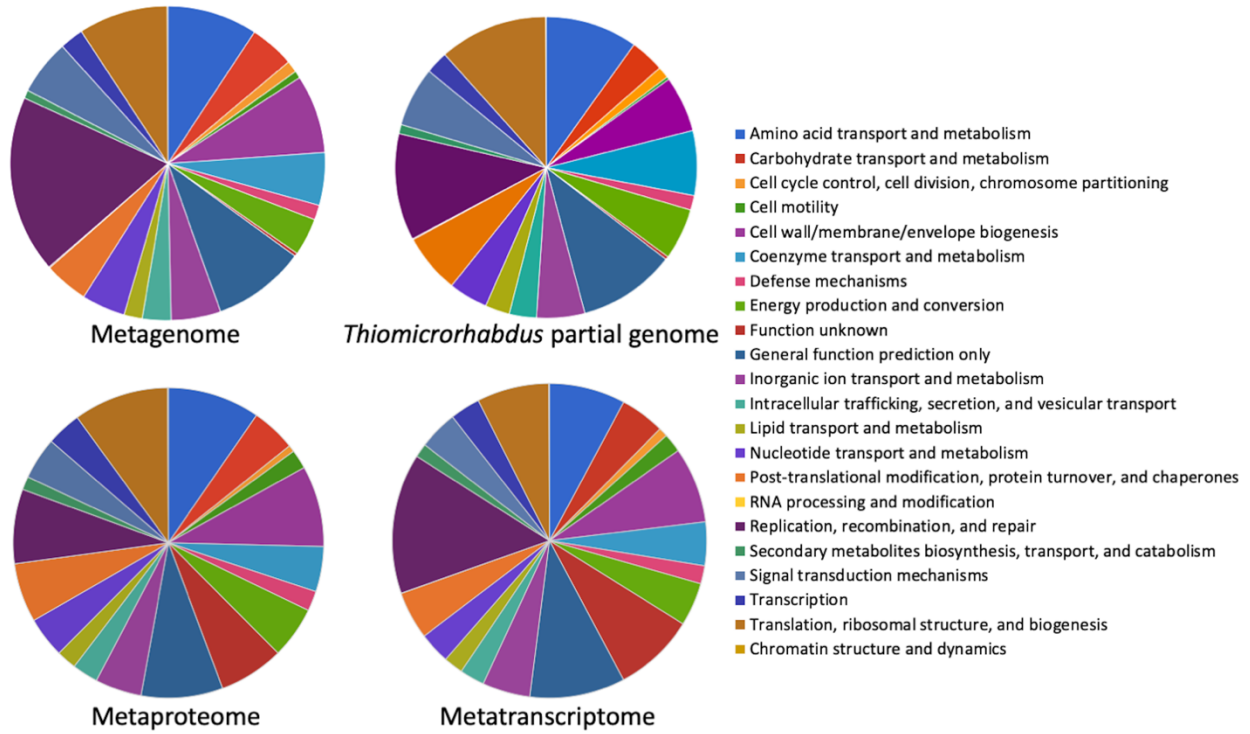


Figure S4.1. Relative abundance of annotated feature COG categories in the metagenome, *Thiomicrothabodus* partial genome, metaproteome, and metatranscriptomes.